Guiding safe and sustainable technological innovation under uncertainty: a case study of III-V/silicon photovoltaics

Blanco Rocha, C.F.

Guiding safe and sustainable technological innovation under uncertainty

A case study of III-V/silicon photovoltaics

Carlos Felipe Blanco R.

Guiding safe and sustainable technological innovation under uncertainty: a case study of III-V/silicon photovoltaics

PhD Thesis, Leiden University, The Netherlands

ISBN: 9789051919974

Cover: Carlos Felipe Blanco

Layout: Carlos Felipe Blanco

Printing: UFB Grafisch Leiden University

Guiding safe and sustainable technological innovation under uncertainty

A case study of III-V/silicon photovoltaics

Proefschrift

ter verkrijging van
de graad van doctor aan de Universiteit Leiden,
op gezag van rector magnificus prof.dr.ir. H. Bijl,
volgens besluit van het college voor promoties
te verdedigen op donderdag 8 september 2022
klokke 10:00 uur
door
Carlos Felipe Blanco Rocha
geboren te Barranquilla, Colombia
in 1980

Promotores:	Prof. dr. ing. M.G. Vijver
	Prof. dr. ir. W.J.G.M. Peijnenburg
Copromotor:	Dr. S. Cucurachi

Promotiecommissie:	Prof. dr. A. Tukker
	Prof. dr. E. van der Voet
	Prof. dr. M.A.J. Huijbregts (Radboud Universiteit)
	Prof. dr. T.H.W. Bäck
	Dr. F. Dimroth (Fraunhofer Institute for Solar Energy Systems)
	Dr. P.A. Behrens

"Data-driven predictions can succeed – and they can fail. It is when we deny our role in the process that the odds of failure rise. Before we demand more of our data, we need to demand more of ourselves."

N. Silver, The Signal and the Noise (2020)

"In so far as the word 'knowledge' has any meaning, the world is knowable; but it is interpretable otherwise, it has no meaning behind it, but countless meanings."

F. Nietzche, The Will to Power (1910)

Table of Contents

Chapter 1

General introduction

1.1. Six decades of photovoltaic technological development

In 1876, William Grylls Adams and Richard Evans Day made an astounding discovery: a solid material, selenium, could generate electricity when exposed to light. Despite the far-reaching consequences of this discovery, it was not until 1954 that the first photovoltaic (PV) cell was created at Bell Laboratories in the United States. This primordial solar cell was made of silicon and had a conversion efficiency of 4% which was later raised to 11%. At a cost-per-watt nearly 600 times higher than that of coal power plants, Bell Laboratories' silicon cell found only limited applications in miniature ship and airplane models and portable radios.[1,2]

It was the space race of the 1960s that put the solar cell as a front-runner technology to power earth-orbiting satellites, where they easily outperformed competing chemical and nuclear power alternatives.[3] While cost was not a limiting factor to put solar cells in space, it presented a very difficult barrier to making them competitive back on Earth. Solar would have to wait until the next millennium to see an enormous drop in price, enough to make them a serious alternative for terrestrial applications (Figure 1-1).

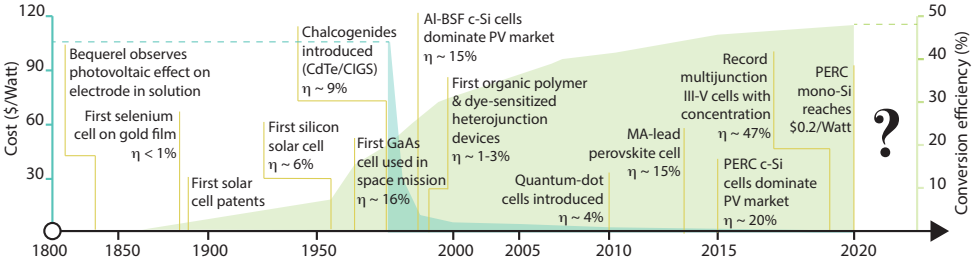

Figure 1-1 Timeline of developments in PV designs overlayed on increases in conversion efficiency and decrease in cost (in 2015 U.S. dollars). Sources: NREL[4], IEA[5].

1.2. A sunny future

There is almost no doubt that in the coming decades PV will take a leading role in energy systems across the world. Hundreds of PV growth projections have been proposed by leading experts from multiple disciplines, including the Intergovernmental Panel on Climate Change (IPCC), academic and research institutions, energy corporations, financial consultants, governments, and NGOs. The average of these projections for the compounded annual growth rate in global PV capacity deployment by the year 2050 is 10.6%, and the interquartile range is 8.6-13.6% for 1,488 scenarios evaluated (Figure 1-2).[6]

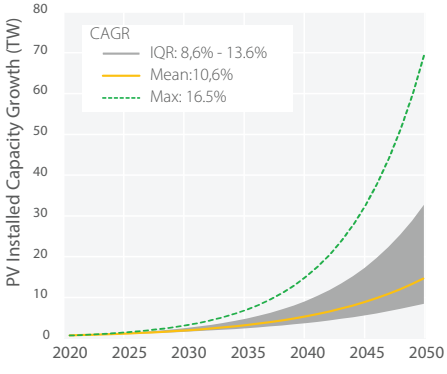

Figure 1-2 Global PV growth projections

The most optimistic scenarios see a total installed PV capacity of 70 TW by the year 2050 (and there is reason to look towards the most optimistic scenarios since most scenarios proposed to date have fallen short of actual PV growth[7]). Such a sharp increase in installed capacity could represent an impressive market share of 35% of the projected total primary energy demand. Taking an average panel conversion efficiency of 20% and a PV cell size of 156.75 x 156.75 mm, such a deployment could require 14 trillion PV cells to be installed on ca. 340 billion square meters of space (roughly 0.2% of the Earth's total land area). For a typical aluminium-glass framed PV panel weight of 11 kg/m^2, this translates to ca. 3.8 billion tonnes of installed materials, mostly glass and aluminium by weight.

1.3. Environmental benefits and trade-offs

For a long time, the environmental benefits of PV remained largely unquestioned. PV is emission-free during operation, which gives it a very strong advantage vs. combustion of fossil fuels that release carbon dioxide and methane as well as other toxic gases and particulate matter to the atmosphere. In addition to this, the PV cells and modules are mostly made of elements that have negligible adverse ecological effects when released into the environment. This means that even when landfilled at their end-of-life (EOL), PV modules are mostly inert. The massive success of the last decade and the expected growth in PV deployment, however, have evoked a closer look at potential environmental pitfalls. Insofar as conventional crystalline silicon cells (c-Si) go, these have been related to land use, the energy intensity of the silicon supply chain, and waste volumes.[8] Some additional concerns have been raised regarding the use of lead for the soldering of the PV module frames. And more recently, concerns have been raised regarding the availability/criticality of materials[9], with pure silicon being included in the EU list of critical raw materials along with other elements such as indium required in more recent PV technologies.

1.4. Multijunction III-V/silicon tandem solar cells

To date, c-Si cells have dominated the PV market due to the availability and stability of silicon and the decades of research and development (R&D) behind the technology. The current commercially available c-Si cells can convert energy from the sun with ca. 21% efficiency, while the record-holding lab prototype exceeded 26% in 2021.[4] The c-Si design has already capitalized from economies of scale (cumulative installed capacity in 2020 was 760 GW[10], provided by billions of panels) and the average cost of a c-Si module was US$0.20/W$_p$ in April 2020.[11] As marginal increases in c-Si efficiency now come at increasing manufacturing prices, c-Si's market dominance in the long term may be challenged if much higher efficiencies at smaller price premiums can be achieved by competing designs, leading to a lower cost per watt. Multijunction IIII-V/silicon tandem cells[12] (III-V/Si) is one emerging concept which combines c-Si bottom cells with top III-V layer absorbers to reach conversion efficiencies beyond c-Si's theoretical limit of 29.4%.[13] With significantly less time and resources invested in research and development, III-V/Si cell efficiencies above 35% have already been demonstrated at lab-scale.[14] If deployed at

large scale, III-V/Si could allow for significant savings of land area, material consumption and waste generation from PV systems.

From May 2017 until April 2021, the SiTaSol project consortium[15] led by Fraunhofer ISE, and including leading industrial partners and research institutes in the field of photovoltaics, worked on developing solutions to bring the high-efficiency but very high-cost III-V/Si technology closer to commercialization. SiTaSol sought to further develop processes which could eventually meet challenging cost targets in order to improve the economic feasibility of such solar cells at large scale. The key priorities of the project were the development of a new metalorganic vapour phase epitaxy (MOVPE) reactor with an efficient use of the precursor gases, enhanced waste treatment, recycling of metals and low-cost preparation of the c-Si growth substrate. The project consortium was also tasked with evaluating the environmental impacts and risks of the technology if it were deployed at large scale. The data generated within the SiTaSol R&D program were used to inform the assessments conducted in this thesis.

1.5. *Ex-ante* environmental assessment

As innovative PV designs such as III-V/Si strive to achieve lower cost-to-output ratios ($/kWh), they become increasingly complex by introducing new materials in different configurations for which the interactions with the environment are less well-known. And yet if an innovation in PV design achieves a competitive ratio, it has a higher chance of being introduced into the market at an accelerated rate. This means it will be propagated across very large-scale production, consumption, and recycling/disposal systems across the globe. Therefore, it is imperative to better understand the environmental implications of newer designs before these large-scale systems are deployed. Once these systems are in place, it is much more difficult to modify the technology's design. This dilemma has been clearly presented by Collingridge[16] and discussed by various authors in the context of sustainability[17–19] (see Figure 1-3 and Box 1-1).

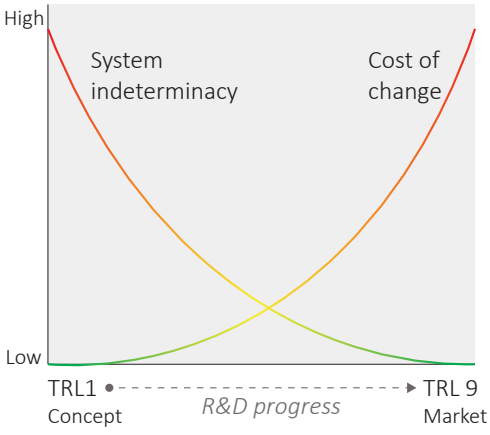

Figure 1-3 The Collingridge Dilemma (TRL: Technology Readiness Level)

In recent years, the recognition of the need for an *ex-ante* environmental assessment approach has shaped a growing sub-discipline with increasing numbers of publications and dedicated working groups across the U.S. and the European Union.[20] Perhaps the strongest backing for *ex-ante* assessments has come from the European Union, whose Horizon 2020 investment framework often requires them to grant funding for proposed R&D programs.

Several authors have attempted to provide methods or guidance frameworks for *ex-ante* assessment, particularly in LCA[21–24].

Box 1-1: Predicting the environmental performance of a future technology

The innovation process in many ways resembles the crossing of a fuzzy maze, where the pathways in close vicinity of the research topic are numerous but easily distingishable, while the ones farther away are also numerous but evolving in time and thus harder to anticipate (Figure 1-4). Developing a commercially successful technology requires extensive trial-and-error, and backward steps are commonplace. Furthermore, technologies are often made of different components which are developed separately and then have to work together. At the same time, extrinsic drivers in the socioeconomic and environmental landscapes evolve constantly, while also being determinant of the future environmental implications of the technology.

To illustrate this situation, we can think of a researcher who is trying to come up with a revolutionary design for the car of the future. At any point in time throughout the R&D process, the researcher will face many unknowns. Some of them will be intrinsic to the technology, e.g., will plutonium fuel be sufficiently stable? Or, what will be the consumption of plutonium per km? Others will be extrinsic, e.g., will the price of plutonium be too high in the future? Or, will the global reserves of plutonium deplete and make the technology non-viable? Will social concerns or environmental regulations become too strict for radioactive fuels in commercial vehicles? A technology that enters the R&D process at TRL 1 will be subject to many changes by the time it enters the market at TRL 9. These changes are likely to have profound implications on the environmental performance of the technology. The decision of when, and under which assumptions to make an *ex-ante* assessment such as an LCA or a risk assessment (RA) is not trivial.

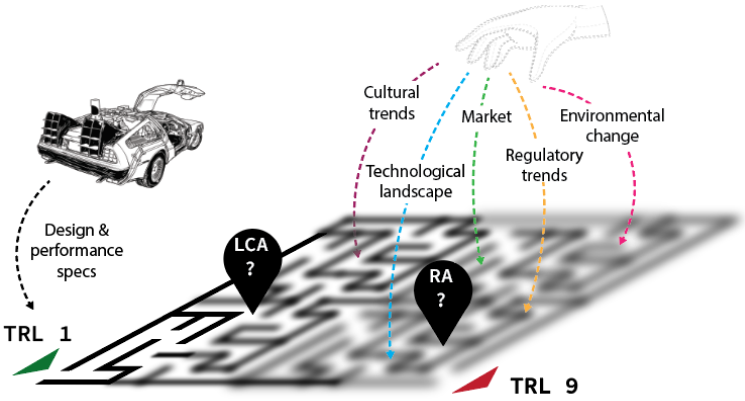

Figure 1-4 The dynamic and uncertain journey of an R&D project

On the central question of how to forecast the evolving and not fully-known future technological configurations and their behaviour in the environment, few of these proposals have placed quantitative uncertainty analysis and global sensitivity analysis[25] (GSA) at the centre of the frameworks.* Rather they have largely relied on scenario analysis and technological roadmaps[26] to explore the implications of different possible futures. One

* Throughout this work we will generally refer to uncertainty as it is considered in the modeling domain. Uncertainty is then an expression of model indeterminacy[29]. Saltelli at al.[25] define uncertainty analysis as "quantifying uncertainty in model output", and sensitivity analysis as "the study of how uncertainty in the output of a model (numerical or otherwise) can be apportioned to different sources of uncertainty in the model input".

noteworthy exception is the work of Ravikumar et al.[27], who proposed the use of GSA to guide prioritization of research in "anticipatory" LCA. In the subsequent chapters of this thesis, uncertainty and sensitivity analysis take an increasingly important role until it they are placed at the centre of the *ex-ante* exercise. As will be demonstrated towards the end of this work, this will expand the capabilities of *ex-ante* assessments, enabling them to answer different questions that can better guide the R&D processes towards safer and more sustainable designs.

1.6. Research aim

The aim of this research is two-fold. On the one hand, it investigates the emerging III-V/Si cell design and the production-consumption systems in which it would be embedded, in order to determine the potential environmental impacts and risks the technology may pose when deployed at a large scale. On the other hand, it adapts and further develops existing *ex-ante* environmental assessment methods to make them more suitable to provide early guidance for the sustainable and safe design of emerging technologies. Five main research questions are posed and answered in this study:

I. What are the environmental hotspots in the emerging PV technologies landscape and what is the magnitude of the variabilities in the life cycle impacts?

II. What are the life-cycle environmental impacts of III-V/Si cells compared to c-Si cells and what are the key opportunities for improvement?

III. What are the potential ecological risks introduced by III-V/Si cells throughout their life cycles?

IV. How can unresolved technological pathways in the development of III-V/Si cells be incorporated in *ex-ante* environmental assessments?

V. How can uncertainty analysis and global sensitivity analysis be used to prioritize research directions towards safer and more sustainable design of III-V/Si tandem technologies?

1.7. Outline of this thesis

Chapter 2 takes a high-level look at the environmental performance of the emerging PV landscape by conducting a systematic review and meta-analysis of LCAs of emerging PV designs. The analysis identifies environmental hotspots and trends across the different technology types and evaluates the magnitude of the variabilities in different impact scores compared to the incumbent silicon PV modules. As the title indicates, the main question answered is whether research and innovation in PV are heading in a positive direction in terms of life cycle environmental impacts. Chapter 2 also introduces an exploratory methodological novelty in that a Random Effects Model[28] is adapted and applied to a meta-analysis of LCA studies. To adapt the model we considered the incumbent technology (c-Si) as the control group, and the emerging PV technologies as the intervention group. Design innovations such as the incorporation of different absorbent

materials (e.g. perovskites, III-V elements, CdTe) are thus seen as "interventions" that can influence the life cycle impact score of PV electricity. The model allows an investigation of variation in the effect of interventions within and between studies and technology types.

Chapter 3 focuses on the III-V/Si technology and conducts an LCA with a high level of resolution. Primary data obtained from lab and pilot tests within the SiTaSol project are used and extrapolated in a first attempt to resemble industrial-scale production as much as possible. A local sensitivity analysis is used to explore the implications of future improvements in the key contributing processes such as MOVPE energy efficiency, hazardous waste treatment and recycling, as well as changes in the background energy supply.

Chapter 4 addresses perhaps the most important learning from the first full-scale LCA conducted in Chapter 3: the unresolved design choices and unknown background system parameters are too numerous so that they cannot be solved and interpreted adequately with a local sensitivity analysis or scenario analysis. While parametric uncertainty (e.g., in the energy consumption of a manufacturing process) can be easily propagated in LCA models, scenario uncertainty (e.g., whether one material or manufacturing method is chosen over another for a given component) is more challenging. We demonstrate how this problem can be overcome by introducing binomial and multinomially distributed factors in the model, which can trigger discrete events stochastically based on their expected chances of success. This allows combining an unlimited number of technological choices or pathways in a single analysis and propagating this uncertainty of process or material selection along with other parametric uncertainties.

GSA is then used to understand which of the uncertain factors contribute the most to uncertainty in the impact scores. Here, two additional novelties are introduced; for the first time, GSA is applied to such a high-dimensional model with tens of thousands of uncertain model inputs (including uncertainty in the background LCA database). This is made possible by introducing a pre-filtering step which leaves non-contributing flows out of the analysis. Second, GSA is applied for the first time to a full-scale LCA model that combines parametric with scenario uncertainties. While the analysis focuses on one component of the technology (the front metal contacts of the PV cell), it establishes the building blocks for a straightforward extrapolation to larger systems and to other types of technologies.

Chapter 5 takes the insights from the technology and the methods obtained in Chapters 3 and 4 and applies them to a different framework, that of ecological risk assessment. Chapter 5 sets out to answer what is seemingly a simple question -*what are the risks posed by III-V material emissions from III-V/silicon tandem PV modules throughout their life cycles?* However, as the common phrase goes, "the dose makes the poison". To understand what the dose is, an integration of mass flow analysis with fate and exposure assessment models is required. Furthermore, these models must be probabilistic, prospective, and dynamic to appropriately reflect the ecological risks that may be potentially introduced by the technology. Compared to LCA models, risk assessment models are more sensitive to

temporal and spatial determinations which introduce an even broader range of uncertainties and variabilities. Risk assessment thus presents a more demanding test for the applicability and usefulness of the uncertainty analysis and global sensitivity analysis methods proposed in previous chapters.

Chapter 6 lays out a framework that encompasses all the methodological developments of the previous chapters, placing quantitative uncertainty analysis and global sensitivity analysis at the forefront of *ex-ante* assessment, and presenting its full potential towards guiding safer and more sustainable technological designs. Having understood the diversity and magnitude of uncertainties and variabilities that can be encountered, it is also recognized that most of the data required to characterize these uncertainties will be unavailable. A Bayesian approach to probability is presented as the most suitable one for defining and characterizing uncertainty, given the largely subjective nature and reliance on expert knowledge. The Bayesian approach completes the puzzle by providing tools and mathematical underpinning to the characterization of uncertainty and its updating with subsequent iterations that fit very naturally the R&D process.

References

1. U.S. Patent and Trademark Office. A Brief History of Solar Panels. *Smithsonian Magazine*.
2. Green, M. A. Silicon photovoltaic modules: a brief history of the first 50 years. *Prog. Photovoltaics Res. Appl.* **13**, 447–455 (2005).
3. Perlin, J. *From space to earth: The story of solar electricity*. (Harvard University Press, 2002).
4. Green, M. A., Dunlop, E. D., Hohl-Ebinger, J., Yoshita, M., Kopidakis, N., & Hao, X. (2022). Solar cell efficiency tables (version 59). *Progress in Photovoltaics: Research and Applications*, **30**(1), 3–12.
5. IEA. Evolution of solar PV module cost by data source, 1970-2020.
6. Jaxa-Rozen, M. & Trutnevyte, E. Sources of uncertainty in long-term global scenarios of solar photovoltaic technology. *Nat. Clim. Chang.* **11**, 266–273 (2021).
7. Ives, M. C. *et al. A new perspective on decarbonising the global energy system*. https://site.energychallenge.info/report/ (2021).
8. Tawalbeh, M. *et al.* Environmental impacts of solar photovoltaic systems: A critical review of recent progress and future outlook. *Sci. Total Environ.* **759**, 143528 (2021).
9. IEA. *The Role of Critical Minerals in Clean Energy Transitions*. (2021).
10. IEA-PVPS. *Snapshot of Global PV Markets 2021*. https://iea-pvps.org/snapshot-reports/snapshot-2021/ (2021).
11. Benda, V. & Černá, L. PV cells and modules – State of the art, limits and trends. *Heliyon* **6**, e05666 (2020).
12. Cariou, R. *et al.* III-V-on-silicon solar cells reaching 33% photoconversion efficiency in two-terminal configuration. *Nat. Energy* **3**, 326–333 (2018).
13. Ehrler, B. *et al.* Photovoltaics Reaching for the Shockley–Queisser Limit. *ACS Energy Lett.* **5**, 3029–3033 (2020).
14. Essig, S. *et al.* Raising the one-sun conversion efficiency of III-V/Si solar cells to 32.8% for two junctions and 35.9% for three junctions. *Nat. Energy* **2**, 17144 (2017).
15. Fraunhofer ISE. SiTaSol: Application relevant validation of c-Si based tandem solar cell processes. https://sitasol.com/.
16. Collingridge, D. *The social control of technology*. (Frances Pinter, 1980).
17. Villares, M., Işıldar, A., van der Giesen, C. & Guinée, J. Does ex ante application enhance the usefulness of LCA? A case study on an emerging technology for metal recovery from e-waste. *Int. J. Life Cycle Assess.* 1–16 (2017) doi:10.1007/s11367-017-1270-6.

18. Hetherington, A. C., Borrion, A. L., Griffiths, O. G. & McManus, M. C. Use of LCA as a development tool within early research: Challenges and issues across different sectors. *Int. J. Life Cycle Assess.* **19**, 130–143 (2014).

19. van der Giesen, C., Cucurachi, S., Guinée, J., Kramer, G. J. & Tukker, A. A critical view on the current application of LCA for new technologies and recommendations for improved practice. *J. Clean. Prod.* **259**, 120904 (2020).

20. Cucurachi, S., van der Giesen, C. & Guinee, J. Ex-ante LCA of emerging technologies. *CIRP Procedia* (2018).

21. Tsoy, N., Steubing, B., van der Giesen, C. & Guinée, J. Upscaling methods used in ex ante life cycle assessment of emerging technologies: a review. *Int. J. Life Cycle Assess.* **25**, 1680–1692 (2020).

22. van der Giesen, C., Cucurachi, S., Guinée, J., Kramer, G. J. & Tukker, A. A critical view on the current application of LCA for new technologies and recommendations for improved practice. *J. Clean. Prod.* **259**, (2020).

23. Thonemann, N., Schulte, A. & Maga, D. How to conduct prospective life cycle assessment for emerging technologies? A systematic review and methodological guidance. *Sustainability (Switzerland)* vol. 12 (2020).

24. Buyle, M., Audenaert, A., Billen, P., Boonen, K. & Van Passel, S. The future of ex-ante LCA? Lessons learned and practical recommendations. *Sustain.* **11**, 1–24 (2019).

25. Saltelli, A. *et al. Global Sensitivity Analysis. The Primer. Global Sensitivity Analysis. The Primer* (John Wiley and Sons, 2008). doi:10.1002/9780470725184.

26. Wright, G., Cairns, G. & Bradfield, R. Scenario methodology: New developments in theory and practice. *Technol. Forecast. Soc. Change* **80**, 561–565 (2013).

27. Ravikumar, D., Seager, T. P., Cucurachi, S., Prado, V. & Mutel, C. Novel Method of Sensitivity Analysis Improves the Prioritization of Research in Anticipatory Life Cycle Assessment of Emerging Technologies. *Environ. Sci. Technol.* **52**, 6534–6543 (2018).

28. Hedges, L. V. Meta-Analysis. *J. Educ. Stat.* **17**, 279–296 (1992).

29. Oreskes, N., Shrader-Frechette, K. & Belitz, K. Verification, Validation, and Confirmation of Numerical Models in the Earth Sciences. *Science (80-.).* **263**, 641–646 (1994).

Chapter 2

Are technological developments improving the environmental sustainability of photovoltaic electricity?

Abstract

Innovation in photovoltaics (PV) is mostly driven by the cost per kilowatt ratio, making it easy to overlook environmental impacts of technological enhancements during early research and development stages. As PV technology developers introduce novel materials and manufacturing methods, the well-studied environmental profile of conventional silicon-based PV may change considerably. Herein, existing trends and hotspots across different types of emerging PV technologies are investigated through a systematic review and meta-analysis of life-cycle assessments (LCAs). To incorporate as many data points as possible, a comprehensive harmonization procedure is applied, producing over 600 impact data points for organic, perovskite (PK), dye-sensitized, tandem, silicon, and other thin-film cells. How the panel and balance of system components affect environmental footprints in comparable installations is also investigated and discussed. Despite the large uncertainties and variabilities in the underlying LCA data and models, the harmonized results show clear positive trends across the sector. Seven potential hotspots are identified for specific PV technologies and impact categories. The analysis offers a high-level guidance for technology developers to avoid introducing undesired environmental trade-offs as they advance to make PV more competitive in the energy markets.

Keywords: environmental impacts, life-cycle assessments, photovoltaics, solar, sustainability

This chapter has been published as: Blanco, C.F., Cucurachi, S., Peijnenburg, W.J.G.M., Beames, A. and Vijver, M.G. (2020). Are Technological Developments Improving the Environmental Sustainability of Photovoltaic Electricity? Energy Technol., 8: 1901064. https://doi.org/10.1002/ente.201901064

2.1. Introduction

Since the introduction of the first solar cell in the early 1950's, the market share of photovoltaic electricity (PV) has expanded exponentially and it is now the fastest growing source of renewable energy.[1] PV was quickly embraced as a clean albeit expensive source of energy, yet today it can compete with conventional fossil-fuel based sources purely on economic grounds.[2] In an effort to drive this advantage even further, many technological enhancements are being pursued to either reduce manufacturing costs or to increase the PV cells' conversion efficiencies.[3] However, as the focus narrows on cost and conversion efficiency, awareness has risen to place equal importance on the potential environmental trade-offs that technological innovations in PV may introduce.

Improving efficiency and lowering costs of PV cells presents technology developers with many technical barriers. Developers have often addressed these barriers by incorporating new materials and modifying cell architectures, spawning numerous alternative cell designs. Technological enhancements aim to increase the light-absorption capacity of the cells, increase conductivity, or replace existing materials of the cell for cheaper ones that fulfil the same function. For example, several thin film technologies completely replaced silicon - a non-toxic and highly abundant material - while aiming for cost reductions. Changes in manufacturing methods may also alter the environmental profile of the PV industry, as they can require more complex equipment and energy-demanding processes. The technological enhancement and diversification are going at a fast pace, making it difficult for relevant stakeholders to keep track of and manage the long-term environmental impacts of successful PV innovations that may disseminate very quickly.

The earlier the stage of development of the technology, the harder it is to produce a realistic assessment of the environmental impacts once it is implemented at commercial scale.[4] But an early assessment is all the more important, given the fact that design changes are easier to make during earlier R&D stages.[5] Stamford & Azapagic made a first step in this direction by assessing the environmental impacts of recent technological improvements of silicon-based PV.[6] However, this was still a retrospective assessment of technological improvements that had already penetrated the market. It was also limited to the currently dominating silicon-based PV systems and did not investigate the technologies that are competing to replace them. Chatzisideris et al.[7] investigated more recent technologies, yet their analysis was based on limited quantitative data prior to 2015 and numerous studies have been published since then.

In this study, we adopt a more prospective and comprehensive approach by assessing the emerging PV technologies that may dominate in the next 10 or more years. Our aim is to discern whether the PV industry is moving forward in terms of environmental sustainability as it develops towards lower costs and/or higher efficiencies. For this, we conduct a systematic review and harmonization of life cycle assessment (LCA) studies of current state-of-the-art and emerging PV. We then apply a novel method to conduct a statistical meta-analysis on the harmonized data. We address 5 specific questions: (i) what –if any-

are the observable trends in the environmental impacts of each type of PV technology; (ii) what the variability of impact scores is within and across different PV technologies; (iii) what the effects are, if any, of technological advances on environmental performance; (iv) how the environmental impacts compare across technology types and across different stages of technological maturity, and (v) which potential hotspots can be anticipated by comparing the relative contributions to impacts from different elements of the PV technologies. Our analysis is meant to ultimately provide valuable guidance for PV technology developers, policymakers and other stakeholders so that they can factor in environmental sustainability considerations during the early R&D stages.

2.2. Methods

2.2.1. Classification of PV technologies

For our analysis we classified the emerging PV technologies as shown in Table 2-1, adapting definitions from Green et al.[8] and NREL[9]. Some of these technologies were already introduced in the market, such as thin-film cadmium telluride (CdTe). Others have been limited to niche applications, implemented only as pilots, or are still in development phase. The table also shows the advantages and disadvantages that have been reported in various literature sources[10,11] for each technology in terms of efficiency, cost and environmental aspects.

2.2.2. Assessment framework and meta-analysis approach

Life cycle assessment (LCA) is a commonly used framework to assess sustainability aspects of emerging technologies, as it provides a holistic accounting of environmental impacts throughout a product's entire life cycle.[12] This holistic approach ensures that environmental trade-offs are identified and quantified, and that new technologies do not result in environmental burdens larger than those of the incumbent technology.[13] We conducted a systematic review and meta-analysis of LCA studies of state-of-the-art and emerging PV by following the guiding principles for meta-analyses contained in the PRISMA statement (Preferred Reporting Items for Systematic Reviews and Meta-Analyses).[14] First we identified potentially relevant publications since 2010 using the Web of Science® tool[15] and the Google Scholar search tool. Then we screened and filtered the results according to the criteria described in section 2.2.3. In a final step we harmonized the quantitative LCA results from the eligible studies, adapting and significantly extending the harmonization approach proposed by the NREL Life Cycle Assessment Harmonization Project (section 2.2.4).[16,17]

Table 2-1. Classification and characteristics of PV technologies and cell types assessed

PV technology	Cell types	Advantages	Shortcomings	PV technology
Silicon	single-Si; multi-Si	Non-toxic; high efficiencies; long-term stability; abundant materials	Energy intensive; high cost	Silicon
Thin-film silicon	amorphous silicon (a-Si); micro-Si (μ-Si);	Low cost; less materials; non-toxic	Low efficiency	Thin-film silicon
Thin-film chalcogenide	Cadmium telluride (CdTe); CIGS, CZTS,	Less materials; low cost; high efficiencies	Critical materials; toxicity of Cd	Thin-film chalcogenide
Dye-sensitized (DSSC)	Ruthenium complex sensitizers; organic dyes	Low cost; flexible; non-toxic; ease of fabrication; ability to operate in diffuse light[38]	Temperature sensitivity of liquid electrolyte; low efficiency[38]	Dye-sensitized (DSSC)
Organic (OPV)	Polymer; Single-wall carbon nanotube (SWCNT)	Low cost; flexible; lightweight; non-toxic; ease of fabrication; can be tailored for application	Stability (short lifetime); low efficiency	Organic (OPV)
Perovskite (PK)	Lead halide, Tin halide	Low cost; flexible; lightweight; ease of fabrication; high efficiencies	Stability (short lifetime); toxicity of lead	Perovskite (PK)
III-V	Gallium arsenide (GaAs)	High efficiency	High cost; material scarcity; toxicity of As	III-V
Quantum dot	Cadmium selenide (CdSe)	High efficiency (potential)	Toxicity of Cd; high cost	Quantum dot
Tandem/hybrid	Silicon HJ; III-V/Si; PK/Si; TF/TF; TF/PK	High efficiency	Expensive; material scarcity; toxicity of As	Tandem/hybrid

2.2.3. Identification, screening and selection of studies

To identify LCA studies of PVs, we searched three different sources. First, we searched the Web of Knowledge® database using the following search strings:

> *(TS=((LCA OR (life cycle assessment OR (life-cycle assessment OR (life-cycle analysis OR life cycle analysis)))) AND (solar OR (photovoltaic* OR PV)))) AND LANGUAGE: (English) AND DOCUMENT TYPES: (Article) Timespan: 2010-2019. Indexes: SCI-EXPANDED, SSCI, A&HCI, ESCI.*

(TI = ((LCA OR (life cycle assessment OR life-cycle assessment)) AND (photovoltaics OR (solar AND cells)))) AND LANGUAGE: (English) AND DOCUMENT TYPES: (Article) Timespan: 2010-2019. Indexes: SCI-EXPANDED, SSCI, A&HCI, ESCI.

A second source was the Google Scholar search tool, where we searched for similar search strings and compared the first 1000 hits to the results obtained in the Web of Knowledge. A third source was the cross-references in the reviewed articles that were not identified in the previous steps. We then screened these results to exclude those with: (i) repeated results from previous work; (ii) focused on a specific geographical implementation; (iii) did not use a PV cell or panel (m^2) or generation of electricity with a PV system (kWh) as the basis for the assessment (functional unit) (see section 2.2.4.1); (iv) did not use own data and/or calculations for the technological system; and (v) assessed PV cells integrated on other devices.

From the screened studies we selected for inclusion only those studies, in which the data provided allowed for the harmonization steps described in section 2.2.4. The full list of included and excluded studies is provided in the Appendix Table A.1-1.

2.2.4. Harmonization

2.2.4.1. Functional unit

We chose the generation of 1 kWh of electricity as a comparative basis (i.e. functional unit in LCA[18]) for the meta-analysis. This functional unit is used frequently in LCA studies of PV electricity generation[19], and accounts for technological advantages or disadvantages from the cell technology that translate to the ancillary PV infrastructure. For example, cells with higher efficiencies require less area to produce 1 kWh. Therefore, they also require smaller infrastructures and correspondingly less materials for the installation. However, many relevant studies reported impacts for a unit area of cell, typically 1 m2. In order to harmonize these units, we calculated the equivalent area required to produce 1 kWh as indicated in Equation 2-1.[20]

$$A = \varepsilon/(\eta \cdot r \cdot PR \cdot LT) \qquad \text{(Eq. 2-1)}$$

Where $\boldsymbol{\varepsilon}$ is electricity output of the PV system (1 kWh), A is the total solar panel area (m^2), η is the solar panel efficiency (%), r is the annual average solar radiation on panels (measured in $kWh{\cdot}year^{-1}{\cdot}m^{-2}$), PR is the performance ratio (i.e., a coefficient that adjusts for conversion losses), and LT is the lifetime of the PV system.

Most LCA studies for PV converge on values of PR = 0.75 and solar radiation = 1700 kWh/m^2, representative of southern Europe and close to the world average, respectively. The panel efficiencies η vary depending on each cell technology. Additional efficiency losses occur when the cells are incorporated into the panels due to the small separations between the cells. Therefore, whenever cell efficiencies were reported instead of panel efficiencies we subtracted 2% to account for these area losses, following the approach of Louwen et al.[21]

Some studies reported electricity output in kWh, but for different operating conditions than the typical ones assumed for Equation 2-1. Adjustments to the impact scores were made according to the proportional difference in the parameters radiation and performance ratio. O'Donoghue et al.[22] refer to this kind of adjustment as *proportional adjustment*, where the adjusting factor is the ratio of the parameter value in the study to the intended harmonized parameter value. This adjustment is possible because usually more than 99% of the total impacts of renewable electricity generation is embedded in the infrastructure, which is represented by the area parameter in Equation 2-1. Following the method of Asdrubali et al.[23] for harmonization in renewables, we combined the three parameter adjustments into a single formula to calculate the harmonized impact scores (Equation 2-2).

$$D_i harm = D_i pub \cdot \frac{r_{pub} \cdot PR_{pub} \cdot LT_{pub}}{r_{harm} \cdot PR_{harm} \cdot LT_{harm}} \quad \text{(Eq. 2-2)}$$

$D_i harm$ is the harmonized impact score, $D_i pub$ is the reported impact score, r_{pub} is the solar radiation assumed in the study, PR_{pub} is the performance ration assumed in the study, LT_{pub} is the lifetime of PV system in the study, r_{harm} is the average solar radiation in southern Europe (1700 kWh/m^2), PR_{harm} is the average performance ratio of 75% and LT_{harm} is the average lifetime. We set a 30 years lifetime for the harmonized value of all PV systems except for perovskites and organic PV, which have many technical barriers to long-term stability. Meng et al.[24] and Cai et al.[25] assess that perovskites may need lifetimes of 15 years to achieve lower costs per kWh than traditional energy sources. However, it is not yet clear what the maximum achievable lifetime of perovskites is. Therefore, we adopt 15 years as a conservative lifetime under the assumption that once the technology becomes cost-competitive the efforts to extend the related lifetime may even slow down further.

2.2.4.2. System boundaries

We also harmonized system boundaries by ensuring that the same life-cycle stages and comparable unit processes were considered across all technologies. For this, we divided the life-cycle inventories of each technology into four broad life-cycle phases: (1) material extraction and assembly of PV cell, (2) material extraction and assembly of panel components; (3) material extraction and assembly of balance-of-system (BOS) components; (4) electricity generation, and (5) end-of-life (EOL) including decommissioning, recycling and/or final disposal. Within these system boundaries, the least common denominator was established as all life-cycle stages up to electricity generation. When necessary, unit processes were excluded, and impact scores were recalculated by subtracting the corresponding contributions. We calculated panel (2) and BOS (3) components separately and added them proportionally in relation to the required area of the installation. The amount of installation required is calculated in ecoinvent[26] as indicated in Equation 2-3.

$$Q_{inst} = \frac{1\ kWh}{LT \cdot Capacity \cdot Yield} \quad \text{(Eq. 2-3)}$$

Based on ecoinvent data for a single-Si slanted-roof installation, Q_{inst} = 1.158E-5 installations are required for the generation of 1 kWh. The yield is proportional to the efficiency of the solar module, therefore we adjusted Q_{inst} in each case by a factor calculated as in Equation 2-4 and added the corresponding impacts for the adjusted area of installation, as follows:

$$\frac{\eta_{si}}{\eta_{em}} \qquad \text{(Eq. 2-4)}$$

In Equation 2-4, η_{si} is the efficiency of the single-Si solar module from ecoinvent, i.e. 13.6%, and η_{em} is the efficiency of the assessed PV technology in each case.

An exception to this proportional adjustment was the inverter, which scales with power and not with area or efficiency. Therefore, the quantity of inverter required for generating 1 kWh was kept constant across all systems. This quantity was calculated as indicated in Equation 2-5.

$$Q_i = \frac{1\ kWh}{P \cdot S \cdot 365 \cdot LT} = 2.2E-5\ units \qquad \text{(Eq. 2-5)}$$

Qi is the amount of inverter units required to generate 1 kWh, P is the power rating of the modelled inverter (2.5 kW/unit), S is the equivalent amount of sunlight hours for the Southern European location (5 hours/day), 365 is the number of days in a year, and LT is the average lifetime of an inverter (10 years). Individual life-cycle inventories for BOS and panel components were updated to reflect the changes proposed by the International Energy Agency PVPS 2015 report.[27]

2.2.4.3. Impact assessment methods

In order to assess impacts in LCA, characterization factors must be used which translate environmental emissions into different types of impacts[28]. Different methods have been proposed to estimate these, and they can use different indicators and units for such. For example, the CML method[13] expresses toxicity impacts in units of kg 1-4 dichlorobenzene equivalents, while the USEtox method[29] uses comparative toxicity units (CTUs). Therefore, we converted all results to the units used by the reference impact assessment methods recommended by the European Commission in the International Reference Life Cycle Data System (ILCD).[30] For some impact categories, conversions are relatively straightforward and can be achieved by a constant factor with acceptable accuracy. In other cases, such as toxicity and resource depletion, the modelling behind each indicator is considerably different across characterization methods. This results in conversion factors that could vary across several orders of magnitude for different product systems, making harmonization of impact indicators impracticable. However, we are mainly focused on the relative change of environmental profile of the emerging PV technology relative to the dominating crystalline silicon systems in 2010. Therefore, we consider it appropriate to approximate these conversion factors according to Equation 2-6.

$$Ie_{ILCD} = \frac{Ir_{ILCD}}{Ir_x} \cdot Ie_x \quad \text{(Eq. 2-6)}$$

The result gives a consistent idea of how much better or worse each system is compared to the reference crystalline silicon system. The resulting conversion factors for each impact category are provided in the Appendix Table A.1-2. In Equation 2-6, Ie_{ILCD} is the impact score of the emerging technology in harmonized ILCD units; Ie_x is the impact score of the emerging technology in the units of the original methodology used by the study; Ir_x is the impact score of a reference single-Si PV system (as modelled in ecoinvent v3.4)[26] in the units of the impact assessment methodology used by the study, and Ir_{ILCD} is the impact score of the reference single-Si PV system in ILCD units.

A flowchart describing the full identification, screening, selection and harmonization process is provided in Appendix Figure A.1-1.

2.2.5. Statistical analysis

In order to discern trends in time, we used linear regression models and Pearson correlation coefficients for impact scores as a function of time (i.e. year in which technology developers firstly describe the PV cell design in literature). Louwen et al.[31] investigated exponential learning curves to assess the greenhouse gas emissions of silicon-based PV over a period of 40 years. However, there is still scant supporting evidence for the existence of such curves for the data at hand in the current study. Furthermore, our interest is not to predict but rather to observe whether the trends exist and if so, whether they are positive or negative.

To investigate the effects of technological development on the environmental performance of PV systems, we used a random effects model.[32,33] Random effects models commonly applied in meta-analyses require the definition of an experimental group (i.e. the population of individuals exposed to a certain treatment), and of a control group (i.e. the population of individuals not exposed to the treatment). Effects are, then, estimated comparing the outcome of the treatment across studies using effect size metrics, such as odds ratios, correlation coefficients, and standardized mean differences.[32,33] We framed our case such that the commercially established single and multi-crystalline PV systems served as a *pseudo*-control group, using the harmonized data compiled from the meta-analysis by Hsu et al. of the National Renewable Energy Laboratory and the Brookhaven National Laboratory.[17] The data in these studies refers to commercial PV systems assessed in the years 2000 to 2008. We defined as *pseudo*-experimental groups the emerging PV technologies assessed in the years 2010 to 2019 (see Appendix Table A.1-1). We consider the diverse technological enhancements as the treatments performed on the experimental groups. The effects of the technological enhancements were interpreted as the changes in the standardized mean differences (SMD)[34] in impact scores. The SMD is equivalent to the difference in mean score between the emerging PV technology and the reference PV system, divided by the standard deviation of the scores. To get a sufficiently large population (N) for each group, we grouped results by PV technology type, rather than by

study. This is admittedly a departure from convention in meta-analysis but is –to an extent- reasonable insofar as the harmonization is comprehensive enough.

2.3. Results and discussion

2.3.1. LCA studies and data points identified and selected

A total of 1024 potential LCA studies were identified in the Web of Knowledge database and Google Scholar. The screening process resulted in 85 studies, of which 40 resulted eligible for the quantitative synthesis. These 40 studies produced 682 data points (LCA impact scores), distributed as shown in Figure 2-1. The studies were produced by 28 lead authors and published in 18 different peer-reviewed journals. As shown in Figure 2-2, the majority of the studies were related to perovskites and thin films. The eligible contributions in the year 2018 doubled those from the next most productive year (2011).

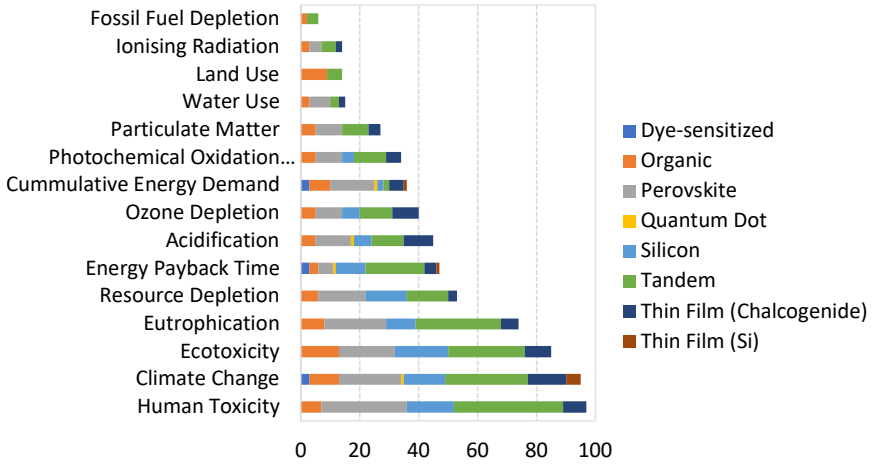

Figure 2-1 Number of impact indicators considered for different PV technologies, 2010-1019.

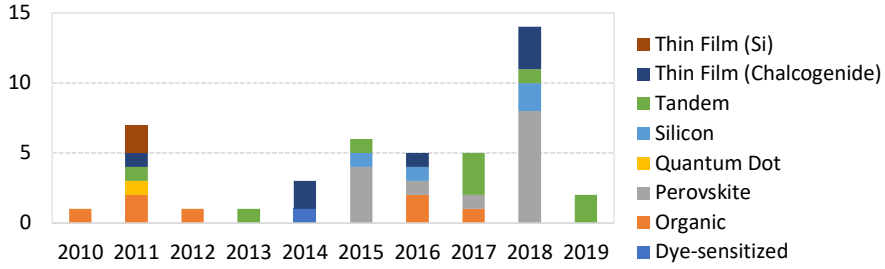

Figure 2-2 Number of LCA studies selected for different PV technologies, 2010-1019.

2.3.2. Trends per technology type

Figure 2-3 shows the impact scores for each of the ILCD impact categories classified by PV technology type and maturity, as a function of the year in which the cell design was introduced. A first important insight can be obtained from looking at the Y scales, which provide both maximum and minimum values as well as an idea of the variability of the scores reported. Most impact scores are within an order of magnitude despite differences in modelling and cell designs. It can be observed that there is no clear trend in time, and the steeper slopes are only present for technology and impact type combinations with few data points. Of the impact-cell type subgroups with more than 10 data points, only four trends with strong correlations were detected. Tandem cells showed a strong positive correlation (increasing impact) with respect to resource depletion and photochemical oxidation, and a strong negative correlation with respect to ozone depletion. The former may be explained by the increased use of transparent conductive oxides in tandem cell manufacturing. Full results of the regression calculations are provided in Appendix Table A.1-3.

For climate change impacts, the scores appear to be stabilizing towards <0.03 kg CO_2 eq. Here, thin-film silicon and chalcogenides appear to perform remarkably well, most likely due to a good balance between conversion efficiency, low material requirements and replacement of energy intensive silicon. A predominance of green data points (perovskites) can be observed on top, suggesting an overall larger footprint for this technology type. On the other hand, state-of-the-art versions of silicon-based technologies are amongst the most competitive from an environmental perspective.

2.3.3. Variability of impact scores

When compared to a single-Si rooftop PV system as a reference (as modelled in ecoinvent v3.4[26]), the relative impacts of all technologies aggregated fell within a factor of 2 (where single-Si = 1, see Figure 2-4). The only exception to this was the category of marine eutrophication. This holds for the 75th percentile in 13 out of 14 ILCD impact categories when outliers were removed (outlier values are considered any values over 1.5 times the interquartile range over the 75th percentile or any values under 1.5 times the interquartile range under the 25th percentile). None of the medians exceed that of the reference system, and 10 categories fall under 1.5 for a 75th percentile. Considering most of the emerging PV systems were assessed based on lab-scale designs that are not representing optimized industrial-scale processes, the landscape looks positive as long as upscaling to industrial scale is reflected in further material and energy optimization.

A closer look at the distribution of scores per technology type is presented in Figure 2-5, for the impact categories with most data points. Perovskites show the largest variability. An interesting thing to note is the apparently lognormal shape of the distributions. In the case of freshwater eutrophication, the normal shaped curved is on a logarithmic x-axis, which also suggests a lognormal distribution for this category. Lognormal distributions are often found in the probabilistic impact scores of individual systems, but we had no reason

to assume the same type of distribution for meta-analyses across different systems. We used the geometric means and standard deviations to summarise the data, which are better suited for skewed distributions (Table 2-2).[35]

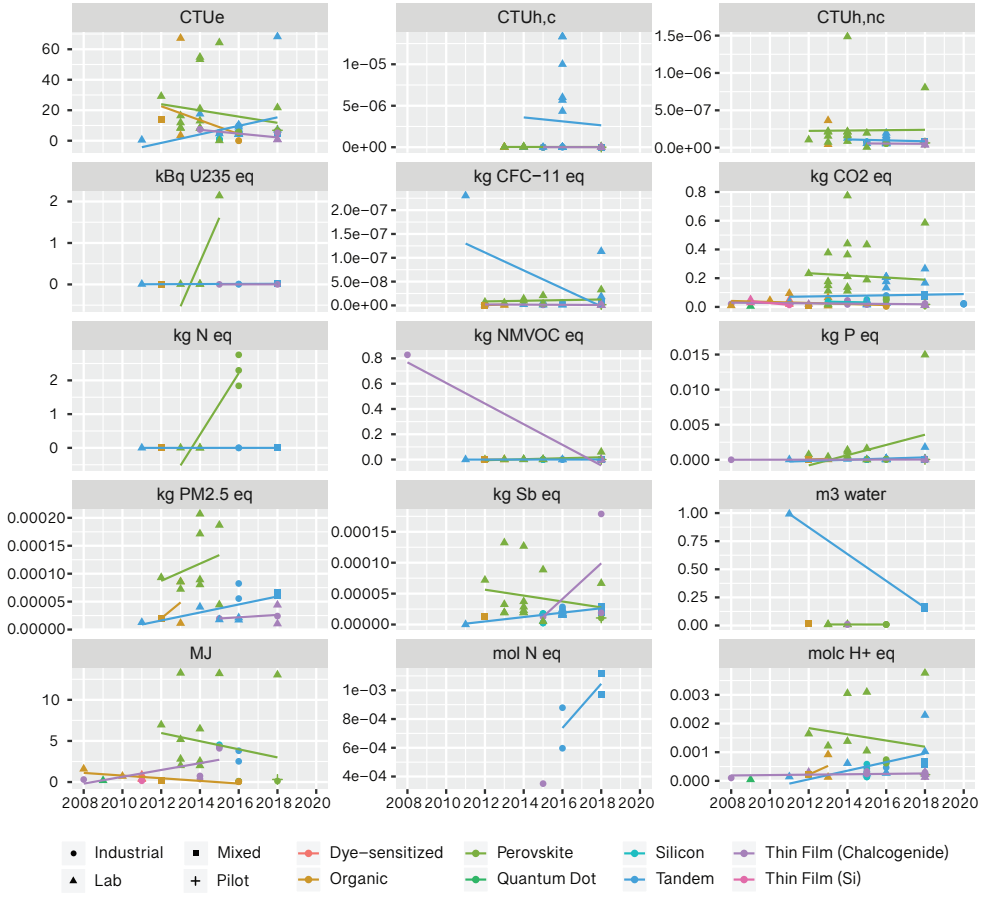

Figure 2-3 Harmonized LCA impact scores of PV technologies as a function of time. CTUe: freshwater ecotoxicity; CTUh,c: human toxicity – cancer effects; CTUh,nc: human toxicity – non-cancer effects; kg CFC-11 eq: ozone depletion; kg CO2 eq: climate change; kg N eq: marine eutrophication; kg NMVOC eq: photochemical oxidation; kg P eq: freshwater eutrophication; kg PM2.5 eq: particulate matter; kg Sb eq: mineral resource depletion; kg U235 eq: ionising radiation; m3 water: water use; MJ: cumulative energy demand; mol H+ eq: acidification; mol N eq: terrestrial eutrophication.

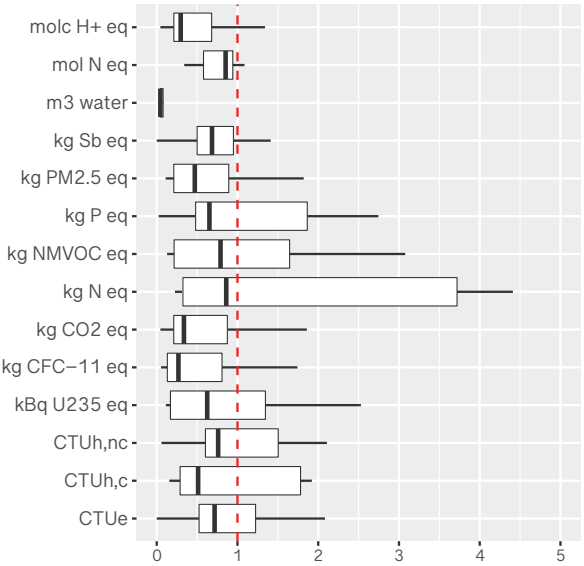

Figure 2-4 Relative LCA impact scores compared to a reference single-Si PV rooftop system as modelled in ecoinvent v3.4[26] (single-Si impact score = 1, indicated by the red dotted line).

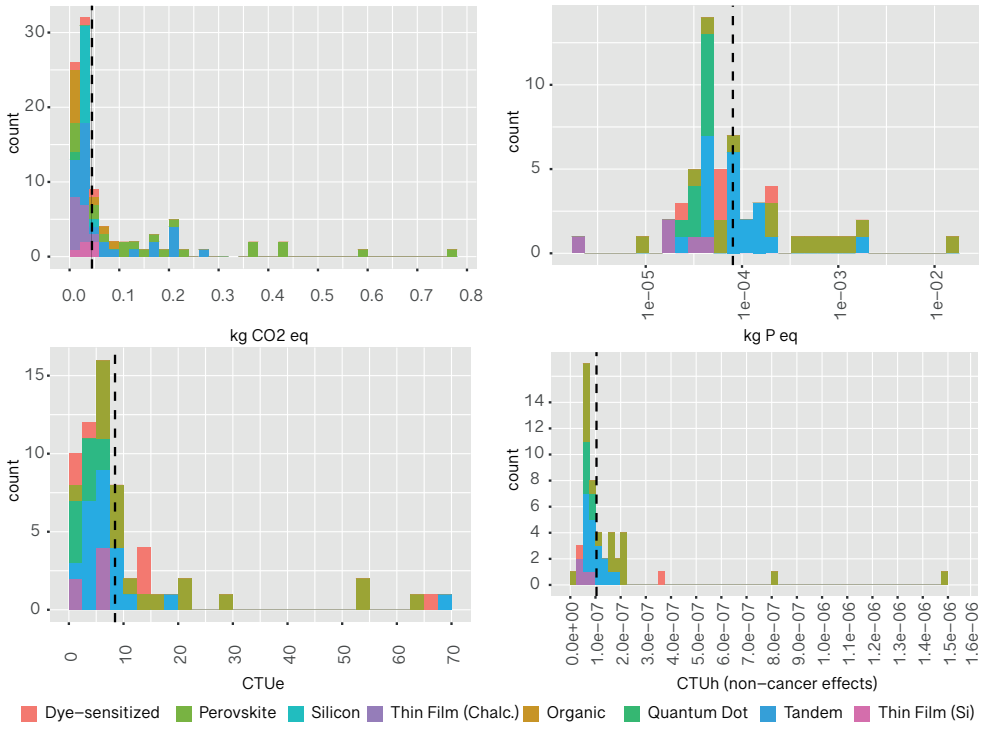

Figure 2-5 Histogram of harmonized impact scores categorized by PV technology type. The black dotted line indicates the score for the reference single-Si rooftop PV system[26].

Table 2-2 Statistics for impact scores, all PV technologies

Impact category	Units	Geometric mean	Geometric standard deviation	Min	Max	n
Freshwater ecotoxicity	CTUe	4.91E+00	6.47	1.73E-03	6.83E+01	62
Human toxicity, cancer effects	CTUh,c	2.09E-08	15.33	1.97E-09	1.33E-05	39
Human toxicity, non-cancer effects	CTUh,nc	9.66E-08	2.28	6.15E-09	1.49E-06	48
Ionising radiation	kBq U235 eq	6.33E-03	7.21	9.34E-04	2.14E+00	14
Ozone depletion	kg CFC-11 eq	2.88E-09	4.33	4.18E-10	2.30E-07	40
Climate change	kg CO2 eq	4.20E-02	3.09	4.34E-03	7.74E-01	95
Marine eutrophication	kg N eq	6.70E-04	89.11	2.48E-05	2.76E+00	14
Photochemical oxidation	kg NMVOC eq	3.16E-04	7.44	4.24E-05	8.28E-01	34
Freshwater eutrophication	kg P eq	8.21E-05	4.32	1.93E-06	1.50E-02	55
Particulate matter	kg PM2.5 eq	4.30E-05	2.41	1.04E-05	2.07E-04	27
Resource depletion	kg Sb eq	1.63E-05	29	1.89E-08	1.79E-04	46
Water depletion	m3 water	2.03E-02	4.29	8.68E-03	9.92E-01	15
Terrestrial eutrophication	mol N eq	7.25E-04	1.60	3.51E-04	1.12E-03	5
Acidification	molc H+ eq	4.10E-04	2.67	4.65E-05	3.76E-03	45

2.3.4. Effects of technological enhancement on environmental impacts

Technological innovations appear to have had positive results on climate change impact scores, as can be seen from the random effects model results plotted in Figure 2-6. The heterogeneity, however, is quite large and we cannot conclude that there is a significant effect overall. Heterogeneity can be attributed to the differences in materials, manufacturing processes or efficiencies of each technology type, but it could also be attributed to modelling differences that were not sufficiently corrected via the harmonization procedure.

We further sub-grouped the data by cell-conversion efficiency and disaggregated by sub-technology types (see Appendix Figure A.1-2). The results did not find a significant reduction in climate change impacts for groups with higher cell-conversion efficiencies

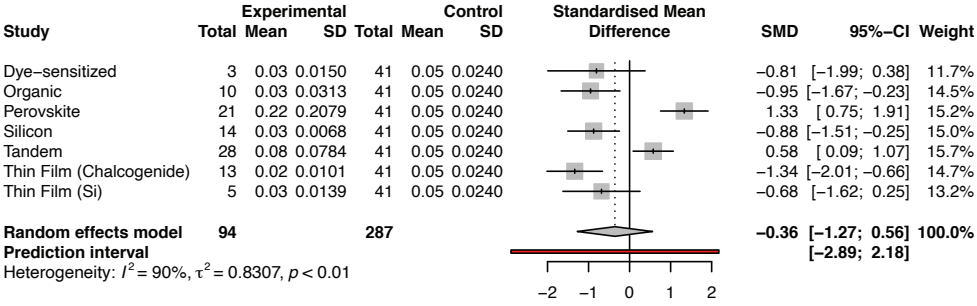

Figure 2-6 Random effects model results for climate change impact.

measured using SMD. The sub-grouping did not reduce the inherent heterogeneity of the data either. The results may suggest that either additional underlying factors (e.g., material choice, manufacturing processes, cost) are better suited than conversion efficiency to represent the relationship between technological enhancements and climate change impacts, or that the strive for reduced efficiency is not necessarily reflected in improved environmental performance of the PV sector. If the latter is the case, PV technologies can still bring about environmental benefits by replacing other types of energy sources (e.g., fossil fuel-based), which are not considered in the current study.

2.3.5. Contribution and hotspots analysis

2.3.5.1. Light absorbing layers and cells

The focus of most LCA studies of emerging PV technologies is on innovations in the light absorbing layers, whether in terms of their materials or configurations. Each type of absorbing layer places some additional requirements on the ancillary components of the cell (e.g., OPV requires encapsulation, perovskites are deposited on a transparent conductive oxide, etc.). Figure 2-7 shows the average contributions of the modules to each impact category for each PV technology. It can be seen that for perovskites and tandem technologies, the main contributions come from the cell, rather than from the panel and balance of system components.

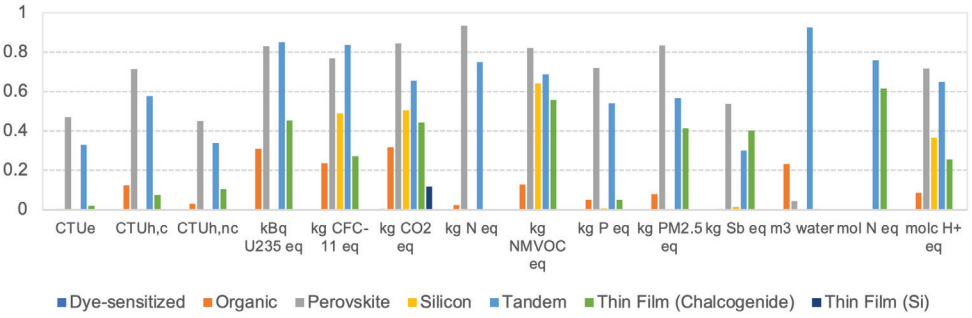

Figure 2-7 Average relative contributions of PV cells as compared to the corresponding PV system.

2.3.5.2. From cells to panels

Based on the 2015 inventory data from IEA PVPS[27], panel contributions for a single-Si roof mounted PV system can range between 4% to water depletion, 11% to climate change and 28% to mineral resource depletion. Within the panel, aluminium and solar glass typically account for over 50% of the contributions in most impact categories, although small amounts of copper weigh heavily on the toxicity categories. Therefore, cells that may require less or no glass and aluminium highly benefit from these avoided emissions in certain installations. Examples of these are roll-to-roll manufactured OPV, perovskites, dye-sensitized cells and thin film chalcogenides. This is an important outcome, since it implies that technologically enhanced PV cells have a good opportunity to offset environmental trade-offs if the new cell design favours less materials-intensive panels. The need for less panel materials can result from lighter cells allowing lamination or lighter panelling, and/or from higher cell efficiencies requiring less panel area per kWh.

2.3.5.3. From panels to PV installations

The BOS is also a main contributor and is in a large part independent of cell design. Particularly the inverter, which is required equally for all systems independent of cell efficiency, contributes on average 11% to impact categories, with 32% to mineral resource depletion and 29% to human toxicity, non-cancer effects for a reference single-Si roof-mounted system. The remainder of the installation is composed of mounting systems and cabling which contribute on average 33% to all impact categories, with 71% contribution to freshwater ecotoxicity, 37% to human toxicity, cancer effects, and 18% to climate change. Here the key contributions come from aluminium and copper, where aluminium from the mounting system represents 87% of the climate change contribution and copper from the electric installation 97% of the contribution to freshwater ecotoxicity.

2.3.5.4. Hotspots in the emerging PV landscape

Figure 2-8 presents a radar plot with relative impacts of the different types of PV cells, where 100% corresponds to the impact score for a reference single-Si roof-mounted system as modelled in ecoinvent 3.4[26]. For each type of PV cell, we have used the geometric mean impact score, following the indications of section 2.3.3. Perovskites dominate the plot and exceed the reference single-Si system by factors of 2 and more in 4 impact categories. These potentially important hotspots are summarized in Table 2-3, along with their possible sources. It is important to highlight that the results discussed earlier represent the impacts of the PV technologies in comparable applications, i.e., roof-mounted installations. However, several of these technologies are finding alternative applications and may end up creating their specific market niches. Some of these technologies can be embedded into other systems (e.g., building integrated or flexible cells integrated on consumer products). From an LCA perspective, this means that the assessed functional unit would change, and this can considerably change the calculation of the life cycle impact scores of the technologies.

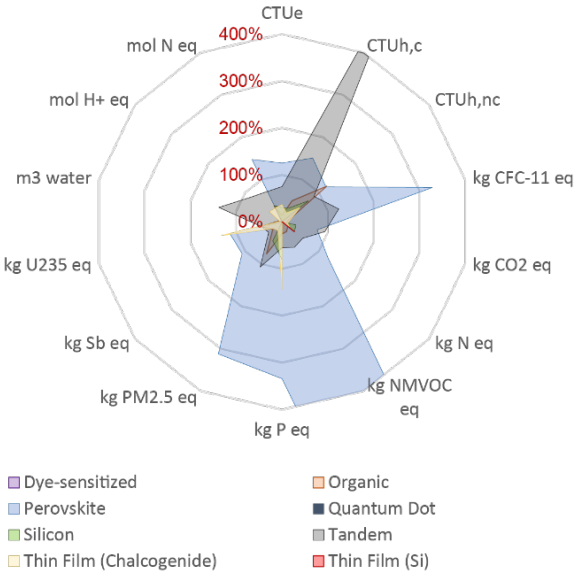

Figure 2-8 Relative ILCD impact scores for different PV technologies, compared to a reference single-Si roof-mounted PV system as modelled in ecoinvent v3.4 (=100%). The plot is truncated at 400% for visualization purposes.

Table 2-3 Key potential environmental hotspots in emerging PV technologies, compared to a reference single-Si roof-mounted PV system.

PV technology	Impact category	Comparative hotspots
Perovskites	Photochemical oxidation	Isopropanol emitted in blocking layer; fluorine-doped tin oxide ; (FTO) glass; gold layer
	Freshwater eutrophication	Fluorine-doped tin oxide (FTO) glass; isopropanol emitted in blocking layer; gold layer; waste streams
	Particulate matter	Fluorine-doped tin oxide (FTO) glass; perovskite layer; gold layer
	Ozone depletion	Fluorine-doped tin oxide (FTO) glass; gold layer; perovskite layer
	Marine eutrophication	Dimethylformamide (DMF) in solution-deposited PK; fluorine-doped tin oxide (FTO) glass
	Human toxicity, cancer effects	Methylammonium iodide (MAI); tin
Tandem	Human toxicity, cancer effects	Dimethylformamide (DMF) and isopropanol solvents in PK/Si

2.4.Conclusions

A comprehensive harmonization effort combined with diverse statistical analyses allowed us to answer important questions about the direction the PV sector is taking in terms of sustainability. This was possible despite the large underlying uncertainties in predicting future evolution of immature technologies, and the wide array of modelling choices across LCA studies which can lead to large variabilities, even in harmonized results. From an overall environmental perspective, thin film silicon and dye-sensitized cells presented a considerable lead, followed by thin film chalcogenide, organic and silicon. As many of the assessments are still based on early design concepts, the results we presented should not be used as arguments to hinder further research on specific technologies. Rather, they may be used constructively to highlight research pathways that can result in more environmentally competitive designs. Emerging concepts that are lagging in this respect can address their shortcomings by aiming to reach higher efficiencies, longer lifetimes, substituting novel materials and/or reducing the energy intensive of their manufacturing processes.

This meta-analysis investigated environmental life cycle impacts based on the LCA method. LCA aggregates environmental emissions and impacts in large production and consumption systems that occur in many different places and times. This temporal and spatial integration is helpful to compare product systems based on their total life cycle emissions, but LCA results do not necessarily reflect actual risk at a specific location or time. Risk assessment can provide an idea of actual risk by combining release, environmental fate and exposure to emissions and comparing them to thresholds on which adverse effects occur.[36] Both frameworks are complementary and necessary.[12,37] We believe future studies incorporating risk assessment results into a meta analyses framework like the one developed in this study could provide a comprehensive and valuable tool for guiding research and policy in the PV sector.

References

1. International Energy Agency. *Renewables 2018 - Market analysis and forecast from 2018 to 2023. IEA* (2018).
2. Lazard. *Levelized Cost of Energy 2017*. (2017).
3. ITRPV, Group, S. P. & ITRPV. *International Technology Roadmap for Photovoltaic. ITRPV Eighth Edition, International Technology Roadmap for Photovoltaic Results 2016, (2017)* www.itrpv.net (2017) doi:http://www.itrs.net/Links/2013ITRS/2013Chapters/2013Litho.pdf.
4. Cucurachi, S., Van Der Giesen, C. & Guinée, J. Ex-ante LCA of Emerging Technologies. *Procedia CIRP* **69**, 463–468 (2018).
5. Collingridge, D. *The social control of technology*. (Frances Pinter, 1980).
6. Stamford, L. & Azapagic, A. Environmental Impacts of Photovoltaics: The Effects of Technological Improvements and Transfer of Manufacturing from Europe to China. *Energy Technol.* **6**, 1148–1160 (2018).
7. Chatzisideris, M. D. & Laurent, A. Ecodesign perspectives of thin-film photovoltaic technologies: A review of life cycle assessment studies. *Sol. Energy Mater. Sol. Cells* **156**, 2–10 (2016).
8. Green, M. A. *et al.* Solar cell efficiency tables (Version 53). *Prog. Photovoltaics Res. Appl.* **27**, 3–12 (2019).
9. NREL. Best Research-Cell Efficiency Chart | Photovoltaic Research | NREL. https://www.nrel.gov/pv/cell-efficiency.html (2019).
10. Rao, S., Morankar, A., Verma, H. & Goswami, P. Emerging Photovoltaics: Organic, Copper Zinc Tin Sulphide, and Perovskite-Based Solar Cells. *J. Appl. Chem.* **2016**, 1–12 (2016).
11. Zakutayev, A. Brief review of emerging photovoltaic absorbers. *Curr. Opin. Green Sustain. Chem.* **4**, 8–15 (2017).
12. Guinée, J. B., Heijungs, R., Vijver, M. G. & Peijnenburg, W. J. G. M. Setting the stage for debating the roles of risk assessment and life-cycle assessment of engineered nanomaterials. *Nat. Nanotechnol.* **12**, 727–733 (2017).
13. Guinée, J. B. *Handbook on life cycle assessment : operational guide to the ISO standards*. (Kluwer Academic Publishers, 2002).
14. Moher, D., Liberati, A., Tetzlaff, J., Altman, D. G. & Group, T. P. Preferred Reporting Items for Systematic Reviews and Meta-Analyses: The PRISMA Statement. *PLoS Med.* **6**, e1000097 (2009).
15. Clarivate. Web of Science. www.webofscience.com.
16. Heath, G. A. & Mann, M. K. Background and Reflections on the Life Cycle Assessment Harmonization Project. *Journal of Industrial Ecology* vol. 16 (2012).

17. Hsu, D. D. *et al.* Life Cycle Greenhouse Gas Emissions of Crystalline Silicon Photovoltaic Electricity Generation. *J. Ind. Ecol.* **16**, S122–S135 (2012).

18. Rebitzer, G. *et al.* Life cycle assessment Part 1: Framework, goal and scope definition, inventory analysis, and applications. *Environment International* vol. 30 701–720 (2004).

19. Frischknecht, R. *et al. Methodology Guidelines on Life Cycle Assessment of Photovoltaic Electricity, 3rd edition, IEA PVPS Task 12*. http://www.iea-pvps.org/fileadmin/dam/public/report/technical/Task_12_-_Methodology_Guidelines_on_Life_Cycle_Assessment_of_Photovoltaic_Electricity_3rd_Edition.pdf (2016).

20. Monteiro Lunardi, M. *et al.* A comparative life cycle assessment of chalcogenide/Si tandem solar modules. *Energy* (2018) doi:10.1016/J.ENERGY.2017.12.130.

21. Louwen, A., Van Sark, W. G. J. H. M., Schropp, R. E. I., Turkenburg, W. C. & Faaij, A. P. C. Life-cycle greenhouse gas emissions and energy payback time of current and prospective silicon heterojunction solar cell designs. *Progress in Photovoltaics: Research and Applications* vol. 23 1406–1428 (2015).

22. O'Donoughue, P. R., Heath, G. A., Dolan, S. L. & Vorum, M. Life Cycle Greenhouse Gas Emissions of Electricity Generated from Conventionally Produced Natural Gas: Systematic Review and Harmonization. *J. Ind. Ecol.* (2014) doi:10.1111/jiec.12084.

23. Asdrubali, F., Baldinelli, G., D'Alessandro, F. & Scrucca, F. Life cycle assessment of electricity production from renewable energies: Review and results harmonization. *Renewable and Sustainable Energy Reviews* (2015) doi:10.1016/j.rser.2014.10.082.

24. Meng, L., You, J. & Yang, Y. Addressing the stability issue of perovskite solar cells for commercial applications. *Nature Communications* vol. 9 5265 (2018).

25. Cai, M. *et al.* Cost-Performance Analysis of Perovskite Solar Modules. *Adv. Sci.* **4**, 1600269 (2017).

26. Wernet, G. *et al.* The ecoinvent database version 3 (part I): overview and methodology. *Int. J. Life Cycle Assess.* **21**, 1218–1230 (2016).

27. Frischknecht, R. *et al. Life Cycle Inventories and Life Cycle Assessments of Photovoltaic Systems*. http://iea-pvps.org/fileadmin/dam/public/report/technical/Future-PV-LCA-IEA-PVPS-Task-12-March-2015.pdf (2015).

28. Pennington, D. W. *et al.* Life cycle assessment Part 2: Current impact assessment practice. *Environ. Int.* **30**, 721–739 (2004).

29. Fantke, P. *et al. USEtox® 2.0, Documentation version 1*. (2017). doi:10.11581/DTU:00000011.

30. European Commission Joint Research Center - Institute for Environmental Sustainability. *ILCD Handbook: Recommendations for Life Cycle Impact Assessment in the European context. Vasa* http://eplca.jrc.ec.europa.eu/uploads/ILCD-Recommendation-of-methods-for-LCIA-def.pdf (2011) doi:10.278/33030.

31. Louwen, A., van Sark, W. G. J. H. M., Faaij, A. P. C. & Schropp, R. E. I. Re-assessment of net energy production and greenhouse gas emissions avoidance after 40 years of photovoltaics development. *Nat. Commun.* **7**, 13728 (2016).

32. Harrer, M., Cuijpers, P., Furukawa, T. A. & Ebert, D. D. *Doing Meta-Analysis in R: A Hands-on Guide*. (PROTECT Lab, 2019). doi:10.5281/zenodo.2551803.

33. Valentine, J. C., Pigott, T. D. & Lau, T. Systematic Reviewing and Meta-Analysis. in *International Encyclopedia of the Social & Behavioral Sciences* (ed. Wright, J. D.) 906–913 (Elsevier, 2015). doi:10.1016/B978-0-08-097086-8.10509-4.

34. Deeks, J., Higgins, J. & Altman, D. Analysing data and undertaking meta-analyses. in *Cochrane Handbook for Systematic Reviews of Interventions* (eds. Higgins, J. & Green, S.) (The Cochrane Collaboration).

35. Martinez, M. N. & Bartholomew, M. J. What Does It Mean? A Review of Interpreting and Calculating Different Types of Means and Standard Deviations. *Pharmaceutics* **9**, (2017).

36. Fairman, R., Mead, C. D. & Williams, W. P. *Environmental Risk Assessment - approaches, experiences and information sources. Environmental Issues* vol. 4 (1998).

37. Franklin, C. Chasing Hazards: Toxicity, Sustainability, and the Hazard Paradox. *Natural Resources & Environment* vol. 29 (2015).

38. Lau, K. K. S. & Soroush, M. Overview of Dye-Sensitized Solar Cells. in *Dye-Sensitized Solar Cells* (eds. Soroush, M. & Lau, K.) 1–49 (Elsevier, 2019). doi:10.1016/B978-0-12-814541-8.00001-X.

Chapter 3

Environmental impacts of III–V/silicon photovoltaics: life cycle assessment and guidance for sustainable manufacturing

Abstract

Multijunction III–V/silicon photovoltaic cells (III–V/Si), which have achieved record conversion efficiencies, are now looking like a promising option to replace conventional silicon cells in future PV markets. As efforts to increase efficiency and reduce cost are gaining important traction, it is of equal importance to understand whether the manufacturing methods and materials used in these cells introduce undesired environmental trade-offs. We investigate this for two state-of-the-art III–V/Si cell design concepts using life cycle assessment. Considering that the proposed III–V/Si technologies are still at an early research and design stage, we use probabilistic methods to account for uncertainties in the extrapolation from lab-based data to more industrially relevant processes. Our study shows that even at this early stage and considering potential uncertainties, the III–V/Si PV systems are well positioned to outperform the incumbent silicon PV systems in terms of life-cycle environmental impacts. We also identify key elements for more sustainable choices in the III–V/Si design and manufacturing methods, including the prioritization of energy efficiency measures in the metalorganic vapour phase epitaxy (MOVPE) process and a reduction in the consumption of indium trichloride in spray pyrolysis.

Keywords: LCA; III-V cells; multijunction cells; photovoltaics; environmental impacts

This chapter has been published as: Blanco, C.F., Cucurachi, S., Dimroth, F., Guinée, J.B., Peijnenburg, W.J.G.M., Vijver, M.G. (2020). Environmental impacts of III–V/silicon photovoltaics: life cycle assessment and guidance for sustainable manufacturing. Energy Environ Sci, 13:4280–90. doi:10.1039/D0EE01039A.

3.1. Introduction

The last few decades have seen a dramatic increase in global efforts to accelerate the market penetration of renewable energy sources like solar photovoltaics (PV). It is well recognized that the success of a technology in the PV landscape is highly dependent on lowering the cost per unit of electricity generated (i.e., $/kWh). Such cost reductions have come either from lowering manufacturing costs, or from increasing conversion efficiency through technological innovation. Numerous alternatives to the conventional silicon-based PV technologies have been introduced with the aim of minimizing the cost/efficiency ratio. Alternative options to silicon-based PV include thin-film cadmium-telluride (CdTe), copper-indium-gallium-selenide (CIGS)[1], perovskite[2], organic[3], dye-sensitized[4], and multijunction III-V cells[5,6]. Yet, while the focus on $/kWh reduction is driving innovation, it is equally important for the industry not to lose sight of the environmental impacts of the proposed technological changes. In order to avoid undesired environmental trade-offs, PV technology developers must constantly aim for the right balance between cost, efficiency and environmental impacts.[7] Even more so in early research and development stages, when more sustainable design choices are cheaper and easier to implement.[8]

This balance between cost, efficiency and environmental impacts is especially relevant for PV systems based on III-V solar cells. III-V cells use crystalline arrangements of elements from groups III and V of the periodic table (e.g., arsenic, phosphorus, aluminium, gallium, indium) to capture sunlight from parts of the spectrum outside of the physical limits of silicon. Despite having achieved record efficiencies amongst the newer generations of PV technologies[9,10], the high production cost of III-V solar cells has so far restricted them to niche applications, such as concentrators, and space and military missions.[11–14] One possible way to reduce cost is to replace the germanium substrate that has been used as a bottom cell with a silicon bottom cell instead (III-V/Si).[11–14] If such innovations become scalable, III-V/Si solar cells could potentially take up a substantial part of the future PV market.[11–14] Rapid shifts in technology and materials, however, may also introduce unforeseen environmental impacts, given that the manufacturing of the new generations of III-V solar cells involves energy intensive processes, and requires the use of highly toxic substances, such as arsine and phosphine. Small amounts of critical or scarce materials, such as indium and gallium, are also consumed in the processing of these cells.[15,16]

In light of the promising technical and economic outlook of III-V/Si PV, in this study we complement the recent technological development efforts by assessing the life cycle environmental impacts of state-of-the-art III-V/Si PV design concepts. In doing so, we investigate whether the ongoing advances in these technologies may bring about undesired environmental trade-offs. Our assessment is also meant to serve as an early guidance for more sustainable design of III-V/Si PV cells that will eventually achieve an optimal balance between cost, efficiency and environmental impacts.

3.2. Methods

We applied the life-cycle assessment (LCA) method[17], which allows identifying and quantifying the environmental trade-offs in globally distributed product systems.[18] We first defined the product system and its boundaries (section 3.2.1) and calculated the total energy and material inputs and outputs of each production step (section 3.2.2). Next, we assessed the impacts of the environmental inputs and outputs using life cycle impact assessment models (section 3.2.3). We then interpreted the results by considering the uncertainty and variability of the data and the influence on the results of various modelling choices (section 3.2.4).

3.2.1. Product system definitions

We used 1 kWh of electricity generated in a slanted-roof PV installation as the basis (i.e., functional unit[18]) to assess the environmental performance of the studied PV systems. Choosing electricity generation (instead of a given area of solar cell, for example) allowed us to account for the environmental benefits of higher cell efficiencies that require less module area and infrastructure materials to produce the same amount of electricity.

A slanted-roof PV installation consists of solar panels, which contain the cells and the balance of system (BOS). The BOS includes the AC/DC inverter, cables and other supporting infrastructure necessary for the functioning of the installations. Multijunction III-V/Si cells have different configurations of ultrathin layers of elements from groups III and V of the periodic table (e.g., gallium, indium, arsenide and phosphide). These layers constitute the top cells, which are placed on top of a silicon substrate, or bottom solar cell. The top and bottom cells are designed to capture different wavelengths of the solar spectrum, allowing them to convert more energy than conventional silicon cells. Some additional intermediate III-V layers are required, e.g., for bonding and tunnel diodes that act as interconnecting layers between sub cells. We modelled two different III-V/Si cell designs based on lab-scale concepts of a 2-terminal III-V/Si cell that are being developed by a team led by Fraunhofer ISE.[19,20] For a comparative reference we used the conventional single-crystalline (single-Si) PV systems that dominate the current PV market, based on data from the ecoinvent v3.4 LCA database.[21] The three different cell designs are presented in Figure 3-1.

The manufacturing of III-V/Si cells starts with the silicon wafer that constitutes the bottom cell. This wafer is similar to the one used in commercially available single-Si PV and its manufacturing process is well documented in the ecoinvent database.[21] The silicon wafer is then grinded and etched to prepare it for coupling with the additional III-V cells.[22] After grinding and etching, the cell is implanted with phosphorus and boron ions which are generated by creating an arc discharge in phosphine and boron trifluoride gas. The ions are then accelerated with specific energies to achieve the desired doping characteristics (e.g., depth of ion concentration and quantity).

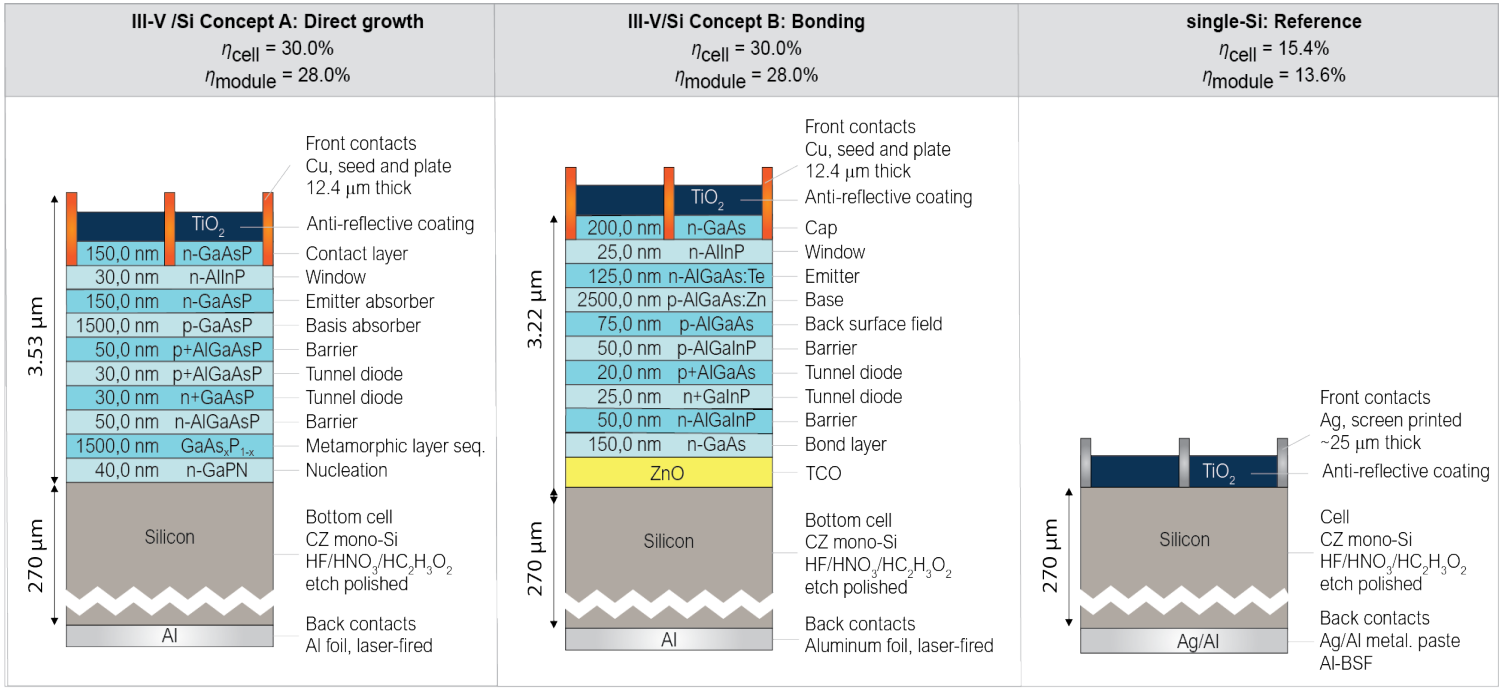

Figure 3-1 Different types of cells assessed in this study. III-V/Si concepts A and B (left and centre) are being developed by a team led by Fraunhofer ISE. The reference single-Si cell (right) has been modelled as in ecoinvent v3.4. ηcell = cell conversion efficiency; ηmodule = module conversion efficiency.

This process is followed by annealing, a thermal treatment that helps to activate the dopants and repair any damage caused by the ion implantation process. A passivation layer, which reflects non-absorbed light back into the cell, is added to the backside of the cell by atomic layer deposition (ALD) of a 10nm film of aluminium oxide (Al_2O_3). This is followed by plasma enhanced chemical vapour deposition (PECVD) of a silicon nitrate (SiN_x) film of 70-100nm.

For the use phase, we considered a system lifetime of 30 years with no degradation, in line with most LCA studies of conventional silicon PV systems. While stability has been a sensitive aspect in LCA studies of some emerging PV technologies such as organic and perovskites[24], III-V multi-junction solar cells are well known for applications in space where reliability is a key concern and significant tests are performed before a product is qualified for a space mission.[25] III-V multi-junction cells are also significantly less sensitive to impurities since the absorber thickness is only on the order of 1-3 μm compared to 100-200 μm for Si. This also relaxes the required diffusion length for photogenerated carriers, an important quantity in any solar cell material. Furthermore, the crystals are formed at high temperatures above 600°C and found to be very stable at operating temperatures up to 120 °C and even above. III-V multi-junction cells have already been deployed in concentrator photovoltaic modules where they operate at around 80°C with irradiance levels up to 1000 suns. All these harsh conditions have not been leading to any significant signs of degradation, making this technology very suitable for next generation photovoltaics with high reliability.[26–28]

We excluded electricity distribution, final disposal/recycling and other end-of-life (EOL) options for the III-V/Si cells. We only focused on cradle to gate because the distribution of electricity is not specific to the III-V/Si system, and it is still too early to understand potential recycling options that may be applicable to the III-V/Si cells. We separately discuss the potential implications of recycling in section 3.3.5.

The process flowcharts for each manufacturing route are presented in Appendix Figures A-2.1 and A-2.2. The systems are split between the foreground, which includes new processes specific to the III-V/Si technology, and the background, which includes all the raw materials, transport, energy and ancillary services further upstream in the supply chain.

3.2.2. Data collection

Input and output data for all background system processes was obtained from the ecoinvent v3.4 database.[21] For the foreground processes, we collected data directly from technology developers and secondary sources such as scientific literature and technical equipment / safety data sheets. We used average European electricity markets as modelled in ecoinvent for all foreground electricity inputs and average global markets for raw materials. Many of the processes for manufacturing the III-V prototypes are still lab-based, which could result in unrealistically high consumption of energy and materials. To account for this, we used proxies or extrapolated data where possible in order to represent

more realistic industrial-scale processes (e.g., use of in-line tools for wet chemical processes instead of single-use baths). We then attached uncertainties to these extrapolations and assumptions as described in section 3.2.4. The full life-cycle inventory of inputs, outputs and data sources for each of the foreground processes is presented in Appendix A-2, along with the corresponding calculations and assumptions.

3.2.3. Impact assessment

The life-cycle impacts were calculated following the methods recommended by the International Reference Life Cycle Data System (ILCD).[29] We calculated impacts across all impact categories recommended by ILCD, including climate change, human toxicity, freshwater ecotoxicity, ionising radiation and depletion of mineral resources (see section 3.3.1).

3.2.4. Uncertainty analysis

For emerging technologies, it is often the case that data is unavailable due to commercial sensitivities, is not fully representative as it may be based on lab-scale processes, or can only be expressed as ranges as the technology has not been fine-tuned.[30] Table 3-1 summarizes the key processes in the foreground with high uncertainty and the parameters used to characterize them. For the background system, we incorporated the uncertainty information supplied by the ecoinvent v3.4 database.[31] We performed an uncertainty analysis by running 1000 Monte Carlo simulations for each alternative PV system.[32] We used a dependent sampling method, which takes the same random values for parameters in processes that are shared by the alternative systems in each Monte Carlo run. This method provides a more realistic comparison and avoids over or underestimation of variance in the LCA model's ouputs.[33] We then tested the significance of the difference in impact scores between each alternative PV system using the modified null hypothesis test method proposed by Heijungs et al.[34]. For this we used the calculation tools for significance testing in LCA developed by Mendoza-Beltrán et al.[35]

3.3.Results and discussion

3.3.1. Environmental profile

Figure 3-2 shows the impacts of the III-V/Si PV systems, taking the single-Si PV system as a comparative reference (100%). The III V/Si systems have lower scores than the single-Si system across all impact categories except for ionizing radiation and mineral resource depletion (concept B only). The high radiation impact, however, is a consequence of choosing the average European electricity market for the foreground processes, where countries like France and Ukraine contribute significant amounts of nuclear energy. It can also be seen that there is only a very slight difference between the direct growth (concept A) and the bonding (concept B) methods used to manufacture the III-V PV system, across all impact categories except mineral resource depletion.

Table 3-1 Uncertainty parameters for foreground data

Parameter	Distribution	Mode	Min	Max	Criteria
Hazardous gas abatement – mass of granulate consumed per mass of gas inflow	Triangular	7.65 kg	2.55 kg	7.65 kg	Max value obtained from empirical lab results. Min value based on expert opinion (Fraunhofer ISE, personal communication). Mode set as max for worst-case scenario.
GaAs substrate manufacturing – process losses during wafer slicing and polishing	Triangular	70%	50%	70%	Based on Lichtensteiger (2015)[62] and Eichler (2012)[63]. Mode set as max for worst-case scenario.
GaAs substrate thickness	Triangular	550 µm	450 µm	650 µm	Based on expert opinion (Joanneum, personal communication).
Equipment electricity consumption – calculated as power input (kW) * operating time (h)	Triangular	75%	60%	90%	We assume equipment not always operates at full power, which is especially the case for heating.
Energy and mass inputs – taken from technical spec sheet	None	Reported value	-	-	We take the value just as reported in the technical specifications sheet.
Energy and mass inputs – taken from commercial brochure	Triangular	Reported value	-20%	+20%	We take the value as reported in the brochure but add uncertainty that can arise from applying the technology in different conditions.
Solvent quantities – taken from peer-reviewed scientific literature, patents & third-party lab protocols for chemical synthesis	Triangular	–30% of reported value	-45%	Reported value	Much larger efforts are placed on recycling of solvents in industrial scale.
Reactant quantities – taken from peer-reviewed scientific literature, patents & third-party lab protocols for chemical synthesis	Triangular	Reported value	-10%	+10%	Reactants are needed in stoichiometric quantities.

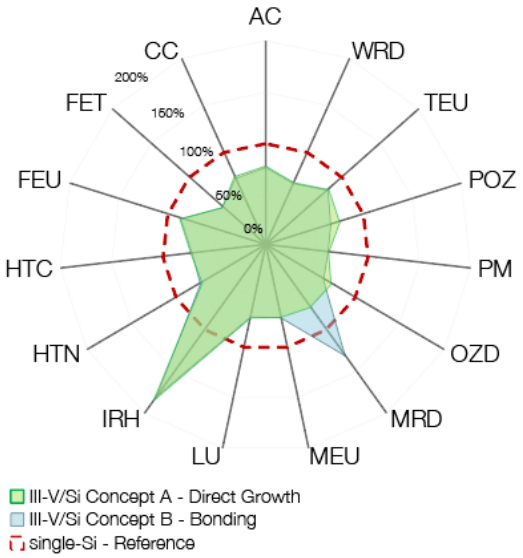

Figure 3-2 Comparative impact results of III-V/Si PV systems manufactured using both III-V/Si concepts and commercial single-Si (slanted-roof) as modelled in ecoinvent v3.4. AC: acidification; CC: climate change; FET: freshwater ecotoxicity; FEU: freshwater eutrophication; HTC: human toxicity, cancer effects; HTNC: human toxicity, non-cancer effects; IRH: ionising radiation, human health; LU: land use; MEU: marine eutrophication; MRD: mineral, fossil and renewable resource depletion; OD: stratospheric ozone depletion; PM: particulate matter; POZ: photochemical ozone formation; TEU: terrestrial eutrophication; WRD: water resource depletion.

3.3.2. Key process contributions to impacts

3.3.2.1. Climate change

The individual process contributions to the climate change impacts of the III-V/Si (concept A) and single-Si systems are shown in Figure 3-3. Process contributions smaller than 1% are not shown. The electricity consumed by the MOVPE reactor is the dominant flow amongst the processes specifically related to the manufacturing of the III-V/Si cell. Even though other processes require similarly high temperatures (e.g., annealing), the throughput of MOVPE is much smaller.

Only 31 four-inch wafers are treated in a one-hour run, while over 100 four-inch wafers per run are processed in the annealing furnace. In an MOVPE reactor, most of the energy spent for heating is lost as radiation in the cooled reactor walls and heaters. At this point, however, it is already challenging to increase the area throughput even more. Some experiments have been made to change resistance heating for induction heating in the past[36], but these changes are not expected to create significant efficiency gains in the overall process.

However, opportunities exist in the future to minimize the thermal mass that must be heated and possibly optimize the source utilization efficiency. Higher growth rates and

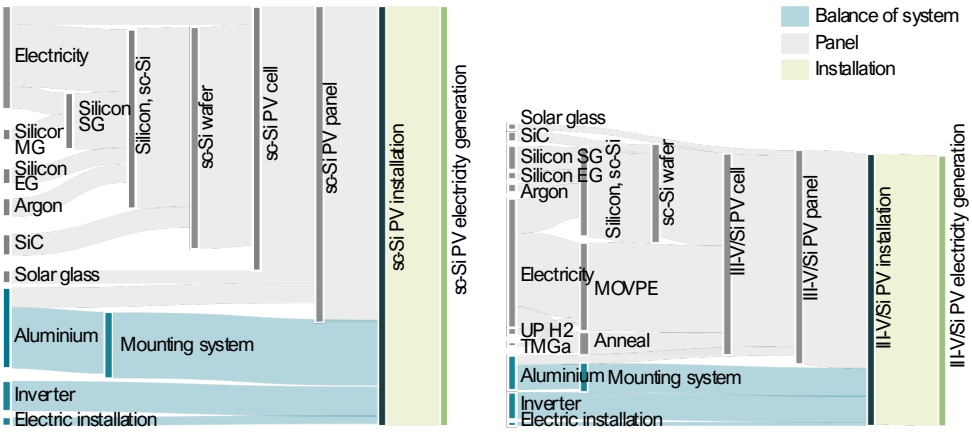

Figure 3-3 Relative contribution of economic flows and foreground processes to the total life cycle climate change impacts of generating electricity with a reference single-Si PV system (left) and a III-V/Si PV system (concept A – Direct Growth, right). BOS flows are indicated in blue, panel flows in grey.

shorter growth time would also result in important energy efficiency improvements. There are some more developed MOVPE tools that already exist in the market like the Aixtron R6 that can handle more than 100 two inch wafers or 31 four inch wafers per run.[37] Recent production type Planetary Reactors® can automatically load/unload 5x200 mm wafers. We further investigate the effects of this potential improvements in section 3.3.4.1.

The manufacturing of the silicon wafer is another dominant process for both III-V/Si and single-Si systems. Here, however, the III-V/Si PV systems draw an advantage from the reduced area required per kWh, which greatly reduces silicon but also panel and balance of system material requirements. The inverter's contribution is not offset by the smaller area because it depends on the power, so its contribution is equal in both III-V/Si and single-Si systems.

Notably, the consumption of ultrapure gases is not an important contribution and, in most cases, falls below the 1% threshold (except for hydrogen and TMGa which contribute 2.06 and 1.15% of the total impact respectively). This is also the case for the front contact metallization. While the manufacturing of engineered nanoparticles does require additional processing energy and materials vs. the bulk silver paste[38,39], the smaller quantity of metal that is used in the nanoink-printed contacts appears to offset the impacts vs. using conventional metallization pastes.

3.3.2.2. Human toxicity, non-cancer effects

Copper feeds are the most important contributors to human toxicity impacts for both III-V/Si and single-Si systems Figure 3-4. Copper is mainly consumed in the inverter and electrical installation, both of which are BOS components and not related to the III-V/Si or single-Si cells. MOVPE also has an important contribution to the toxicity impact categories as well, due to the large fraction of the electricity mix in the average European market that is coal based. Coal mining releases zinc, nickel, copper and other metal

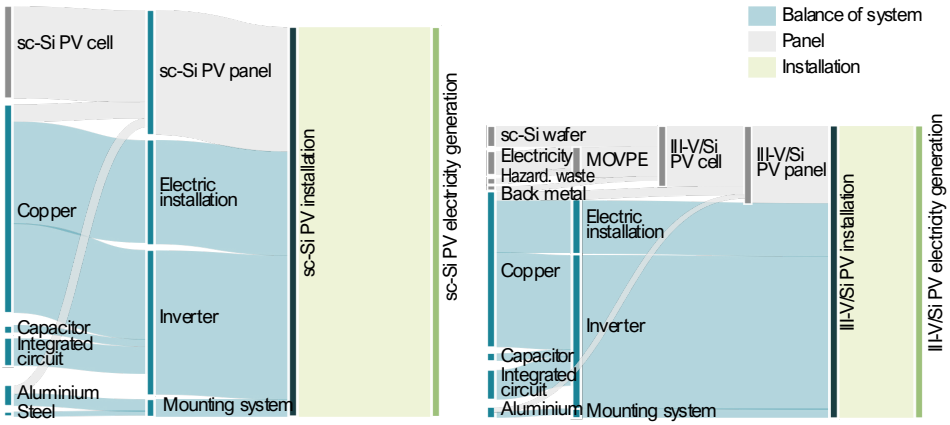

Figure 3-4 Relative contribution of economic flows and foreground processes to the total life cycle human toxicity (non-cancer effects) impacts of generating electricity with a reference single-Si PV system (left) and a III-V/Si PV system (concept A – Direct Growth, right). BOS flows are indicated in blue, panel flows in grey.

emissions to water during the treatment of coal mining spoils, resulting in an important contribution to the total impact. In comparison to these life cycle impacts, the contribution of hazardous waste treatment of arsine and phosphine gases is very small (1.8%).

3.3.2.3. Freshwater ecotoxicity

The freshwater ecotoxicity impacts of both III-V/Si and single-Si systems are largely dominated by the metal components in the BOS. Here, the largest contributor is the treatment of scrap copper waste from the electrical installation. Copper as an input raw material also has important contributions to the installation of inverters. The use of toxic hydride gases in MOVPE again has a minor contribution in this category (5%), where the relevant contribution mostly derives from the coal-based fraction of electricity consumed. Powering the MOVPE reactor with a renewable source of electricity could reduce freshwater ecotoxicity impacts by up to 4%.

3.3.2.4. Mineral resource depletion

In this impact category, the bonding concept (B) performs considerably worse than the direct growth concept (A) and the single-Si reference systems. In concept B, the largest contributions to resource depletion result from the consumption of indium (47%), tantalum (25%), cadmium (6%) and silver (5%). The consumption of indium occurs mainly during the spray pyrolysis process which consumes indium trichloride in the solution. Tantalum is entirely consumed in the inverter, which is a BOS component required for all systems. Tantalum could also be used as anti-reflection coating layer; however, we have considered titanium dioxide instead. The other important components are the aluminium alloy for the panel and arsine.

Notably, the contributions to resource depletion from gallium and indium consumed in the MOVPE process are negligible in comparison. This may be attributable to the

low quantities of metalorganic precursors required per cell and the high precursor efficiencies achieved in the Aixtron reactor we modelled (gallium: 38%, indium: 27%, aluminium: 38%). To put these values in perspective, we calculated the consumption of these metals (both identified as critical materials by the European Commission[15]) for a large-scale yearly production of 1 GWp of III-V/Si cells. Such large-scale manufacturing would consume 818 kg of indium per year. The global refinery production of indium was 760 tonnes in 2019 (estimated).[40] Therefore, the III-V/Si market would demand 0.1% of current global supply.

On the other hand, manufacturing 1 GWp of III-V/Si cells would consume approximately 80 tonnes of gallium, ca. 25% of the current world production of primary gallium (320 tonnes in 2019, estimated[40]). The reason behind the low impact score of gallium in this category is that the ILCD impact assessment method we used is based on a rough estimate of total gallium reserves rather than production[41]. According to the U.S. Geological Survey, gallium contained in world resources of bauxite can exceed 1 million tons, and a considerable quantity is also contained in zinc resources.[40] Various authors have investigated the criticality of gallium and noted that current supply is still much lower than its actual potential.[42,43] As a result, such an increase in demand for III-V/Si cells would not necessarily compromise exploitable reserves, but could significantly change the future supply and market dynamics for gallium.

3.3.3. Uncertainty analysis

Figure 3-5 shows the results of the Monte Carlo simulations and presents the difference in impacts between the conventional single-Si systems and the III-V/Si systems. The positive values indicate a larger impact of single-Si. The Monte Carlo results show that the III-V/Si PV systems are overall likely to perform better environmentally than the commercial single-Si systems modelled in ecoinvent. In most cases, positive results appear to fall well within 75% confidence intervals. The exceptions to this are the impact categories of ionising radiation, where both III-V/Si systems perform worse than single-Si by a factor of between 1 and 2, and resource depletion, where concept A (direct growth) performs worse by a factor of around 0.1-0.5. It can also be seen that concept A performs slightly better than concept B (bonding) in all impact categories, although the difference appears to be relatively small (except for the resource depletion impact category). The modified null hypothesis test with an alpha value of 0.05 further confirmed the statistical significance of these differences.

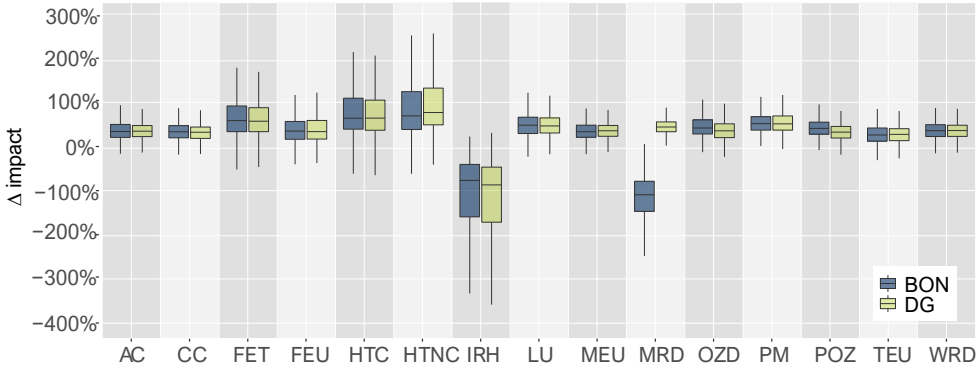

Figure 3-5 Monte Carlo simulation results for comparative impacts of III-V/Si PV systems vs. the reference single-Si PV system. Values are normalized to the deterministic impact score of the reference single-Si PV system. Positive values indicate a better performance of the III-V/Si systems. The middle line shows the median; the bottom and top edges of the box indicate the 25th and 75th percentiles respectively. The whiskers show minimum and maximum values, with outlier points removed.

3.3.4. Sensitivity analysis

3.3.4.1. Technological advances and supply chain optimizations

The reference single-Si PV system from ecoinvent v3.4 is representative of technologies installed before the year 2010.[21] However, several technological advances in single-Si PV have been made since then. For example, the aluminium back surface field (Al-BSF) technology has given way to the passivated emitter and rear contact (PERC) cells resulting in higher module conversion efficiencies.[44] There have also been considerable optimizations in the energy and materials used in the silicon supply chain, as well as in metallization, module and balance of system components.[45] These optimizations can also be expected to benefit the III-V/Si PV systems, but to a lesser extent. We therefore tested how these improvements could affect the comparative advantages and disadvantages of the III-V/Si PV systems vs. newer PERC single-Si systems.

As shown in Figure 3-6, the improved supply chains for silicon and BOS reduce the comparative climate change impact score of the reference single-Si system (Al-BSF) by 34%. These same material reductions lower the climate change impact of the III-V/Si systems by 24% because of the smaller impact of the silicon bottom solar cell and the improved panel and BOS infrastructure. Further implementation of PERC technologies and raising single-Si module conversion efficiencies to 17, 18 and 19% result in additional reductions of 13.3%, 2.7% and 2.3% respectively.

It is also expected that the fabrication of the III-V layers in the III-V/Si tandem cell will improve with the maturity of the technology in the future.[46–48] One of the largest contributions to the climate change impact is the energy consumption during the MOVPE process, which currently accounts for 8.8 kWh for one single 156x156 mm^2

wafer. This consumption was estimated based on a pilot MOVPE reactor design that can process 31 x 4-inch wafers per hour. By comparison, some modern day silicon chemical vapour deposition (CVD) reactors can process over 1000 wafers per hour[49], with energy consumptions as low as 0.014 kWh per wafer. If a similar performance is achieved with the III-V/Si process, this could result in an energy reduction in MOVPE of more than 99%, making the impact contribution of MOVPE almost negligible.

Figure 3-6 shows how such expected reductions in MOVPE energy consumption would decrease the comparative climate change impact score of the III-V/Si systems. There is roughly a 5% total impact reduction for each 30% MOVPE energy efficiency improvement. In the best scenario with negligible MOVPE energy consumption, the climate change impact score of the III-V/Si PV system comes down to 38 g CO_2eq per kWh electricity generated. In such situation, III-V/Si systems would perform better than the most advanced PERC Si systems in all impact categories except ozone depletion and photochemical ozone formation. In the former category, a small disadvantage (~3%) remains attributable to the methyl chlorides required for the production of metalorganic compounds. In the latter category, the remaining disadvantage (~5%) is attributable to the hydrogen gas consumed in the MOVPE process. Similar graphs for other impact categories are provided in the Appendix Figure A-2.2.

Next to energy efficiency improvements and increased throughput in MOVPE, external policies to increase the participation of renewables in the European energy mix can have an equally important effect. If we take the 2040 projections in the Sustainable Development Scenario proposed by the International Energy Agency[50], with 73% renewables, 16% nuclear, 10% natural gas and 1% coal, the contributions to climate change and human toxicity impacts from MOVPE alone would be reduced by more than 90%.

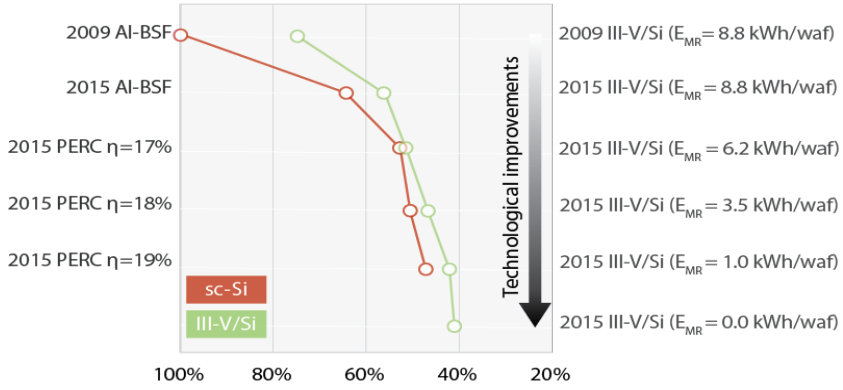

Figure 3-6 Change in climate change impact scores as a result of technological improvements. 2009: Reference data (2009) for silicon, module and BOS supply chains from ecoinvent v3.4; 2015: Updated IEA PVPS data (2015) for silicon, module and BOS supply chains; η: module efficiency; E_{MR}.: Energy consumption of MOVPE process per wafer.

3.3.4.2. Hazardous gas abatement

One parameter that is highly uncertain due to unavailability of data is the hazardous gas abatement process for MOVPE exhaust gases. The consumption of adsorbing granulate in this process was calculated from an experimental run conducted by Fraunhofer ISE in Freiburg, Germany. However, the precise granulate composition is undisclosed by the manufacturer and we used secondary data from literature.[51] We tested this assumption by modelling an additional worst-case scenario where the granulate had a composition of 80% copper oxide and 20% activated silica. We also assumed that none of the granulate is recycled or regenerated, which is not a realistic situation as important efforts in the industry to recover copper content are already being applied. With this setup, the increase in climate change impacts is negligible, and for freshwater ecotoxicity the impact of the hazardous waste process increased by 4%. For human toxicity, the impacts are more significant, and showed an increase of nearly 12%. These increases are mostly attributed to the consumption of copper oxide for preparation of the adsorbent granulate. In this worst-case scenario for hazardous waste, III-V/Si still outperforms single-Si with an 18% lower impact score. Reducing the amount of copper in the granulate may be an effective way to balance the impacts of increasing adsorbent requirements.

3.3.4.3. Carrier gases and inert atmospheres

Carrier or inert gases for processes like MOVPE, PECVD, ion implant and annealing are consumed in large volumes. Therefore, any change in their quantities or environmental profile could propagate throughout the whole system. Some authors have argued for the technical and environmental advantages of hydrogen over nitrogen for MOVPE[52,53], but overall there appears to be some room for flexibility. Based on our model, nitrogen performs better than hydrogen in terms of climate change by a factor of approximately 3 (1.04 vs. 0.32 kg CO_2eq per m^3 of gas). It also performs better in terms of photochemical ozone formation and particulate matter. In all other categories, it performs worse by an equal factor of 3. This indication appears unaffected by the different purification processes required for each gas.

The sourcing of these carrier and inert gases also merits closer inspection from an environmental perspective. We tested two options for hydrogen; on-site generation with a proton exchange membrane system (PEM) and procuring of commercially available liquefied hydrogen produced off-site via steam methane reforming (SMR). The latter option scored better by a factor of almost 3 in terms of climate change (2.77 vs 1.04 kg CO_2eq per cubic meter of gas) and by a factor of approximately 25 in terms of human health and freshwater ecotoxicity. The poor performance of the PEM system is related to the coal-based fraction of the energy mix. However, this could change significantly if the PEM system is powered with renewable electricity.

3.3.4.4. GaAs substrate (bonding method only)

The vertical gradient freeze (VGF) crystal growth method for GaAs substrates is quite energy intensive. It also consumes much more gallium because the substrate is considerably thicker than the III-V layers (by two orders of magnitude). Therefore, the reuse rate that is achievable for this substrate will be of high importance. There is a realistic potential for reuse >100 times, in which case the GaAs substrate would only be a minor contribution to the overall environmental footprint (ca. 2 g CO_2eq or 3% of total contribution). If the recycling rate falls to 30 times, the GaAs substrate would add 7 g CO_2eq, or 9% impact contribution. In this pessimistic scenario, the climate change impacts of the III-V/Si system would still be 20% less than the reference single-Si system.

3.3.4.5. Laser treatment vs. wet chemical processing

The laser processes involved (epitaxial lift-off and front-contact sintering) have also been attempted using wet chemical processing. We compared both alternatives to investigate whether there is an overall preference for laser-based methods, which are mostly dependent on energy inputs. For the lift-off process, the laser treatment contributed 1 g CO_2eq (ca. 1.5%), while a chemical treatment using approx. 1.4 gr of hydrogen fluoride per wafer would only contribute 0.17 g CO_2eq. (ca. 0.2%).

In sintering the nanoink-printed front contacts, the laser treatment contributed a negligible amount to all impact categories. We modelled an alternative lab-based process for chemical sintering of the nanoink, using 50 mL of formic acid, 5 mL of ethanol and 42 L of ultrapure nitrogen to sinter a 1 cm^2 sample. This process would contribute an additional 0.2 kg CO_2eq. to climate change, multiplying the total impact of the III-V/Si systems by a factor of nearly 3. An industrial setup for such process would have to be able to sinter a cell area 60 times larger using the same quantities of chemicals in order to keep the impact contribution within 5%. This suggests that laser sintering is a clearly preferred method from an environmental perspective.

3.3.4.6. Silver vs. copper nanoink for front contacts

Silver nanoink showed a slightly higher impact (+1-3%) than copper in most impact categories, when using the laser-based sintering method. However, these small relative differences would not make a noticeable change in the overall impact of the III-V/Si PV systems. On the other hand, silver nanoink can be sintered by thermal treatment in open air, i.e., it would not require the use of formic acid, ethanol and nitrogen. Therefore, if the chemical sintering method is chosen over laser sintering, then silver nanoink would be a much better option.

3.3.5. Potential recycling of III-V materials

The environmental benefits and technical feasibility of recycling important quantities of materials like glass, aluminium and silver from conventional silicon PV

modules have been discussed by various authors.[54] However, even after many years there are still important economic barriers hindering this and today only approximately 10% of silicon PV panels are recycled.[55] III-V/Si cells could present additional technical and economic challenges because of the complexity of the crystalline layers. Yet it may still be the case that waste management regulations or constricting markets promote the case for recycling of critical elements like gallium and indium from III-V/Si cells.

Scant work has been conducted to date on recycling of III-V cells, but significant work has been published on recycling of light-emitting diodes (LEDs) which have similar compositions of III-V materials and are also grown via MOVPE.[56–61] These methods, which include combinations of mechanical, chemical and thermal processing, have been able to recover more than 90% of gallium and indium. Yet they tend to be quite energy intensive, in some cases requiring processing temperatures of up to 1000°C to be sustained for long periods of time. A detailed assessment of such options is out of scope for this work, but some preliminary calculations can help to set expectations. Each modelled III-V/Si cell contains approximately 2.3 mg of indium and 220 mg of gallium (for concept A). Sourcing these quantities from virgin product adds a CO_2 footprint of 0.7 and 54 g CO_2eq respectively. These amounts set an upper threshold for the carbon emissions of the proposed recycling processes if environmental benefits are to be derived. For a comparative reference, annealing 100 cells at similarly high temperatures for 1 hour added 40 g CO_2eq per cell. Therefore, beyond criticality considerations discussed in section 3.3.2.4, it seems challenging for the recovery of III-V materials to deliver significant environmental benefits.

An additional incentive for recovery/recycling of III-V materials from the cells could be the avoidance of possible leaching of toxic arsenic compounds to soil and groundwater. Following a similar calculation as before, each III-V/Si cell contains 360 mg of arsenic. In a pessimistic scenario where the entirety of arsenic leached and infiltrated into groundwater, this would raise the freshwater ecotoxicity impact of the III-V/Si systems by roughly 260%. Note however that this is highly unlikely since the arsenic would be contained in a III-V crystal lattice and would be much less soluble under normal atmospheric conditions.

3.4. Conclusions

We can conclude that the environmental outlook of III-V/Si PV systems looks promising if module conversion efficiencies of 28% or above can be reached with a cost competitive product. Our results demonstrate that the higher conversion efficiency of III-V/Si tandem cells can indeed compensate for the impacts of the additional processes and materials used in its manufacturing. Since the operation phase of the III-V/Si system has negligible environmental inputs and outputs, the impacts are almost entirely (>99.99%) embedded in the infrastructure. The

infrastructure increases proportionally to the total module area required for the generation of 1 kWh, and the cell area is inversely proportional to cell efficiency. This creates a strong negative correlation between cell conversion efficiency and environmental impact, which reduces not only the impacts of the III-V/Si cell but also of the smaller panel framework and mounting system needed to produce the same amount of electricity.

We further showed through a sensitivity analysis that, factoring in technological advances of the past decade for single-PV and further process optimizations during upscaling of III-V/Si, the difference between both systems may eventually become narrower. In such a scenario, the deciding factors may then turn to limitations like space availability in urban areas (favouring III-V/Si) or criticality of specific materials like gallium (favouring single-Si).

Having probed every processing step and their commercially and technically viable alternatives, our investigation produced several important takeaways for III-V technology developers to prioritize in their designs. First, energy efficiency measures in the MOVPE process are the most effective way to improve the environmental profile of III-V PV technologies. Additional room for noticeable improvement in CO_2 footprint is in the thermal processing, where rapid thermal annealing or other more energy efficient methods can be pursued. Second, with respect to hazardous gases like arsine and phosphine, we have found that the toxic impacts (from an LCA perspective) are mostly attributed to the use of (primary) copper in the scrubber granulate that is required to absorb the gases. This is due to the fact that, under standard operating conditions, negligible quantities of arsine and phosphine are emitted directly to the environment.

Mining copper for the granulate does result in direct environmental emissions of heavy metals and other pollutants. Therefore, the industry's increasing focus on reusing copper in adsorbent granulates is well placed in order to manage the use of these gases sustainably. Third, on-site generation of carrier gases is only preferable when the electricity source powering the systems is mostly renewable. Fourth, epitaxial lift-off and bonding is also an environmentally acceptable manufacturing route insofar as GaAs substrate can be reused at least dozens of times, and the indium trichloride consumption for spray pyrolysis can be reduced or alternative adhesives proposed. In the bonding route, chemical lift-off is preferred over laser lift-off. Finally, chemical sintering of copper ink can introduce significant environmental burdens from the formic acid, therefore a laser sintering method is preferable.

While keeping these elements in mind, it is still the case that larger and more easily achievable improvements for both III-V and single-Si PV systems may come from improving the life cycle impacts of silicon wafers, panel frame and BOS components, where a large fraction of most impacts resides. These can come from

reducing the silicon wafer thickness and losses, and from using recycled or substitute materials for panel (aluminium) and electric components (copper).

References

1. Lee, T. D. & Ebong, A. U. A review of thin film solar cell technologies and challenges. *Renew. Sustain. Energy Rev.* **70**, 1286–1297 (2017).

2. Correa-Baena, J.-P. *et al.* The rapid evolution of highly efficient perovskite solar cells. *Energy Environ. Sci.* **10**, 710–727 (2017).

3. Kippelen, B., Brédas, J.-L., Kanwal, A., Miller, S. & Chhowalla, M. Organic photovoltaics. *Energy Environ. Sci.* **2**, 251 (2009).

4. Zhang, S., Yang, X., Numata, Y. & Han, L. Highly efficient dye-sensitized solar cells: Progress and future challenges. *Energy and Environmental Science* vol. 6 1443–1464 (2013).

5. Philipps, S. & Warmuth, W. *Photovoltaics Report*. Fraunhofer ISE (2018).

6. Cotal, H. *et al.* III–V multijunction solar cells for concentrating photovoltaics. *Energy Environ. Sci.* **2**, 174–192 (2009).

7. Zhou, Z. & Carbajales-Dale, M. Assessing the photovoltaic technology landscape: Efficiency and energy return on investment (EROI). *Energy Environ. Sci.* **11**, 603–608 (2018).

8. Arvidsson, R. *et al.* Environmental Assessment of Emerging Technologies: Recommendations for Prospective LCA. *J. Ind. Ecol.* **22**, 1286–1294 (2018).

9. NREL. Best Research-Cell Efficiency Chart | Photovoltaic Research | NREL. https://www.nrel.gov/pv/cell-efficiency.html (2019).

10. Green, M. A. *et al.* Solar cell efficiency tables (Version 53). *Prog. Photovoltaics Res. Appl.* **27**, 3–12 (2019).

11. Dimroth, F. III-V Solar Cells - Materials, Multi-Junction Cells - Cell Design and Performance. in *Photovoltaic Solar Energy* 371–382 (John Wiley & Sons, Ltd, 2017). doi:10.1002/9781118927496.ch34.

12. Cariou, R. *et al.* Monolithic Two-Terminal III-V//Si Triple-Junction Solar Cells with 30.2% Efficiency under 1-Sun AM1.5g. *IEEE J. Photovoltaics* **7**, 367–373 (2017).

13. Cariou, R. *et al.* III – V-on-silicon solar cells reaching 33 % photoconversion efficiency in two-terminal configuration. *Nat. Energy* **3**, 1–5 (2018).

14. Essig, S. *et al.* Raising the one-sun conversion efficiency of III-V/Si solar cells to 32.8% for two junctions and 35.9% for three junctions. *Nat. Energy* **2**, 17144 (2017).

15. European Commission. *Communication from the Commission to the European Parliament, the Council, the Eureopean Economic and Social Committee and the Committe of the Regions on the 2017 list of Critical Raw Materials for the EU*. https://eur-lex.europa.eu/legal-content/EN/TXT/?uri=CELEX:52017DC0490 (2017).

16. Graedel, T. E., Harper, E. M., Nassar, N. T., Nuss, P. & Reck, B. K. Criticality of metals and metalloids. *Proc. Natl. Acad. Sci.* **112**, 4257–4262 (2015).

17. ISO14040. Environmental management — Life cycle assessment — Principles and framework. *The International Organization for Standardization* (2006) doi:10.1136/bmj.332.7550.1107.

18. Guinée, J. B. *Handbook on life cycle assessment : operational guide to the ISO standards.* (Kluwer Academic Publishers, 2002).

19. Feifel, M. *et al.* Direct growth of III-V/Silicon triple-junction solar cells with 19.7% efficiency. *IEEE J. Photovoltaics* **8**, 1590–1595 (2018).

20. Fraunhofer ISE. Photovoltaic Trend: Tandem Solar Cells Record Efficiency for Silicon-based Multi-junction Solar Cell. (2019).

21. Wernet, G. *et al.* The ecoinvent database version 3 (part I): overview and methodology. *Int. J. Life Cycle Assess.* **21**, 1218–1230 (2016).

22. Schwartz, B. & Robbins, H. Chemical Etching of Silicon. *J. Electrochem. Soc.* **123**, 1903 (1976).

23. Feifel, M. *et al.* MOVPE Grown Gallium Phosphide-Silicon Heterojunction Solar Cells. *IEEE J. Photovoltaics* **7**, 502–507 (2017).

24. Blanco, C. F., Cucurachi, S., Peijnenburg, W. J. G. M., Beames, A. & Vijver, M. G. Are Technological Developments Improving the Environmental Sustainability of Photovoltaic Electricity? *Energy Technol.* 1901064 (2020) doi:10.1002/ente.201901064.

25. American Institute of Aeronautics and Astronautics. *Standard: Qualification and Quality Requirements for Space Solar Cells (AIAA S-111A-2014). Standard: Qualification and Quality Requirements for Space Solar Cells (AIAA S-111A-2014)* (American Institute of Aeronautics and Astronautics, Inc., 2014). doi:10.2514/4.102806.001.

26. Gerstmaier, T., Zech, T., Röttger, M., Braun, C. & Gombert, A. Large-scale and long-term CPV power plant field results. in *AIP Conference Proceedings* vol. 1679 030002 (American Institute of Physics Inc., 2015).

27. Muller, M., Jordan, D. & Kurtz, S. Degradation analysis of a CPV module after six years on-Sun. in *AIP Conference Proceedings* vol. 1679 020004 (American Institute of Physics Inc., 2015).

28. Algora, C. Reliability of III-V concentrator solar cells. in *Microelectronics Reliability* vol. 50 1193–1198 (Elsevier Ltd, 2010).

29. European Commission Joint Research Center - Institute for Environmental Sustainability. *ILCD Handbook: Recommendations for Life Cycle Impact Assessment in the European context. Vasa* http://eplca.jrc.ec.europa.eu/uploads/ILCD-Recommendation-of-methods-for-LCIA-def.pdf (2011) doi:10.278/33030.

30. Gavankar, S., Anderson, S. & Keller, A. A. Critical Components of Uncertainty Communication in Life Cycle Assessments of Emerging Technologies. *J. Ind. Ecol.* **19**, 468–479 (2015).

31. Weidema, B. *et al. Overview and methodology: Data quality guidelines for the ecoinvent database version 3.* https://www.ecoinvent.org/files/dataqualityguideline_ecoinvent_3_20130506.pdf (2011).

32. Heijungs, R. & Lenzen, M. Error propagation methods for LCA—a comparison. *Int. J. Life Cycle Assess.* **19**, 1445–1461 (2014).

33. Henriksson, P. J. G. *et al.* Product carbon footprints and their uncertainties in comparative decision contexts. *PLoS One* **10**, 1–11 (2015).

34. Heijungs, R., Henriksson, P. J. G. & Guinée, J. B. Measures of difference and significance in the era of computer simulations, meta-analysis, and big data. *Entropy* **18**, 361 (2016).

35. Mendoza Beltran, A. *et al.* Quantified Uncertainties in Comparative Life Cycle Assessment: What Can Be Concluded? *Environ. Sci. Technol.* **52**, 2152–2161 (2018).

36. Li, K. H. *et al.* Induction-heating MOCVD reactor with significantly improved heating efficiency and reduced harmful magnetic coupling. *J. Cryst. Growth* **488**, 16–22 (2018).

37. AIXTRON SE. AIX R6 Sets New Standards in LED Manufacturing. https://www.aixtron.com/en/investors/AIX R6 Sets New Standards in LED Manufacturing_n347 (2014).

38. Slotte, M., Metha, G. & Zevenhoven, R. Life cycle indicator comparison of copper, silver, zinc and aluminum nanoparticle production through electric arc evaporation or chemical reduction. *Int. J. Energy Environ. Eng.* **6**, 233–243 (2015).

39. Pourzahedi, L. & Eckelman, M. J. Comparative life cycle assessment of silver nanoparticle synthesis routes. *Environ. Sci. Nano* **2**, 361–369 (2015).

40. U.S. Geological Survey. *Mineral Commodity Summaries. Mineral Commodity Summaries* http://pubs.er.usgs.gov/publication/mcs2020 (2020) doi:10.3133/mcs2020.

41. European Commission, Joint Research Centre & Institute for Environment and Sustainability. *Characterisation factors of the ILCD Recommended Life Cycle Impact Assessment methods. Database and supporting information.* https://eplca.jrc.ec.europa.eu/uploads/LCIA-characterization-factors-of-the-ILCD.pdf (2012).

42. Frenzel, M., Ketris, M. P., Seifert, T. & Gutzmer, J. On the current and future availability of gallium. *Resour. Policy* **47**, 38–50 (2016).

43. Frenzel, M., Mikolajczak, C., Reuter, M. A. & Gutzmer, J. Quantifying the relative availability of high-tech by-product metals – The cases of gallium, germanium and indium. *Resour. Policy* **52**, 327–335 (2017).

44. M. Lunardi, M., Alvarez-Gaitan, J. P., Chang, N. L. & Corkish, R. Life cycle assessment on PERC solar modules. *Sol. Energy Mater. Sol. Cells* **187**, 154–159 (2018).

45. Frischknecht, R. *et al. Life Cycle Inventories and Life Cycle Assessment of Photovoltaic Systems.* http://iea-pvps.org/index.php?id=315 (2015).

46. Brien, D. *et al.* Modelling and simulation of MOVPE of GaAs-based compound semiconductors in production scale Planetary Reactors. *J. Cryst. Growth* **303**, 330–333 (2007).

47. Dauelsberg, M. *et al.* Modeling and process design of III-nitride MOVPE at near-atmospheric pressure in close coupled showerhead and planetary reactors. *J. Cryst. Growth* **298**, 418–424 (2007).

48. Beckers, A. *et al.* 45-3: Invited Paper: Enabling the Next Era of Display Technologies by Micro LED MOCVD Processing. *SID Symp. Dig. Tech. Pap.* **49**, 601–603 (2018).

49. Reber, S. *et al.* Advances in equipment and process development for high-throughput continuous silicon epitaxy. *27th Eur. Photovolt. Sol. Energy Conf. Exhib.* 2466–2470 (2012) doi:10.4229/27THEUPVSEC2012-3CV.2.34.

50. IEA. *World Energy Outlook 2019*. (OECD Publishing, 2019). doi:10.1787/78a72c2c-en.

51. Wang, X. *et al.* Arsine adsorption in copper-exchanged zeolite under low temperature and micro-oxygen conditions. *RSC Adv.* **7**, 56638–56647 (2017).

52. Schön, O., Schineller, B., Heuken, M. & Beccard, R. Comparison of hydrogen and nitrogen as carrier gas for MOVPE growth of GaN. *J. Cryst. Growth* **189–190**, 335–339 (1998).

53. Meijer, A., Huijbregts, M. A. J., Schermer, J. J. & Reijnders, L. Life-cycle assessment of photovoltaic modules: Comparison of mc-Si, InGaP and InGaP/mc-Si solar modules. *Prog. Photovoltaics Res. Appl.* (2003) doi:10.1002/pip.489.

54. Deng, R., Chang, N. L., Ouyang, Z. & Chong, C. M. A techno-economic review of silicon photovoltaic module recycling. *Renewable and Sustainable Energy Reviews* vol. 109 532–550 (2019).

55. Lunardi, M. M., Alvarez-Gaitan, J. P., Bilbao, J. I. & Corkish, R. A Review of Recycling Processes for Photovoltaic Modules. in *Solar Panels and Photovoltaic Materials* (ed. Zaidi, B.) (IntechOpen, 2018). doi:10.5772/intechopen.74390.

56. Van Den Bossche, A., Vereycken, W., Vander Hoogerstraete, T., Dehaen, W. & Binnemans, K. Recovery of Gallium, Indium, and Arsenic from Semiconductors Using Tribromide Ionic Liquids. *ACS Sustain. Chem. Eng.* **7**, 14451–14459 (2019).

57. Maarefvand, M., Sheibani, S. & Rashchi, F. Recovery of gallium from waste LEDs by oxidation and subsequent leaching. *Hydrometallurgy* **191**, (2020).

58. Zhan, L., Zhang, Y., Ahmad, Z. & Xu, Z. Novel Recycle Technology for Recovering Gallium Arsenide from Scraped Integrated Circuits. *ACS Sustain. Chem. Eng.* **8**, 2874–2882 (2020).

59. Zhan, L., Wang, Z., Zhang, Y. & Xu, Z. Recycling of metals (Ga, In, As and Ag) from waste light-emitting diodes in sub/supercritical ethanol. *Resour. Conserv. Recycl.* **155**, (2020).

60. Zhan, L., Xia, F., Xia, Y. & Xie, B. Recycle Gallium and Arsenic from GaAs-Based E-Wastes via Pyrolysis-Vacuum Metallurgy Separation: Theory and Feasibility. *ACS Sustain. Chem. Eng.* **6**, 1336–1342 (2018).

61. Zhang, Y., Zhan, L., Xie, B., Xu, Z. & Chen, C. Decomposition of Packaging Materials and Recycling GaAs from Waste ICs by Hydrothermal Treatment. *ACS Sustain. Chem. Eng.* **7**, 14111–14118 (2019).

62. Lichtensteiger, L. Kerf-free wafer slicing and thinning for semiconductor applications. in *2013 10th China International Forum on Solid State Lighting, ChinaSSL 2013* 85–88 (IEEE, 2015). doi:10.1109/SSLCHINA.2013.7177320.

63. Eichler, S. Green Gallium Arsenide (GaAs) Substrate Manufacturing. in *CS MANTECH Conference* (2010).

Chapter 4

Assessing the sustainability of emerging technologies: a probabilistic LCA method applied to advanced photovoltaics

Abstract

A key source of uncertainty in the environmental assessment of emerging technologies is the unpredictable manufacturing, use, and end-of-life pathways a technology can take as it progresses from lab to industrial scale. This uncertainty has sometimes been addressed in life cycle assessment (LCA) by performing scenario analysis. However, the scenario-based approach can be misleading if the probabilities of occurrence of each scenario are not incorporated. It also brings about a practical problem; considering all possible pathways, the number of scenarios can quickly become unmanageable. We present a modelling approach in which all possible pathways are modelled as a single product system with uncertain processes. These processes may or may not be selected once the technology reaches industrial scale according to given probabilities. An uncertainty analysis of such a system provides a single probability distribution for each impact score. This distribution accounts for uncertainty about the product system's final configuration along with other sources of uncertainty. Furthermore, a global sensitivity analysis can identify whether the future selection of certain pathways over others will be of importance for uncertainty in the impact score. We illustrate the method with a case study of an emerging technology for front-side metallization of photovoltaic cells.

Keywords: life cycle assessment; uncertainty analysis; global sensitivity analysis; emerging technologies; LCA; sustainability assessment

This chapter has been published as: Blanco, C.F., Cucurachi, S., Guinée, J.B., Vijver, M.G., Peijnenburg, W.J.G.M., Trattnig, R. and Heijungs, R. (2020) Assessing the sustainability of emerging technologies: A probabilistic LCA method applied to advanced photovoltaics, Journal of Cleaner Production, 259, 120968, https://doi.org/10.1016/j.jclepro.2020.120968.

4.1. Introduction

Whenever a new technology is proposed, the main concern from an environmental perspective is whether it will satisfy certain societal needs at the expense of introducing unwanted environmental burdens. This has happened often in the past, sometimes resulting in global-scale environmental issues that were not foreseen. Life cycle assessment (LCA) is until now the only environmental assessment method that can systematically reveal undesired environmental trade-offs that may result when an existing technology is replaced by a new one[1]. Because of this, the application of LCA in early research and development (R&D) stages has gained considerable traction in recent years[2] and is even recognized by the European Union as an essential component of the R&D projects it is funding[3].

The LCA method was originally developed to study systems for which sufficient information about material and energy inputs and outputs, as well as the cause-effect relationships throughout the entire supply-chain of a technology is obtainable. This is already challenging for well-established technologies, let alone for technologies that are in development and have not yet been commercialized. In both cases, many uncertainties arise from missing or inaccurate data, spatial and temporal variability of process parameters, spatial and temporal variability of characterization models, and inaccuracy of characterization models, amongst other sources[4–6]. The standard approach for dealing with these uncertainties in LCA is to represent them using stochastic parameters with probability distributions (e.g., uniform, normal or lognormal) instead of fixed values, and then propagate them by random sampling and calculation of the resulting impacts in numerous Monte Carlo simulations. Rather than a single impact score, this approach produces a probability distribution for the impact score which can also be described by its mean, mode, variance, percentiles, and/or other statistical descriptors[7].

For emerging technologies, the challenge of dealing with uncertainty is even greater because these technologies have not been tested in a real operating environment and many design aspects have not been settled yet[8–11]. At any given point in time during the R&D process, there are many unknowns as to how the numerous technical and economic roadblocks to a successful marketable product will be eventually overcome, if they are overcome at all. In addition to this, the technology must be evaluated in the future economic and environmental context in which it will be deployed. An LCA model that attempts to forecast the impacts of such an unproven and immature technology therefore has potentially larger and more diverse sources of uncertainty (Table 4-1).

Following the typology of Huijbregts et al.[4], some of these uncertainties can be represented as "parameter" uncertainties, e.g., when the quantities of material and energy inputs and outputs required in each manufacturing step may decrease as a result of future process optimizations. If reasonable estimates for the expected changes in these quantities is within reach, then this type of variation can be incorporated via the aforementioned Monte Carlo

Table 4-1 Additional uncertainty sources specific to LCA of emerging technologies.

LCA phase	Uncertainty source	Uncertainty type	Context in LCA of emerging technologies
Goal and scope	Functional unit	Scenario	The technology may ultimately be used in ways different than the one projected initially, or it may be used for multiple/different purposes.
	System boundary: end-of-life (EOL)	Scenario	The possibilities for reuse/recycling often develop after the technology has been deployed, and/or when it is economically feasible. It is not known if and how this will happen. Regulations may change with respect to EOL requirements.
Inventory	Unit process	Scenario	The manufacturing methods will most likely change as the technology moves from the lab to industrial scale.
	Flow quantities	Parameter	Cost and process optimizations will likely lead to reduced or substituted material and energy input/output flows.
	Allocation	Parameter	The parameters used to establish the criteria for allocation of multifunctional processes might change in time. E.g., forecasted market values in the case of economic allocation.
Impact assessment	Characterization model	Model	Novel materials may have unknown or insufficiently studied impact mechanisms or pathways.
	Characterization model: fate	Parameter	Landscape parameters that affect transport and fate of substances may change in time, e.g., global temperature.
	Characterization model: exposure	Parameter	Parameters that affect exposure e.g., population densities or diets may change in time.
	Characterization model: effect	Model	Marginal changes may result in exponentially larger effects as the baseline condition deteriorates. E.g., impact of increased radiative forcing on ecosystems.

methods using most LCA software. Other perhaps more consequential types of uncertainty are related to which specific manufacturing steps will ultimately enable the early design or concept to become technically and economically feasible. Numerous and widely diverse engineering solutions are proposed and tested during early R&D stages, and these may or may not be a part of a technology's future product system configuration once it reaches maturity. We refer to these different possible configurations as "technological pathways", each of which is further pursued and investigated in subsequent R&D stages in order to find the one that ensures technical and economic feasibility. This type of uncertainty can be classified as "scenario uncertainty" and has often been addressed in LCA by modelling each technological pathway as a separate scenario[2,8,12].

Assessing and comparing different scenarios is useful when a design choice can be made on sustainable grounds[13]. However, the usefulness of this approach is more limited when there is no choice, rather a technological pathway that will eventually emerge as the –often only - economically and technically viable option. If the LCA results are meant to guide funding decisions that must be made with the *current* state of information, a comparative assessment of two or more scenarios can be misleading, even more so if the probability of one occurring is higher than the other. Another limitation is of a more practical nature; considering all the different possible technological pathways, the number of scenarios will most likely become unmanageable and their interpretation confusing if not impracticable.

To address these limitations, in this paper we propose a probabilistic approach in which all technological pathways being pursued by the developer are combined in a single product system. The competing pathways are activated or deactivated in each Monte Carlo run according to their probabilities of success by stochastic triggers or switches that are built into the LCA model. This type of model setup builds upon those proposed by other authors for combining different scenarios and/or modelling choices in single product systems[4,14–16]. It has been shown that these models allow the joint propagation of parameter, scenario and model uncertainties, producing a single probability distribution for the studied system's impact score.

The framing and methods we propose extend and refine the previous work of these authors in various ways. First, in applying this approach to emerging technologies we propose a clear separation between (i) uncertainty about the potential success of competing technological pathways, and (ii) uncertainty introduced by subjective modelling choices or preferences related to allocation, system boundaries, and future external scenarios. The former constitutes an inherent uncertainty about the product system and its effect is appropriately reflected by a single output impact score distribution. The latter, on the other hand, is best investigated as separate scenarios, in order to distinguish the effects of subjective choices and make them more transparent.

To further differentiate between (i) and (ii), we note that the stochastic triggers we use in (i) to activate technological pathways are objective parameters with a *true* value: each pathway either can or cannot overcome the technical and economic barriers the technology concept faces, but this is unknown at present by the developer. This true value –the uncertainty of which is adequately characterized by a Bernoulli distribution - will only be found by future R&D and testing. On the other hand, subjective value choices as in (ii) do not have an empirical "true" value and their joint propagation risks masking the effect of such subjective choices, reducing model transparency[15].

Second, our method investigates the effects of uncertainty about the probabilities (chances of success) of each pathway/scenario, which most likely exists in early R&D. This uncertainty about the input probabilities is often called second-order uncertainty[17,18]. We characterize these uncertainties using different types of probability distributions for these

parameters other than uniform, allowing for a more refined and realistic representation of the expectations of technology developers.

Finally, we demonstrate the application of a global sensitivity analysis (GSA) method that is suitable for such a model and highlights which uncertainties - including those from competing technological pathways as well as second-order uncertainties - are most relevant from an environmental perspective. Our aim with this is to identify incentives to more actively pursue research towards resolving the most sensitive ones. If they cannot be resolved, the information can and should be used to select the more relevant pathways that merit further investigation via e.g., local sensitivity analysis. In this case, the definition of scenarios for further investigation as a subsequent step becomes more objective and systematic, as the modeller will have quantitative criteria to select those that are most relevant.

4.2.Methods

4.2.1. Configuring the parametrized product system

To perform LCA calculations on a single system that combines different technological pathways, we use random parameters that activate or deactivate the inputs from the competing processes according to their underlying probabilities of occurrence (i.e., chances of success). To each competing process, we attach a random trigger that takes on a value of 0 or 1, so that it activates or deactivates the process flow according to a defined Bernoulli distribution function. The Bernoulli distribution is a discrete distribution that has two possible outcomes: success (=1) occurs with probability π, and failure (=0) occurs with probability 1- π, where $0<p<1$ [19].

Step 1: Identify the relevant technological pathways. The first step is to screen for the possible technological pathways that are being pursued, and the corresponding unit processes that are to be included in the single product system. This can be aided by a quick-scan lab-scale LCA and by eliciting expert knowledge and expectations of technology developers. The result of this step is a tree of possibilities that includes a number of pathways to fulfil the intended function(s) of the technology. This step would screen for alternative competing unit processes in all life-cycle stages, including manufacturing but also use and end-of-life options.

Step 2: Set up the product system. The competing unit processes (process X and process Y) are connected as providing simultaneous inputs to process Z as shown in Figure 4-1.

Step 3: Determine the required flows. Each competing process may contribute in a different way. For example, process Z may use either 1 kg of the product made by process X or 2 kg of the product made by process Y. Both quantities are added to the process Z as if they occur simultaneously, so the inputs of process Z are 1 kg of product from process X and 2 kg of product from process Y.

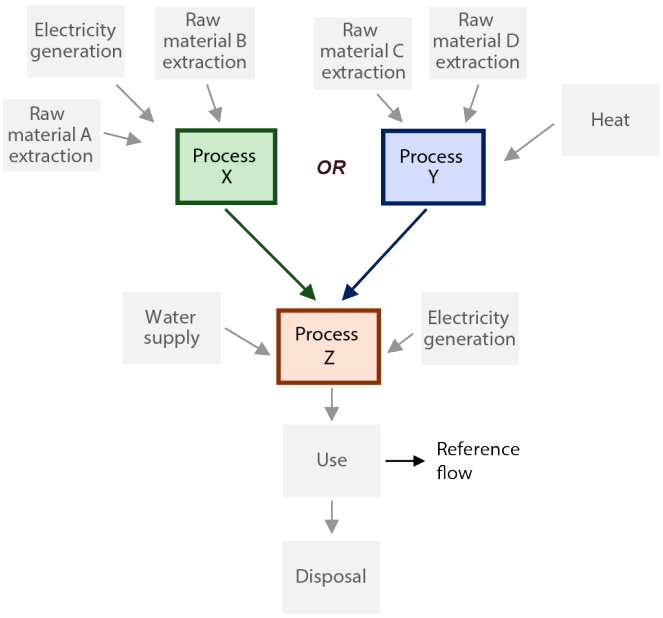

Figure 4-1 Product system with a process (Z) that requires an input from two competing, mutually exclusive process (X or Y).

Step 4: Determine the probabilities of occurrence of each flow. The probability of occurrence of X or Y will most likely be determined based on expert knowledge or expectations from the technology developers about technical and/or economic feasibility. For example, they may be estimated by looking at trends in related technologies, or by using economic forecasts for each alternative as a proxy. The criteria should be tightly linked to the functional unit of the technology, and the chances each option has of contributing to this function in an optimal (technical and economic) way. We define π as the probability of process X being selected, where π is a value between 0 and 1. Then the probability of process Y being selected is 1- π.

Step 5: Define parameter T. We will use a random number *T* to switch each flow on or off, by taking 1 for 'on' and 0 for 'off'. We generate T from a Bernoulli distribution, which is equivalent to a binomial distribution with 1 single trial (n=1) and probability π.

$$T \sim bin(n=1, \pi)$$

If there are more than two competing unit processes for the same element of the technology's product system, the generalized version of the Bernoulli distribution can be used, namely the categorical distribution. In this case we would define the probability of process X as π_x, the probability of process Y as π_y, and the probability of process Z would be $\pi_z = 1 - (\pi_x + \pi_y)$. A similar result can be achieved by nesting the alternatives so that their combined probabilities result in the desired individual probabilities (see Appendix Section A.3.1 for implementation notes).

Step 6: Apply the triggers to each flow. Because they are competing processes, only one flow can be activated at a time. This is achieved by multiplying process Z's input from process X by *[T]* and the input from process Y by *[1-T]*.

Step 7: If applicable and known, add uncertainty to the probability of occurrence (success) of each flow. The probabilities of each flow occurring may be given as a range, rather than fixed. For example, "the chance of using process X instead of process Y may be between 30% and 50%". In this case, a uniform distribution with minimum 0.3 and maximum 0.5 can be used. The uncertainty about the probabilities can be characterized in even more detail by using non-uniform distributions. Such is the case when a range of probabilities is expected, but there is more confidence around a certain value. For example, the chance of using process X instead of process Y is between 30% and 50%, but most likely 40%. This can be characterized by a triangular distribution with min 0.3, max 0.5 and mode 0.4. To implement this, the uncertainty distribution is directly applied to parameter π in the equations above. Wide ranges can be used in this step when there is limited knowledge about the probabilities. The relevance of this second-order uncertainty will be investigated afterwards in the global sensitivity analysis, indicating whether further efforts are necessary to make the predictions more accurate.

Step 8: Run the Monte Carlo simulation. The Monte Carlo simulation is run for the single product system. In each run, uncertain flows and characterization factors will take on random values according to their underlying probability distributions, and the effects propagated towards the calculation of the impact score. In the same way, the random triggers will randomly activate or deactivate the alternative technological pathways, according to their chances of success. The sampling in each run is done in a dependent way as recommended by Henriksson et al.[20] and Mendoza Beltran et al.[21], in order to ensure that shared unit processes across both systems take the same random values in each run. The inventory or impact assessment output will represent a future system that has a probability π of using process X and a probability π *-1* of using process Y.

Step 9: Global sensitivity analysis. Several sensitivity indices and the corresponding algorithms to calculate or estimate them have been proposed for GSA[22]. These methods can calculate or estimate how much each uncertain input contributes to the model's output variance, for all or a subset of uncertain input parameters. For our model we propose the delta moment-independent sensitivity measures[23] which had previously been implemented in LCA by Cucurachi et al.[24]. Various methods have been proposed to estimate the delta measures[25,26]; we used the *betaKS3* MatLab subroutine developed and provided by E. Plischke and E. Borgonovo upon request[27] (see Appendix Section A.3.2).

The sensitivity measure and corresponding estimation algorithm we propose present several important advantages for our model: (i) it accounts for possible correlations between uncertain input parameters; (ii) it has a significantly faster computation time and less memory usage, which is essential for models with tens or hundreds of thousands of uncertain parameters as in the case of large LCA databases like ecoinvent[28]; (iii) it is

independent of the model and only requires the values taken by the uncertain input parameters and the outputs (impact scores) in each Monte Carlo run, making them easy to apply in LCA; (iv) it is moment-independent, i.e. reflects expected changes in the actual output distribution rather than an approximated curve fit (typically a lognormal distribution with an estimated mean and variance). This is especially important in our framing given that, as we will show, the superposition of different technological pathways may produce output impact score distributions with more than one peak (multimodal or heteroscedastic). In such cases, variance-based sensitivity measures would not provide accurate estimates of importance. Finally, (v) it can take uncertain input parameters with discrete distributions, such as the binomially distributed triggers we used.

4.2.2. Case study of emerging photovoltaic technologies

We applied the method to a real-life case study in order to determine whether it was computationally feasible, if the results are in line with expectations and to further explore what types of conclusions can be drawn from the analysis. For this, we chose an emerging technology for metallization of the front electric contacts of photovoltaic (PV) cells that uses silver or copper metallic nanoinks. The special properties of the nanoparticles in the ink enhance the cell's performance by reducing the shadow, i.e. the area of cell that is covered by the metallic patterns and does not receive sunlight. It can also reduce the amount of silver required vs. traditional screen-printing methods. The case study is an ideal situation to investigate whether secondary materialization is occurring, while many possible configurations of the manufacturing and mainstream use of the technology are yet to be resolved. The concept of secondary materialization, introduced by Williams et al.[29], suggests that *"technological progress tends to increase energy and material use associated with products and is thus a counterforce to efficiency improvements attributed to dematerialization"*.

Preparation of the metallic nanoinks starts with the manufacturing of metallic nanoparticles via one of two possible routes; physical (or "top-down") methods apply energy to fracture larger particles to nanoscale sizes, and chemical (or "bottom-up") methods create the nanoscale particles from even smaller molecules using chemical reactions [30]. We based our calculations for these processes on the life-cycle inventories reported by Pourzahedi and Eckelman[31] and Slotte and Zevenhoven[32]. The nanoinks consist of a solution of metallic nanoparticles in alcohol/hydrocarbon (for silver) or polymer (for copper) and are deposited in patterns on the front side of the cell by inkjet printing to form an initial "seed layer". The printed patterns then have to be sintered, using either a thermal (laser) or a chemical process that consolidates the metallic particles in the pattern [33]. Sintering of silver nanoparticles can be done in open air, while copper nanoink requires an oxygen-free atmosphere to avoid formation of undesired oxides on the contacts[34]. Once sintered, the fingers are grown to a final thickness of 12.5μm by electroplating. Three busbars are placed on the cell using the conventional screen-printing methods that are used for the fingers in most commercially available silicon PV cells.

Figure 4-2 and Table 4-2 show the different competing alternatives and the parameter values used in the model. Additional calculation notes are presented in Appendix Section A.3.3.

In addition to the five stochastic triggers *T1-T5* and their uncertain probabilities of success π*1*- π*5*, we also included three input parameters subject to the more conventional form of uncertainty commonly addressed in LCA. First, we varied the amount of sintering gas mixture consumed per PV cell, dividing it by a random, triangularly distributed value (*P6*) with min:1, mode:5 and max:10. Second, we considered uncertainty in the amount of electrolyte solution consumed in electroplating per PV cell, i.e. how many cells can be treated per batch. We represented this by a parameter *P7* that divided the amount of solution required by a random, triangularly distributed value with min:10, mode:50 and max:100. Finally, we considered a potential increase in cell conversion efficiency of between 0.5 and 2%. We represented this by a parameter *P8* that multiplied the PV cell area required to produce 1 kWh by a uniformly distributed value between 0.98 and 0.995.

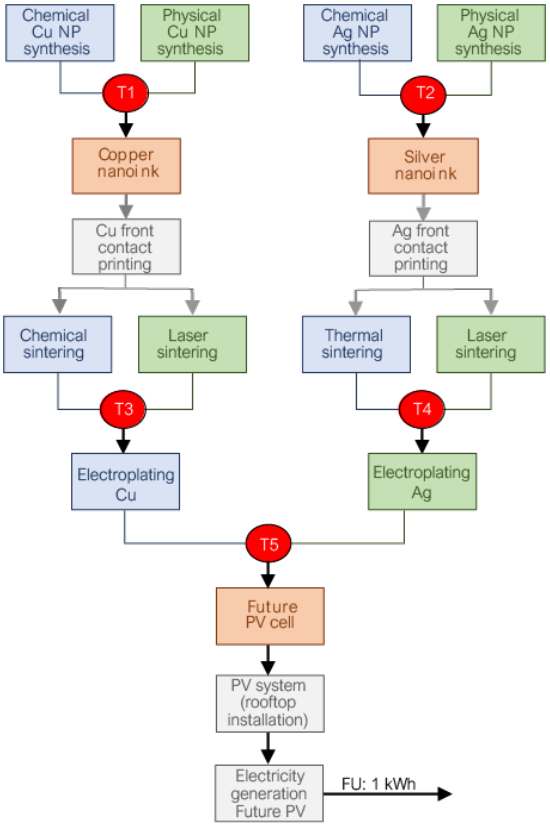

Figure 4-2. Product system for the generation of electricity using a solar cell with nanoink-printed front contacts, considering different alternative manufacturing pathways. T variables identify the triggers that select one or the other of the competing alternatives.

Table 4-2 Parameter definitions for possible manufacturing pathways of nanoink printed front contacts in photovoltaic cells. T variables identify the triggers (Figure 4-2) and π values the probability for the least likely unit process in the competing pair.

T	Description	π	Expected chance of success	Uncertainty about chance of success π: type	Uncertainty about chance of success π: parameters	Justification
T1	Synthesis route for Cu nanoparticles. Success = chemical route, failure = physical route.	π1	0.7	Triangular	Min: 0.5 Mode: 0.7 Max: 0.8	Chemical methods provide more control over particle size and shape, which may ultimately be more important for the nanoink.
T2	Synthesis route for Ag nanoparticles. Success = chemical route, failure = physical route.	π2	0.7	Triangular	Min: 0.5 Mode: 0.7 Max: 0.8	Chemical methods provide more control over particle size and shape, which may ultimately be more important for the nanoink.
T3	Sintering method for Cu nanoink. Success = chemical sintering, failure = laser sintering.	π3	0.2	Triangular	Min: 0.1 Mode: 0.2 Max: 0.3	Based on initial trials, the chemical sintering method had not performed as well as the laser methods. In addition to this, it may be easier to upscale the laser process.
T4	Sintering method for Ag nanoink. Success = thermal sintering, failure = laser sintering.	π4	0.5	Uniform	Min: 0 Max: 1	At the time of assessment, there was no particular indication of the performance of each method.
T5	Metallic nanoink used for seed printing of front contacts. Success = Cu nanoink, failure = Ag nanoink.	π5	0.8	Triangular	Min: 0.5 Mode: 0.5 Max: 0.8	Based on preliminary tests for technical feasibility, copper-based nanoink seemed “more promising”, while silver-based nanoink was not discarded.

We then ran a (dependent) Monte Carlo simulation of n=1000 runs to calculate and compare the impact scores of the nanoink printed PV cell with a conventional screen-printed PV cell. For this comparison we defined the functional unit as the generation of 1 kWh of electricity. For the conventional cell, we used the inventory data for single-Si

photovoltaics from the LCA database ecoinvent v2[28], and incorporated uncertainty in the background input/output flows provided by ecoinvent. We focused on four impact categories: climate change, ozone depletion, human toxicity and freshwater aquatic ecotoxicity, all based on the ReCiPe impact assessment method[35].

We then used the modified null hypothesis significance test proposed by Heijungs et al. (2016) to determine whether the differences in impact scores between the types of systems were statistically significant. The choice of the modified version of the test responds to the fact that it is well suited for early stages in technology development, where we the size (or relevance) of the difference is important. In other words, differences that are not relevant enough should not provide a basis to deter continued research and development while the potential benefits of the technology are still uncertain. To implement the modified null hypothesis significance test we used the excel based tools developed by Mendoza-Beltrán et al.[21].

4.3. Results and discussion

4.3.1. Comparative impact assessment of PV systems

The distribution of the climate change impact scores for both types of PV systems (nanoink-printed and conventional screen-printed cells) are shown in Figure 4-3. The impact score distributions of both systems mostly overlap around 0.08 kg CO_2eq, except for an additional peak around 0.15 kg CO_2eq for the nanoink-printed cells. This is in line with our expectation to find multimodal output distribution curves, and further strengthens the case for the use of moment-independent global sensitivity measures (this is further discussed in Section 3.2). By looking at the impact contributions of the individual foreground processes, we were able to determine that the additional peak around 0.15 kg CO_2eq corresponded to the chemical sintering pathway for the copper nanoink option

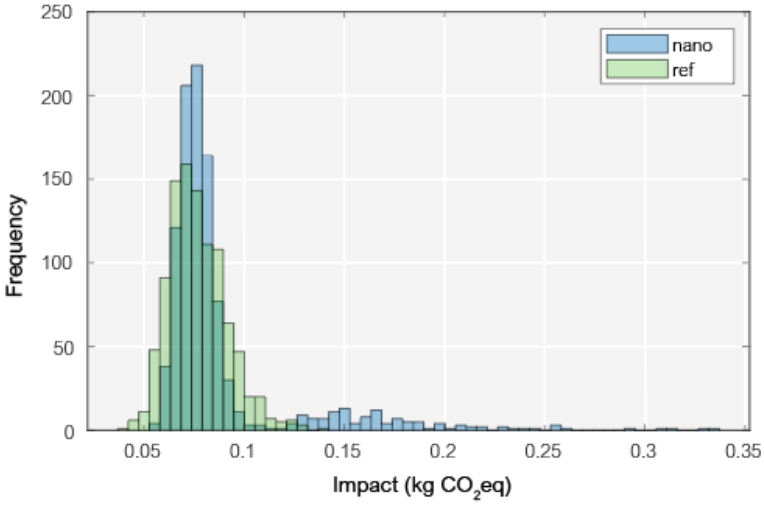

Figure 4-3 Comparison of climate change impacts of a PV system with nanoink-printed cells (nano) and a conventional screen-printed cells (ref)

which had a low probability of success (hence the lower frequencies), but was the only pathway that could result in impacts in this higher range.

Having a single probability distribution for the impact scores, we can draw general conclusions about the expected impacts of the nanoink-printed PV technology. For climate change, for example, the impacts will range between 0.05-0.2 kg CO_2 eq, and the impact will remain below 0.167 kg CO_2 eq for the 95th percentile. These and other statistics are summarized in Table 4-3.

The boxplot in Figure 4-4 shows the mean and percentiles for the *differences* in impact scores, relative to the reference system and for the four impact categories investigated. A positive percentage value (above the dotted red line) means a higher impact score for the nanoink printed cells. The medians (central black lines) of all values are higher, suggesting a slightly worse performance for the nanoink-printed cells. However, the difference in performance does not appear to be strongly conclusive, given that an important part of the boxes (25th and 75th percentiles) in all cases remains below 0%.

Table 4-3 Statistical descriptors for the impact score distributions of the nanoink-printed PV system and the conventional screen-printed system (Ref system).

Statistical parameter	Nanoink printed system	Ref system
Climate change (kg CO2 eq)		
Arithmetic mean	0,088	0,077
Geometric mean	0,083	0,076
Median	0,077	0,075
5th percentile	0,064	0,057
95th percentile	0,167	0,103
Ozone depletion (kg CFC-11 eq)		
Arithmetic mean	1,73E-08	1,54E-08
Geometric mean	1,62E-08	1,50E-08
Median	1,50E-08	1,49E-08
5th percentile	1,17E-08	1,03E-08
95th percentile	3,25E-08	2,25E-08
Human toxicity (kg 1,4 DCB eq)		
Arithmetic mean	0,229	0,212
Geometric mean	0,185	0,173
Median	0,170	0,159
5th percentile	0,085	0,081
95th percentile	0,534	0,502
Freshwater ecotoxicity (kg 1,4 DCB eq)		
Arithmetic mean	0,0026	0,0024
Geometric mean	0,0024	0,0022
Median	0,0023	0,0021
5th percentile	0,0013	0,0013
95th percentile	0,0049	0,0043

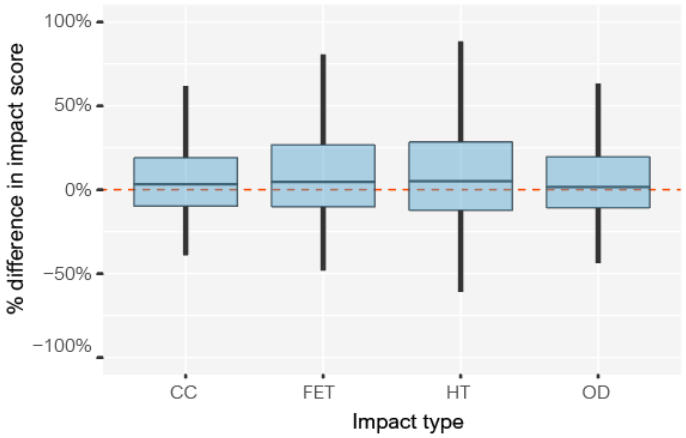

Figure 4-4 Distribution of difference in impact scores of nanoink-printed cell, relative to the impact score of the screen-printed cell (ref). CC: Climate Change; OD: Ozone Depletion; HT: Human Toxicity; FET: Freshwater Ecotoxicity.

In order to discern whether these differences were statistically significant or not, we used the modified null hypothesis significance test [36] with an alpha-value of 0.05 and a d-value of 0.2. The test concluded that only the climate change and freshwater ecotoxicity impact scores of the reference screen-printed cell was lower. For the other impact categories, the differences were not statistically significant.

4.3.2. Global Sensitivity Analysis (GSA)

The Borgonovo delta sensitivity measures[23] are listed for the stochastic triggers and other uncertain foreground parameters in Table 4-4**.** The most important contribution to variance in the climate change impact score comes from trigger T3, which selects between the chemical and laser sintering for the copper nanoink pathway. This is followed in order of importance by trigger T5, which selects between the copper and silver nanoink front contacts for the cell. The third most important parameter was not a trigger, but the amount of gas mixture that could be used to treat each cell in the chemical sintering procedure. The three most sensitive parameters are therefore in the copper nanoink with chemical sintering route. These can all be traced to the potentially very large impact contribution that can result from formic acid consumption in the chemical sintering route for copper.

Table 4-4 Delta sensitivity measure estimates for the climate change impacts of the PV system with nanoink printed front contacts.

Uncertain input parameter	δ est.	Rank
π1: Chance of success of T1	0.01	10
π2: Chance of success of T2	0.00	6
π3: Chance of success of T3	0.02	5
π4: Chance of success of T4	0.02	4
π5: Chance of success of T5	0.02	9
T1: Chem. vs. phys. synthesis of Cu nanoparticles	0.00	12
T2: Chem. vs. phys. synthesis of Ag nanoparticles	0.01	11
T3: Chem. Vs. laser sintering: Cu ink	0.20	1
T4: Thermal vs. laser sintering: Ag ink	0.01	13
T5: Cu vs. Ag printed front contacts	0.10	2
Qty. of gas mix required for Cu nanoink sintering	0.04	3
Qty. of solution required for electroplating	0.01	7
Cell conversion efficiency increase	0.01	8

4.3.3. Factor fixing

With the sensitivity ranking obtained from the GSA, we proceeded to factor fixing[37] in order to investigate further how the environmental profile of the technology would change if the most sensitive parameters were fixed. In this case, we tested trigger T3, which by the final stages of this study was looking less likely to favour a chemical sintering route for copper nanoink due to various technical challenges. Therefore, we updated T3 to a constant value of 0 so that the laser sintering route was always chosen for copper-based nanoink. We then ran a similar Monte Carlo simulation for the updated system and produced the results shown in Figure 4-5.

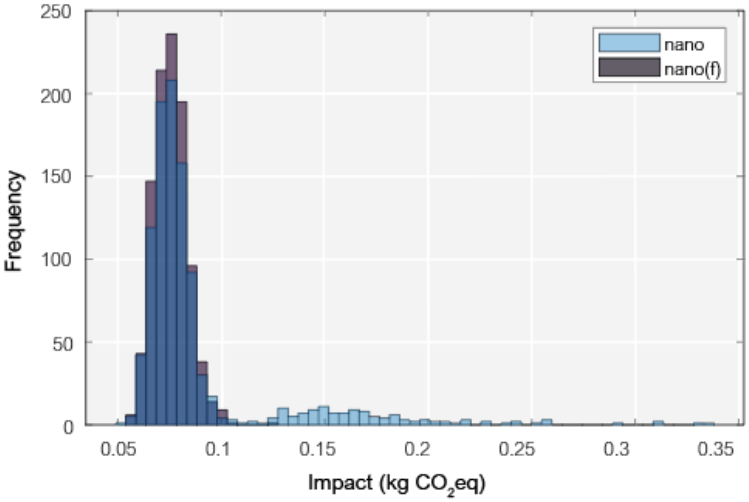

Figure 4-5 Comparison of climate change impacts of a PV system with nanoink-printed cells with both laser and chemical sintering alternatives for copper nanoink (nano) and with only laser sintering alternative for copper nanoink (nano(f)).

With all other triggers left to vary freely, the impact profile of this updated technology improved considerably. The peak around 0.15 kg CO_2eq disappeared, and the spread of the impact score distribution diminished noticeably. The geometric mean of the climate change impact score for the updated system decreased by 10% (75 g CO2 eq) and the 95th percentile by 46% (90 g CO2 eq). The geometric means for ozone depletion, human toxicity and freshwater ecotoxicity decreased by 15%, 3% and 8% respectively.

We performed a similar significance test on the updated results in order to confirm if – under these new constraint –statistically significant differences could be observed. The results indicate that discarding the chemical sintering of copper nanoink as an optional pathway results in a statistically significantly lower climate change impact score for the nanoink-printed cells vs. the conventional screen-printed cells. For other impact categories, there are no statistically significant differences.

4.3.4. Insights from the application of the method

An important aspect addressed in our method is the fact that the chances of success π are uncertain and must be determined using subjective criteria to a certain degree. The implementation of Step 7 allowed us to factor this in and investigate the relevance of these uncertainties by including the uncertain parameters π in the global sensitivity analysis. The results of our case study suggested that these second-order uncertainties about the probabilities of success π of each trigger did not have important effects on the model's output variance.

There are theoretical reasons to believe that uncertainty about the probability π has no influence on the overall result in a Monte Carlo type of sampling. After all, when we sample from a binomial distribution with probability π and sample size n (say, 1000), the expected number of times we have chosen a certain technological pathway is $n \times \pi$. When we modify the setup and use a binomial distribution with probability equal to $\pi+\varepsilon$, where ε is, for instance normally distributed with mean 0 and standard deviation σ, the expected number of times we have chosen this technological pathway is $n \times \pi + 0 = n * \pi$, because the expected value of this normal distribution is 0.

To further verify this, we fixed parameter $\pi 3$ in order to give a certain chance of success for *T3* of 20% and repeated the Monte Carlo simulation. The results are shown in Figure 4-6, showing only a very small shift in the distribution curves as expected. Further exploration of this perhaps unexpected finding is out of scope for this study, but we believe worthy of investigation in future work. Nevertheless, addressing uncertain probabilities in the method makes an important step in moving from probability theory to possibility theory [38], without yet making the full turn.

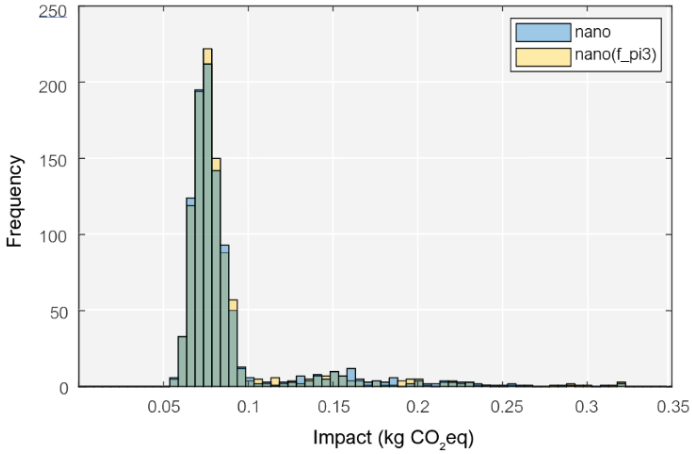

Figure 4-6. Comparison of climate change impacts of a PV system with nanoink-printed cells with uncertain chance of success for chemical sintering alternatives for Cu nanoink (nano) and with certain probability of success (nano(f_pi3)).

4.4. Conclusions

The application of the probabilistic method to the case study proved that calculation of such a model is feasible and the results fall within expectations as verified by the shapes of the distributions in Figure 4-6. Additionally, we demonstrated the important analytical possibilities offered by the method, and successfully addressed the conceptual and practical limitations of the scenario approach for the specific case of uncertain technological pathways. This probabilistic approach better represents the fundamental reality of the technological system under scrutiny when these pathways will only be resolved in a future stage. In early R&D stages, and with the existing state of knowledge of the system, these possible branches of the technology are better represented as a single system with a single range of potential impacts and specific probabilities attached to each value. This interpretation is fundamentally different from making numerous *if/then* conclusions about the system's environmental performance in different scenarios. It can especially provide a more robust basis and –if desired- a more conservative basis for considering future environmental impacts in current decisions.

The proposed framing also demonstrated to be better suited for a global sensitivity analysis that allowed us to identify the most sensitive parameters from a wider spectrum of uncertainty sources, including whether the future selection of one unit process instead of another is relevant for the variance in the system's impact score. The combination of the probabilistic LCA model with GSA can now be used to answer two fundamental questions about the sustainability of an emerging technology in a more robust and realistic way. The first question being whether an emerging technology with unresolved pathways is likely to outperform the incumbent technology, and to what degree of confidence. The second question being to what extent the assessment depends on the chances of success of the technological pathways being pursued.

References

1. Guinée, J. B. *Handbook on life cycle assessment : operational guide to the ISO standards.* (Kluwer Academic Publishers, 2002).

2. Cucurachi, S., Van Der Giesen, C. & Guinée, J. Ex-ante LCA of Emerging Technologies. *Procedia CIRP* **69**, 463–468 (2018).

3. European Commission Joint Research Centre. European Platform on LCA - Funded Research Programs. http://eplca.jrc.ec.europa.eu/EUFRP/ (2019).

4. Huijbregts, M. A. J., Gilijamse, W., Ragas, A. M. J. & Reijnders, L. Evaluating Uncertainty in Environmental Life-Cycle Assessment . A Case Study Comparing Two Insulation Options for a Dutch One-Family Dwelling. *Environ. Sci. Technol.* **37**, 2600–2608 (2003).

5. Igos, E., Benetto, E., Meyer, R., Baustert, P. & Othoniel, B. How to treat uncertainties in life cycle assessment studies? *Int. J. Life Cycle Assess.* 1–14 (2018) doi:10.1007/s11367-018-1477-1.

6. Lloyd, S. M. & Ries, R. Characterizing, Propagating, and Analyzing Uncertainty in Life-Cycle Assessment: A Survey of Quantitative Approaches. *J. Ind. Ecol.* **11**, 161–179 (2008).

7. Groen, E. A., Heijungs, R., Bokkers, E. A. M. & de Boer, I. J. M. Methods for uncertainty propagation in life cycle assessment. *Environ. Model. Softw.* **62**, 316–325 (2014).

8. Arvidsson, R. *et al.* Environmental Assessment of Emerging Technologies: Recommendations for Prospective LCA. *J. Ind. Ecol.* **22**, 1286–1294 (2018).

9. Bergerson, J. A. *et al.* Life cycle assessment of emerging technologies: Evaluation techniques at different stages of market and technical maturity. *J. Ind. Ecol.* jiec.12954 (2019) doi:10.1111/jiec.12954.

10. Hetherington, A. C., Borrion, A. L., Griffiths, O. G. & McManus, M. C. Use of LCA as a development tool within early research: Challenges and issues across different sectors. *Int. J. Life Cycle Assess.* **19**, 130–143 (2014).

11. Villares, M., Işıldar, A., van der Giesen, C. & Guinée, J. Does ex ante application enhance the usefulness of LCA? A case study on an emerging technology for metal recovery from e-waste. *Int. J. Life Cycle Assess.* 1–16 (2017) doi:10.1007/s11367-017-1270-6.

12. Valsasina, L. *et al.* Life cycle assessment of emerging technologies: The case of milk ultra-high pressure homogenisation. *J. Clean. Prod.* **142**, 2209–2217 (2017).

13. Höjer, M. *et al.* Scenarios in selected tools for environmental systems analysis. *J. Clean. Prod.* **16**, 1958–1970 (2008).

14. Mendoza Beltran, A., Heijungs, R., Guinée, J. & Tukker, A. A pseudo-statistical approach to treat choice uncertainty: the example of partitioning allocation methods. *Int. J. Life Cycle Assess.* **21**, 252–264 (2016).

15. Gregory, J. R., Noshadravan, A., Olivetti, E. A. & Kirchain, R. E. A Methodology for Robust Comparative Life Cycle Assessments Incorporating Uncertainty. *Environ. Sci. Technol.* **50**, 6397–6405 (2016).

16. Azari Jafari, H., Yahia, A. & Amor, B. Assessing the individual and combined effects of uncertainty and variability sources in comparative LCA of pavements. *Int. J. Life Cycle Assess.* **23**, 1888–1902 (2018).

17. Borsotto, M., Zhang, W., Kapanci, E., Pfeffer, A. & Crick, C. A junction tree propagation algorithm for Bayesian networks with second-order uncertainties. in *Proceedings - International Conference on Tools with Artificial Intelligence, ICTAI* 455–462 (2006). doi:10.1109/ICTAI.2006.14.

18. Sankararaman, S. & Mahadevan, S. Separating the contributions of variability and parameter uncertainty in probability distributions. *Reliab. Eng. Syst. Saf.* **112**, 187–199 (2013).

19. Forbes, C. S., Evans, M., Hastings, N. & Peacock, B. *Statistical Distributions*. (Wiley, 2011).

20. Henriksson, P. J. G. *et al.* Product carbon footprints and their uncertainties in comparative decision contexts. *PLoS One* **10**, 1–11 (2015).

21. Mendoza Beltran, A. *et al.* Quantified Uncertainties in Comparative Life Cycle Assessment: What Can Be Concluded? *Environ. Sci. Technol.* **52**, 2152–2161 (2018).

22. Borgonovo, E. & Plischke, E. Sensitivity analysis: A review of recent advances. *Eur. J. Oper. Res.* **248**, 869–887 (2016).

23. Borgonovo, E. A new uncertainty importance measure. *Reliab. Eng. Syst. Saf.* **92**, 771–784 (2007).

24. Cucurachi, S., Borgonovo, E. & Heijungs, R. A Protocol for the Global Sensitivity Analysis of Impact Assessment Models in Life Cycle Assessment. *Risk Anal.* **36**, 357–377 (2016).

25. Plischke, E., Borgonovo, E. & Smith, C. L. Global sensitivity measures from given data. *Eur. J. Oper. Res.* **226**, 536–550 (2013).

26. Derennes, P., Morio, J. & Simatos, F. A nonparametric importance sampling estimator for moment independent importance measures. *Reliab. Eng. Syst. Saf.* **187**, 3–16 (2019).

27. Borgonovo, E. & Iooss, B. Moment-Independent and Reliability-Based Importance Measures. in *Handbook of Uncertainty Quantification* (eds. Ghanem, R., Higdon, D. & Owhadi, H.) 1265–1287 (Springer International Publishing, 2017). doi:10.1007/978-3-319-11259-6_37-1.

28. Frischknecht, R. *et al.* The ecoinvent database: Overview and methodological framework. *Int. J. Life Cycle Assess.* **10**, 3–9 (2005).

29. Williams, E. Environmental effects of information and communications technologies. *Nature* **479**, 354 (2011).

30. Kamyshny, A. & Magdassi, S. Metallic Nanoinks for Inkjet Printing of Conductive 2D and 3D Structures. in *Nanomaterials for 2D and 3D Printing* (eds. Kamyshny, A. & Magdassi, S.) 119–160 (Wiley-VCH Verlag GmbH & Co. KGaA, 2017). doi:10.1002/9783527685790.ch7.

31. Pourzahedi, L. & Eckelman, M. J. Comparative life cycle assessment of silver nanoparticle synthesis routes. *Environ. Sci. Nano* **2**, 361–369 (2015).

32. Slotte, M. & Zevenhoven, R. Energy requirements and life cycle assessment of production and product integration of silver, copper and zinc nanoparticles. *J. Clean. Prod.* **148**, 948–957 (2017).

33. Renn, M. J., Schrandt, M., Renn, J. & Feng, J. Q. Localized Laser Sintering of Metal Nanoparticle Inks Printed with Aerosol Jet® Technology for Flexible Electronics. *J. Microelectron. Electron. Packag.* **14**, 132–139 (2017).

34. Hermerschmidt, F. *et al.* Truly Low Temperature Sintering of Printed Copper Ink Using Formic Acid. *Adv. Mater. Technol.* **3**, 1800146 (2018).

35. Goedkoop, M. *et al. Report I: Characterisation. ReCiPe : A life cycle impact assessment method which comprises harmonised category indicators at the midpoint and the endpoint level* (2009).

36. Heijungs, R., Henriksson, P. J. G. & Guinée, J. B. Measures of difference and significance in the era of computer simulations, meta-analysis, and big data. *Entropy* **18**, 361 (2016).

37. Saltelli, A. *et al. Global Sensitivity Analysis. The Primer. Global Sensitivity Analysis. The Primer* (John Wiley and Sons, 2008). doi:10.1002/9780470725184.

38. Dubois, D. & Prade, H. M. *Possibility Theory : an Approach to Computerized Processing of Uncertainty*. (Springer US, 1988).

Chapter 5

Probabilistic and prospective ecological risk assessment of III-V/silicon tandem photovoltaics

III-V/silicon tandem solar cells offer one of the most promising avenues for high-efficiency, high-stability photovoltaics. However, a key concern is the potential environmental release of group III-V elements, especially arsenic. To inform long-term policies on the energy transition and energy security, we develop and implement a framework that fully integrates future PV demand scenarios with dynamic stock, emission and fate models in a probabilistic ecological risk assessment. We examine three geographical scales: local (including a floating utility-scale PV and waste treatment); regional (city-wide) and continental (Europe). Our probabilistic assessment considers a wide range of variations for over one hundred uncertain technical, environmental and regulatory parameters. We find that significant III-V/silicon PV penetration in energy grids at all scales presents low-to-negligible risks to soil and freshwater organisms. Risks are further abated if recycling is considered at the panels' end-of-life.

Keywords: III-V/silicon cells; risk assessment; toxicity; photovoltaics; safe-by-design; sustainable innovation

This chapter is based on the manuscript *High-efficiency III-V/Si tandem solar cells pose low toxicity risks to soil and freshwater ecosystems* (Blanco, C.F., Quik, J.T.K., Hof, M., Behrens, P., Cucurachi, S., Peijnenburg, W.J.G.M., Dimroth, F., Vijver, M.G.). In preparation for submission to *Energy Environ. Sci.*

5.1. Introduction

Recent decades have seen a dramatic increase in photovoltaic electricity (PV) in energy markets worldwide.[1] Next to lower manufacturing costs, a key driver for increased PV adoption has been the environmental benefits when compared to fossil and nuclear-based electricity generation.[2,3] An important factor for the success of the currently dominating crystalline silicon (c-Si) PV technologies is that silicon has low toxicity[4]. This has set a benchmark against which emerging PV technologies such as III-V/silicon tandem cells (III-V/Si) would be judged. III-V/Si tandem cells stack thin light-absorbing layers of Group III and V elements (gallium, indium, arsenide, phosphide) on top of a c-Si wafer to achieve record-breaking conversion efficiencies for non-concentrating systems that can exceed 35%.[5] Manufacturing III-V/Si with current technology is very expensive and important research efforts are underway to make them more economically attractive.[6–9] However, concerns regarding potentially toxic releases of III-V metals and metalloids to the environment could hinder investment and stall further development and deployment of the technology. As a result, III-V/Si may miss out on important cost-reductions that could be achieved via technological breakthroughs and/or learning by doing.

Investigating the potential environmental impacts and risks of innovative PV designs such as III-V/Si during early research and development stages can assist in making designs more competitive from an environmental perspective.[10–12] The environmental impacts of emerging PV technologies have often been assessed in a prospective way using life cycle assessment (LCA) with future projections.[13] Blanco et al.[14] recently investigated the LCA impacts of commercially viable III-V/Si cell concepts and concluded that they could perform similar or better than silicon PV across most environmental impact categories, including climate change, fresh water ecotoxicity, eutrophication, and others. The LCA approach, however, only allows a comparison of impact indicators in a relative sense, where environmental emissions are aggregated across space and time.[15] To determine whether the emissions pose actual risks, they must be evaluated in a specified temporal and spatial context. Such an evaluation can be performed by means of ecological risk assessment.[16] However ecological risk assessments for emerging technologies are challenging from a modelling and data availability perspective and have not been conducted so far for III-V/Si PV systems. In this study we address this important knowledge gap by assessing the ecological risks of metal and metalloid releases that may take place during the life cycle of III-V/Si PV systems.

Recent studies of toxicity of emerging PV technologies have a large degree of heterogeneity and focus selectively on single or small subsets of PV system components, life-cycle stages, release mechanisms and/or toxicity endpoints.[17–20] To avoid these shortcomings, we adopt a comprehensive approach by screening for relevant emissions in all life-cycle stages of III-V/Si panels and estimating the risks posed by these emissions in plausible and well-defined PV demand scenarios at three geographical scales: local, regional and continental. Furthermore, we recognize that a holistic and forward-looking assessment such as this introduces numerous and large uncertainties and variabilities.[21]

We therefore use a probabilistic risk assessment approach to explicitly consider these in an integrated PV demand-emission-fate model and quantify uncertainty in the outcomes of the assessment, i.e., risk indicators.[22] We then use global sensitivity analysis to reveal which factors contribute most to this uncertainty. While the III-V/Si technology is still in development, this information is equally or more important than the magnitude of the risk indicators, as it can help prioritize further research and development of the technology as well as simplify the assessment by disregarding trivial uncertainties and variabilities.

5.2. Methods

5.2.1. Overview of modelling framework

To assess the ecological risks from III-V/Si panels in future PV demand scenarios we developed an integrated model that consists of five steps. First, demand for installed PV capacity (in MW or GW) over a one-hundred-year modelling period (2031-2130) is determined for each geographical scale (continental, regional, local) based on relevant PV demand scenarios and stated policies (section 5.2.2). Second, a dynamic stock model is used to determine the amount of PV panels that would be manufactured, installed, operated, recycled and discarded each year in order to satisfy the demand required in the previous steps, while accounting for accidental panel breakage and panels reaching the end of their useful life (section 5.2.3). Third, potential releases of arsenic, gallium and indium (direct emissions) from PV panels to the environment at each life-cycle stage are calculated with a specific emission model developed for each release mechanism (section 5.2.4). Fourth, the environmental distribution and fate of the emitted masses across different environmental compartments (soil, freshwater, air) in each year is determined using a dynamic fate model. Predicted environmental concentrations (PEC) in each compartment are then calculated from the resulting mass in each compartment and the compartment's volume (section. 5.2.5). Finally, a risk quotient (RQ) is calculated as the ratio of PEC to the predicted no-effect concentration (PNEC) that has been reported in literature for each compartment (section 5.2.6).

All components of the model allow for the consideration of probability distributions for input parameters. The model's input parameter descriptions and the corresponding distributions used in this case study are reported in Appendix Table A.4-1. Further details on calculations and assumptions for each step are also documented in Appendix Section A.4. The model was built on the statistical software *R* supported by macro-enabled Microsoft Excel spreadsheets. The annotated *R* scripts and Excel spreadsheets are available for download in https://github.com/jormercury/solar-simplebox.

5.2.2. Demand projections

In the first step we determined the quantity of installed III-V/Si panels required to meet PV electricity demand scenarios for three geographical scales:

- *SKY_EUR,* a continental scale where we based future PV demand on the Shell Sky Scenario[23] for Europe, which is the most ambitious with regards to electrification and future participation of PV from the Shell family of scenarios. We combined the Sky projections for total PV demand with the IEA's "High GaAs" scenario, in which III-V cells comprise 5% of the distributed and 15% of the utility-scale PV demand.[24]
- *RES_AMS,* a regional scale representing the city of Amsterdam and based on the municipality's stated ambitions in their Regional Energy Strategy (RES v1.0)[25]. Here we also applied III-V/Si market shares from the IEA "High GaAs" scenario.
- *UTI_LOC*, a local scale reflecting a utility PV plant consisting of 50 MW of floating III-V/Si panels installed on a lake area of 0.9 km^2 in addition to 50,000 distributed panels (14 MW) installed on rooftops in the surrounding area and draining towards the lake. End-of-life (EOL) PV treatment is also assumed to take place within this area. As such the local scale is meant to represent an unlikely worst-case scenario for the local water compartment.*

The growth in installed PV capacity over the period 2031-2130 in both the SKY_EUR and the RES_AMS scenarios were modelled using logistic-growth curves. In SKY_EUR, we assumed an initial capacity addition of 100 MW_p and stabilizing at 430 GW_p. We took an annual growth rate of 14.1% from the 75th percentile of 1100 different PV deployment scenarios in Europe that were reviewed and harmonized by Jaxa-Rozen et. al.[26] In the RES_AMS scenario we assumed an initial capacity addition of 0.1 MW_p in the year 2031 and stabilizing at 110 MW_p following a higher growth rate of 20%. For the UTI_LOC scenario the amounts of PV panels installed were kept constant throughout the modelling period, with replacement of broken panels and those that reach their EOL.

With an expected 28% panel conversion efficiency, III-V/Si panels will have a rating of 280 W_p per m^2 of panel. Thus, every 1 MW_p of planned installed capacity would require a PV installation with an effective area of 3,571 m^2.

5.2.3. Dynamic stock flows

Yearly stock flows of III-V/Si panels (quantified as m^2 of PV panel) were calculated using a dynamic stock model[27–29] for a one-hundred year modelling period. In the stock model, additional panels are manufactured each year to meet the increasing demand, to replace broken panels, and to replace panels that reached the end of their useful life (due to long-term degradation). In lieu of specific panel lifetime data, we assumed a normal distribution for III-V/Si panel lifetime of each yearly cohort centred at 30 years and with a standard deviation of 5. Accidental panel breakage rates of 0.06-0.12%/year were taken based on panel crack statistics reported by the International Energy Agency.[30]

* In their Regional Energy Strategy, the Amsterdam municipality has marked floating PV as a last resort, only to take place if the regional and national goals cannot be satisfied with installation on rooftops and other public infrastructure.

5.2.4. Emissions of III-V metals and metalloids

Based on III-V/Si cell design specifications proposed by a European project[31], each m^2 of panel would contain 8.81 g of arsenic (As), 15.06 g of gallium (Ga) and 0.1 g of indium (In).[31] The As, Ga and In content in each panel is subject to environmental release depending on the specific conditions and dissolution processes that can take place during manufacturing, operation (use phase), end-of-life (EOL) phase (Figure 5-1).

Manufacturing. III-V substances enter the supply chain of III-V/Si cells in the metalorganic vapour phase epitaxy process (MOVPE) which is used to grow the absorber III-V layers on top of the silicon wafer. These substances are supplied from hydride gases and metalorganic precursors (arsine, trimethylgallium and trimethylindium). The fraction not deposited on the solar cells is distributed in two waste streams: a gas stream that is captured by a scrubber, and a solid stream composed of materials that deposit on the different elements of the reactor and on filters which are cleaned periodically. In the scrubber, a dry zeolite/copper-based granulate adsorbs the toxic substances.

The current best practice in the industry is to reintroduce the used scrubber granulate into the smelting process for copper, in which case the III-V content is captured as an acceptable impurity in the metal. It is likely that the valuable metals (indium, gallium) will be eventually separated and recovered. For arsenic there is no economic case at present, however there is technical feasibility for arsenic recovery from the used adsorbent granulates. Such recoveries may become economically viable when the arsenic content in waste is sufficient (e.g., ~100 ton/year)[†]. Recovery may also be driven by resource scarcity of critical materials like indium and gallium.[32] Recovery processes will have an associated efficiency, typically between 95-99%, and the remaining fraction (rejects) would be disposed in an underground hazardous waste storage facility.

The solid waste stream from MOVPE that deposits in the reactor is periodically removed as a standard cleaning procedure. This waste is also discarded in an underground hazardous waste storage facility. These types of facilities in Europe are typically installed on sealed and carefully monitored abandoned mine shafts, where potential migration of contaminants is deemed implausible.

Use phase (operation). Two processes were modelled to estimate potential releases during operation: dissolution at the cracked surface of III-V materials directly exposed to rain, and transport of III-V materials on non-exposed parts that get dissolved by water ingress and are transported to the crack where it is then released. We modelled the former process following the method proposed by Celik et al.[33], which is based on an application of the Noyes-Whitney equation[34]. The latter process was modelled using equations 5-1 and 5-2, where $trans_{crack}$ is the transport of dissolved metal to the crack (g/s), J_{crack} is the flux of dissolved metal to the crack (g/m^2/s), D is the diffusion coefficient of metal (m^2/s), C_s is the saturated mass concentration of metal in water in g/m^3, C_b is the concentration of

[†] Personal communication from UMICORE.

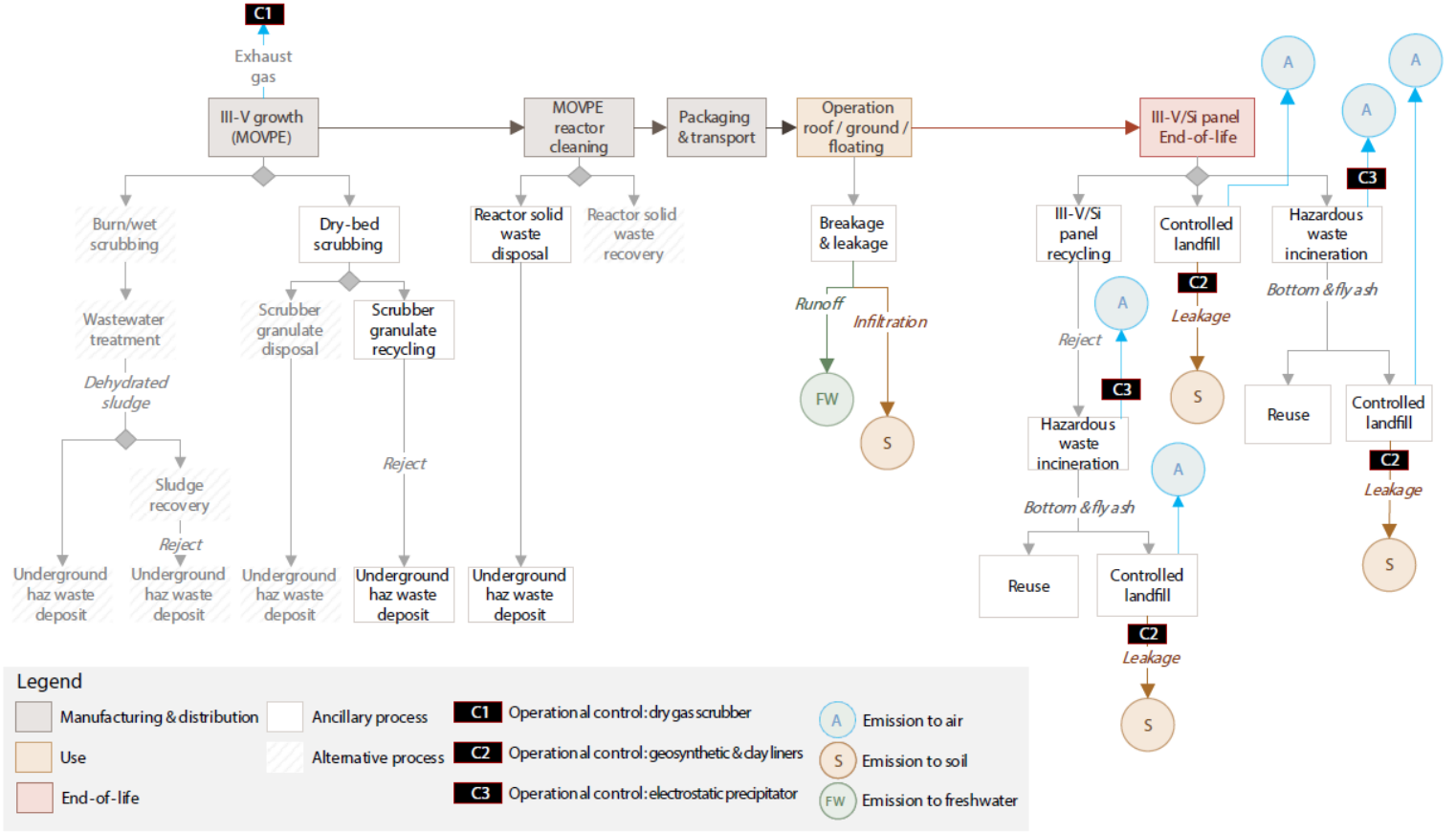

Figure 5-1 Identification of potential sources of III-V emissions in the life cycle of III-V/Si PV panels

metal in bulk solvent (rainwater) in g/m^3, and $distance_{cr}$ is the average travel distance of the metal from any point in the panel to the crack (m), calculated using the method of Mathai et al.[35] Cracked panels were assumed to leach for one year after which they would be replaced.

$$trans_{crack} = J_{crack} \cdot A_{cr\_side} \quad \text{(Eq. 5-1)}$$

$$J_{crack} = D \cdot \frac{Cs - Cb}{distance_{cr}} \quad \text{(Eq. 5-2)}$$

End-of-life phase: Recycling. The European Waste Management Directive for electronic products -including photovoltaic panels- requires that 85% is collected for treatment and preparation for reuse/recycling.[36] It is likely, however, that the panels are disassembled to recover the easily recyclable materials such as aluminium and glass.[‡] We modelled two scenarios for each scale: with and without recovery of III-V materials. In former case we assumed recovery efficiencies for these processes based on existing patents and published recycling methods for similar technologies[37–39].

End-of-life phase: Incineration. In incineration facilities, it has been found that 20-80% of arsenic in waste may remain in the bottom ash while the rest is volatized.[40] The volatized fraction is directed to emission control mechanisms at the stack such as electrostatic precipitators (ESP) with removal efficiencies that typically range between 99.5-99.9%.[41] Arsenic that is not vaporised in the incinerated panels is emitted to air and the remaining fraction is collected as secondary waste with bottom ash, fly ash and filters. Gallium and indium do not form volatile organic compounds, so we assumed 100% remains in the bottom ash. In Europe, secondary waste from incineration facilities is typically either sent to a controlled landfill or reused in construction material.[42]

End-of-life phase: landfill. Two main processes drive emissions from landfilled PV waste: leaching from the waste to the leachate within the landfill, and leakage of the leachate from the landfill to the surrounding soil. The former will be largely regulated by a waste/leachate partitioning coefficient (k_W) which can be determined empirically from leaching tests or field measurements. Leaching and subsequent leakage from the landfill will also be largely regulated by the effective infiltration (I), the amount of rainfall that infiltrates and passes through the landfill's containment structures such as clay or geosynthetic liners. We use a simplified version of EPA's Composite Model for Leachate Migration with Transformation Products (EPACMTP)[43], where the mass balance for a landfill cell is given by equations 5-3 and 5-4.

$$A_W \cdot D_{LF} \cdot \rho_W \cdot \frac{dC_w}{dt} = A_W \cdot I \cdot C_L(t) \quad \text{(Eq. 5-3)}$$

$$C_L(t) = K_W \cdot C_W(t) \quad \text{(Eq. 5-4)}$$

When modelling emissions we took a conservative approach and assumed that all III-V elements in the PV cells are fully soluble. This is a common starting point for metals risk

[‡] Ibid.

assessment within the EU.[44] Another important consideration is that, once released, metals and metalloids can exist in different forms like organic complexes with dissolved organic matter, inorganic complexes with dissolved anions, or free hydrated metal ions. This applies especially to arsenic, which can exist in four oxidation states with different toxicities: –3, 0, +3, and +5. In this study, we assume that arsenic dissolves entirely to its most toxic form (*arsenite*, +3). Indium and gallium may also exist in different oxidation states, but once released to the environment tend to revert to their +3 oxidation state.[45]

5.2.5. Predicted environmental concentrations

We then modelled the distribution of the emitted III-V substances in the environment using SimpleBox v4, a widely used tool for fate modelling developed by the Netherlands Institute of Public Health and the Environment (RIVM).[46] For the SKY_EUR continental scale we used the landscape settings for the European continent that were established for the European Union System for the Evaluation of Substances (EUSES).[47] In the SimpleBox model, the continental scale contained the regional AMS_RES scale embedded, which in turn contained the embedded local UTI_LOC scale (SimpleBox calculates exchanges between embedded scales). To model the regional AMS_RES and UTI_LOC landscape we derived surface water and soil coverage data from GIS data made available by the Amsterdam municipality[48], and weather data provided by the Royal Netherlands Meteorological Institute (KNMI)[49].

To conduct dynamic PEC calculations we coupled a probabilistic implementation of the SimpleBox model using the @Risk add-in (Palisade, v8.1.0) with the deSolve[72] package in R. SimpleBox is based on the original implementation as described in Schoorl et al.[46,50] with the addition of a local scale with an air, soil, water and sediment compartment based on van de Meent et al.[51] In this implementation, the model matrix of all rate constants is read from the SimpleBox Excel spreadsheets and combined with the annual III-V emissions (calculated in section 5.2.4), using the event function in deSolve.

5.2.6. Predicted no-effect concentrations and risk quotients

We took the PNEC values recommended by the European Chemicals Agency (ECHA) in the registration dossiers for each substance.[52–54] Depending on each case, these were derived by ECHA from EC10 or EC50 (concentration at which 10% or 50% of the target organism presents the observed effect), LC50 (lethal concentration for 50% of the observed organisms) and LOEC (lowest observed effect concentration) values reported in literature. An assessment factor is applied to account for uncertainty in extrapolation from lab to field results, or for the limited availability of datapoints.[55]

Arsenic. The PNEC value recommended by ECHA for freshwater organisms is 5.6 μg/L, after application of an assessment factor of 3. For soil, the recommended PNEC is 2.9 mg/kg soil (dry weight) after an assessment factor of 2 has been applied.

Gallium. One NOEC for freshwater organisms was reported in the ECHA database of 10,300 μg/L.[52] Following ECHA guidelines[55], an assessment factor of 100 should be

applied for a single NOEC value, resulting in a PNEC of 103 µg/L. There was only one datum for soil organisms reported in literature, an EC50 of 0.271 g/kg soil (dw) for rice plants in acidic soil (no effects were observed in neutral soils).[56] Applying an assessment factor of 100 gives a PNEC of 2.7E-3 g/kg soil (dw). For soil, ECHA recommends using the Equilibrium Partitioning Method as an alternative calculation method when only one datum is available and choosing the lowest PNEC obtained from both methods. The Equilibrium Partitioning Method uses the PNEC in water to estimate PNEC in soil according to Equation 5-5:

$$PNEC_{soil} = \frac{K_{sw}}{\rho_{soil}} \cdot PNEC_{water} \cdot 1000 \qquad \text{(Eq. 5-5)}$$

In Equation 5-5, K_{sw} is the soil water partition coefficient for gallium and ρ_{soil} is the density of soil phase, 2500 kg/m^3. This would result in a PNEC of 4E-2 g/kg soil (dw). We therefore take the lower PNEC of 2.7E-3 g/kg soil (dw).

Indium. The toxicity data for indium (In3+) were taken from the ECHA database, which recommends a PNEC of 40.6 µg/L after applying an assessment factor of 3. For terrestrial organisms, the recommended value is 7.3E-3 g/kg soil (dw), after applying an assessment factor of 10.[53].

RQs for each compartment were calculated as the PEC/PNEC ratio, where RQ values approaching or exceeding 1 indicate a potential situation of concern.

5.2.7. Uncertainty and sensitivity analysis

We used the Monte Carlo uncertainty propagation method[57] to determine uncertainty in the PECs and RQs as a result of uncertainties and variabilities in the model's input parameters. For the Monte Carlo simulation we pre-sampled 1,000 sets of random values for these parameters from their underlying distributions, and recalculated PECs and RQs for each set of values throughout the period 2031-2130. This produced a probability distribution for each PEC and RQ in each year, from which summary statistics (geometric mean, 25th and 75th percentiles) were derived.

Finally, we conducted a global sensitivity analysis using the moment-independent sensitivity importance measure proposed by Borgonovo[58,59] to rank all uncertain parameters in terms of their contribution to uncertainty in the resulting RQs in freshwater and natural soil compartments for all scales. We calculated these sensitivity measures using the *sensiFdiv* function in the *sensitivity* package for R developed by Iooss et al.[60]

5.3.Results and discussion

5.3.1.III-V/Si panel stock flows

The calculated stocks of III-V/Si panels installed and reaching their end-of-life in each year of the modelling period are shown in Figure 5-2. In Europe, carrying capacity is reached after the year 2110, while for Amsterdam it is reached at around the year 2080.

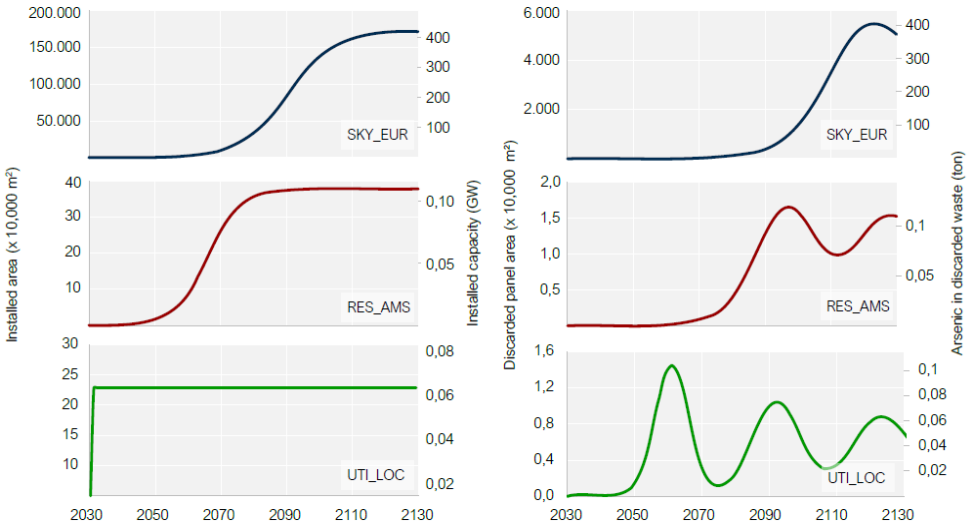

Figure 5-2 Projected III-V/Si PV demand (left) and discarded materials (right) for the three scales.

The steep ramp-up followed by stabilization in the demand growth curves (left) produces a ripple in the amount of PV materials that are available for recycling or final disposal at end-of-life (right). These oscillations are somewhat smoothened by uncertainty in the lifetime each cohort which varies around 30 years. As will be seen in sections 5.3.2 and 5.3.3, these oscillations in EOL stocks are then reflected in the emissions and PEC's.

5.3.2. III-V metals and metalloid emissions

The yearly emissions from the PV stocks during operation (USE) and disposal (EOL) in each scale are shown in Figure 5-3. These emissions were calculated for the single "base case" value for each parameter listed in Appendix Table A.4-1 (see Appendix Figure A.4-1 for the probabilistic results of the emissions model). Emissions from the use phase are several orders of magnitude lower than the emissions from the EOL phase, even when recycling is considered. At the largest scale (European continent, SKY_EUR), the quantity of arsenic emitted during the use phase starts stabilizing towards the end of the modelling period around 30 kg/year. In the regional (Amsterdam, RES_AMS) and local (UTI_LOC) scales, where they may be more concentrated, total emissions amount to grams which are then distributed over the respective areas of 220 km^2 and 16 km^2. This indicates that in all scenarios, the only relevant emissions are expected to occur at EOL.

In the end-of-life phase, total life-cycle emissions approach 1 ton/year in the SKY_EUR scenario at continental scale for the soil and air compartments. The quantities emitted to the air compartment are larger than quantities to soil at the beginning of the modelling period. This can be explained by the immediacy of the emissions during incineration: emissions which are not captured by the electrostatic precipitator during/after incineration, will be immediately released into the air compartment. On the other hand,

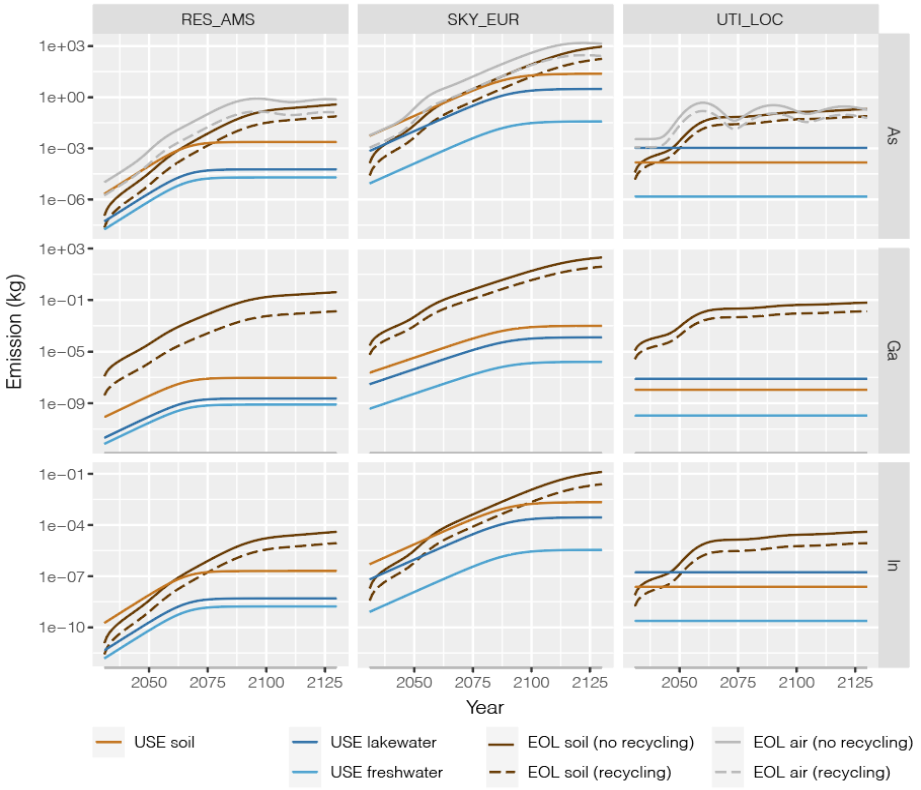

Figure 5-3 Life cycle emissions of III-V materials from III-V/Si PV installations in three different scenarios. EOL: End-of-Life phase; USE: Use phase.

emissions in a landfill are subject to a retardation factor represented by the large waste/leachate partitioning coefficients (K_w) of Equations 5-3 and 5-4. Towards the end of the modelling period, the emissions from landfill to the soil compartment are of similar magnitude than those to air in all scales. No air emissions are foreseen for gallium and indium due to their negligible volatilities.

5.3.3. Environmental fate of III-V metals and metalloids

The resulting PECs in soil and freshwater compartments are shown in Figure 5-4. At the end of the 100-year modelling period, the 75th percentile PEC of arsenic in freshwater in the local scale remains 1 to 2 orders of magnitude below the drinking water limits established by the World Health Organisation (without considering background levels or emissions). In the regional and continental scales, the PEC is 3-4 orders of magnitude lower. In soil, the 75th percentile PEC of arsenic is 5 orders of magnitude lower than the average concentration found in natural soils (1-40 mg/kg).[61] The geometric means are closer to the lower boundaries, suggesting skewed distributions with a long tail extending to the higher PEC values. The expected environmental concentrations of gallium and indium are in the nanogram range and lower, indicating negligible effects of this emissions from an ecological risk perspective.

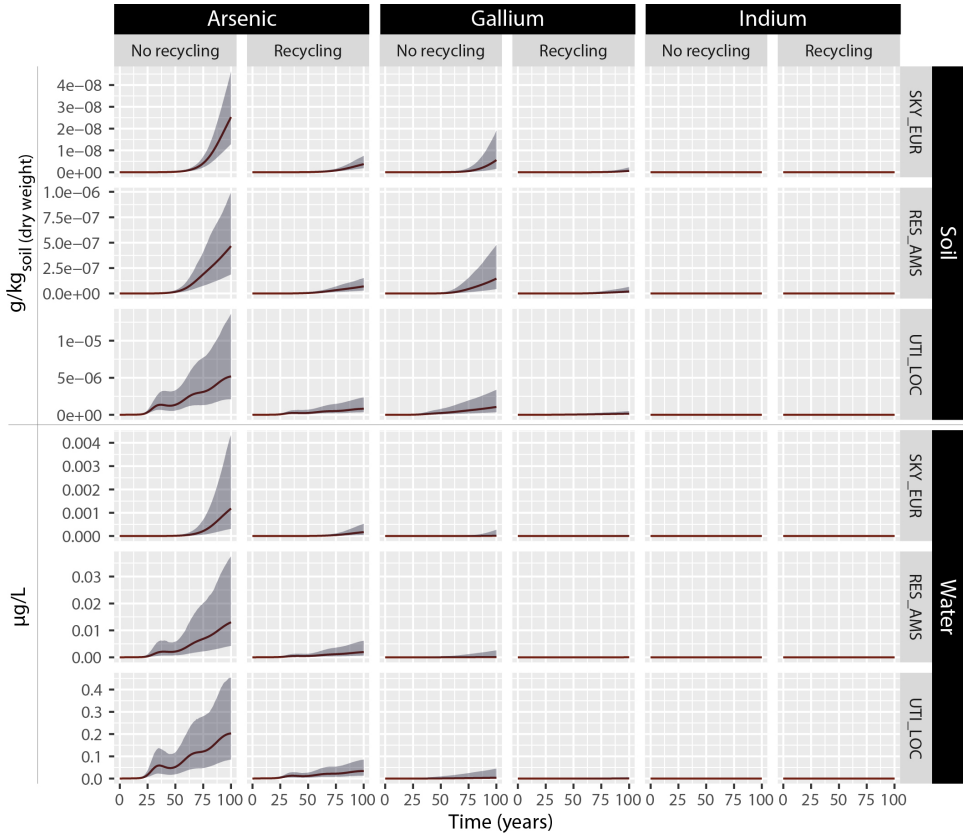

Figure 5-4 Predicted environmental concentrations of arsenic in soil and freshwater compartments in all scales, with and without recycling. The shaded area encloses the 25th and 75th percentiles and the solid line shows the geometric mean.

5.3.4. Ecological risks to freshwater and soil organisms

Figure 5-5 summarizes the RQs in the 100th year of simulation. As the scale volumes reduce in size (from continental to regional to local), the PECs and RQs increase. The local freshwater compartment presents the highest RQ for arsenic at ca. 0.1 for the upper range.

This could become a potential hotspot which may require consideration against background arsenic concentrations in the event a similar deployment is planned. The risk quotients for all other scales, compartments and metals are below 0.01. In all cases, recycling of the III-V content of the cells would reduce risks by one order of magnitude.

For the worst-case local scenario conditions for arsenic in which RQ approaches 0.1, some of the underlying assumptions merit further inspection with the aim of identifying potential risk attenuating mechanisms. A key starting assumption was that all emitted arsenic dissolves to its most toxic ion, arsenite (As(III)), which is assumed to persist as such.

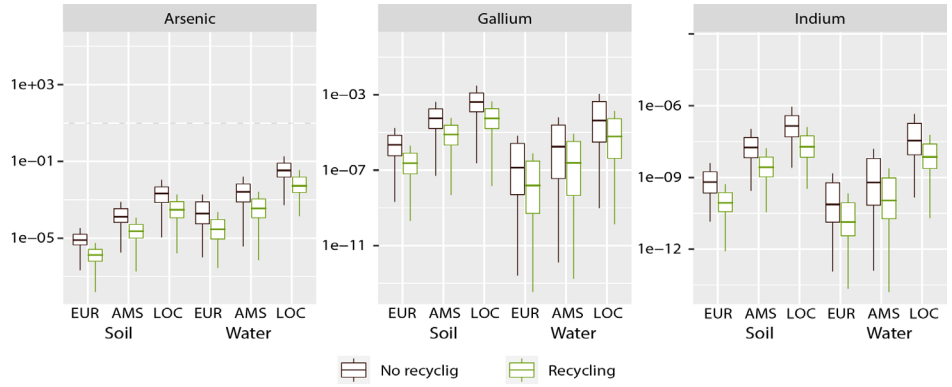

Figure 5-5 Risk Quotients for arsenic, gallium and indium in soil and freshwater compartments in all scales, with and without recycling.

However, arsenic undergoes several transformation processes which result in arsenate ions (As(V)) or even less toxic methylated organic forms.[62,63] The PNEC for As(III) is approximately 5 times lower than for As(V) in plant species.[61] A study of landfill leachate in Nordic countries found that arsenic in leachate is typically 80% arsenate, 10% arsenite and the rest is methylated.[64] Even lower percentages of As(III) (<5%) and higher amounts of methylated forms were reported by Pinel-Raffaitin and colleagues in landfill leachates sampled in France.[63]

In situ mechanisms to address As(III) mobilization in leakage from cracked panels during operation may be implemented as an additional precaution, especially in floating PV plants. Shumlas et al.[65], for example, reported accelerated oxidation of As(III) to As(V) when exposed to sunlight on layered manganese oxide. While such applications were developed for wastewater treatment in the case of arsenic, *in situ* mitigation concepts have already been proposed for perovskite PV cells where accidental lead leakage is immediately sequestered by lead-absorbing coatings.[66]

5.3.5. Sensitivity ranking of variable and uncertain parameters

The sensitivity rankings for all uncertain and variable model inputs in the integrated model and for all scales and compartments are shown in Figure 5-6. The most sensitive parameters are the waste/leachate partitioning coefficient in the landfill, the landfill cell depth, the fraction of vapourised arsenic captured in the incinerator's ESP, and the fraction of PV collected for recycling. For the landfill partitioning coefficient, the range of possible values spans several orders of magnitude.[67] It is likely that a large part of this dispersion is irreducible due to widely different landfill chemistries and environmental conditions that can be encountered. Further studying of the specific behaviour of arsenic in waste when exposed to leachate can however reduce the uncertainty. This has already been strongly advocated by Söderberg et al.[68] who reviewed 245 articles on soil/solution partitioning of metals in different media and found that none posterior to the EPA report[67] of 2005 investigated this parameter in waste disposal systems.

Figure 5-6 Sensitivity ranking of model parameters. L: local scale, R: regional scale, C: continental scale.

It is also noteworthy that despite the complexity and spatial dependency of the fate model, most of the parameters in this model component ranked low in terms of their contribution to uncertainty in the risk quotient. The sensitivity hotspots are clearly found in the EOL phase emissions model.

5.3.6. Recommendations for safe and sustainable III-V/Si PV installations

The most influential parameters identified in the global sensitivity analysis can offer opportunities to improve the design, not only of the photovoltaic cell, but of the configuration of large-scale deployments and the ancillary/complementary technological systems.

Waste/leachate partitioning coefficient. Despite its large variability, this highly influential factor can be addressed to some extent by controlling landfill chemistry, especially the pH of the leachate. It is likely that a construction and demolition (CDW) waste landfill with low organic waste content will produce leachate in higher pH ranges than a municipal solid waste (MSW) landfill where organic matter is being degraded and more acidic conditions emerge. Reaction of the ethyl vinyl acetate (EVA) encapsulation in PV panels with infiltrated water in the landfill may also produce acidic conditions, even in CDW landfills, by formation of acetic acid on the surface of discarded PV waste. Thus, delamination prior to disposal and/or replacement of the EVA encapsulation for alternative materials[69] in the panel's design may further reduce risks. This measure could also reduce leakage during operation of cracked panels, however the contribution of this release mechanism to the overall risk is already negligible.

Landfill depth. Stacking discarded PV waste in landfills more vertically rather than horizontally can have a significant retardation factor. Figure 5-7 shows the shift in the distribution curve of arsenic emissions to soil after the landfill depth is fixed at its higher range (10 m). The distribution is shifted significantly to the left and its tail size reduced.

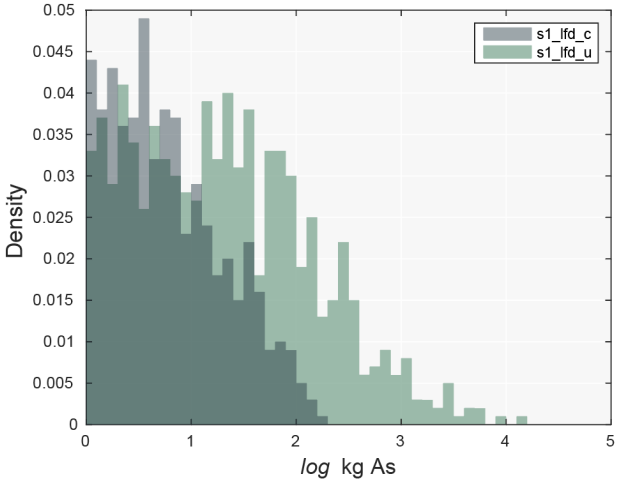

Figure 5-7 Change in distribution of arsenic emissions to soil (s1_lfd_u) as a result of fixing parameter landfill depth at lf.d = 10 m (s1_lfd_c).

Incinerator abatement efficiency (electrostatic precipitator). The fraction of vapourised arsenic that gets captured in the incinerator's electrostatic precipitator (thus prevented from direct release to the air compartment), also has an important influence. Even though the abatement efficiency range (98-99.9%) left small room for improvement, the results suggest that efforts to implement best available practice and marginal further improvements in abatement efficiency can result in noticeable risk reductions.

PV collection for recycling rate. By reintroducing III-V materials in PV waste into new economic products, they are effectively prevented from being released into the environment. The analysis not only showed an order of magnitude difference between the recycling and no-recycling scenario, but within the recycling scenario any efforts to increase collection above 85% will also result in important risk reductions.

The global sensitivity analysis also reveals where mitigation mechanisms may not be as effective in relation to the effort/cost required to implement them. For example, reducing arsenic content of the cells in the design and manufacturing within what is feasible will not have a noticeable effect on the risk profile of the III-V/Si technology. The same applies to measures to further reduce the cracking of panels – the use phase emissions are already too low to offer significant risk reduction.

5.3.7. Critical reflection on limitations and directions for future research

The integrated model we developed is complex in that it incorporates numerous interconnected cause-effect mechanisms to ensure all relevant factors are given consideration. Producing the data for such a model can be very time consuming, if the data is available at all. Therefore, some important assumptions and rough estimates were necessarily made. First, while the underlying landfill model is a good approximation for a monofill, the waste/leachate partitioning values (K_w) from EPA we used were taken from municipal solid waste (MSW) landfills, which will have phases where leachate has lower pH. This may significantly accelerate the release of arsenic from PV waste to the leachate. Second, we opted not to include a detailed speciation model for the dissolution of III-V species during use phase when exposed to acid rain or acetic acid attack. These models can increase the complexity of the assessment significantly, and they depend on a very large variability of water and waste chemistries which are difficult to determine at this stage. Given that the use phase emissions were considerably lower than the EOL emissions we decided to make conservative assumptions in this respect, although this may be an important aspect to incorporate if more detailed risk assessments are needed. Third, the dynamic emissions we calculated are largely dependent on the demand scenarios, more specifically the growth rates assumed for PV deployment (and the assumption of logistic growth curves). The market dynamics for PV are difficult to predict, with many forecasts having proved overly pessimistic in recent years.[70] Further coupling and updating of expected PV growth rates (specifically for III-V/Si markets) may shift the time-dependent results in a way that has important implications.

5.4. Conclusions

Our assessment indicates that the ecological risks from III-V materials emissions throughout the lifetime of III-V/Si PV panels do not pose a cause for concern, even under the worst-case situation modelled in the local scale. The main source of potentially toxic releases would be the above-ground disposal of III-V/Si cells in landfills. We find that the relevant increases in concentrations occur mostly in soil, while the contribution to the freshwater compartment was negligible across all scales. In soil, the mobility of III-V materials is very low, and releases will be diluted on the order of hundreds or thousands of years. Tighter regulations for landfill containment and monitoring systems will dilute these processes further. In the case of gallium and indium, these elements have much lower reactivity, so the emissions that do occur will have negligible effects. Nevertheless, at smaller scales with the co-occurrence of intense PV utilization and disposal, the risks may increase so that careful monitoring of the efficacy of control measures is required, particularly around landfill and incineration abatement, collection of used PV panels and increased recycling of arsenic. These factors will become increasingly important considering potential future expansion of markets for other arsenic containing electronic waste, such as that from discarded integrated circuits and LED diodes.

It is important to also consider that current social and regulatory trends in the European context have a clear direction towards reducing waste and increasing circularity of the economy. As an example, Germany sends less than 1% of its construction and demolition waste to landfills as of 2021.[71] European regulations have set demanding thresholds for electronic waste recycling, and numerous patents have demonstrated technologies for recovering materials from LEDs, integrated circuits, and photovoltaic devices with III-V materials grown via MOVPE. These recycling techniques can only be expected to become more efficient and cost-effective in time. Furthermore, the growing concerns over resource availability and supply risks of III-V materials like indium and gallium will provide further incentives. Considering these factors, a low-emission and low-risk scenario for the life cycle of future III-V/Si is likely.

As a final note, we highlight the value of the integrated model developed in this work for the early-stage assessment of chemical risks from emerging technologies. The model can be readily extended to other technologies beyond PV. In the past, such complex integrated models have seldom been applied at early R&D stages because of the time consuming and significant effort to construct and set up the models and the numerous uncertainties faced. But the framework and calculation algorithms we have made available make the rapid screening of different scenarios possible, while preserving the complexity and wide variety of influential factors found in real life. Furthermore, it is an ideal tool to prioritize research and data collection on influential factors during subsequent R&D stages.

References

1. Lazard. *Lazard's Levelized Cost of Energy Analysis - Version 12.0*. https://www.lazard.com/media/450784/lazards-levelized-cost-of-energy-version-120-vfinal.pdf (2018).
2. Jager, W. Stimulating the diffusion of photovoltaic systems: A behavioural perspective. *Energy Policy* **34**, 1935–1943 (2006).
3. Leenheer, J., de Nooij, M. & Sheikh, O. Own power: Motives of having electricity without the energy company. *Energy Policy* **39**, 5621–5629 (2011).
4. European Chemicals Agency. Silicon - Registration Dossier. https://echa.europa.eu/registration-dossier/-/registered-dossier/16144/7/1 (2020).
5. Jain, N. & Hudait, M. K. III–V Multijunction Solar Cell Integration with Silicon: Present Status, Challenges and Future Outlook. *Energy Harvest. Syst.* **1**, 121–145 (2014).
6. Dimroth, F. III-V Solar Cells - Materials, Multi-Junction Cells - Cell Design and Performance. in *Photovoltaic Solar Energy* 371–382 (John Wiley & Sons, Ltd, 2017). doi:10.1002/9781118927496.ch34.
7. Cariou, R. *et al.* III-V-on-silicon solar cells reaching 33% photoconversion efficiency in two-terminal configuration. *Nat. Energy* **3**, 326–333 (2018).
8. Essig, S. *et al.* Raising the one-sun conversion efficiency of III-V/Si solar cells to 32.8% for two junctions and 35.9% for three junctions. *Nat. Energy* **2**, 17144 (2017).
9. Lee, K. H. *et al.* Assessing material qualities and efficiency limits of III–V on silicon solar cells using external radiative efficiency. *Prog. Photovoltaics Res. Appl.* **24**, 1310–1318 (2016).
10. Arvidsson, R. *et al.* Environmental Assessment of Emerging Technologies: Recommendations for Prospective LCA. *J. Ind. Ecol.* **22**, 1286–1294 (2018).
11. Hetherington, A. C., Borrion, A. L., Griffiths, O. G. & McManus, M. C. Use of LCA as a development tool within early research: Challenges and issues across different sectors. *Int. J. Life Cycle Assess.* **19**, 130–143 (2014).
12. van der Giesen, C., Cucurachi, S., Guinée, J., Kramer, G. J. & Tukker, A. A critical view on the current application of LCA for new technologies and recommendations for improved practice. *J. Clean. Prod.* **259**, 120904 (2020).
13. Blanco, C. F., Cucurachi, S., Peijnenburg, W. J. G. M., Beames, A. & Vijver, M. G. Are Technological Developments Improving the Environmental Sustainability of Photovoltaic Electricity? *Energy Technol.* 1901064 (2020) doi:10.1002/ente.201901064.
14. Blanco, C. F. *et al.* Environmental impacts of III–V/silicon photovoltaics: life cycle assessment and guidance for sustainable manufacturing. *Energy Environ. Sci.* **13**, 4280–4290 (2020).

15. Sleeswijk, A. W., Heijungs, R. & Erler, S. T. Risk Assessment and Life-cycle Assessment: Fundamentally different yet reconcilable. *Greener Manag. Int.* (2003).

16. Guinée, J. B., Heijungs, R., Vijver, M. G. & Peijnenburg, W. J. G. M. Setting the stage for debating the roles of risk assessment and life-cycle assessment of engineered nanomaterials. *Nat. Nanotechnol.* **12**, 727–733 (2017).

17. Zimmermann, Y. S., Schäffer, A., Corvini, P. F. X. & Lenz, M. Thin-film photovoltaic cells: Long-term metal(loid) leaching at their end-of-life. *Environ. Sci. Technol.* **47**, 13151–13159 (2013).

18. Celik, I., Song, Z., Heben, M. J., Yan, Y. & Apul, D. S. Life cycle toxicity analysis of emerging PV cells. in *Conference Record of the IEEE Photovoltaic Specialists Conference* vols 2016-Novem 3598–3601 (IEEE, 2016).

19. Babayigit, A., Ethirajan, A., Muller, M. & Conings, B. Toxicity of organometal halide perovskite solar cells. *Nat. Mater.* **15**, 247 (2016).

20. Zeng, C. *et al.* Ecotoxicity assessment of ionic As(III), As(V), In(III) and Ga(III) species potentially released from novel III-V semiconductor materials. *Ecotoxicol. Environ. Saf.* **140**, 30–36 (2017).

21. Collingridge, D. *The social control of technology*. (Frances Pinter, 1980).

22. U.S. Environmental Protection Agency. *Risk Assessment Forum White Paper: Probabilistic Risk Assessment Methods and Case Studies*. http://epa.gov/raf/prawhitepaper/index.htm (2014).

23. Shell International B.V. Sky Scenario. *Shell Scenarios SKY Meeting the Goals of the Paris Agreement* https://www.shell.com/energy-and-innovation/the-energy-future/scenarios/shell-scenario-sky.html (2018).

24. IEA. *The Role of Critical Minerals in Clean Energy Transitions*. (2021).

25. City of Amsterdam. Policy: Renewable energy. *Policy: Sustainability and energy* https://www.amsterdam.nl/en/policy/sustainability/renewable-energy/.

26. Jaxa-Rozen, M. & Trutnevyte, E. Sources of uncertainty in long-term global scenarios of solar photovoltaic technology. *Nat. Clim. Chang.* **11**, 266–273 (2021).

27. Deetman, S., Pauliuk, S., van Vuuren, D. P., van der Voet, E. & Tukker, A. Scenarios for Demand Growth of Metals in Electricity Generation Technologies, Cars, and Electronic Appliances. *Environ. Sci. Technol.* **52**, 4950–4959 (2018).

28. Pauliuk, S. & Heeren, N. ODYM—An open software framework for studying dynamic material systems: Principles, implementation, and data structures. *J. Ind. Ecol.* **24**, 446–458 (2020).

29. van der Voet, E., Kleijn, R., Huele, R., Ishikawa, M. & Verkuijlen, E. Predicting future emissions based on characteristics of stocks. *Ecol. Econ.* **41**, 223–234 (2002).

30. Köntges, M. *et al. Review of Failures of Photovoltaic Modules*. https://iea-pvps.org/wp-content/uploads/2020/01/IEA-PVPS_T13-01_2014_Review_of_Failures_of_Photovoltaic_Modules_Final.pdf (2014).

31. Fraunhofer ISE. SiTaSol: Application relevant validation of c-Si based tandem solar cell processes. https://sitasol.com/.

32. Licht, C., Peiró, L. T. & Villalba, G. Global Substance Flow Analysis of Gallium, Germanium, and Indium: Quantification of Extraction, Uses, and Dissipative Losses within their Anthropogenic Cycles. *J. Ind. Ecol.* **19**, 890–903 (2015).

33. Celik, I., Song, Z., Phillips, A. B., Heben, M. J. & Apul, D. Life cycle analysis of metals in emerging photovoltaic (PV) technologies: A modeling approach to estimate use phase leaching. *J. Clean. Prod.* **186**, 632–639 (2018).

34. Noyes, A. A. & Whitney, W. R. The rate of solution of solid substances in their own solutions. *J. Am. Chem. Soc.* **19**, 930–934 (1897).

35. Mathai, A. M., Moschopoulos, P. & Pederzoli, G. Random points associated with rectangles. *Rend. del Circ. Mat. di Palermo* **48**, 163–190 (1999).

36. European Parliament; Council of the European Union. *Directive 2012/19/EU of the European Parliament and of the Council of 4 July 2012 on waste electrical and electronic equipment (WEEE)*. (2012). doi:10.3000/19770677.L_2012.197.eng.

37. Van Den Bossche, A., Vereycken, W., Vander Hoogerstraete, T., Dehaen, W. & Binnemans, K. Recovery of Gallium, Indium, and Arsenic from Semiconductors Using Tribromide Ionic Liquids. *ACS Sustain. Chem. Eng.* **7**, 14451–14459 (2019).

38. Maarefvand, M., Sheibani, S. & Rashchi, F. Recovery of gallium from waste LEDs by oxidation and subsequent leaching. *Hydrometallurgy* **191**, (2020).

39. Zhan, L., Xia, F., Xia, Y. & Xie, B. Recycle Gallium and Arsenic from GaAs-Based E-Wastes via Pyrolysis-Vacuum Metallurgy Separation: Theory and Feasibility. *ACS Sustain. Chem. Eng.* **6**, 1336–1342 (2018).

40. Jung, C. ., Matsuto, T., Tanaka, N. & Okada, T. Metal distribution in incineration residues of municipal solid waste (MSW) in Japan. *Waste Manag.* **24**, 381–391 (2004).

41. Hasselriis, F. & Licata, A. Analysis of heavy metal emission data from municipal waste combustion. *J. Hazard. Mater.* **47**, 77–102 (1996).

42. Blasenbauer, D. *et al.* Legal situation and current practice of waste incineration bottom ash utilisation in Europe. *Waste Manag.* **102**, 868–883 (2020).

43. U.S. Environmental Protection Agency Office of Solid Waste. *EPA's Composite Model for Leachate Migration with Transformation Products (EPACMTP) Technical Background Document*. (2003).

44. European Chemicals Agency. *Guidance on Information Requirements and Chemical Safety Assessment - ECHA*. https://echa.europa.eu/guidance-documents/guidance-on-information-requirements-and-chemical-safety-assessment (2011).

45. Jensen, H., Gaw, S., Lehto, N. J., Hassall, L. & Robinson, B. H. The mobility and plant uptake of gallium and indium, two emerging contaminants associated with electronic waste and other sources. *Chemosphere* **209**, 675–684 (2018).

46. Hollander, A., Schoorl, M. & van de Meent, D. SimpleBox 4.0: Improving the model while keeping it simple…. *Chemosphere* **148**, 99–107 (2016).

47. Vermeire, T. G. *et al.* European Union System for the Evaluation of Substances (EUSES). Principles and structure. *Chemosphere* **34**, 1823–1836 (1997).

48. City of Amsterdam. Maps Data. *2019* https://maps.amsterdam.nl/open_geodata/?LANG=en.

49. The Royal Netherlands Meteorological Institute (KNMI). Klimatologie - Metingen en waarnemingen. https://www.knmi.nl/nederland-nu/klimatologie-metingen-en-waarnemingen.

50. Schoorl, M., Hollander, A. & van de Meent, D. *SimpleBox 4.0 A multimedia mass balance model for evaluating the fate of chemical substances.* https://www.rivm.nl/bibliotheek/rapporten/2015-0161.pdf (2015).

51. van de Meent, D., Zwart, D. & Posthuma, L. Screening-Level Estimates of Environmental Release Rates, Predicted Exposures, and Toxic Pressures of Currently Used Chemicals. *Environ. Toxicol. Chem.* **39**, 1839–1851 (2020).

52. European Chemicals Agency. Gallium - Registration Dossier - ECHA. *Gallium* https://echa.europa.eu/registration-dossier/-/registered-dossier/23228/6/2/4.

53. European Chemicals Agency. Indium - Registration Dossier - ECHA. *Indium* https://echa.europa.eu/registration-dossier/-/registered-dossier/22264.

54. European Chemicals Agency. Arsenic - Registration Dossier - ECHA. *Arsenic* https://echa.europa.eu/registration-dossier/-/registered-dossier/22366.

55. ChemSafetyPro. How to Calculate Predicted No-Effect Concentration (PNEC).

56. Su, J. Y., Syu, C. H. & Lee, D. Y. Growth inhibition of rice (Oryza sativa L.) seedlings in Ga- and In-contaminated acidic soils is respectively caused by Al and Al + In toxicity. *J. Hazard. Mater.* **344**, 274–282 (2018).

57. Firestone, M. *et al. Guiding Principles for Monte Carlo Analysis - Technical Panel.* https://www.epa.gov/risk/guiding-principles-monte-carlo-analysis (1997).

58. Borgonovo, E. A new uncertainty importance measure. *Reliab. Eng. Syst. Saf.* **92**, 771–784 (2007).

59. Plischke, E. & Borgonovo, E. Fighting the Curse of Sparsity: Probabilistic Sensitivity Measures From Cumulative Distribution Functions. *Risk Anal.* risa.13571 (2020) doi:10.1111/risa.13571.

60. Iooss, B., Da Veiga, S., Janon, A. & Pujol, G. Global Sensitivity Analysis of Model Outputs. (2021).

61. World Health Organization. *Environmental Health Criteria 224 Arsenic and Arsenic Compounds Second Edition.* (2001).

62. Jain, C. K. & Ali, I. Arsenic: Occurrence, toxicity and speciation techniques. *Water Res.* **34**, 4304–4312 (2000).

63. Pinel-Raffaitin, P., Le Hecho, I., Amouroux, D. & Potin-Gautier, M. Distribution and Fate of Inorganic and Organic Arsenic Species in Landfill Leachates and Biogases. *Environ. Sci. Technol.* **41**, 4536–4541 (2007).

64. Harstad, K. *Handling and assessment of leachates from municipal solid waste landfills in the Nordic countries*. (2007). doi:https://doi.org/https://doi.org/10.6027/TN2006-594.

65. Shumlas, S. L. *et al.* Oxidation of arsenite to arsenate on birnessite in the presence of light. *Geochem. Trans.* **17**, 5 (2016).

66. Li, X. *et al.* On-device lead sequestration for perovskite solar cells. *Nature* **578**, 555–558 (2020).

67. Allison, J. D. & Allison, T. L. *Partitioning Coefficients for Metals in Surface Water, Soil and Waste*. https://cfpub.epa.gov/si/si_public_record_report.cfm?Lab=NERL&dirEntryId=135783 (2005).

68. Uddh Söderberg, T. *et al.* Metal solubility and transport at a contaminated landfill site – From the source zone into the groundwater. *Sci. Total Environ.* **668**, 1064–1076 (2019).

69. Adothu, B. *et al.* Newly developed thermoplastic polyolefin encapsulant–A potential candidate for crystalline silicon photovoltaic modules encapsulation. *Sol. Energy* **194**, 581–588 (2019).

70. Creutzig, F. *et al.* The underestimated potential of solar energy to mitigate climate change. *Nat. Energy* **2**, 17140 (2017).

71. Ferdous, W. *et al.* Recycling of landfill wastes (tyres, plastics and glass) in construction – A review on global waste generation, performance, application and future opportunities. *Resour. Conserv. Recycl.* **173**, 105745 (2021).

Chapter 6

A framework for guiding Safe and Sustainable-by-Design innovations

Abstract

Assessing the safety and sustainability of technologies while they are still in early research & development stages is the most effective way to avoid undesired outcomes. However, the journey from idea to market is highly uncertain and involves intensive trial-and-error as developers attempt to optimise material choices and configurations. As designs evolve quickly, assessing their environmental impacts while numerous factors remain undetermined is not straightforward. Thus, assessors often revert to evaluating a limited subset of possible scenarios which are then used to guide design choices. However, selecting scenarios for hundreds of undetermined factors without a systematic sensitivity screening may preclude important improvement opportunities. To provide the best guidance, the evaluated scenarios should be defined by the factors that are most influential on the future environmental impacts of the technology. In this chapter we propose a broad approach that accomplishes this by incorporating a wide spectrum of undetermined factors –both intrinsic and extrinsic to the technology design– in integrated assessment models. These models are then screened for highly sensitive factors using global sensitivity analysis. Strategies to further reduce uncertainty on the most influential factors are proposed for a second iteration, and the residual factors for which uncertainty cannot be further reduced and remain influential are selected as a basis for development of "sensitive" scenarios. We demonstrate the framework by applying it to the life cycle assessment and ecological risk assessment of an emerging photovoltaic technology.

Keywords: life cycle assessment, ecological risk assessment, emerging PV, safe-by-design, sustainable-by-design

This chapter is based on the manuscript: Blanco, C.F., Behrens, P., Vijver, M.G., Peijnenburg, W.J.G.M., Quik, J.T.K., Rodrigues, J., Cucurachi, S. (2022). A framework for guiding Safe and Sustainable-by-Design innovations. In preparation for submittal to *Environ. Int.*

6.1. Introduction

Safety and sustainability criteria are taking an increasingly central role in guiding policy decisions for supporting and regulating new technology development.[1] To better support decision-making during the early research and development (R&D) stages, safety and sustainability practitioners have scrambled to propose diverse prospective methods and criteria such as *ex-ante* LCA[2] and prospective risk assessment.[3] However, there is an important challenge in producing such environmental indicators, i.e. accounting for the uncertain evolution of technical, environmental and socioeconomic factors – both intrinsic and extrinsic to the technologies – that influence the future environmental implications of the technologies once they are deployed at commercial scale[2–6].

Traditional *ex-post* assessments of well-established technologies are already prone to inaccuracy and/or imprecision due to uncertainty and variability.[7,8] A risk/impact estimate may deviate from its actual value in response to spatial and temporal variability of the underlying processes, as well as imprecise or unavailable data regarding the technology's design and operational parameters.[9–11] Errors may also be introduced in the broader environmental impact/risk assessment models, which are composed of mathematical relationships that can only offer limited approximations.[12] At the very least, the impacts of existing technologies can –to some extent– be measured and validated empirically. Bereft of this possibility, even more uncertainty surrounds *ex-ante*/prospective assessments.[13]

To further illustrate this challenge, we take the case of an emerging photovoltaic technology, III-V/Si tandem cells (III-V/Si).[14,15] These cells have achieved record conversion efficiencies by adding layers of elements from groups III and V of the periodic table (e.g. gallium, indium, arsenic) on top of a silicon substrate to increase light absorption. However, especially the use of arsenic may raise concerns about the safety and sustainability of III-V/Si. Whether the trade-off between potential toxicity and improved solar cell performance is desirable depends on many factors. For example, at end-of-life (EOL) the panels could be recycled, and the arsenic recovered, or they could be incinerated or disposed of in a landfill or underground waste deposit. The extent to which arsenic is recovered from PV panels at EOL will depend on economic factors along with regulatory concerns surrounding e-waste or supply risks.[16,17] Finally, there will be the ease and feasibility of current and future methods for physically separating the arsenic from the other panel constituents will be determinant. Since arsenic can take various forms once released, from high-toxicity (+3 oxidation) to a low-toxicity (methylated) state, uncertainty regarding the form of arsenic to which organisms are ultimately exposed will also be of importance.

The influence of these numerous and interrelated factors which span multiple domains will remain unknown until the assessments are conducted and complemented with some form of sensitivity analysis[18]. A common strategy that has been applied across numerous modelling disciplines to deal with uncertain factors of presupposed relevance is scenario analysis. This approach has provided more confidence in the assessments, especially in

the presence of epistemic uncertainties. However, the number of uncertain factors and plausible scenarios that result from their combined interactions can easily be in the tens or even hundreds, especially when considering interactions across social, technical, and economic domains that influence a technology's performance. What is often observed in practice is that a handful of scenarios are selected, which can help as a benchmarking exercise and to identify hotspots.[19,20] In this approach, however, the actual relevance of the selected scenarios to safety and sustainability implications is not evaluated before they are selected, whilst leaving potentially important scenarios outside of the analysis.

In this chapter, we present a framework to identify the scenarios of most interest that can result from the different configurations of the most influential factors and use these to prioritize R&D efforts towards safe and sustainable-by-design (SSbD) innovation. We illustrate the framework by diving deeper into the case study of III-V/Si cells introduced above. The framework follows five steps (Figure 6-1): i) identify and map uncertain factors, with special attention to those specific to the forward-looking or *ex-ante* nature of the assessments; (ii) propose methods for the characterization and propagation of the uncertainties in these factors; (iii) identify the least sensitive factors and fix them to reduce model complexity (iv) apply strategies to reduce uncertainty in the most sensitive factors; (v) in a second iteration, select remaining sensitive factors as a basis to develop relevant scenarios based on sensitivity, e.g. "sensitive scenarios". Sensitive scenarios will highlight opportunities for most effective safety and sustainability improvements for technology designs that are in the early R&D.

We developed this framework considering two different types of environmental assessments: life cycle assessment (LCA), and human and ecological risk assessment

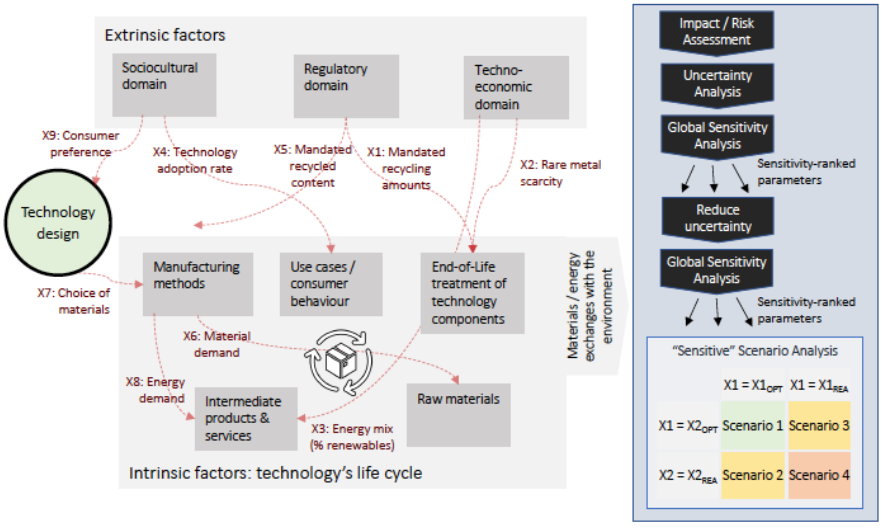

Figure 6-1 Framework for guiding safe and sustainable-by-design innovation. Red arrows show examples of uncertain/evolving factors (X#) that may influence the material and energy exchanges associated to the technology's life cycle, and the concomitant impacts and risks. Global Sensitivity Analysis (GSA) can be used to prioritize the most influential factors for targeting at the design stage.

(HERA). An introduction to each is provided by Guinée et al.[21] and ECHA[22], respectively. The combined use of LCA and HERA is seen as a promising approach for addressing the potential environmental concerns of emerging technologies[23,24]. Although we focus on these two methods, the framework we propose can be applied to other types of technology assessment models.

6.2. Methodological framework

6.2.1. Factors that determine the future environmental performance of emerging technologies

The adoption of a new technology by society will trigger changes in the environment. These changes – whether desirable or undesirable – are quantified using indicators such as concentration of pollutants in air, area of ecosystem degraded, or risk quotients for endpoints such as aquatic species reproduction. Indicators vary in response to changes in factors that interact across different domains, forming a cause-effect chain (Figure 6-1, left). Some factors are farther removed from the technology design itself but may have a larger influence on the indicator. For example, they can reside in regulatory trends, which may set increasingly strict limitations on materials usage, or in social/economic/cultural trends, which may determine how much of the technology is used and where. In an LCA model, for example, a factor such as X8 may represent the amount of electricity that will be required by a chosen manufacturing method (X7). A change either in X8 or X7 will mediate the quantity of CO_2 emitted, but this also depends on the source of electricity that is supplied (X3). These relationships -amongst others- determine the technology's carbon footprint. Extrapolating this analysis to entire life cycles and related processes in the socioeconomic domains, as well as to other types of indicators beyond carbon footprint, makes evident that the number of cause-effect chains and the undetermined factors within them may easily fall in the hundreds or thousands.

6.2.2. Sources of uncertainty in models of the future

Uncertainty has been comprehensively studied in *ex-post* assessment models. A good overview is provided by Lloyd and Ries[25], who classify uncertainties according to different LCA modelling components: parameter (input data), model (mathematical relationships), and scenario (normative choices). A similar set of uncertainty sources has been described in risk assessment[26]. *Ex-ante* assessments introduce additional sources of uncertainty due to the forward-looking nature of the assessments. Table 6-1 extends our previous work[13] and proposes a comprehensive typology for these new sources, along with relevant examples found in both HERA and LCA *ex-ante* models. It is important to note that there can be overlap between uncertainty types. For example, uncertainty in a physical constant such as a soil/water partitioning coefficient for a novel substance can be considered either parameter or model uncertainty. Uncertainty in a physical constant can even be classified as scenario uncertainty whereby each scenario represents a future world where the constant has a different value from a range of possible values.

6.2.3. Model parametrization: putting uncertainty types at the same level

The first step in our framework is to translate as many uncertainties as possible to a parameter type of uncertainty. This requires all potentially influential factors, such as those listed in Table 6-1 to be represented as variable parameters in a single integrated model. This is straightforward for the "parameter" types of uncertainties listed. Scenario uncertainties of type I, III, V and VII, which are often assessed independently, can also be parametrized using the approach we demonstrated in Chapter 4, where alternative scenarios exist simultaneously in a model and are activated or deactivated stochastically using binomially distributed parameters as triggers.[13] Model uncertainties can be incorporated in a similar way, as described by Saltelli et al.[27] and Mendoza-Beltrán et al.[28]

6.2.4. Characterization of *ex-ante* uncertainty

The second step involves expressing the range of possible values for all parameters - including triggers for alternative models and scenarios- as probability distributions. Since we are referring to future events, we must first specify what is meant by probability. We will advocate for a Bayesian interpretation of probability, but briefly describe other approaches as well to support our case:

- A *frequentist* approach determines probability distributions by conducting numerous tests (or collecting numerous samples) and recording the frequencies of occurrence of each value. Such tests or samples can only be collected once a technology is deployed so the approach is of limited use in *ex-ante* assessments.
- The *classical* approach determines the likelihood of occurrence of each value, based on all possible values. This approach can be useful in *ex-ante* assessments, e.g., if we know beforehand that there are only three possible processing routes for a given component of the technology. This gives each route 1/3 chance of success. An important limitation of this approach is that all possible values are given equal odds of occurrence.
- The *Bayesian* or *subjective* approach uses probability distributions to represent the degree of belief that an observer has in a particular outcome.[29,30] The Bayesian approach has been applied in risk assessment[31] and to a lesser extent in LCA[32]. It is especially useful for *ex-ante* assessment, if not essential; many possible future states cannot be simulated in a frequentist way. While frequentists have long argued that subjectivity is a strong limitation (or outright invalidating the scientific nature of the exercise), it is also a key strength in that it incorporates other sources of relevant information where actual measurement data is scant or unavailable. Bayes' Theorem provides a formal method for updating the beliefs (represented by so-called *prior* probability distributions) once new data becomes available to produce a *posterior* distribution.[30] This naturally fits the research & development process, which iterates a technology through additional testing and gradual upscaling in order to optimize it until it is ready for commercialization.

The question then is how best to establish prior distributions for uncertainties and variabilities of the types listed in Table 6-1, and then how to update them. Prior distributions must reflect beliefs about parameters that describe the uncertainty of the true (future) state of a factor, e.g., the probability that manufacturing method A will be used instead of B for a particular component once the technology reaches industrial scale. The most conservative attempt would be to start with flat or "non-informative" prior distributions, which distribute probabilities evenly across all possible parameter values. However, there is a trade-off regarding how informative subsequent posteriors will be. Wolpert et al.[33] describe this situation very well and offer that -with important caveats and limitations- "collateral evidence" such as that obtained from field studies of similar environmental systems, expert elicitation, and laboratory studies of the related process can be used to inform priors.[33]

Another often-applied rule of thumb in Bayesian statistics is to choose priors from a "conjugate distribution family". Conjugate priors ensure that the functional form of the resultant posterior distribution is the same as that of the prior, i.e. a PERT prior probability density function will be updated to a PERT posterior probability density function.[30] Conjugate priors also make the estimation of posterior distributions a far simpler and more intuitive exercise once additional data or observations are obtained (see Box 6-1).

6.2.5. Propagation of uncertainty and variability

Two approaches for propagating uncertainties are commonly applied; analytic and numerical[34]. The models' complexity and the fact that integrated assessments require interaction between different types of models make analytical solutions impractical for this type of framework.[35] The preferable alternative is Monte Carlo simulation[36,37], which generates numerous random samples from the underlying probability distribution of the model's input parameters and calculates an equal number of values for the model's output. The frequency distribution of the obtained values is used to construct a probability distribution.

When propagating uncertainty, it is often the case that two or more elements in a model share a source of uncertainty. When this happens, the values for both parameters are dependent.[35] Correlations have been identified between many elements of *ex-post* LCA models.[38,39] They also exist amongst the *ex-ante* uncertain parameters listed in Table 6-1. For example, a future increase in ambient temperature may affect the amount of cooling needed to safely operate a novel battery technology, increasing energy consumption and CO_2 emissions of the system. The same factor may affect precipitation and cloud cover. Both mechanisms will have a global warming impact that to some extent depends on the same uncertain factor.

Table 6-1 Uncertain factors in ex-ante assessments of emerging technologies. Factors are classified according to their modelling domain and whether they are extrinsic or intrinsic to decision-making during the R&D process.

Type	Domain	Intrins.(I)/ Extrins.(E)	Uncertain factor	Uncertainty type	LCA component	HERA component	Context and examples
I	Technology design	I	Material choice	Scenario	Inventory (foreground)	Similarity estimates	Different materials will be tested and selected based on optimized performance; more recently safety, chemical simplicity and recyclability are also considered. See Blanco et al.[13] (metallization of PV cells)
II	Technology design	I	Material quantity	Parameter	Inventory (foreground)	Emission scenario	Quantities of materials used in the design may vary as the design gets optimized.
III	Technology manufacturing	I	Manufacturing route	Scenario	Inventory (foreground)	Emission scenario	Manufacturing/synthesis methods may change when upscaling to industrial scale. See Picchino et al.[40] (chemicals)
IV	Technology manufacturing	I	Material and energy use	Parameter	Inventory (background)	Emission scenario	Process optimizations likely lead to reduced material and energy consumption. See Cucurachi et al.[41] (silicon PV cells)
V	Techno-economic	E	External industries processes	Scenario	Inventory (background)	Emission scenario	Analogous to (III) but applied to external suppliers.
VI	Techno-economic	E	External industries materials & energy use	Parameter	Inventory (background)	Emission scenario	Analogous to (IV) but applied to external suppliers. See Harpprecht et al.[42] (metals)
VII	Techno-economic	E	External markets composition	Scenario	Inventory (background)	Emission scenario	Changes in market compositions for products and services in the supply chain. See Mendoza-Beltran et al.[43] (energy) and Harpprecht et al.[42] (metals)
VIII	Technology use	I/E	Function of technology	Scenario	Goal and scope	Emission scenario	The technology may ultimately be used in different ways. It may be used for multiple/different purposes. See Hiremath et al.[44] (batteries) and Hischier et al.[45] (engineered nanomaterials).
IX	Technology use	I/E	Survival/Failure rates	Parameter	Inventory (foreground)	Emission scenario	Failures (due to e.g. obsolescence, degradation or misuse) may cut the technological products' lifetimes short. See Miller et al.[46] (online commerce)

Type	Domain	Intrins.(I)/ Extrins.(E)	Uncertain factor	Uncertainty type	LCA component	HERA component	Context and examples
X	Technology use	I	Functional performance	Parameter	Goal and scope	Emission scenario	Operational performance parameters may deviate from expected values. See Gong et al.[47] (perovskite PV).
XI	Technology EOL	I/E	Recycling	Scenario	Inventory (foreground)	Emission scenario	The development of recycling methods often lags behind technology deployment. It is not known whether and how this will happen. See Raugei and Winfield[48] (battery recycling)
XII	Regulatory	E	Material use & emission thresholds	Parameter/ scenario	Inventory (background)	Emission scenario	Regulation may impose new limits on emissions, use or choice of materials and energy sources.
XIII	Environment /landscape	E	Characterization model: fate	Parameter	Impact assessment	Fate	Landscape parameters that may affect transport and fate of the substances can change in time, e.g. changing averages for ambient temperatures, wind speeds or ocean water pH can affect how substances are distributed in the environment.
XIV	Environment /landscape	E	Characterization model: exposure	Parameter	Impact assessment	Exposure	Parameters that affect exposure e.g. population densities or diets can change in time.
XV	Environment /landscape	E	Characterization model: effect	Model	Impact assessment	Effect	Marginal changes may result in exponentially larger effects as the baseline condition deteriorates. e.g. impact of increased radiative forcing on ecosystems.
XVI	Techno-economic	E	Allocation	Parameter	Inventory (foreground)	N.A.	The parameters used to establish the criteria for allocation of multifunctional processes may change in time. e.g. forecasted market values in the case of economic allocation in LCA.
XVII	Techno-economic	E	Resources	Parameter	Impact assessment	N.A.	Availability of natural resources may change over time. This can particularly affect LCA impact categories related to resource depletion. See Baustert et al.[49] (water scarcity)

Integrating models presents an important opportunity to account for dependencies between parameters across different processes, scales and domains. This is not trivial to our goal: a factor that has dependencies can have additional indirect influence on the model's output, i.e., it may become more relevant. A convenient way to address correlations is to isolate each shared source of uncertainty or variability in one single parameter. The random values for the Monte Carlo simulation can be pre-sampled, ensuring the same value for all occurring instances of the shared parameter is used within each Monte Carlo run.[50] This strategy already prepares the data required for the next step.

6.2.6. Global sensitivity analysis: screening for relevant factors

A global sensitivity analysis (GSA) reveals "how uncertainty in the output of a model (numerical or otherwise) can be apportioned to different sources of uncertainty in the model input"[51]. In our framework, GSA is used as the "sieve" which selects the most relevant factors from all those identified. The characteristics of the integrated models we use place certain constraints on the type of GSA that can be performed. First, it is likely that the resulting models will be highly dimensional with numerous uncertainty parameters. This requires calculation algorithms for sensitivity indices that can be performed in a reasonable computational time. Second, the models are usually integrated by passing output data as input data between them (as in the integration of economic demand with emissions and fate models in Chapter 5), which makes analytical GSA methods not practicable. "Black box" or model-independent GSA methods such as the *delta* measure introduced by Borgonovo[52] are thus favoured. Third, the introduction of binomial and other discrete distributions for parameters may sometimes result in multimodal output distributions. Therefore, variance-based methods may not be suitable and moment-independent methods are preferred.[52,53]

As we showed in Chapter 4, and elsewhere[13,41], one GSA method that meets these requirements is the Borgonovo delta sensitivity measure[54]. The Borgonovo *delta* represents the influence of a parameter as its ability to shift the model's output distribution curve. This is illustrated by Figure 6-2, where the red probability distribution curve is the environmental risk of a technology when all uncertain factors are left to vary freely across their entire spectrum of possibilities, according to their underlying distributions (*unconditional*). If one factor in the risk model can be fixed at a value representing one scenario, the curve will shift by moving along the x-axis (lower or higher risk depending on the value assumed by the parameter) and will become narrower (lower uncertainty/dispersion in the model output or risk score). The new blue curve (conditional) is the environmental risk for the specified scenario. For an environmental indicator, it is usually desirable that the output distribution curve moves towards the origin on the x-axis (lower risk/impact) and becomes narrower (less uncertainty). The curve *shift* is defined by Borgonovo as the non-overlapping area between both curves. The *delta* sensitivity measure is the probability-weighted average of all possible shifts induced by the parameter when it is fixed at its possible values.[54]

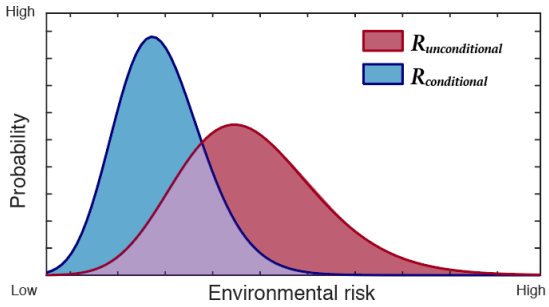

Figure 6-2 Graphical representation of Borgonovo's delta sensitivity measure in an environmental model. The non-overlapping area (blue + red) represents the shift in the curve when the model is evaluated conditional to an uncertain fixed at one of its possible values (Adapted from Borgonovo[52]).

6.2.7. Second iteration: further reducing uncertainty

The first GSA iteration may result in several factors that have higher sensitivity. Before producing recommendations or making any decisions on the technology design, three avenues can be used first to further reduce uncertainty in the model. For subjective probabilities: structured expert knowledge elicitation protocols such as DELHPI, aimed at reducing bias while furthering consensus[55,56]. Some of these methods have even been extended to incorporate the experts' beliefs regarding their own uncertainty[57–59] For other uncertain factors, more refined modelling can be applied specifically to the nature of the parameter, e.g. hydrological, geochemical, or economic models based on market research. A third recourse is to collect additional data from lab or pilot-scale tests, such as leaching tests or process consumption and emissions measurements. Bayesian inference can then be used to update the probability distributions for the factors for which new data was obtained (see Box 6-1).

6.2.8. Proposing safe and sustainable by design strategies

Once the possibilities to further reduce uncertainty have been exhausted, a second uncertainty propagation and GSA iteration will produce the residual most relevant factors. These factors can then be used to construct "sensitive" scenarios, which by this point will likely consist of a much smaller, but highly relevant subset. These scenarios can be used to engage with technology developers and other stakeholders (e.g., suppliers, consumers, policymakers, funding agencies and environmental advocacy groups) around the prioritization of design changes and/or other measures that can be taken to show the most efficient measures towards a safe and sustainable deployment of the technology.

The sensitive scenarios point to the factors which are most influential *while still subject to considerable change*. This presents an opportunity to influence these factors by attempting to fix them at a desirable value or at least reduce their uncertainty/variability towards a smaller and more desirable range (shift the distribution to the left and make it narrower). Because the factors can span different model domains, their nature may vary significantly as will the possible ways to influence them. A well-tested guiding principle that has been

applied for several decades in risk management is the hierarchy of risk control measures, which leads the decision-maker to prioritize strategies according to the order (i) elimination, (ii) substitution, (iii) engineering control, (iv) procedural control and (v) personal protective equipment. Such strategies are already very visible in proposals for emerging PV technologies, such as in-situ sequestration of lead in perovskite solar cells[60] (engineering control), replacement of lead for tin (substitution)[61], and administrative management of the risk (e-waste regulations[17,62]).

6.3. Case study of an emerging solar energy technology

6.3.1. III-V/Si photovoltaic system

To demonstrate the proposed framework, we apply it to the III-V/Si PV technology. In Chapter 3 we conducted a life cycle assessment of this technology largely based on lab-scale and pilot data from a European R&D project.[63,64] In the following sections we take this as a starting point and develop the different steps of the framework. The iterations result in different versions of the LCA and RA models, each representing our state of knowledge at different points in time as the R&D project advanced.

6.3.2. Life cycle assessment

The manufacturing of III-V/Si cells involves numerous processing steps, most of which are already at industrial scale and used in the mainstream silicon PV industry. Two key steps, however, are still early-stage concepts which could only be tested at lab and pilot-scale. The first is the deposition of the top cell's III-V layers, which are grown via Metalorganic Vapour Phase Epitaxy (MOVPE).[65] In the initial phase of the project (*t=0*) we considered state-of-the-art MOVPE reactors that are currently used in related industries. These reactors have a high energy consumption with low throughputs (7 round 4" wafers per run at 3.5-hour runtime). For a future III-V/Si PV industry, this would not be economically viable or environmentally advantageous.[64] Therefore, this was an R&D priority and by the end of the project (*t=1*), a pilot-scale reactor achieved a throughput of 31 round 4" wafers per run at 2.5 hours runtime.

It was determined, however, that even larger throughputs would be required to make the technology economically feasible. Further projections of throughput increase and runtime reductions were elicited from experts, based on what they would consider feasible future improvements in the reactor (*t=2*). Such improvements include switching to larger wafers (square M2 wafers) and increasing throughput to 50 wafers per run at 0.5 hours runtime. A PERT distribution was used to represent this uncertain evolution via two factors: MOVPE power consumption per wafer area and MOVPE process runtime. The distributions' minimum, mode and maximum parameters were adjusted accordingly between *t=0* and *t=2* based on the R&D achievements and experts' projections for what would ultimately be feasible.

The second key processing step is the metallization of the front contacts, for which a decision had to be made between nanosilver and nanocopper ink as described in Chapter 4.[13] The analysis made in this previous work represented the state of knowledge at an initial state of the project (*t=0*). Additional research and testing were conducted, showing more promising results for copper. We use this Boolean factor to illustrate Bayesian updating within the framework (see Box 6-1) and how it can be updated in an intermediate step (*t=1*) and towards the end of the project (*t=2*) based on the results of lab tests.

Box 6-1 – Bayesian updating applied to uncertainty in material compositions

In building an *ex-ante* LCA of an emerging photovoltaic cell design, it was found that two alternative materials for the front metallic contacts were under consideration: nanosilver and nanocopper particles.[13] The material that shows best electrical properties will ultimately be incorporated in the cell design, but this may depend on evolving intrinsic and extrinsic factors. Thus, we want to use a probability distribution to represent the chance of copper performing better than silver, so that the choice of material can be used in a probabilistic LCA model. The competition between copper and silver can be simulated as a binomial process, where the success of copper over silver in any given trial is described by Equation 6-1:

$$x \sim bin(1, p) \qquad \text{(Eq. 6-1)}$$

If copper is successful, $\boldsymbol{x}$ will take a value of 1 while if silver is successful, $\boldsymbol{x}$ will take a value of 0. The uncertain parameter of interest is $\boldsymbol{p}$, which is the probability of copper having better properties than silver in a random trial*. We don't know this probability and must make a subjective estimate of it. The data we have is the following: Six trials have been conducted to date. Copper showed better properties (success) on 4 of the 6 trials.

Establishing a prior: Choosing a beta distribution to describe $\boldsymbol{p}$ greatly simplifies inference of binomial parameters.* From the data we have, we set the mean $\boldsymbol{\mu}$=4/6 from a sample size $\boldsymbol{n}$=6. The parameters $\boldsymbol{\alpha_0}$ and $\boldsymbol{\beta_0}$ of the (prior) beta distribution for $\boldsymbol{p}$ can be calculated from $\boldsymbol{\mu}$ and $\boldsymbol{n}$ using Equations 6-2 and 6-3. Our prior beta distribution for $\boldsymbol{p}$ is then specified by parameters $\boldsymbol{\alpha_0}$ = 4 and $\boldsymbol{\beta_0}$ = 2 (Figure 6-3, "Prior").

$$\alpha_0 = \mu \cdot n \qquad \text{(Eq. 6-2)} \qquad\qquad \beta_0 = (1-\mu) \cdot n \qquad \text{(Eq. 6-3)}$$

Updating to a posterior: A posterior distribution for $\boldsymbol{p}$ can be obtained when additional testing is performed. Following the analytical updating procedure of DeGroot[66], if 3 additional laboratory tests (trials) are performed and copper shows better performance in 2 out of 3 tests, the posterior distribution (Figure 6-3, Post1) will also have a beta form, this time with $\boldsymbol{\alpha_1} = \alpha_0 + 2$ and $\boldsymbol{\beta_1} = \beta_0 + 1$. Here, 2 and 1 represent successes and failures of copper to perform better than silver in the new trials, respectively. If an additional test is performed where copper is again successful, we again update our posterior beta distribution (Post2) with $\alpha_2 = \alpha_1 + 1$ and $\beta_2 = \beta_1 + 0$ (Post2).

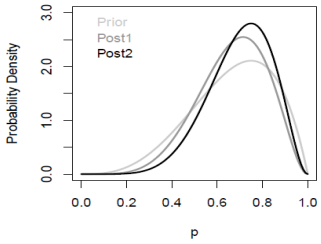

Figure 6-3 Bayesian updating of the probability of success of copper over silver

The x-axis in Figure 6-3 plots $\boldsymbol{p}$, which is the chance of success of copper, and the y-axis plots the probability of the x-value for parameter $\boldsymbol{p}$ being correct. Updating $\boldsymbol{p}$ with new test results moves the chances in favour of copper but also reduces the spread of the distribution curve.

Some additional parameters in the background silicon supply chain and other non-cell components were also updated between *t=0* and *t=2* to better reflect state-or-the-art, following the work of Cucurachi et al.[41] Table 6-2 summarizes how we represented the evolution of these factors in the model using different probability distributions.

The resulting impact score distributions for climate change for each snapshot of the technology is shown in Figure 6-4. The figure clearly illustrates how successive iterations reduce not only the impact (by any measure of central tendency) but the dispersion as well. The Bayesian updating of the front metallization route in favour of copper with a laser sintering route shifted the distribution slightly to the left and reduced dispersion at *t=1*. In the final period of the R&D project (*t=2*), two key achievements resulted in a significant improvement and reduction in uncertainty: the successful demonstration of the pilot reactor with significantly lower power requirements, and the decision to fully abandon the silver metallization route as well as the chemical sintering method in favour of the copper with laser sintering route.

In the first iteration (*t=0*), the global sensitivity analysis (Figure 6-5) highlighted the sensitivity importance of the power consumption of the MOVPE tool (*P_movpe_tool*)*, followed by MOVPE runtime (*RT_movpe*) and panel lifetime (LT_panel). A second tier of importance consisted of several factors in the background silicon supply chain as well as the choice between copper and silver nanoink (*Cu_vs_Ag*) for the front metallization, and the chances of success of the different nanoparticle synthesis and ink sintering routes (*p1-p5*). In the case of binomially distributed factors, the underlying probabilities p_x of each were more influential than the factors themselves. This contrasts with the result we had obtained for similar distributions in the simplified case study of Chapter 4.

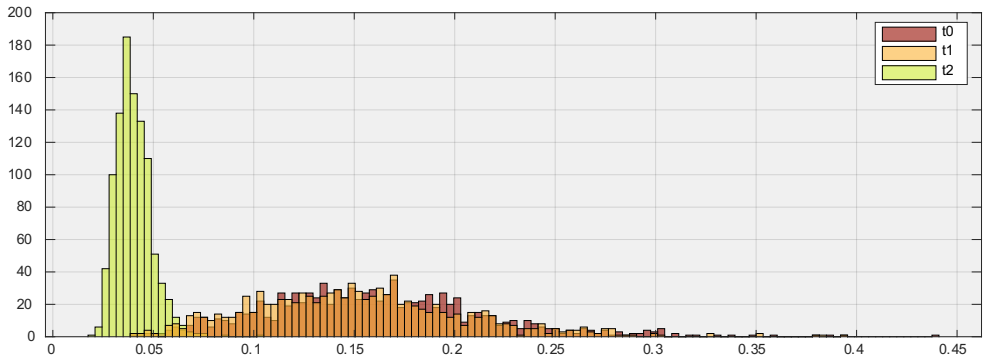

Figure 6-4 Frequency distribution for climate change impact scores (in kg CO2 eq) of the emerging III-V/Si technology in three successive snapshots in time: t0=midpoint through the R&D project, t1=after additional lab tests for different front metallization configurations, and t2=at the end of the R&D project.

* See Table 6-2 for factor/parameter definitions.

Table 6-2 - Evolution of key factors in an LCA model of the III-V/Si tandem photovoltaic technology

Factor Id	Factor description	Initial model (t=0)	Final model (t=2)
MOVPE			
P_movpe	MOVPE tool power load per processed wafer area	pert (min=1, mode=509, max=509, shape=4)	pert(min=13.3, mode=119, max=119, shape=4)
RT_movpe	MOVPE runtime	pert(min=0.5, mode=3.5, max=3.5)	pert(min=0.5, mode=1, max=2.5)
Scru_cons	Scrubber granulate consumption	triang(min=2.55, mode=7.65, max=7.65)	No change
Front metal*			
Cu_v_Ag	Choice of Cu nanoink vs. Ag nanoink	bin(1, p_1) p_1 ~ beta(4,2)	1 (resolved)
Synth_Ag	Choice of chemical vs physical synthesis for Ag	bin(1, p_2) p_2 ~ pert(1000, 0.5,0.7,0.8)	N/A
Synth_Cu	Choice of chemical vs physical synthesis for Cu	bin(1, p_3) p_3 ~ pert(1000, 0.5,0.7,0.8)	No change
Sint_Cu	Choice of laser vs. chemical sintering for Cu	bin(1, p_4); p_4 ~ pert(min=0.1, mode=0.2, max=0.3, shape=4)	1 (resolved)
Sint_Ag	Choice of laser vs. chemical sintering for Ag	bin(1, p_5); p_5 ~ unif(1000, 0,1)	N/A
Performance parameters			
Eff_panel	Panel efficiency	pert(min=0.25, mode=0.28, max=0.31, shape=4)	No change
PR_syst	Performance ratio of PV system	pert(min=0.8, mode=0.85, max=0.9, shape=4)	No change
LT_panel	Panel lifetime	norm(30, 5)	No change
Background supply chain			
Cu_scrub	Scrubber granulate copper fraction	pert(min=0.2, mode=0.3, max=0.7, shape=4)	No change
Cu_rec	Recycling of copper from granulate	bin(n=1, p= 0.5)	No change
Al_panel	Aluminium in panel	lnorm(gm= 2.63, gsd=1)	unif(1000, min=1.6, max=2)
Glass_panel	Glass in panel	lnorm(gm=10.08, gsd=1.22)	unif(1000, min=5.04, max=7.56)
Elec_panel	Electricity to manufacture panel	lnorm(gm=4.71, gsd=1)	unif(1000, min=12.22, max=15.27)
Elec_siem	Electricity consumption Siemens process	lnorm(gm=110, gsd=1)	unif(1000, min=34.1, max=44.3)
Heat_siem	Heat consumption Siemens process	lnorm(gm=185, gsd=1)	unif(1000, min=57.24, max=74.52)
Elec_CZ	Electricity consumption Czochralski process	lnorm(gm=85.6, gsd=1.22)	unif(1000, min=43.4, max=69.3)
Si_CZ	Silicon consumption for Czochralski process	lnorm(gm=1.07, gsd=1)	triang(1000, min=0.4, mode=0.66, max=0.75)

**For the Front metal components, the five uncertain choices are represented by two uncertain factors each: the choice (a variable equal to 1 or 0) and the chances of success for the given choice, which is represented by an uncertain factor p_x. The initial model then has 25 uncertain factors in total.*

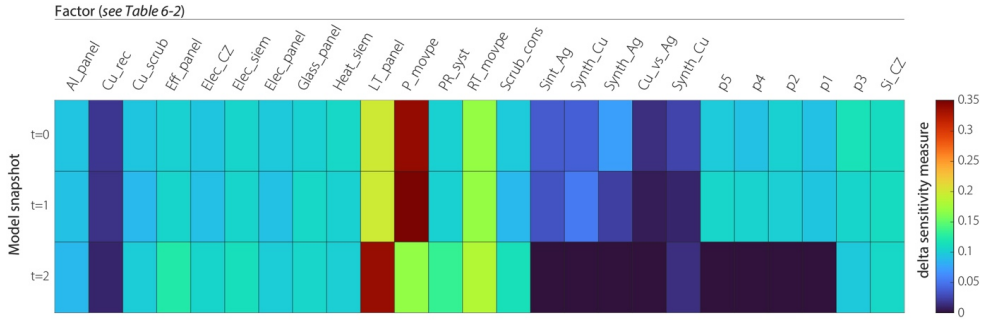

Figure 6-5 Delta sensitivity measures (relative to other factors) in three successive snapshots in time: t=0: midpoint through the R&D project, t=1: after additional lab tests for different front metal configurations, and t=2: at the end of the R&D project. The description of each factor is provided in Table 6-2.

At the end of the R&D project (*t=2)*, the influence of MOVPE power consumption is largely reduced and the most sensitive factor by a considerable margin is now the panel's lifetime. This presents an interesting opportunity; on one hand, III-V cells have been designed in the past to withstand extreme radiation for their applications in space and there is a good case for III-V/Si cells to last longer than conventional silicon ones. Following the hierarchy of risk controls suggested in section 6.2.8, this would constitute a very effective engineering control. In addition to this, the high efficiency of III-V/Si cells means that they are less likely to become obsolete before they reach their end-of-life.

6.3.3. Risk assessment

In Chapter 5 we conducted a detailed prospective ecological risk assessment of the III-V/silicon tandem PV technology throughout its various life cycle stages, with a focus on the III-V materials that constitute the top cell (gallium, arsenide, indium). The model underpinning the assessment presented reflects the current state-of-knowledge and concluded that the risks are low to negligible in the explored scenarios. An earlier preliminary version of the assessment was conducted ca. 2 years earlier with more limited knowledge.[67] Here we present for illustration purposes how this first version of the model was refined and how the conclusions changed considerably after applying the framework. The key model settings and assumptions that changed are described in Table 6-3.

Figure 6-6 shows the distribution for the risk quotient obtained for arsenic emissions to soil in a no-recycling scenario (no arsenic recovered from PV panels collected for disposal). A global sensitivity analysis of this preliminary model highlighted the leaking rate and the leaching rate as the most sensitive parameters. Thus, increased focus was placed on the landfill emissions component of the model during the final 2 years of the R&D program. The model was refined as presented in Chapter 5, with leaching processes reparametrized in terms of a solid/waste partitioning coefficient (k_{sw}) for which more than 100 datapoints were available. Leakage processes were also reparametrized in terms of landfill infiltration, for which again more than 100 datapoints were available.

Table 6-3 - Evolution of key factors in the ecological risk assessment model of the III-V/Si tandem photovoltaic technology

Factor description	Preliminary model (t=0)	Current model (t=1)	Future model (t=2)
PV capacity demand	Steady state 5 GW capacity addition per year	Dynamic, logistic growth curve based on >1000 datapoints.	No change
Arsenic waste leaching in landfill	Constant rate (% mass/year). Empirical, based on two datapoints, a lognormal distribution was assumed with mean 0.8 and variance 0.3.	Dynamic, calculated from empirical solid/waste partitioning coefficient (k_{sw}) based on >100 datapoints.	Leachate pH controlled resulting in higher k_{sw} (now sampled only from the upper quartile of the distribution used in t=1).
Leakage of landfill leachate to surrounding soil compartment	Constant leakage rate of landfill leachate to the surrounding soil compartment (%/year): based on 1 datum, a lognormal distribution was assumed with mean 2.0 and variance 0.7.	Constant, calculated from landfill infiltration rates based on >100 datapoints.	No change
Landfill cell depth	Not applicable	Empirical, exponential distribution with a peak at 10 and lower value 0.5m. based on >100 datapoints.	Increased landfill depths (PERT distribution with min=5, mode=7.5 max=10 m.)
Recycling rate	85%-99.9% panels collected	85%-99.9% panels collected	Increased to 95%-99.9% panels collected
Incinerator abatement	98-99.9% arsenic captured in electrostatic precipitator	No change	Improved to 99.5-99.9% arsenic captured in electrostatic precipitator

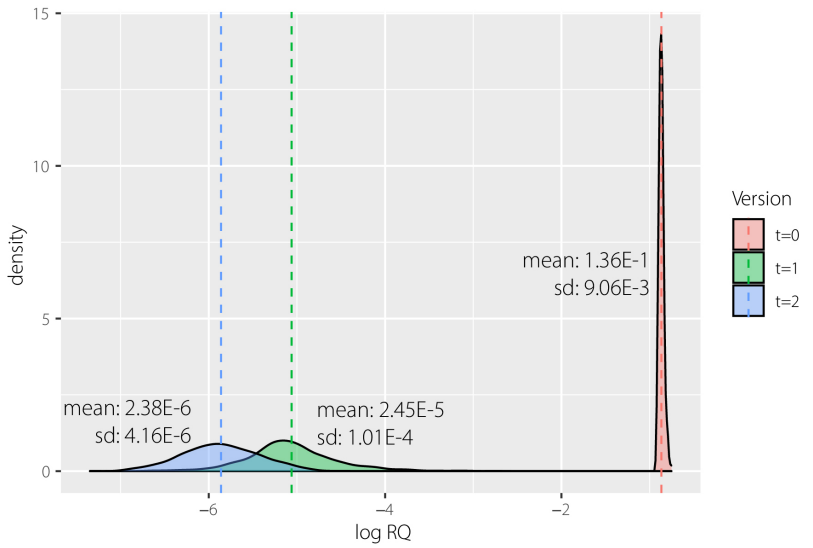

Figure 6-6 Frequency distribution of risk quotient for III-V/Si arsenic emissions to soil in the European continent

Both processes -along with the growth in PV demand- were modelled dynamically rather than steady-state, recognizing the relevance of the temporal dimension and to reflect more realistic scenarios. As a result, the risk quotient for arsenic in the soil compartment in Europe was reduced by several orders of magnitude, becoming negligible. We note that dispersion increased considerably with the model refinement that took place between *t=0* and *t=1*. This is likely attributed to the refined landfill model where the new parameters – especially the waste/leachate partitioning coefficient - introduced a large variability. Arguably, it is best to first improve accuracy, even if it at the expense of precision.[12]

The GSA in Chapter 5 (corresponding to *t=1*) pointed to four factors to target and strategies to address them: the waste/leachate partitioning in the landfill, the landfill depth, the recycling rate, and the incinerator abatement. The combined effect of these actions can be evaluated in an "optimistic" future scenario *t=2*, where the risk could be reduced by an additional order of magnitude as a result of specific strategies. Figure 6-6 shows how the risk is further reduced by nearly an order of magnitude.

6.4.Discussion

6.4.1. Insights obtainable through the framework

Applying our framework to the LCA of the III-V/Si PV system highlighted a very interesting point regarding the lifetime of PV panels, which resulted in the most sensitive factor after three iterations. While it is common in LCAs of PV to standardize the lifetime parameter to a fixed value[68] e.g., 25 or 30 years, there is an important variability coming from two different sources. On one hand there is the stability of the cell/panel and its ability to withstand weathering and degrade slowly. Some opportunities for improvement in this sense lie within the grasp of the technology developer. III-V/Si cells already present an important advantage as they can withstand high radiation for long periods of time without degrading.

Further work on improved cell coatings and panel glass framing may offer important avenues for more sustainable design. On the other hand, there is the proper maintenance and protection of the panel during its use phase. Together with the decision to use the panel throughout its entire useful life and not replace it earlier than needed, this opportunity is on the side of the consumer. Our analysis indicates that if the technology developer undertakes all foreseeable actions to improve the manufacturing and design, then the influence the consumer has over the panel reaching its EOL too early will significantly outweigh additional marginal improvements that can be achieved on the design side. Furthermore, we note that the performance ratio (*PR_syst*), which can also be influenced by the user via adequate maintenance/cleaning and proper installation setup, had a moderate ranking in sensitivity (Figure 6-5). In a way, these recommendations follow the progression of the hierarchy of risk controls, where engineering controls (design changes) are exhausted and administrative controls (e.g., consumer behaviour) follow next.

To better illustrate the potential implications of improved panel lifetime management, we can observe the shift in the climate change impact score distributions when panel lifetime is fixed at its min (25 years) and max (35 years) values for a pessimistic and optimistic case, respectively. For the distributions in Figure 6-7, the mode shifts from ca. 0.045 in the pessimistic case to 0.03 kg CO2 eq. in the optimistic case, an impressive potential for impact reduction of 33%. After three iterations, the LCA model was simplified from 25 underspecified factors to 15, without ignoring the remaining 10. Rather they were systematically assessed and then fixed at an average value, since their uncertainty was proven unimportant. Of the remaining 15 factors, it would now be justifiable to prioritize 3 or 4 factors (panel lifetime and MOVPE process parameters).

6.4.2. Feasibility and resources required

One concern is whether applying all the steps of the framework is possible considering the time and resources typically allocated to such assessments. Fortunately, despite there being large theoretical work underpinning each step of the framework, the tools for implementation have been developed over time and can now be run in matters of minutes with average computational power.[41] Compared to the effort typically invested in conventional ex-post assessments, the only step that may require significant additional time and data collection is the characterization of uncertainty with probability distributions. In practice, many information exchanges will and should take place between a sustainability practitioner and a technology developer. Framing these exchanges in the context of uncertainty as we have presented here will provide more structure to the conversations and optimize the learning process (for both the practitioner and the technology developer, as we have often observed in practice).

Furthermore, the most time-consuming refinement is expected to happen during the second iteration, which will -after GSA- only consider a handful of uncertain factors in the model. The alternatives to our proposed approach could be equally or more time-consuming, e.g., developing and communicating numerous ad-hoc scenarios or developing more detailed modelling such as process engineering upscaling for all

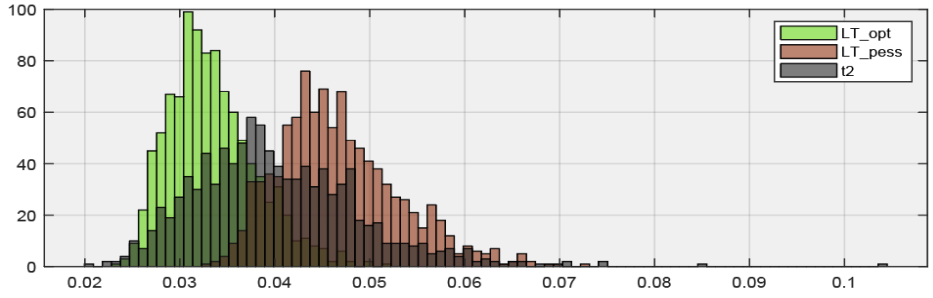

Figure 6-7 Frequency distribution for climate change impact scores (in kg CO2 eq) of the emerging III-V/Si technology in three "sensitive scenarios": with a short panel lifetime of 25 years (LT_pess), with a long panel lifetime of 35 years (LT_opt) and with an uncertain panel lifetime distributed according to the final model at the end of the R&D project.

uncertain parameters. Our framework ensures that the additional resources required by *ex-ante* are devoted to the things that matter.

6.4.3. On subjective probability distributions

Another concern is whether it is realistic, robust, and transparent to introduce largely subjective probability distributions that may cause some confusion about models' operations and outputs. Here we argue that exactly the opposite is the case; the subjective assumptions are not only clearly stated but they are represented in a way that obeys the rules of probability. Their effects are systematically introduced, analysed and interpreted. Two types of subjective information are introduced in our framework when subjective distributions are used. First, the shape of the distribution (e.g., uniform, PERT, triangular) and second, the parameters of the distribution (e.g., min, max and mode). The case study offers a good example of how we introduced boundaries and realistic assumptions in the energy consumption of the MOVPE process. We chose a PERT distribution bounded by the maximum power loading, which is given by the best result achieved to date. This is reasonable as it was already established that the current consumption is not economically viable. The minimum is a very low value which resembles that of in-line tools used in high-throughput production of commercial silicon cells which have 30 or more years advantage. For a conservative approach, we set the mode equal to the maximum. We could have chosen a triangular shape using this minimum and maximum boundaries. However, a PERT shape is more realistic in that increases in energy efficiency get more difficult with each subsequent attempt.

This example shows how relevant and objective information which would be lost otherwise is included in the distribution. On the other hand, making no assumption is in many ways an assumption. For example, not attaching probability to different scenarios may well result in the unconscious attachment of equal probability to each scenario during the interpretation and/or decision-making phase.[13] Interpretation and decision-making will necessarily involve probabilistic weighing, whether it is done by the practitioner or the decision-maker, consciously or unconsciously. Given the rigor introduced here, we advocate it is best to place probabilistic weighing as much as possible within the scope of the assessment itself. In addition to this, it must be recognized that *ex-ante* assessments must be conducted in a low-information environment. Therefore, all information available should be used, including beliefs, constraints and plausibilities that narrow the space for ambiguity.

6.5.Conclusions

The popular expression "you are only as strong as your weakest link" has great relevance in the context of *ex-ante* environmental assessments for safe and sustainable designs. If an element of an integrated model has a resolution far coarser than the rest, then there is a high chance that the benefits of increased precision in the rest of the model are lost. In the same way, if great effort is spent in modifying a factor that has only limited influence on

the environmental outcomes, then this effort is lost. Scenario analysis has proven to be a useful tool in *ex-ante* assessments; however, with the proposed framework we are pushing back against overreliance on scenario analysis without a previous and comprehensive sensitivity screening. Selecting scenarios to assess only based on preconceived notions may often result in that the compared scenarios are not significantly different therefore are not useful to act upon. This shifts an already stretched focus from decision-makers to aspects that are ultimately unimportant.

Our framework successfully addresses this shortcoming with robust systematic and quantitative methods to support decision-making. It also offers a useful structure for the information exchange between environmental modellers and technology developers throughout the R&D process. Furthermore, it iteratively simplifies models by allowing non-influential factors to be fixed. Less complex models will allow for clearer and more meaningful analysis, as well as communication and discussion of the findings amongst stakeholders.

There are important improvements of the framework that may be of interest for *ex-ante* LCA and RA researchers to further develop. We particularly see two valuable future developments. First, the incorporation of multivariate Bayesian approaches which can allow inference on more complex or underspecified distributions. Second, the incorporation of strategies to deal with correlations between observations from lab/pilot test results. In combination, these two improvements could significantly strengthen the framework and broaden its applicability.

References

1. Patinha Caldeira, C. *et al.* Safe and Sustainable by Design chemicals and materials Review of safety and sustainability dimensions, aspects, methods, indicators, and tools. (2022) doi:10.2760/879069 (online),10.2760/68587 (print).
2. van der Giesen, C., Cucurachi, S., Guinée, J., Kramer, G. J. & Tukker, A. A critical view on the current application of LCA for new technologies and recommendations for improved practice. *J. Clean. Prod.* **259**, 120904 (2020).
3. Fernandez-Dacosta, C. *et al.* Can we assess innovative bio-based chemicals in their early development stage? A comparison between early-stage and life cycle assessments. *J. Clean. Prod.* **230**, 137–149 (2019).
4. Villares, M., Işıldar, A., van der Giesen, C. & Guinée, J. Does ex ante application enhance the usefulness of LCA? A case study on an emerging technology for metal recovery from e-waste. *Int. J. Life Cycle Assess.* 1–16 (2017) doi:10.1007/s11367-017-1270-6.
5. Hetherington, A. C., Borrion, A. L., Griffiths, O. G. & McManus, M. C. Use of LCA as a development tool within early research: Challenges and issues across different sectors. *Int. J. Life Cycle Assess.* **19**, 130–143 (2014).
6. Frischknecht, R., Büsser, S. & Krewitt, W. Environmental assessment of future technologies: How to trim LCA to fit this goal? in *International Journal of Life Cycle Assessment* vol. 14 584–588 (2009).
7. Lloyd, S. M. & Ries, R. Characterizing, Propagating, and Analyzing Uncertainty in Life-Cycle Assessment. *J. Ind. Ecol.* **11**, 161–179 (2007).
8. Hertwich, E. G., McKone, T. E. & Pease, W. S. Parameter Uncertainty and Variability In Evaluative Fate and Exposure Models. *Risk Anal.* **19**, 1193–1204 (1999).
9. Igos, E., Benetto, E., Meyer, R., Baustert, P. & Othoniel, B. How to treat uncertainties in life cycle assessment studies? *Int. J. Life Cycle Assess.* 1–14 (2018) doi:10.1007/s11367-018-1477-1.
10. Ramsey, M. H. Uncertainty in the assessment of hazard, exposure and risk. *Environ. Geochem. Health* **31**, 205–217 (2009).
11. Huijbregts, M. Application of uncertainty and variability in LCA. *Int. J. Life Cycle Assess.* (1998).
12. Heijungs, R. On the number of Monte Carlo runs in comparative probabilistic LCA. *Int. J. Life Cycle Assess.* **25**, 394–402 (2020).
13. Blanco, C. F. *et al.* Assessing the sustainability of emerging technologies: A probabilistic LCA method applied to advanced photovoltaics. *J. Clean. Prod.* **259**, 120968 (2020).
14. Essig, S. *et al.* Raising the one-sun conversion efficiency of III-V/Si solar cells to 32.8% for two junctions and 35.9% for three junctions. *Nat. Energy* **2**, 17144 (2017).

15. Cariou, R. *et al.* Monolithic Two-Terminal III-V//Si Triple-Junction Solar Cells with 30.2% Efficiency under 1-Sun AM1.5g. *IEEE J. Photovoltaics* **7**, 367–373 (2017).

16. European Commission. *Critical Raw Materials Resilience: Charting a Path towards greater Security and Sustainability*. https://eur-lex.europa.eu/legal-content/EN/TXT/?uri=CELEX:52020DC0474 (2020).

17. European Parliament; Council of the European Union. *Directive 2012/19/EU of the European Parliament and of the Council of 4 July 2012 on waste electrical and electronic equipment (WEEE)*. (2012). doi:10.3000/19770677.L_2012.197.eng.

18. Hirt, L. F., Schell, G., Sahakian, M. & Trutnevyte, E. A review of linking models and socio-technical transitions theories for energy and climate solutions. *Environ. Innov. Soc. Transitions* **35**, 162–179 (2020).

19. Tsoy, N., Steubing, B., van der Giesen, C. & Guinée, J. Upscaling methods used in ex ante life cycle assessment of emerging technologies: a review. *Int. J. Life Cycle Assess.* **25**, 1680–1692 (2020).

20. Cucurachi, S., van der Giesen, C. & Guinee, J. Ex-ante LCA of emerging technologies. *CIRP Procedia* (2018).

21. Guinée, J. B. *et al.* Life cycle assessment: Past, present, and future. *Environ. Sci. Technol.* **45**, 90–96 (2011).

22. European Chemicals Agency. *Guidance on Information Requirements and Chemical Safety Assessment Part A: Introduction to the Guidance Document*. https://echa.europa.eu/documents/10162/13643/information_requirements_part_a_en.pdf/4d25d209-00a8-4a1b-97e5-5adae231b205 (2011).

23. Guinée, J. B., Heijungs, R., Vijver, M. G. & Peijnenburg, W. J. G. M. Setting the stage for debating the roles of risk assessment and life-cycle assessment of engineered nanomaterials. *Nat. Nanotechnol.* **12**, 727–733 (2017).

24. Kuczenski, B., Geyer, R. & Boughton, B. Tracking toxicants: Toward a life cycle aware risk assessment. *Environ. Sci. Technol.* **45**, 45–50 (2011).

25. Lloyd, S. M. & Ries, R. Characterizing, Propagating, and Analyzing Uncertainty in Life-Cycle Assessment: A Survey of Quantitative Approaches. *J. Ind. Ecol.* **11**, 161–179 (2008).

26. U.S. EPA (U.S. Environmental Protection Agency). *Guidelines for Human Exposure Assessment*. https://www.epa.gov/risk/guidelines-human-exposure-assessment (2019).

27. Saltelli, A. *et al. Global Sensitivity Analysis. The Primer. Global Sensitivity Analysis. The Primer* (John Wiley and Sons, 2008). doi:10.1002/9780470725184.

28. Mendoza Beltran, A., Heijungs, R., Guinée, J. & Tukker, A. A pseudo-statistical approach to treat choice uncertainty: the example of partitioning allocation methods. *Int. J. Life Cycle Assess.* **21**, 252–264 (2016).

29. Jaynes, E. T. *Probability Theory: The Logic of Science. Probability Theory* (Cambridge University Press, 2003). doi:10.1017/CBO9780511790423.

30. Sivia, D. S. *Data analysis : a Bayesian tutorial.* (New York: Oxford University Press, 2006).

31. Smith, C. & Kelly, D. *Bayesian Inference for Probabilistic Risk Assessment. Springer Series in Reliability Engineering* (Springer London, 2006). doi:10.1007/978-1-84996-187-5.

32. Lo, S.-C., Ma, H. & Lo, S.-L. Quantifying and reducing uncertainty in life cycle assessment using the Bayesian Monte Carlo method. *Sci. Total Environ.* **340**, 23–33 (2005).

33. Wolpert, R. L., Steinberg, L. J. & Reckhow, K. H. Bayesian Decision Support Using Environmental Transport-And-Fate Models. in *Case Studies in Bayesian Statistics* 241–293 (Springer, New York, NY, 1993). doi:10.1007/978-1-4612-2714-4_5.

34. Groen, E. A., Heijungs, R., Bokkers, E. A. M. & de Boer, I. J. M. Methods for uncertainty propagation in life cycle assessment. *Environ. Model. Softw.* **62**, 316–325 (2014).

35. Rodrigues, J. F. D., Moran, D., Wood, R. & Behrens, P. Uncertainty of Consumption-Based Carbon Accounts. *Environ. Sci. Technol.* **52**, 7577–7586 (2018).

36. Firestone, M. *et al. Guiding Principles for Monte Carlo Analysis - Technical Panel.* https://www.epa.gov/risk/guiding-principles-monte-carlo-analysis (1997).

37. Liu, J. S. *Monte Carlo Strategies in Scientific Computing*. (Springer, 2004). doi:10.1007/978-0-387-76371-2.

38. Groen, E. A. & Heijungs, R. Ignoring correlation in uncertainty and sensitivity analysis in life cycle assessment: what is the risk? *Environ. Impact Assess. Rev.* **62**, 98–109 (2017).

39. Heijungs, R., Guinée, J. B., Mendoza Beltrán, A., Henriksson, P. J. G. & Groen, E. Everything is relative and nothing is certain. Toward a theory and practice of comparative probabilistic LCA. *Int. J. Life Cycle Assess.* **24**, 1573–1579 (2019).

40. Piccinno, F., Hischier, R., Seeger, S. & Som, C. From laboratory to industrial scale: a scale-up framework for chemical processes in life cycle assessment studies. *J. Clean. Prod.* **135**, 1085–1097 (2016).

41. Cucurachi, S., Blanco, C. F., Steubing, B. & Heijungs, R. Implementation of uncertainty analysis and moment-independent global sensitivity analysis for full-scale life cycle assessment models. *J. Ind. Ecol.* (2021) doi:10.1111/jiec.13194.

42. Harpprecht, C., Oers, L., Northey, S. A., Yang, Y. & Steubing, B. Environmental impacts of key metals' supply and low-carbon technologies are likely to decrease in the future. *J. Ind. Ecol.* jiec.13181 (2021) doi:10.1111/jiec.13181.

43. Mendoza Beltran, A. *et al.* When the Background Matters: Using Scenarios from Integrated Assessment Models in Prospective Life Cycle Assessment. *J. Ind. Ecol.* **24**, 64–79 (2020).

44. Hiremath, M., Derendorf, K. & Vogt, T. Comparative Life Cycle Assessment of Battery Storage Systems for Stationary Applications. *Environ. Sci. Technol.* **49**, 4825–4833 (2015).

45. Hischier, R., Salieri, B. & Pini, M. Most important factors of variability and uncertainty in an LCA study of nanomaterials – Findings from a case study with nano titanium dioxide. *NanoImpact* **7**, 17–26 (2017).

46. Miller, S. A. & Keoleian, G. A. Framework for analyzing transformative technologies in life cycle assessment. *Environ. Sci. Technol.* **49**, 3067–3075 (2015).

47. Gong, J. *et al.* Perovskite photovoltaics: life-cycle assessment of energy and environmental impacts. *Energy Environ. Sci.* **8**, 1953–1968 (2015).

48. Raugei, M. & Winfield, P. Prospective LCA of the production and EoL recycling of a novel type of Li-ion battery for electric vehicles. *J. Clean. Prod.* **213**, 926–932 (2019).

49. Baustert, P. *et al.* Integration of future water scarcity and electricity supply into prospective LCA: Application to the assessment of water desalination for the steel industry. *J. Ind. Ecol.* (2022) doi:10.1111/jiec.13272.

50. Lesage, P., Mutel, C., Schenker, U. & Margni, M. Uncertainty analysis in LCA using precalculated aggregated datasets. *Int. J. Life Cycle Assess.* **23**, 2248–2265 (2018).

51. Saltelli, A. Sensitivity Analysis for Importance Assessment. *Risk Anal.* **22**, 579–590 (2002).

52. Borgonovo, E. A new uncertainty importance measure. *Reliab. Eng. Syst. Saf.* **92**, 771–784 (2007).

53. Plischke, E., Borgonovo, E. & Smith, C. L. Global sensitivity measures from given data. *Eur. J. Oper. Res.* **226**, 536–550 (2013).

54. Plischke, E. & Borgonovo, E. Fighting the Curse of Sparsity: Probabilistic Sensitivity Measures From Cumulative Distribution Functions. *Risk Anal.* risa.13571 (2020) doi:10.1111/risa.13571.

55. O'Hagan, A. Expert Knowledge Elicitation: Subjective but Scientific. *Am. Stat.* **73**, 69–81 (2019).

56. Hanea, A. M., McBride, M. F., Burgman, M. A. & Wintle, B. C. Classical meets modern in the IDEA protocol for structured expert judgement. *J. Risk Res.* **21**, 417–433 (2018).

57. Wang, X., Gao, Z. & Guo, H. Delphi Method for Estimating Uncertainty Distributions. *Int. J. Inf.* **15**, 449–460 (2012).

58. Morgan, M. G. Use (and abuse) of expert elicitation in support of decision making for public policy. *Proc. Natl. Acad. Sci.* **111**, 7176–7184 (2014).

59. Czembor, C. A., Morris, W. K., Wintle, B. A. & Vesk, P. A. Quantifying variance components in ecological models based on expert opinion. *J. Appl. Ecol.* **48**, 736–745 (2011).

60. Li, X. *et al.* On-device lead sequestration for perovskite solar cells. *Nature* **578**, 555–558 (2020).

61. Cao, J. & Yan, F. Recent progress in tin-based perovskite solar cells. *Energy Environ. Sci.* **14**, 1286–1325 (2021).

62. Department of Toxic Substances Control. *Photovoltaic (PV) Modules – Universal Waste Management*. (2020).

63. Fraunhofer ISE. SiTaSol: Application relevant validation of c-Si based tandem solar cell processes. https://sitasol.com/.

64. Blanco, C. F. *et al.* Environmental impacts of III–V/silicon photovoltaics: life cycle assessment and guidance for sustainable manufacturing. *Energy Environ. Sci.* **13**, 4280–4290 (2020).

65. Dimroth, F. III-V Solar Cells - Materials, Multi-Junction Cells - Cell Design and Performance. in *Photovoltaic Solar Energy* 371–382 (John Wiley & Sons, Ltd, 2017). doi:10.1002/9781118927496.ch34.

66. DeGroot, M. H. Conjugate Prior Distributions. in *Optimal Statistical Decisions* 155–189 (John Wiley & Sons, Inc., 2005). doi:10.1002/0471729000.ch9.

67. Blanco, C. F., Cucurachi, S., Peijnenburg, W. J. G. M. & Vijver, M. G. *D6.3 Assessment of environmental health and safety concerns of the materials developed*. https://sitasol.com/ (2020).

68. Frischknecht, R. *et al. Methodology Guidelines on Life Cycle Assessment of Photovoltaic Electricity, 3rd edition, IEA PVPS Task 12*. http://www.iea-pvps.org/fileadmin/dam/public/report/technical/Task_12_-_Methodology_Guidelines_on_Life_Cycle_Assessment_of_Photovoltaic_Electricity_3rd_Edition.pdf (2016).

Chapter 7

General Discussion

7.1. The role of early-stage environmental assessments

Every four years, millions of American voters and keen observers abroad point their web browsers to the *FiveThirtyEight* website, one of the most successful platforms for monitoring and forecasting of presidential U.S. elections.[1] Few events could be more influential to modern society since the second half of the 20th century, and Nate Silver (the site's founder) rose to prominence by applying powerful statistical predictive models to the heated topic with unprecedented success. In perhaps the only enjoyable book ever written about probability and statistics, *The Signal and The Noise: Why Many Predictions Fail – but Some Don't*, Silver -a strong advocate for Bayesian thinking- writes:

> *Good innovators typically think very big and they think very small. New ideas are sometimes found in the most granular details of a problem where few others bother to look. And they are sometimes found when you are doing your most abstract and philosophical thinking, considering why the world is the way that it is and whether there might be an alternative to the dominant paradigm. Rarely can they be found in the temperate latitudes between these two spaces, where we spend 99 percent of our lives. The categorizations and approximations we make in the normal course of our lives are usually good enough to get by, but sometimes we let information that might give us a competitive advantage slip through the cracks. The key is to develop tools and habits so that you are more often looking for ideas and information in the right places-and in honing the skills required to harness them into W's* (wins) *and L's* (losses) *once you've found them.*[2]

If early-stage environmental assessments are to play a contributing role in technological innovation, we must look through the cracks and in the granular details that Silver points to. How can we do this then, in the face of overwhelming dearth of data, rapidly evolving technology designs and limited time to adjust and reinterpret our models? Perhaps the two most challenging aspects of the whole *ex-ante* safety and sustainability assessment exercise are model development and data collection. This gives four approaches to where/how to focus the limited knowledge-gathering resources at our disposal:

a) Rapid screening, based on highly simplified models and limited data collection. This approach has often been the *go-to* for chemical safety of novel materials and various techniques such as *read-across* have been developed.[3]

b) Keep models simple and focus the resources on improving data collection as much as possible. This has often been the approach of practitioners in the rising field of *ex-ante* LCA.[4]

c) Accept uncertainty due to limited data and devote the resources to refine the models as much as possible.

d) Only produce the assessments when the technology is fully developed, allowing for both models and data collection to be refined to the standard of conventional *ex-post* assessments.

Approach (d) runs into the well-documented issues of the *Pacing Problem*[5] and the *Collingridge Dilemma*[6] which were discussed in the introductory chapter of this text. Approach *(a)* entails a high likelihood of producing meaningless results due to a combination both inadequate data and models. Furthermore, while it may be a suitable approach for chemicals which are developed much more rapidly than technological products or services[7], it may fall short in the latter given the difficulty to apply techniques such as *read-across* to entire technological product systems. Approach *(b)* tries to improve on the data but will likely leave us with inadequate explanations if relevant cause-effect mechanisms are omitted. Approach *(c)* on the other hand, opens as many opportunities as possible to improve the technology's design while there is still considerable room for trial and error. The more important role of the early-stage assessment is then that of an *enabler* rather than an arbitrator or judge. Approach *(c)* is very well suited to the task.

7.2. New insights obtained in this work

The five content chapters in this text underpin the perspective presented above and progressively lay the groundwork for an overarching methodological framework that takes important steps in a new direction for early-stage sustainability assessments. The insights obtained in each chapter are summarized below. As anticipated in the introductory chapter, these insights are methodological but also technical in that they contributed to a better understanding of the potential advantages and drawbacks of future large-scale III-V/silicon PV deployment.

- *What are the environmental hotspots in the emerging PV technologies landscape and what are the variabilities in the life cycle impacts?*

Chapter 2 initiates with a high-level investigation of environmental hotspots in the emerging PV landscape. Which PV technologies are presenting comparative hotspots (vs. conventional c-Si PV) and why? A systematic review and meta-analysis of over LCA studies conducted in the past decade found that most hotspots for the emerging PV landscape were found in perovskite cells. While perovskite cells are perhaps the most promising alternative from a cost and energy security perspective, their short lifetime (due to poor stability of the perovskite layer) means increased material intensity and larger environmental drawbacks per kWh of electricity generated. The variabilities in the impacts reported across and within technology types were found to be large, spanning several orders of magnitude despite a considerable effort in harmonizing system boundaries and other aspects of the underlying LCA models. While PV technologies are typically classified according to the light-absorbing materials used in the cell, the choice of encapsulation, panel framing and other ancillary installation components were found to have a larger influence than the cell in many cases. It becomes evident that broad consideration must be given to fully installed PV systems if they are to be compared.

- *What are the environmental impacts in the life cycle of III-V/silicon tandem PV modules compared to conventional silicon modules and what are the key opportunities for improvement?*

Chapter 3 developed an LCA model of the III-V/Si with a high granularity representation of the manufacturing processes and synthesis methods for all precursors in the III-V supply chain. The contribution analysis clearly highlighted the MOVPE power consumption and the silicon materials in the bottom cell as the most relevant contributors. From an LCA perspective, toxicity concerns regarding direct emissions of III-V materials during manufacturing and waste treatment do not appear to be relevant compared to the toxic emissions of fossil-based electricity generation. Thus, MOVPE power consumption is more relevant to toxic releases than the arsenic content of the III-V top cells. Evidently, reduction of power consumption during MOVPE is the most effective way to reduce most types of impacts. Alternatively, shifting background energy mixes to more renewable sources would greatly benefit PV deployment by making more advanced technologies such as III-V more competitive from an environmental standpoint.

- *How can unresolved technological pathways in the development of III-V/silicon tandem modules be incorporated in environmental assessments?*

Chapter 4 built on the experience obtained in developing an LCA model and addressed one of the main challenges/sources of uncertainty encountered: the numerous pathways (resulting from all possible design choices) that the technology could take as it evolved through its Technology Readiness Level (TRL) journey. The proposed solution was to combine all possible pathways in a single product system, represented by the corresponding (groups of) unit process(es) which would be triggered stochastically according to their chances of success. The realization that uncertainties of a very different nature than the ones usually accounted for in LCA (e.g., in flow quantities) can also be parametrized and jointly propagated revealed the potential of combined uncertainty analysis and global sensitivity analysis to deal with the numerous and diverse types of uncertainty encountered in *ex-ante*/prospective assessments. This was then picked up and fully developed in Chapter 6.

- *What are the potential ecological risks introduced by III-V/silicon tandem modules throughout their life cycles?*

Chapter 5 is developed following the realization that numerous cause-effect chains must be considered to link adoption of a technology with environmental outcomes, and that there will be equally numerous uncertainties. An LCA model calculates numerous indicators for a fixed unitary demand (the functional unit). Risk assessment models calculate endpoint indicators for a given emission. A gap needs to be filled to connect technological uptake with actual emissions. This is achieved by integrating PV demand scenarios at different spatial scales with a risk assessment model for emissions in the life cycle of the III-V/Si panels manufactured, installed and discarded in these scenarios. Time is also an important consideration, given the delayed migration of metals and metalloids in the environment (typically in the order of tens or hundreds of years). The only way to appropriately answer this question in a prospective way was to develop a fully integrated probabilistic and dynamic demand-emissions-fate model. Such a model is unprecedented

for emerging PV technologies (and other consumer technologies as far as we are aware). Within each scale, a very wide spectrum of possibilities was considered, represented in more than one-hundred uncertain/variable parameters describing processes in the emissions and fate modelling during all relevant life cycle stages.

- *How can uncertainty analysis and global sensitivity analysis be used to prioritize research directions towards safer and more sustainable design of III-V/silicon tandem technologies?*

The probabilistic framework that gradually emerged from the previous chapters and took full shape in Chapter 6 is largely based on combined uncertainty analysis and global sensitivity analysis. This powerful combination provides solutions at different levels for the data limitations and concomitant uncertainty issues in the *ex-ante* problem. First and foremost, it fully reveals the uncertainties by characterizing them in a systematic and cohesive way, making any ensuing investigations/discussions more transparent. Second, it prevents the modelling effort from shying away from greater resolution or more complex representation of cause-effect chains in fear of missing data. Third, it allows focusing on the most relevant uncertain factors for refining further research: a valuable recourse given the time and resource constraints already discussed. This is in essence the so-called factor fixing for model simplification described by Saltelli et al.[8]. Here we stress that, in contrast to strategy (b) of Section 7.1, models are simplified in a way that does not significantly affect the outcomes of interest (e.g., risk or impact indicators), rather than in an arbitrary or ad-hoc manner with no prior knowledge of factor importance. Finally, but no less importantly, experience proved the framework equally useful in facilitating communication between stakeholders with very different backgrounds and different ways of understanding and dealing with uncertainties in their own domain expertise.

As a result, over a four-year period, the studied III-V/Si technology evolved from a highly undetermined system to a system with reduced uncertainty and a much better outlook regarding environmental performance. These are perhaps the two most important outcomes that can be achieved with an early-stage assessment. Throughout the course of the III-V/Si case study, concrete design choices such as laser-sintered copper metallization over other alternatives shifted the indicators of interest (e.g., LCA impact scores, risk quotients) significantly in the desired direction. Moreover, application of the framework revealed the boundary where additional design improvements by technology developers reach their effectiveness limits, i.e. diminishing returns. At this point, efforts from other actors in the technology's value chain such as consumers and end-of-life service providers can have a larger positive influence on the environmental performance of the technological system.

7.3. Limitations and future research directions

A limitation of this work is that the methods used were developed in parallel to the R&D program for the III-V/Si technology which was ongoing[9]. This meant that not all the right questions were asked to key stakeholders such as technology developers and other

relevant actors in the supply chain from the beginning. It also meant that several aspects of the III-V/Si technological system were not fully fitted to the framework, even though they would have provided ideal testing grounds. Such is the case of probability distributions of technological parameters used in the models, which could have been obtained from more structured expert elicitation protocols as suggested in Chapter 6. The opportunity is now ripe to apply the framework from the beginning of an R&D program to fully demonstrate its strength.

Another limitation is that substantial interdisciplinary work is required to build and apply the underlying models. This knowledge may not always be available and will likely go beyond that of a single LCA or Risk Assessment practitioner. A close collaboration between practictioners and technology developers starting from the lower TRL levels is very beneficial (if not a necessity) in this respect, and is largely what made this III-V/Si PV case study possible. It must also be reckoned that the time invested in the III-V/Si LCA and risk assessments here presented was more than would be available for typical R&D projects. However, this included considerable time invested in methods development and this work has provided an important step forward by integrating concepts and developing software tools that can easily be adapted to case studies from other technological domains. This greatly reduces the amount of research that will be required for new case studies, allowing practitioners to focus much more on the specifics of their technology.

Additional work can be done in this front to further facilitate implementation by modellers and minimize coding requirements, e.g., using *Shiny* interfaces for the *R* scripts and improving the coupling of macro-enabled Microsoft Excel spreadsheets with R in the probabilistic dynamic risk assessment model of Chapter 5. On the LCA side, recently published work[10] associated to this thesis developed algorithms and a. user interface for applying the GSA methods proposed in Chapter 4 in a much more efficient way, but there is still room for improvement on visualization and interpretation of the GSA results.

Further work can also be done to strengthen the conceptual power and applicability of the framework. New case studies can help to demonstrate the applicability of Bayesian probabilities and expert elicitation protocols which can fully incorporate all kinds of scarce and diverse data that becomes available. Subsequent iterations of the assessments as the technology advances from low TRL to market-readiness may provide opportunities to conduct Bayesian inference which would make parameter estimation more robust. This can also lead to greater consensus amongst experts in elicitation processes. This framework may also serve as a bridge to machine learning, although the importance of model over data must be stressed. Machine learning is reliant on data and produces data rather than explanations. To guide safe and sustainable innovation, explanations are needed. That is, we need to understand the factors that matter in the technological system (and beyond), their relationships, how they can be influenced and how their changes reflect on different environmental impact and risk indicators.

7.4.Policy and societal implications

The story of a research & development (R&D) program is a story about uncertainty. While uncertainty may be uncomfortable -*an inconvenience*- for modelers, technology developers, decision-makers and their stakeholders, it is an unavoidable and central aspect of innovation. Yet we must not allow it to be paralysing. This work offers an upside to the 'inconvenience' in that it can be an important source of opportunities for safer and more sustainable designs. A deep body of work has already been developed to analyse uncertainty in natural sciences as well as finance, economics and engineering. Very sophisticated methods, more recently including machine learning and artificial intelligence, are now being introduced in these fields, helping the technological and economic dimensions of technology advance at ever larger strides. Safety and sustainability assessment cannot fall behind; if anything, it must stay ahead.

Of course, there is an underlying call for non-technical audiences -especially key decisionmakers and policymakers- to become more comfortable with the language of uncertainty *and* (global!) sensitivity. At the same time, our technical assessments must be better at interpreting and communicating these aspects. But the key message that emerges from this work is that existing uncertainties -about both positive and negative outcomes- must compel us to find a right balance between avoiding risks and hindering technological development that could have otherwise offered unforeseen societal benefits.

References

1. FiveThirtyEight. *ABC News Internet Ventures* https://fivethirtyeight.com/.
2. Silver, N. *The Signal and the Noise: Why So Many Predictions Fail—But Some Don't.* (Penguin Group, 2012).
3. European Chemicals Agency. *Read-Across Assessment Framework (RAAF).* https://echa.europa.eu/documents/10162/13628/raaf_en.pdf/614e5d61-891d-4154-8a47-87efebd1851a (2017).
4. Adrianto, L. R. *et al.* How can LCA include prospective elements to assess emerging technologies and system transitions? The 76th LCA Discussion Forum on Life Cycle Assessment, 19 November 2020. *Int. J. Life Cycle Assess. 2021 268* **26**, 1541–1544 (2021).
5. Downes, L. *The Laws of Disruption: Harnessing the New Forces That Govern Life and Business in the Digital Age*. (Basic Books, 2009).
6. Collingridge, D. *The social control of technology*. (Frances Pinter, 1980).
7. Wassenaar, P. N. H., Rorije, E., Vijver, M. G. & Peijnenburg, W. J. G. M. Evaluating chemical similarity as a measure to identify potential substances of very high concern. *Regul. Toxicol. Pharmacol.* **119**, 104834 (2021).
8. Saltelli, A. *et al. Global Sensitivity Analysis. The Primer. Global Sensitivity Analysis. The Primer* (John Wiley and Sons, 2008). doi:10.1002/9780470725184.
9. Fraunhofer ISE. SiTaSol: Application relevant validation of c-Si based tandem solar cell processes. https://sitasol.com/.
10. Cucurachi, S., Blanco, C. F., Steubing, B. & Heijungs, R. Implementation of uncertainty analysis and moment-independent global sensitivity analysis for full-scale life cycle assessment models. *J. Ind. Ecol.* (2021) doi:10.1111/jiec.13194.

Appendix

Supplementary Information

A.1. Supplementary information to Chapter 2

Table A.1-1 Screened and eligible LCA studies of emerging PV technologies

Year	Authors	Title	PV technology	Eligible	Reason for exclusion
2010	García-Valverde et al.[1]	Life cycle analysis of organic photovoltaic technologies	Organic	Y	
2010	Ito et al.[2]	Life-cycle analyses of very-large scale PV systems using six types of PV modules	Silicon Thin Film Silicon	N	Impact scores not harmonizable
2010	Reijnders[3]	Design issues for improved environmental performance of dye-sensitized and organic nanoparticulate solar cells	Dye-sensitized Organic	N	Not LCA
2011	Bravi et al.[4]	Life cycle assessment of a micromorph photovoltaic system	Thin Film	Y	
2011	Espinosa et al.[5]	Life-cycle analysis of product integrated polymer solar cells	OPV	N	Integrated on other device
2011	Fthenakis & Kim[6]	Photovoltaics: Life-cycle analyses	Silicon Thin Film Silicon Thin Film Chalcogenide	N	Uses data from other studies
2011	Held & Ilg[7]	Update of environmental indicators and energy payback time of CdTe PV systems in Europe	Thin Film	Y	
2011	Kim & Fthenakis[8]	Comparative life-cycle energy payback analysis of multi-junction a-SiGe and nanocrystalline/a-Si modules	Tandem	Y	
2011	Nieves Espinosa et al.[9]	A life cycle analysis of polymer solar cell modules prepared using roll-to-roll methods under ambient conditions	Organic	Y	
2011	Şengül et al.[10]	An environmental impact assessment of quantum dot photovoltaics (QDPV) from raw material acquisition through use	Quantum Dot	Y	
2011	van der Meulen & Alsema[11]	Life-cycle greenhouse gas effects of introducing nano-crystalline materials in thin-film silicon solar cells	Thin Film	Y	
2012	Emmott et al.[12]	Environmental and economic assessment of ITO-free electrodes for organic solar cells	OPV	N	System boundaries not harmonizable Impact scores not harmonizable
2012	Espinosa et al.[13]	Solar cells with one-day energy payback for the factories of the future	OPV	N	Functional unit not harmonizable

2012	Fthenakis[14]	Sustainability metrics for extending thin-film photovoltaics to terawatt levels	Thin Film Chalcogenide Thin Film Silicon	N	Not LCA
2012	Kim et al.[15]	Life Cycle Greenhouse Gas Emissions of Thin-film Photovoltaic Electricity Generation: Systematic Review and Harmonization	Thin Film Chalcogenide Thin Film Silicon	N	Uses data from other studies
2012	Nieves Espinosa et al.[16]	Life cycle assessment of ITO-free flexible polymer solar cells prepared by roll-to-roll coating and printing	Organic	Y	
2012	Raugei et al.[17]	Potential Cd emissions from end-of-life CdTe PV	Thin Film Chalcogenide	N	Not LCA
2012	Yue et al.[18]	Deciphering the uncertainties in life cycle energy and environmental analysis of organic photovoltaics	OPV	N	Uses data from other studies Geographical focus
2012	Zuser & Rechberger[19]	Considerations of resource availability in technology development strategies: The case study of photovoltaics	Thin Film Chalcogenide Thin Film Silicon	N	Not LCA
2013	Eisenberg et al.[20]	Comparative alternative materials assessment to screen toxicity hazards in the life cycle of CIGS thin film photovoltaics	Thin Film Chalcogenide	N	Not LCA
2013	Espinosa et al.[21]	OPV for mobile applications: an evaluation of roll-to-roll processed indium and silver free polymer solar cells through analysis of life cycle, cost and layer quality using inline optical and functional inspection tools	OPV	N	Integrated on other device
2013	Fthenakis et al.[22]	Direct Te Mining: Resource Availability and Impact on Cumulative Energy Demand of CdTe PV Life Cycles	Thin Film Chalcogenide	N	Uses data from other studies
2013	Kim & Fthenakis[23]	Life Cycle Energy and Climate Change Implications of Nanotechnologies	Quantum Dot	N	Uses data from other studies
2013	Mohr et al.[24]	Environmental life cycle assessment of roof-integrated flexible amorphous silicon/nanocrystalline silicon solar cell laminate	Tandem	Y	
2013	Parisi et al.[25]	Development of dye sensitized solar cells: a life cycle perspective for the environmental and market potential assessment of a renewable energy technology	Dye-sensitized	N	Uses data from other studies Impact scores not harmonizable

2014	Collier et al.[26]	Life cycle environmental impacts from CZTS (copper zinc tin sulfide) and Zn3P2 (zinc phosphide) thin film PV (photovoltaic) cells	Thin Film	Y	
2014	Espinosa & Krebs[27]	Life cycle analysis of organic tandem solar cells: When are they warranted?	OPV	N	Functional unit not harmonizable System boundaries not harmonizable Impact scores not harmonizable
2014	Espinosa et al.[28]	Large scale deployment of polymer solar cells on land, on sea and in the air	OPV	N	Functional unit not harmonizable System boundaries not harmonizable Impact scores not harmonizable
2014	Kim et al.[29]	Life cycle assessment of cadmium telluride photovoltaic (CdTe PV) systems	Thin Film	Y	
2014	Mann et al.[30]	The energy payback time of advanced crystalline silicon PV modules in 2020: a prospective study	Silicon	N	Technology not in development
2014	Parisi et al.[31]	The evolution of the dye sensitized solar cells from Grätzel prototype to up-scaled solar applications: A life cycle assessment approach	Dye-sensitized	Y	
2014	Wender et al.[32]	Illustrating Anticipatory Life Cycle Assessment for Emerging Photovoltaic Technologies	Silicon Thin Film Silicon Thin Film Chalcogenide	N	Uses data from other studies
2015	Espinosa et al.[33]	Ecodesign of organic photovoltaic modules from Danish and Chinese perspectives	OPV	N	Geographical focus
2015	Fabini[34]	Quantifying the Potential for Lead Pollution from Halide Perovskite Photovoltaics	Perovskite	N	Not LCA
2015	Gong et al.[35]	Perovskite photovoltaics: life-cycle assessment of energy and environmental impacts	Perovskite	Y	
2015	Louwen et al.[36]	Life-cycle greenhouse gas emissions and energy payback time of current and prospective silicon heterojunction solar cell designs	Tandem	Y	

2015	Nieves Espinosa et al.[37]	Solution and vapour deposited lead perovskite solar cells: Ecotoxicity from a life cycle assessment perspective	Perovskite	Y	
2015	Prado-Lopez et al.[38]	Tradeoff Evaluation Improves Comparative Life Cycle Assessment: A Photovoltaic Case Study	Silicon Thin Film Silicon Thin Film Chalcogenide	N	Uses data from other studies
2015	Scott et al.[39]	Reducing the life cycle environmental impacts of kesterite solar photovoltaics: comparing carbon and molybdenum back contact options	Thin Film Chalcogenide	N	System boundaries not harmonizable
2015	Serrano-Lujan et al.[40]	Tin- and Lead-Based Perovskite Solar Cells under Scrutiny: An Environmental Perspective	Perovskite	Y	
2015	Wetzel & Borchers[41]	Update of energy payback time and greenhouse gas emission data for crystalline silicon photovoltaic modules	Silicon	Y	
2015	Zhang et al.[42]	Life Cycle Assessment of Titania Perovskite Solar Cell Technology for Sustainable Design and Manufacturing	Perovskite	Y	
2016	Babayigit et al.[43]	Toxicity of organometal halide perovskite solar cells	Perovskite	N	Not LCA
2016	Bergesen & Su[44]	A framework for technological learning in the supply chain: A case study on CdTe photovoltaics	Thin Film Chalcogenide	N	Not LCA
2016	Celik et al.[45]	Life Cycle Assessment (LCA) of perovskite PV cells projected from lab to fab	Perovskite	Y	
2016	Chatzisideris et al.[46]	Ecodesign perspectives of thin-film photovoltaic technologies: A review of life cycle assessment studies	Silicon Thin Film Chalcogenide Thin Film Silicon Tandem III-V	N	Uses data from other studies
2016	Hengevoss et al.[47]	Life Cycle Assessment and eco-efficiency of prospective, flexible, tandem organic photovoltaic module	Organic	Y	
2016	Kim et al.[48]	Review of life cycle assessment of nanomaterials in photovoltaics	Silicon Thin Film Chalcogenide Quantum Dot	N	Uses data from other studies
2016	Leccisi et al.[49]	The Energy and Environmental Performance of Ground-Mounted Photovoltaic Systems—A Timely Update	Thin Film	Y	

2016	Scott et al.[50]	Can Carbon Nanomaterials Improve CZTS Photovoltaic Devices? Evaluation of Performance and Impacts Using Integrated Life-Cycle Assessment and Decision Analysis	Thin Film Chalcogenide	N	System boundaries not harmonizable
2016	Tsang et al.[51]	A comparative human health, ecotoxicity, and product environmental assessment on the production of organic and silicon solar cells	Organic	Y	
2016	Tsang et al.[52]	Life-cycle assessment of cradle-to-grave opportunities and environmental impacts of organic photovoltaic solar panels compared to conventional technologies	OPV	N	Uses data from other studies
2017	Celik et al.[53]	Environmental analysis of perovskites and other relevant solar cell technologies in a tandem configuration	Tandem	Y	
2017	Celik et al.[54]	Environmental Impacts from Photovoltaic Solar Cells Made with Single Walled Carbon Nanotubes	Organic	Y	
2017	dos Reis Benatto et al.[55]	Life-Cycle Assessment of Solar Charger with Integrated Organic Photovoltaics	OPV	N	Integrated on other device
2017	Hauck et al.[56]	Environmental benefits of reduced electricity use exceed impacts from lead use for perovskite based tandem solar cell	Perovskite	N	System boundaries not harmonizable
2017	Itten & Stucki[57]	Highly Efficient 3rd Generation Multi-Junction Solar Cells Using Silicon Heterojunction and Perovskite Tandem: Prospective Life Cycle Environmental Impacts	Tandem	Y	
2017	Khaenson et al.[58]	A comparison of the environmental impact of solar power generation using multicrystalline silicon and thin film of amorphous silicon solar cells: case study in Thailand	Silicon Thin Film Silicon	N	Geographical focus
2017	Lunardi et al.[59]	A life cycle assessment of perovskite/silicon tandem solar cells	Tandem	Y	
2017	Vellini et al.[60]	Environmental impacts of PV technology throughout the life cycle: Importance of the end-of-life management for Si-panels and CdTe-panels	Silicon Thin Film Chalcogenide	N	Impact scores not harmonizable
2017	Zhang et al.[61]	Comparison of life cycle environmental impacts of different perovskite solar cell systems	Perovskite	Y	
2018	Alberola-Borràs et al.[62]	Perovskite Photovoltaic Modules: Life Cycle Assessment of Pre-industrial Production Process	Perovskite	Y	
2018	Alberola-Borràs et al.[63]	Relative impacts of methylammonium lead triiodide perovskite solar cells based on life cycle assessment	Perovskite	Y	

2018	Alberola-Borràs et al.[64]	Evaluation of multiple cation/anion perovskite solar cells through life cycle assessment	Perovskite	N	Functional unit not harmonizable Uses data from other studies
2018	Amarakoon et al.[65]	Life cycle assessment of photovoltaic manufacturing consortium (PVMC) copper indium gallium (di)selenide (CIGS) modules	Thin Film	Y	
2018	Celik et al.[66]	Energy Payback Time (EPBT) and Energy Return on Energy Invested (EROI) of Perovskite Tandem Photovoltaic Solar Cells	Perovskite	Y	
2018	Celik et al.[67]	Life cycle analysis of metals in emerging photovoltaic (PV) technologies: A modeling approach to estimate use phase leaching	Thin Film Chalcogenide Perovskite Quantum Dot	N	System boundaries not harmonizable
2018	Lunardi et al.[68]	A comparative life cycle assessment of chalcogenide/Si tandem solar modules	Tandem	Y	
2018	Lunardi et al.[69]	Life cycle assessment on PERC solar modules	Silicon	Y	
2018	Mokhtarimehr et al.[70]	Environmental assessment of vacuum and non-vacuum techniques for the fabrication of Cu2ZnSnS4 thin film photovoltaic cells	Thin Film	Y	
2018	Moore et al.[71]	Portfolio Optimization of Nanomaterial Use in Clean Energy Technologies	OPV	N	Not LCA
2018	Munshi et al.[72]	Thin-film CdTe photovoltaics – The technology for utility scale sustainable energy generation	Thin Film	N	Not LCA Uses data from other studies
2018	Pallas et tal.[73]	Green and Clean: Reviewing the Justification of Claims for Nanomaterials from a Sustainability Point of View	Perovskite Thin Film Silicon Tandem OPV Dye-sensitized	N	Uses data from other studies
2018	Ravikumar et al.[74]	Novel Method of Sensitivity Analysis Improves the Prioritization of Research in Anticipatory Life Cycle Assessment of Emerging Technologies	Thin Film Chalcogenide Thin Film Ribbon	N	Uses data from other studies

2018	Salim et al.[75]	A Fuzzy Based Model for Standardized Sustainability Assessment of Photovoltaic Cells	Silicon Thin Film Chalcogenide Thin Film Silicon Tandem III-V	N	Uses data from other studies
2018	Sinha & Wade[76]	Addressing Hotspots in the Product Environmental Footprint of CdTe Photovoltaics	Thin Film	Y	
2018	Soares et al.[77]	LCA study of photovoltaic systems based on different technologies	Silicon Thin Film Chalcogenide	N	Uses data from other studies
2018	Stamford & Azapagic[78]	Environmental Impacts of Photovoltaics: The Effects of Technological Improvements and Transfer of Manufacturing from Europe to China	Silicon	Y	
2018	Zhou et al.[79]	Assessing the photovoltaic technology landscape: efficiency and energy return on investment (EROI)	Thin Film Chalcogenide OPV	N	Not LCA Uses data from other studies
2019	Billen et al.[80]	Comparative evaluation of lead emissions and toxicity potential in the life cycle of lead halide perovskite photovoltaics	Perovskite	N	System boundaries not harmonizable
2019	Pallas et al.[81]	Life cycle assessment of emerging technologies at the lab scale: The case of nanowire-based solar cells	Tandem	Y	
2020	Blanco et al.[82]	Environmental impacts of III-V/silicon photovoltaics: life-cycle assessment and guidance for sustainable manufacturing	Tandem	Y	

Table A.1-2 Conversion factors for LCA impact category indicators

LCIA method	Version	Impact category	Indicator unit	Conversion factor	Resulting ILCD indicator unit
CED		Cumulative Energy Demand	CED	1	MJ
CML	2014	Abiotic Depletion Potential	CML-ADP	1	kg Sb eq
CML	2014	Abiotic Depletion Potential	CML-ADPf		MJ
CML	2014	Acidification potential	CML-AP	1.19	kg SO2 eq
CML	2014	Climate change	CML-CC	1	kg CO2 eq
CML	2014	Eutrophication potential	CML-EP	0.28	kg PO4 eq
CML	2014	Freshwater aquatic ecotoxicity potential	CML-FAETP	42.15	kg 1,4 DB eq
CML	2014	Human toxicity potential	CML-HTP		kg 1,4 DB eq
CML	2014	Land Use	CML-LU		m2.y
CML	2014	Marine aquatic ecotoxicity potential	CML-MAETP		kg 1,4 DB eq
CML	2014	Ozone depletion potential	CML-ODP	1	kg CFC-11 eq
CML	2014	Photochemical oxidation potential	CML-POCP	10.86	kg C2H4 eq
CML	2014	Terrestrial ecotoxicity potential	CML-TETP		kg 1,4 DB eq
CML	2014	Water depletion potential	CML-WDP	1	m3 water
EPBT		Energy payback time	EPBT	1	years
ILCD	2011	Resource use, minerals and metals	ILCD-ADP	1	kg Sb eq
ILCD	2011	Acidification	ILCD-AP	1	molc H+ eq
ILCD	2011	Climate change	ILCD-CC	1	kg CO2 eq
ILCD	2011	Freshwater ecotoxicity	ILCD-FET	1	CTUe
ILCD	2011	Freshwater eutrophication	ILCD-FEU	1	kg P eq
ILCD	2011	Human toxicity potential - cancer effects	ILCD-HT_CE	1	CTUh,c
ILCD	2011	Human toxicity potential - non cancer effects	ILCD-HT_NCE	1	CTUh,nc
ILCD	2011	Ionizing radiation	ILCD-IR	1	kBq U235 eq
ILCD	2011	Marine eutrophication	ILCD-MEUP	1	kg N
ILCD	2011	Ozone depletion	ILCD-ODP	1	kg CFC-11 eq
ILCD	2011	Respiratory inorganics	ILCD-PM	1	kg PM2.5 eq
ILCD	2011	Photochemical ozone formation	ILCD-POCP	1	kg NMVOC eq
ILCD	2011	Terrestrial eutrophication	ILCD-TEUP	1	mol N eq
ILCD	2011	Water resource depletion	ILCD-WRD	1	m3 water
Impact 2002+	2011	Aquatic acidification	IM2-AC	1.21	kg SO2 eq
Impact 2002+	2011	Climate change	IM2-CC	1	kg CO2 eq

Impact 2002+	2011	Ozone layer depletion	IM2-OD	1	kg CFC-11 eq
Impact 2002+	2011	Terrestrial ecotoxicity	IM2-TE		kg TEG eq
Recipe	2008	Agricultural land occupation	R8-ALO(H)		m2.y
Recipe	2008	Climate change (H)	R8-CC(H)	1	kg CO2 eq
Recipe	2008	Fossil depletion	R8-FD(H)		MJ
Recipe	2008	Freshwater ecotoxicity (H)	R8-FET(H)	544.78	kg 1,4 DB eq
Recipe	2008	Freshwater eutrophication potential	R8-FEU(H)	1	kg P eq
Recipe	2008	Human toxicity (H)	R8-HT(H)		kg 1,4 DB eq
Recipe	2008	Ionising radiation	R8-IR(H)	1	kBq U235
Recipe	2008	Marine ecotoxicity (H)	R8-MET(H)		kg 1,4 DB eq
Recipe	2008	Marine eutrophication potential	R8-MEU(H)	2.76	kg N eq
Recipe	2008	Mineral resource depletion	R8-MRD(H)	1.66E-06	kg Fe eq
Recipe	2008	Natural land transformation	R8-NLT(H)		m2
Recipe	2008	Ozone depletion (H)	R8-OD(H)	1	kg CFC-11 eq
Recipe	2008	Particulate matter	R8-PMF(H)	0.28	kg PM10 eq
Recipe	2008	Photochemical oxidant formation	R8-POF(H)	1	kg NMVOC eq
Recipe	2008	Terrestrial acidification	R8-TA(H)	1.32	kg SO2 eq
Recipe	2008	Terrestrial ecotoxicity (H)	R8-TET(H)		kg 1,4 DB eq
Recipe	2008	Urban land occupation	R8-ULO(H)		m2.y
Recipe	2008	Water depletion	R8-WD(H)	1	m3 water
TRACI	v2.1	Acidification	TR-AC	1.21	kg SO2 eq
TRACI	v2.1	Climate change	TR-CC	1	kg CO2 eq
TRACI	v2.1	Ecotoxicity	TR-ET	1	CTUe
TRACI	v2.1	Eutrophication	TR-EU	0.13	kg N

Table A.1-3 Pearson's correlations for impact as a function of year for each cell type

Impact Category	Cell type	Pearson's Correlation (Impact = *f*(Year))	Number of observations
CTUe	Organic	-0.35	7
CTUe	Perovskite	-0.20	19
CTUe	Silicon	NA	10
CTUe	Tandem	0.31	20
CTUe	Thin Film (Chalcogenide)	-0.84	6
CTUh,c	Organic	NA	2
CTUh,c	Perovskite	-0.07	10
CTUh,c	Silicon	NA	6

CTUh,c	Tandem	-0.04	17
CTUh,c	Thin Film (Chalcogenide)	-0.13	4
CTUh,nc	Organic	NA	2
CTUh,nc	Perovskite	0.01	19
CTUh,nc	Silicon	NA	6
CTUh,nc	Tandem	-0.14	17
CTUh,nc	Thin Film (Chalcogenide)	-0.12	4
kBq U235 eq	Organic	NA	3
kBq U235 eq	Perovskite	0.82	4
kBq U235 eq	Tandem	0.66	5
kBq U235 eq	Thin Film (Chalcogenide)	1.00	2
kg CFC-11 eq	Organic	0.59	5
kg CFC-11 eq	Perovskite	0.15	9
kg CFC-11 eq	Silicon	NA	6
kg CFC-11 eq	Tandem	-0.56	11
kg CFC-11 eq	Thin Film (Chalcogenide)	-0.44	9
kg CO2 eq	Dye-sensitized	NA	3
kg CO2 eq	Organic	-0.28	10
kg CO2 eq	Perovskite	-0.07	21
kg CO2 eq	Quantum Dot	NA	1
kg CO2 eq	Silicon	-0.27	14
kg CO2 eq	Tandem	0.05	28
kg CO2 eq	Thin Film (Chalcogenide)	-0.33	13
kg CO2 eq	Thin Film (Si)	-0.84	5
kg N eq	Organic	NA	3
kg N eq	Perovskite	0.94	6
kg N eq	Tandem	0.93	5
kg NMVOC eq	Organic	0.54	5
kg NMVOC eq	Perovskite	0.44	9
kg NMVOC eq	Silicon	NA	4
kg NMVOC eq	Tandem	0.64	11
kg NMVOC eq	Thin Film (Chalcogenide)	-0.95	5
kg P eq	Organic	0.49	5
kg P eq	Perovskite	0.37	15
kg P eq	Silicon	NA	10
kg P eq	Tandem	0.34	20
kg P eq	Thin Film (Chalcogenide)	0.68	5
kg PM2.5 eq	Organic	0.51	5
kg PM2.5 eq	Perovskite	0.26	9
kg PM2.5 eq	Tandem	0.59	9
kg PM2.5 eq	Thin Film (Chalcogenide)	0.23	4
kg Sb eq	Organic	NA	3
kg Sb eq	Perovskite	-0.22	16
kg Sb eq	Silicon	NA	10

kg Sb eq	Tandem	0.78	14
kg Sb eq	Thin Film (Chalcogenide)	0.53	3
m3 water	Organic	NA	3
m3 water	Perovskite	-0.92	7
m3 water	Tandem	-1.00	3
m3 water	Thin Film (Chalcogenide)	NA	2
MJ	Dye-sensitized	NA	3
MJ	Organic	-0.84	7
MJ	Perovskite	-0.20	15
MJ	Quantum Dot	NA	1
MJ	Silicon	NA	2
MJ	Tandem	NA	2
MJ	Thin Film (Chalcogenide)	0.60	5
MJ	Thin Film (Si)	NA	1
mol N eq	Tandem	0.81	4
mol N eq	Thin Film (Chalcogenide)	NA	1
molc H+ eq	Organic	0.52	5
molc H+ eq	Perovskite	-0.18	12
molc H+ eq	Quantum Dot	NA	1
molc H+ eq	Silicon	NA	6
molc H+ eq	Tandem	0.54	11
molc H+ eq	Thin Film (Chalcogenide)	0.31	10

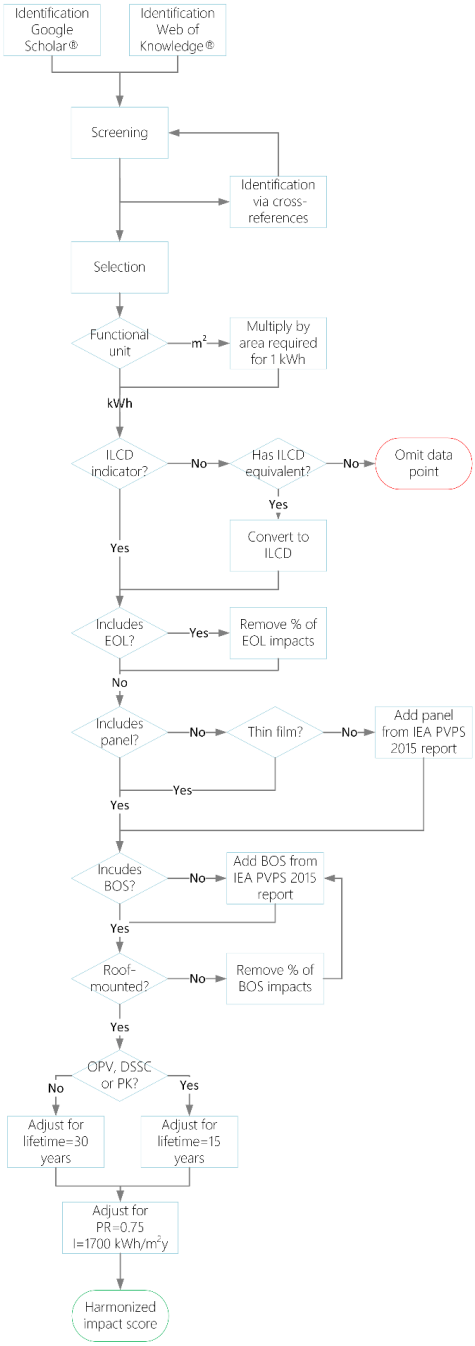

Figure A.1-1 Identification, screening, selection and harmonization procedure flowchart

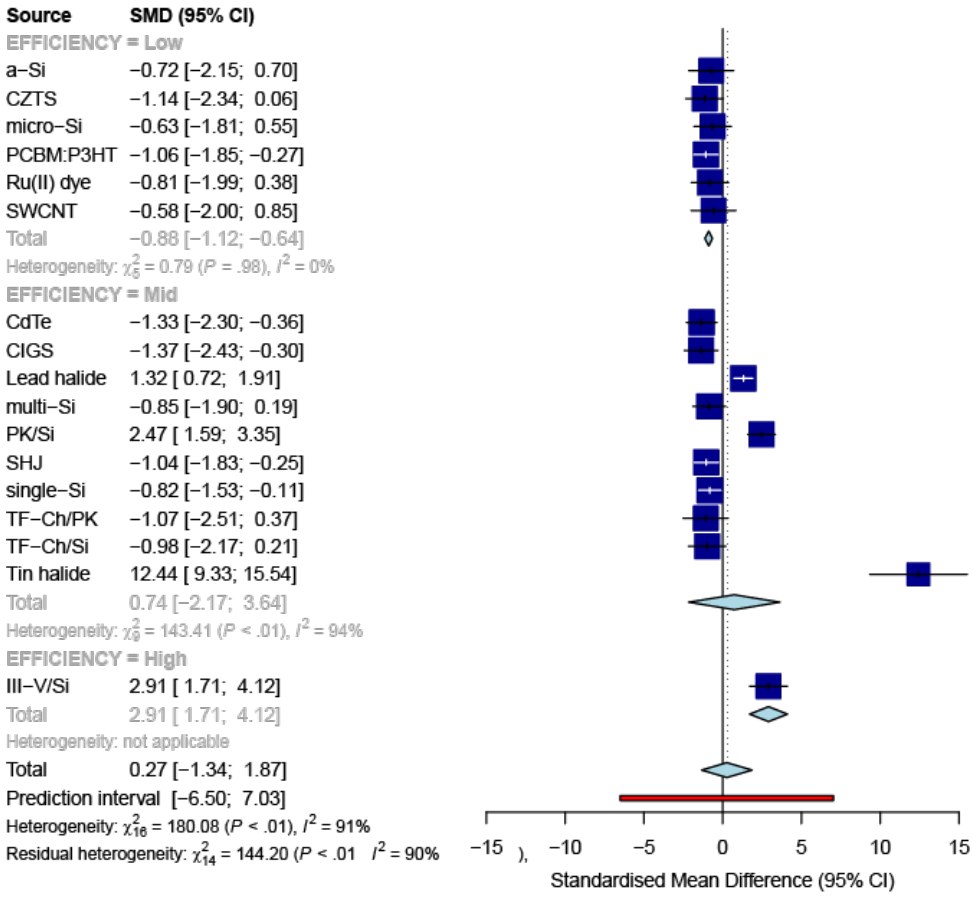

Figure A.1-1 Random effect model results sub-grouped by cell conversion efficiencies.

A.2. Supplementary Information to Chapter 3

A.2.1. System flowcharts and boundaries

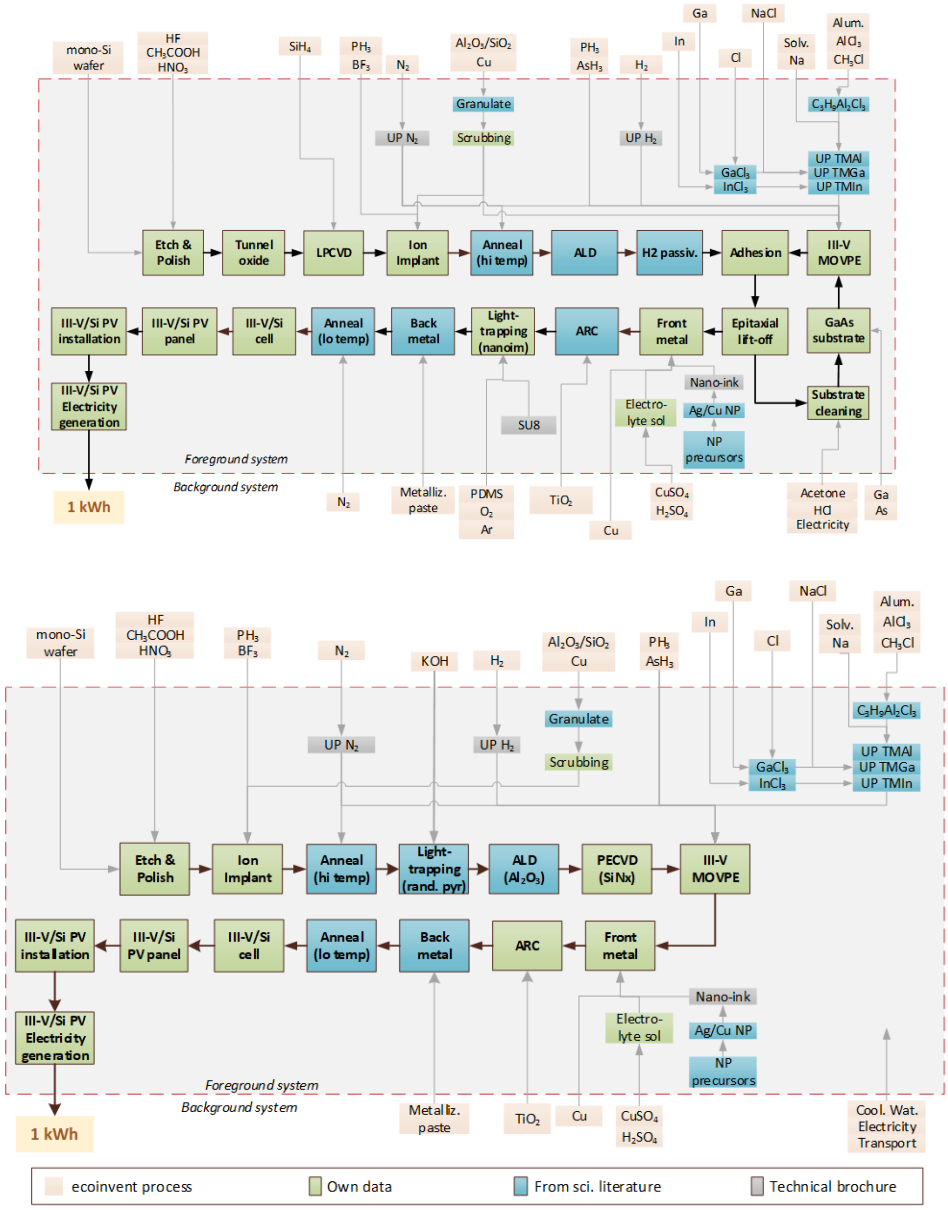

Figure A.2-1 System flowchart for Concept A (direct growth, bottom) and Concept B (bonding, top). UP = Ultrapure

A.2.2. Life-cycle inventories: process descriptions and input/output data

A.2.2.1. Overview and general assumptions

Most of the foreground processes are sensitive to the wafer area that can be processed per run since materials and energy consumption scale proportionally with the treatable wafer area. We based our models on the use of a large MOVPE reactor prototype designed by AIXTRON, which can handle a run of 31 round 4-inch wafers. We assumed that all other processing steps would handle wafers of the same area.

We also note that some lab-based processes described below have been modelled considering only process inputs, while waste emissions have not been fully characterized. The characterization of waste streams and emissions is more relevant in industrial-scale implementations where recycling and reuse take a central role and differ significantly from waste management in a lab environment. However, based on extrapolation from similar processes, it is likely that these emissions would only have relatively minor contributions to the life cycle impacts of the electricity generation process.

A.2.2.2. Silicon wafer preparation

Table A.2-1 Process inputs and outputs for silicon wafer preparation

Input	Flow type	Quantity	Data source
CZ single-Si wafer	Eco	100 units	TopSil, personal communication
HF	Eco	0.3 L	TopSil, personal communication
HNO3	Eco	1.6 L	TopSil, personal communication
HC2H2O2	Eco	0.1 L	TopSil, personal communication
Treatment of wastewater from PV cell production	Eco	2 L	TopSil, personal communication
Output	**Flow type**	**Quantity**	**Data source**
Polished Si wafer	Eco	100 units	TopSil, personal communication

A.2.2.3. Ion implantation (p-n junction)

Table A.2-2. Process inputs and outputs for ion implantation

Input	Flow type	Quantity	Data source
Phosphine (PH_3)	Eco	3.4 g	Fraunhofer, personal communication
Boron trifluoride (BF_3)	Eco	3.4 g	Fraunhofer, personal communication
Ultrapure nitrogen (N_2)	Eco	14 m^3	Fraunhofer, personal communication
Cooling water	Eco	5 m^3	Fraunhofer, personal communication
Electricity, high voltage	Eco	100 kWh	Fraunhofer, personal communication
Compressed air	Eco	15 m^3	Fraunhofer, personal communication
Hazardous waste incineration	Eco	0.009 kg	Calculated
Output	**Flow type**	**Quantity**	**Data source**
Doped wafer area (3400 wafers)	Eco	26.69 m^2	Fraunhofer, personal communication

A.2.2.4. Tube furnace annealing – high temperature

We assumed the use of a 4.2kW power furnace which can handle 100 wafers per batch. The wafers cannot be inserted at 1000°C; this must be done at <400°C, and then the temperature is ramped up at a rate of 10°C per minute. The annealing time is 1 hour at 1000°C and the temperature is then ramped down for removal of the wafers. We assume a worst-case scenario where the furnace operates at full power during ramp up and processing time. We assume no power is consumed during ramp-down. Annealing is conducted in an inert environment of ultrapure nitrogen, which flows at a rate of 30 SLM (standard litres per minute) during insertion and removal, and 15 SLM during annealing.

Table A.2-3. Process inputs and outputs for high temperature tube furnace annealing

Flow type	Flow type	Quantity	Data source
Ultrapure nitrogen	Eco	0.9 m^3	AZUR, personal communication
Electricity	Eco	10.668 kWh	Calculated
Output	**Flow type**	**Quantity**	**Data source**
Annealing of 1 m^2 of cell	Eco	1 unit	Calculated

A.2.2.5. Atomic layer deposition (ALD)

This step considers the deposition of a 10nm film of Al_2O_3 on the rear side. Process data for this step is based on Louwen et al.[83], who reviewed various specifications and found average electricity use to be 0.29 kWh/m^2, with values ranging 0.15 to 0.51 kWh/m2 (−48% to +76%). No materials input data and output data were available for this step.

A.2.2.6. Back-side passivation

Back-side passivation is conducted by plasma-enhanced chemical vapour deposition (PECVD) of a SiNx layer.

Table A.2-4. Energy and material inputs and outputs for PECVD back-side passivation

Input	Flow type	Quantity	Data source
Electricity	Eco	39,93 Wh	Fraunhofer, personal communication
Cooling water	Eco	5,27 L	Fraunhofer, personal communication
Nitrogen	Eco	12,57 L	Fraunhofer, personal communication
Compressed dry air	Eco	5,02 L	Fraunhofer, personal communication
Silane (SiH_4)	Eco	0,03 L	Fraunhofer, personal communication
NH_3	Eco	0,06 L	Fraunhofer, personal communication
Output	**Flow type**	**Quantity**	**Data source**
Back-side passivation of 1 cell	Eco	1 unit	Fraunhofer, personal communication

A.2.2.7. III-V Metalorganic Vapor Phase Epitaxy (MOVPE)

Table A.2-5. Process inputs and outputs for MOVPE III-V direct growth

Input	Flow type	Quantity	Data source
TMGa	Eco	11.48 g	Aixtron, personal communication
TMIn	Eco	0.1 g	Aixtron, personal communication
TMAl	Eco	0.17 g	Aixtron, personal communication
AsH3	Eco	11.76 g	Aixtron, personal communication
PH3	Eco	17.84 g	Aixtron, personal communication
H2	Eco	3.34 m3	Aixtron, personal communication
N2	Eco	3.44 m3	Aixtron, personal communication
Cooling water	Eco	27.51 m3	Aixtron, personal communication
Electricity	Eco	105.06 kWh	Aixtron, personal communication
Hazardous waste treatment	Eco	0.035 kg	Calculated
Output	**Flow type**	**Quantity**	**Data source**
III-V layer area	Eco	2905 cm^2	Aixtron, personal communication

A.2.2.8. Front metal contacts

We based our model on a "seed and plate" metallization technique, which involves nanoink printing of a seed layer of fingers, then electroplating to increase the thickness of the fingers. Conventional screen-printing methods are considered for 3 busbars that cross the fingers.

A.2.2.8.1. Seed layer (nano) inkjet printing

Materials: The pattern to be printed on the cells for the seed layer consists of 6 fingers 2 mm wide, 75 mm long and 0.1 μm thick (height) on average. The total quantity of nanoink required is calculated by the total volume of this pattern multiplied by the density of the nanoink (reported by the manufacturer). To this quantity, we added 10% to account for ink that remains in the filter and is discarded as hazardous waste. Therefore, we have the following inputs, per cell:

 # fingers Finger width Finger length Finger thickness Ink density Loss factor (Eq. A.2-1)

$$6 \cdot \left(2\ mm \cdot \frac{1\ m}{1E3\ mm}\right) \cdot \left(75\ mm \cdot \frac{1\ m}{1E3\ mm}\right) \cdot \left(0.1\mu m \cdot \frac{1\ m}{1E6\ \mu m}\right) \cdot \frac{1.27E3\ kg}{m^3} \cdot 110\% = 1.25E-7\ kg\ Cu\ ink$$

Printer electricity. A sample tested at Joanneum Research Center facilities was approximately 10 cm. long and took 5 minutes to print, with only 2 nozzles in use out of a total possible of 210. We estimated the printing speed as:

$$\frac{10\ cm}{5\ min} \cdot \frac{210\ nozzles}{2\ nozzles} \cdot \frac{60\ min}{1\ h} \cdot \frac{1\ m}{100\ cm} = \frac{126\ m}{h} \quad \text{(Eq. A.2-2)}$$

The total length of the 6 printed fingers is 0.45 m, and the printer has a maximum power rating of 1kW. We assume it operates at 75% power on average. To calculate electricity consumption of the printing process (per cell) we have:

$$\frac{0.45\ m}{cell} \cdot \frac{1\ h}{126\ m} \cdot 1\ kW \cdot 75\% = \frac{0.027\ kWh}{cell} \quad \text{(Eq. A.2-3)}$$

A.2.2.8.2. Seed layer sintering: laser

Laser electricity: The length of the pattern that has to be sintered is calculated from the data in the previous section (0.45 m). We used a laser scan speed of 0.01 m/s, and the optical power delivered by the laser is 1.4 W. The wall-plug to optical efficiency of YAG type lasers is typically around 25%[84], so we estimate the electricity consumption for laser sintering as:

$$\frac{0.45\ m}{cell} \cdot \frac{s}{0.01\ m} \cdot \frac{1\ h}{3600\ s} \cdot 1.4E-3\ kW \cdot \frac{1}{25\%} = \frac{5.6E-5\ kWh}{cell} \quad \text{(Eq. A.2-4)}$$

Materials: Laser-sintering of both Cu and Ag ink is done in open air.

Table A.2-6. Process inputs and outputs for seed-layer inkjet printing

Input	Flow type	Quantity	Data source
Cu nanoink	Eco	1.25E-7 kg	Joanneum, personal communication
Electricity	Eco	0.0271 kWh	Joanneum, personal communication
Output	**Flow type**	**Quantity**	**Data source**
Finger seed layers for 1 cell	Eco	1 unit	Joanneum, personal communication

A.2.2.8.3. Seed layer sintering: chemical (Cu ink only)

Sintering of Cu ink requires a reducing environment, while Ag ink can be sintered in open air. For the Cu ink, a sintering test was conducted at Joanneum Research Center facilities, where for a 1cm^2 sample 5 mL of ethanol (3.95 g @ 789g/L), 50 mL formic acid, and 70 L of ultrapure nitrogen were required.

A.2.2.8.4. Fingers electroplating

Electroplating consists of submerging the cell with the seed pattern in an electrolyte bath, where the patterned cell will serve as an ion-receiving cathode and a copper in the solution will serve as an anode. For copper, the electrolyte solution consists of a mix of cupric sulphate and sulphuric acid. Driving an electric current through the solution will force the metallic ions from the cathode to deposit on the seed pattern until the desired geometry is obtained.

Electricity: A conventional electroplating setup is used, where 10 mA of applied current with an average voltage of 0.5 V provides 250 nm of plating per minute. The electrical power can be calculated from the current and voltage:

$$P = I \cdot V = \left(10\ mA \cdot \frac{1\ A}{1000\ mA}\right) \cdot (0.5\ V) = 5E-3\ W = 5E-6\ kW \quad \text{(Eq. A.2-5)}$$

The amount of electricity consumed is calculated by multiplying the power by the time required to plate the desired finger thickness of 12.5µm.

$$\frac{5E-6\ kW}{cells}\cdot\frac{1\ min}{0.25\ \mu m}\cdot 12.5\ \mu m\cdot\frac{1\ h}{60\ min}=\frac{4.16E-6\ kWh}{cell}$$ (Eq. A.2-6)

Materials: Pure metal anodes donate the ions that ultimately deposit on the pattern (cathode). The ions are first passed from the electrolyte solution to the cathode, and are then replenished from the anode to the solution. Therefore, the anode is sacrificed according to the amount of metal deposited in the cell, and we assume 10% losses.

(Eq. A.2-7)

$$Cu:\ 6\cdot\left(2\ mm\cdot\frac{1\ m}{1E3\ mm}\right)\cdot\left(75\ mm\cdot\frac{1\ m}{1E3\ mm}\right)\cdot\left(12.4\ \mu m\cdot\frac{1\ m}{1E6\ \mu m}\right)\cdot\frac{8.96E3\ kg}{m^3}\cdot 110\%=1.09E-4\ kg\ Cu$$

We consider a standard cupric sulphate electrolyte solution that consists of 200 g cupric sulphate and 25 mL sulphuric acid in sufficient deionized water to prepare 1 L of electrolyte solution. This amount of solution is used for electroplating on one cell; however, we consider that it can be used for the production of 10-100 wafers based on lab experience, and test the sensitivity of this parameter.

Table A.2-7. Energy and material inputs and outputs for electroplating of fingers

Input	Flow type	Quantity	Data source
Copper	Eco	1.09E-4 kg	Joanneum, personal communication
Electricity	Eco	4.16E-6 kWh	Joanneum, personal communication
Electrolyte solution	Eco	0.1 L	Joanneum, personal communication
Output	**Flow type**	**Quantity**	**Data source**
Electroplating of 1 cell	Eco	1 unit	Joanneum, personal communication

A.2.2.8.5. Busbars screen printing

Screen printing electricity: We use data from a screen printer running a squeegee motor with a power of 1.16 kW. The printer can process a sheet of 400x400mm in 30 seconds.

$$\frac{1\ sheet}{4\ cells}\cdot 1.16\ kW\cdot 30\ s\cdot\frac{1\ h}{3600\ s}=\frac{2.41E-3\ kWh}{cell}$$ (Eq. A.2-8)

Curating electricity: Cu busbars are grown over the Cu fingers by screen-printing. However, instead of co-firing, the Cu busbars are curated at lower temperature (250°C) in an atmosphere of pure nitrogen[85]. This is done in a furnace that has a power rating of 3.4 kW and can process 1000 cells per batch, for a curating time of 10 minutes.

$$\frac{3.4\ kW}{1000\ cells}\cdot 10\ min\cdot\frac{1\ h}{60\ min}=\frac{5.67E-4\ kWh}{cell}$$ (Eq. A.2-9)

Materials: We consider 3 busbars, 1 mm wide, 156 mm long and 13.5 µm thick on average. We assume 10% losses from the paste during screen-printing. Per cell, we have:

(Eq. A.2-10)

$$3\cdot\left(1\ mm\cdot\frac{1\ m}{1E3\ mm}\right)\cdot\left(156\ mm\cdot\frac{1\ m}{1E3\ mm}\right)\cdot\left(13.5\ \mu m\cdot\frac{1\ m}{1E6\ \mu m}\right)\cdot\frac{8.96E3\ kg}{m^3}\cdot 110\%=6.23E-5\ kg\ Cu$$

Table A.2-8. Energy and material inputs and outputs for screen printing of busbars

Input	Flow type	Quantity	Data source
Copper	Eco	6.23E-5 kg	Joanneum, personal communication
Electricity	Eco	3E-3 kWh	Joanneum, personal communication
Output	**Flow type**	**Quantity**	**Data source**
Screen printing of 1 cell	Eco	1 unit	Joanneum, personal communication

A.2.2.9. Rear-side metal contacts

Data for the rear-side metal contacts are taken from the inventories for existing single-Si PV cells (ecoinvent v3.4)[86].

A.2.2.10. Tube furnace annealing - low temperature

The data for this process was calculated as for the high temperature annealing in section 2.4; however we discard ramp up energy and gas flow requirements, since the cells can be inserted and removed at this lower process temperature (<400°C).

A.2.2.11. Carrier gases

A.2.2.11.1. Ultrapure hydrogen

Two alternatives are considered for the supply of ultrahigh purity hydrogen: off-site source (commercially available hydrogen produced from Steam Methane Reforming) and on-site generation with a proton exchange membrane (PEM) system. In both alternatives, additional purification with a two-step adsorber/getter is considered.

Off-site generation: Commercial H_2 gas + adsorber/getter. Commercial production of hydrogen gas is modelled based on the steam methane reforming process (SMR), which accounts for over 90% of the world production. This production method was modelled in an LCA study by NREL[87] and more recently by other authors[88,89]. We use the process data reported by Cetinkaya et al.[89], which is in close accordance with figures reported by Mehmeti et al.[88] The inputs required for generating electricity that is consumed in the SMR process are also included in the inventory.

Table A.2-9. Process inputs and outputs for production of hydrogen via steam methane reforming

Input	Flow type	Quantity	Data source
Concrete	Eco	5.26E-06 m^3	Cetinkaya et al.[89]
cast iron	Eco	0.049 g	Cetinkaya et al.[89]
steel, low-alloyed	Eco	4.029 g	Cetinkaya et al.[89]
aluminium, cast alloy	Eco	0.033 g	Cetinkaya et al.[89]
water, deionised	Eco	19,776.2 g	Cetinkaya et al.[89]
natural gas; 44.1 MJ/kg	Env	165 MJ	Cetinkaya et al.[89]
Coal, hard, unspecify., in ground	Env	132.49 g	Cetinkaya et al.[89]
Oil, crude, in ground	Env	8.76 g	Cetinkaya et al.[89]

Output	Flow type	Quantity	Data source
Hydrogen	Eco	1 kg	Cetinkaya et al.[89]

The purifier (adsorber + getter) commercialized by SAES Gas handles a flow of 100 Nm^3/h at an average power consumption of 26kW, therefore 0.26kWh/Nm^3. It also consumes 60 L/min of cooling water, therefore 0.036 m^3 water/Nm^3. In this case we include transportation from SMR plant to consumer, using the same values as for liquid hydrogen specified in EcoInvent v3.4.

Table A.2-10. Process inputs and outputs for purification of hydrogen

Input	Flow type	Quantity	Data source
Hydrogen	Eco	0.08988 kg	SAES product spec sheet
Electricity	Eco	0.26 kWh	SAES product spec sheet
Cooling water	Eco	0.036 m^3	SAES product spec sheet
transport, freight train	Eco	0.0004 t*km	EcoInvent v3.4
transport, freight, light commercial vehicle	Eco	1.62E-05 t*km	EcoInvent v3.4
transport, freight, lorry, unspecified	Eco	0.00051 t*km	EcoInvent v3.4
Output	**Flow type**	**Quantity**	**Data source**
Ultrapure hydrogen	Eco	1 Nm^3	SAES / Proton product spec sheets

On-site generation: PEM on-site generator + adsorber/getter. The proton exchange membrane (PEM) generator commercialized by Proton delivers 30 Nm^3/hr, consuming 5.8 kWh / Nm^3 on average. (For consistency check, we compare with Mehmeti et al.[88] who separately report a consumption of 54.6 kWh/kgH2 = 4.5 kWh/Nm^3. Balahi et al.[90] report a consumption of 4.775 kWh/Nm^3). The Proton PEM generator also requires 26.9 L/h of deionized water per hour and 167 L/min coolant. The purifier (adsorber + getter) commercialized by SAES Gas handles a flow of 100 Nm^3/h at an average power consumption of 26kW, therefore 0.26kWh/Nm^3. It also consumes 60 L/min of cooling water, therefore 0.036 m^3 water/Nm^3. Data for the combined processes is presented in Table A.2-11.

Table A.2-11. Process inputs and outputs for onsite generation and purification of hydrogen

Input	Flow type	Quantity	Data source
Electricity	Eco	6.022 kWh	SAES / Proton product spec sheets
DI water	Eco	0.897 kg	Proton product spec sheet
Cooling water	Eco	0.34 m^3	SAES product spec sheet
Output	**Flow type**	**Quantity**	**Data source**
Ultrapure hydrogen	Eco	1 Nm^3	SAES / Proton product spec sheets

A.2.2.11.2. Ultrapure nitrogen

We consider the use of commercially available liquid nitrogen, which is produced via cryogenic air separation and delivered to consumers in the European market as per EcoInvent v3.4.[86] Although the nitrogen produced via this method is of high purity (99.9999%), we consider additional purification on-site using data for a commercially available SAES purifier.

Table A.2-12. Process inputs and outputs for purification of nitrogen for MOVPE application

Input	Flow type	Quantity	Data source
Nitrogen	Eco	1.25 kg	EcoInvent v3.4
Electricity	Eco	3.3E-4 kWh	SAES product spec sheet
Cooling water	Eco	6.4E-4 m^3	
Output	**Flow type**	**Quantity**	**Data source**
Ultrapure nitrogen	Eco	1 Nm^3	SAES product spec sheets

A.2.2.11.3. Hydride gases

Hydride gases arsine and phosphine were taken directly from the EcoInvent v3.4 database.[86] It is known that further purification may be required to reduce acids and humidity that result from cylinder use, and this can be achieved by commercially available purifiers that use an adsorbent medium. However, no specific data for this purification process was available at the time of this report. It is flagged, however, as an important follow-up area due to the potential generation of significant amounts of hazardous waste in the form of adsorbent media.

A.2.2.12. Metalorganic precursors

We used the input/output data for the synthesis of metalorganic precursors for III-V MOVPE reported by Smith et al. (2018)[91].

A.2.2.13. Scrubbing of MOVPE and ion implant exhaust gas

We assumed dry scrubbing systems, in which the main component is an adsorbent granulate. Energy is only required to operate the equipment systems and monitors, but not for the reaction, therefore it was assumed negligible. Based on tests run at Fraunhofer ISE facilities, 17 kg of hydride gases (arsine or phosphine) from an MOVPE reactor were absorbed in 130 kg of granulate.

Granulate composition is not disclosed by manufacturers, but a review of literature, patents, safety data sheets and technical brochures indicates that the industry is moving towards chemisorption by copper oxide catalyst impregnated on a supporting medium of alumina (Al_2O_3) or silicate (SiO_2)[92–95]. Another option is the use of zeolite (a microporous aluminosilicate mineral) exchanged with a copper cation. After adsorption, the granulate

is collected and reprocessed externally into new copper for other industrial uses. No information could be found on intermediate processing steps.

For the zeolite based adsorbent, we modelled the process described Wang and colleagues[96] for the adsorption of arsine, which is similar to the process described by Li and colleagues[97] for phosphine. We chose the best performing alternative presented by the authors, a copper-loaded zeolite, which is produced by impregnating the zeolite in a 50 mL solution of copper II nitrate with a concentration of 0.2 mol/L $Cu(NO_3)_2$. Based on the preparation procedure reported by the authors, the inputs and outputs are:

Table A.2-13. Process inputs and outputs for purification of scrubbing of arsine and phosphine

Input	Flow type	Quantity	Data source
Zeolite adsorbent	Eco	7.65 kg	Fraunhofer, personal communication
Hazardous waste, for underground deposit	Eco	-8.65 kg	Calculated as mass of adsorbent + mass of treated gas.
Output	**Flow type**	**Quantity**	**Data source**
III-V waste gas treatment	Eco	-1 kg	Fraunhofer, personal communication

Table A.2-14. Process inputs and outputs for production of copper zeolite adsorbent granulate

Input	Flow type	Quantity	Data source
Zeolite powder	Eco	10 g	Wang et al.[96]
Copper II nitrate	Eco	2.95 g	Wang et al.[96]. Based on molar mass of $Cu(NO_3)_2$. Authors report 10% Cu(II) content by weight in final adsorbent. Starting mass of zeolite is 10 g
Output	**Flow type**	**Quantity**	**Data source**
Zeolite adsorbent	Eco	12.95 g	Wang et al.[96].

A.2.2.14. III-V MOVPE growth on GaAs substrate

Table A.2-15. Process inputs and outputs for MOVPE III-V growth on GaAs substrate

Input	Flow type	Quantity	Data source
TMGa	Eco	5.26 g	Aixtron, personal communication
TMIn	Eco	1.23 g	Aixtron, personal communication
TMAl	Eco	3.17 g	Aixtron, personal communication
AsH3	Eco	19.96 g	Aixtron, personal communication
PH3	Eco	4.15 g	Aixtron, personal communication
H2	Eco	0.93 m3	Aixtron, personal communication
N2	Eco	2.24 m3	Aixtron, personal communication
Cooling water	Eco	17.89 m3	Aixtron, personal communication
Electricity	Eco	68.33 kWh	Aixtron, personal communication
Hazardous waste treatment	Eco	0.024 kg	Calculated

Output	Flow type	Quantity	Data source
III-V layer area	Eco	2905 cm^2	Aixtron, personal communication

A.2.2.15. Bonding

The bonding process as described by Heitmann et al.[98] requires 4 steps: HF clean, spray pyrolysis, adhesion and hot press. For the hot-press we used parameters from a commercial wafer bonding tool (https://www.suss.com/en/products-solutions/wafer-bonder/sb6-sb8-gen2). The tool has a power rating of 4.2kW and can process up to 8 wafers simultaneously. We assumed a bonding time of 20 minutes.

Table A.2-16. Process inputs and outputs for bonding

Input	Flow type	Quantity	Data source
HF	Eco	3.44 g	Fraunhofer ISE, personal communication
Spray pyrolysis solution	Eco	120 mL	Fraunhofer ISE, personal communication
Electricity	Eco	0.175 kWh	Fraunhofer ISE, personal communication
Output	**Flow type**	**Quantity**	**Data source**
Bonding of 1 III-V/Si cell	Eco	1 unit	

Table A.2-17. Process inputs and outputs for bonding of spray pyrolysis solution.

Input	Flow type	Quantity	Data source
Zinc 2,4 pentanedione	Eco	1.7 g	Fraunhofer ISE, personal communication
Methanol	Eco	20.0 g	Fraunhofer ISE, personal communication
Indium trichloride	Eco	1.32 g	Fraunhofer ISE, personal communication
Output	**Flow type**	**Quantity**	**Data source**
Spray pyrolysis solution	Eco	1 L	

There are several routes for the industrial synthesis of zinc 2,4 pentanedione (which is a metal acetylacetonate)[99]; we consider a reaction of the zinc chloride salt with acetylacetone and use stoichiometric calculations to estimate the amounts and assume 10% losses.

Table A.2-18. Process inputs and outputs for preparation of zinc 2,4 pentadionate.

Input	Flow type	Quantity	Data source
Vinyl acetate	Eco	0.22 kg	
Zinc chloride	Eco	0.15 kg	

Output	Flow type	Quantity	Data source
Zinc 2,4 pentanedione	Eco	0.34 kg	

Table A.2-19. Process inputs and outputs for synthesis of zinc chloride.

Input	Flow type	Quantity	Data source
Hydrochloric acid	Eco	0.08	
Zinc	Eco	0.07	
Output	**Flow type**	**Quantity**	**Data source**
Zinc chloride	Eco	0.14	

A.2.2.16. Lift-off

A.2.2.16.1. Laser lift-off

For lift-off practiced on a 10x10mm sample, the total energy consumption of the laser equipment was measured at 0.002 kWh (we disregard power consumption during startup and shutdown, assuming a large number of cells can be processed continuously). To this, we add 0.04 kWh for the ventilation equipment, which must operate after processing on the GaAs sample for safety reasons. The laser stage has an area of 762 x 432 mm, so we assume that 70 x 40 samples can be ventilated at a given time. Extrapolating this linearly to a cell (area 78.3 cm2), we get a total of:

$$\left(\frac{0.002\ kWh}{10\times10\ mm^2}+\frac{0.04\ kWh}{70\times40\times10\times10\ mm^2}\right)\cdot\frac{100\ mm^2}{cm^2}\cdot\frac{78.3\ cm^2}{cell}=\frac{0.16\ kWh}{cell} \qquad \text{(Eq. A.2-11)}$$

A.2.2.16.2. Chemical lift-off

To compare the laser lift-off with a chemical method, we modelled a wet chemical process used to etch the bonding layer. Based on projections for state of the arte wet-chemical etching system, we assumed a consumption of 1,25 ml of 50% HF etching solution per wafer. The recyclability of the etching solution is very high, therefore we disregarded the wastewater treatment from this process.

A.2.2.17. GaAs substrate reuse and reclaim

We assumed that the GaAs substrate can be reused 100 times. However, this requires periodical chemical-mechanical polishing (CMP) of the GaAs substrate[100] which is done every 5 reuse cycles. We assume 98% process losses.

Table A.2-20. Process inputs and outputs for reclaiming of GaAs substrate

Input	Flow type	Quantity	Data source
CMP slurry	Eco	0.2 L	Matovu et al.[100]
electricity	Eco	2 kWh	

Output	Flow type	Quantity	Data source
Reclaim of 1 GaAs substrate	Eco	1 unit	

Table A.2-21. Energy and material inputs and outputs for CMP slurry

Input	Flow type	Quantity	Data source
Activated silica	Eco	100 g	Matovu et al.[100]
Hydrogen peroxide	Eco	33.33 g	Matovu et al.[100]
Water, deionised		866.67 g	Matovu et al.[100]
Output	**Flow type**	**Quantity**	**Data source**
CMP slurry	Eco	1 L	

A.2.2.18. III-V/Si PV electricity generation

The III-V/Si cells can be a drop-in replacement for commercially available single-Si PV systems. To make all infrastructure and BOS components equal in the III-V/Si and single-Si systems, we duplicated the ecoinvent (v3.4) process for generation of 1 kWh from a roof-mounted installation. We then replaced the single-Si cell for the III-V cell in the panel which was supplied to the installation, using the same cell area. The area of cell required to generate a given amount of electricity is inversely proportional to the conversion efficiency of the cell, so we applied the increased efficiency factor to the electricity output of the III-V/Si plant. The efficiency of the single-Si module in ecoinvent is 15.4%, and for the III-V/Si module is 30%, giving a conversion factor of (0.3/0.154) = 2.22. We applied this directly to the output of the III-V/Si installation, where instead of generating 1kWh it would generate 2.22 kWh with the same ancillary infrastructure and BOS components.

A.2.3. Sensitivity analysis of technological improvements

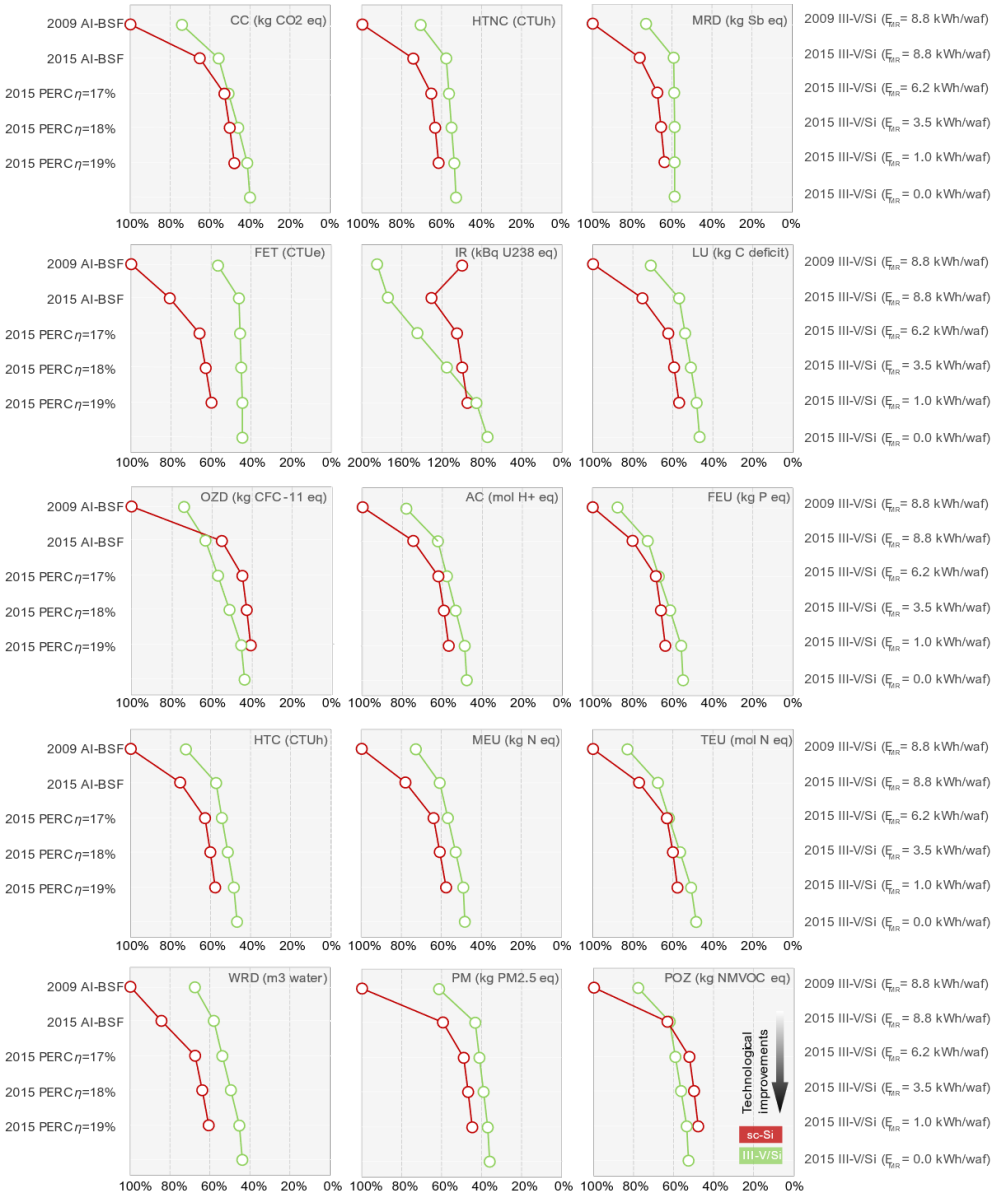

Figure A.2-2 Change in impact scores as a result of technological improvements. 2009: Reference data (2009) for silicon, module and BOS supply chains from ecoinvent v3.4; 2015: Updated IEA PVPS data (2015) for silicon, module and BOS supply chains; η: module efficiency; EMR.: Energy consumption for a single MOVPE run of 37 wafers (2905 cm2).

A.3. Supplementary information to Chapter 4

A.3.1. Implementation notes: Setting up an uncertain product system

The Bernoulli and Categorical distributions are not available in the most commonly used LCA software packages. They can be implemented in MatLab (or Python, following similar algorithms) using the Binomial and Multinomial distributions, which are a general case of each. Section A.3.1.3 presents an alternative for implementation in publicly available software packages (e.g. OpenLCA, SimaPro, GaBi) that allow the use of uncertain user-defined parameters and formulas.

In the following code snippets, values in blue are examples, which can be replaced by the user according to their case. The code is designed for matrix-based LCA calculations as described by Heijungs and Suh[101].

A.3.1.1. Product system with two alternative, mutually exclusive processes: using the binomial distribution in MatLab.

n = 1;	Number of trials, always 1

x = 4088;
y = 4089;
z = 4090;
	Column number for process X in the technology matrix
	Column number for process Y in the technology matrix
	Column number for process Z in the technology matrix

fx = 2; fy = 4;	Quantity of product from process X going to process Z Quantity of product from process Y going to process Z
Px = 0.3;	Probability of process X
T = binornd(n,Px);	Random number from Binomial Distribution. Will give T a value of 1 depending on the probability Px.
A(x,z) = fx·T; A(y,z) = fy·(1-T);	Multiply the flows in the technology matrix by the corresponding trigger value

The corresponding function in Python to generate a random number from a binomial distribution, using the same variable designations as above is:

numpy.random.binomial(n, Px, size=None)

A.3.1.2. Setting up a product system with three or more alternative, mutually exclusive processes: using the multinomial distribution in MatLab.

n = 1;	Number of trials, always 1

x = 4088;
y = 4089;
w = 4090;
z = 4091;
	Column number for process X in the technology matrix
	Column number for process Y in the technology matrix
	Column number for process W in the technology matrix
	Column number for process Z in the technology matrix

fx = 2;
fy = 4;
fw = 3;
	Quantity of product from process X going to process Z
	Quantity of product from process Y going to process Z
	Quantity of product from process W going to process Z

Px = 0.2; Py = 0.2; Pw = 0.6;	Probability of process X Probability of process Y Probability of process W
p = [Px Py Pw];	Create vector with probabilities of each event
T = mnrnd(n,p);	Random number from Multinomial Distribution. Will create a random vector *r* equal to either [1 0 0], [0 1 0] or [0 0 1] based on the respective probabilities Px, Py and Pz.
A(x,z) = fx·T(1); A(y,z) = fy·T(2); A(w,z) = fw·T(3);	Multiply the flows in the technology matrix by the corresponding trigger value

The corresponding function in Python to generate a random number from a multinomial distribution, using the same variable designations as above is:

numpy.random.multinomial(n, p, size=None)

A.3.1.3. Setting up a product system with two or more alternative, mutually exclusive processes. Using the round() function and user-defined (local) parameters in OpenLCA, SimaPro or GaBi.

OpenLCA and SimaPro allow flow quantities to be entered as formulas rather than fixed numbers. These formulas contain parameters that can be uncertain, hence sampled randomly according to given probability distributions. For the case presented in section A.3.1.1 we can model this as:

$$T = round(rand() + (0.5 - Px)) \quad \text{(Eq. A.3-1)}$$

Alternatively, we can define a local parameter Pd which is has a uniform distribution with min: *0.5-Px* and max: *1+0.5-Px*. Then,

$$T = round(Pd) \quad \text{(Eq. A.3-2)}$$

Then we can multiply the incoming flows from processes X and Y by the corresponding quantities, *T* and *T-1*. Note that in the equation above, *rand()* selects a uniformly distributed

value between 0 and 1, which will round to 0 on 50% of the cases and to 1 on the other 50%. By adding *0.5 – Px*, the random number will round to 0 on *Px* of the cases and to 1 on 1-Px of the cases.

The parameter(s) will be recalculated in each Monte Carlo run, making T adopt a value of 1 or 0 according to the probability Px.

If there are more than two competing unit processes for the same element of the technology's product system, the same method can be applied by nesting the alternatives so that their combined probabilities result in the desired individual probabilities (see Figure A.3-1). For example, we may have three alternative competing processes X, Y and W with probabilities of 25, 35 and 40% respectively. In this case we set the probability of process XY as 60% (25 + 35), the probability of process X as 41.6% (so that when multiplied by 60% we get 25%) and the probability of process Y as 58.3% (so that when multiplied by 60% we get 35%). The probability of process W is set at 40%.

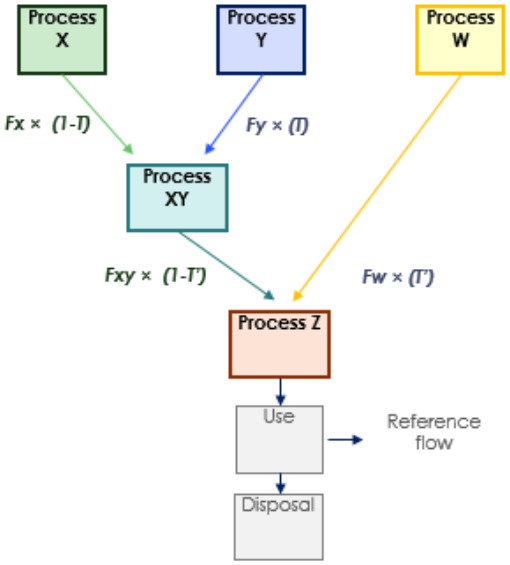

Figure A.3-1 Product system configuration for more than 2 competing alternative unit processes

A.3.2. Global sensitivity analysis: MatLab implementation

To estimate the Borgonovo delta uncertainty importance measures [102] we used a MatLab function *betaKS3.mat* [103] developed by Elmar Plischke and provided by the authors upon request. The *betaKS3* function takes two main inputs: a matrix *X* with all of the uncertain input parameters (rows) and their sampled value in each MC run (columns), and a vector *Y* with the impact score in each MC run. For all other options we used the default settings.

For the case study we only supplied the uncertain inputs in the foreground system, which were the focus of our investigation. Additional options for the betaKS3 function include the partition size, which we set at 15, and used Monte Carlo sample size of 10,000.

However, the uncertain inputs can also include variable and uncertain parameters from the ecoinvent background. These may be found in both the technology (A) and the environmental (B) matrix. The delta method accounts for interactions between parameters, and only those parameters that somehow affect the output can be provided to the function to reduce computational intensity. Therefore, three filters can be applied to the total set of uncertain input parameters from the A and B matrices to significantly reduce computational time:

- From the A and B matrices, include only uncertain flows from processes that are part of the calculated product system.
- From the B matrix, include only uncertain environmental flows that have a characterization factor for the impact type that is being assessed.
- From the A matrix, include only economic flows from processes that have an environmental flow *at any point upstream* that has a characterization factor for the impact type that is being assessed.

For our case study, we also include the values in each MC run of the different probabilities [Px, Py, Pw…] used to set the triggers for the alternative processes of the emerging technology. These can be appended to the input matrix at the end.

The function returns a vector with the sensitivity index for each parameter in the same order as they were listed in the input matrix *X*. The scores can be ranked (while recording the original position) in order to find out the relative importance of each to the variance in the impact score.

Code snippets for implementation of the filters in MatLab are provided below. For the code, we have stored all the uncertain flows in the LCA database along with their position (row | column) and their MC sampled values in two matrices: *inDA* (economic flows), *inDB* (environmental flows). These matrices have the following structure:

Row	Col	Run 1	Run 2	Run 3…	…Run N
1	1	*3.26*	*3.17*	*3.48*	*3.21*
1	2	*0.24*	*0.23*	*0.25*	*0.24*
1	5	*1.17*	*1.22*	*1.09*	*1.21*
…	…	…	…	…	…
# flows	# processes	*25.38*	*24.17*	*27.19*	*23.02*

In the code below, we apply the two filters (i) and (ii) to these matrices, copying them subsequently to inDA ➔ inDAf1, and inDB ➔ inDBf1 ➔ inDBf2.

Apply filter (i) to matrices A and B:

N = 10000	Number of Monte Carlo runs
s = A\f;	Calculates the scaling vector for the demand vector f, from the technology matrix A.
inDAf1 = [inDA zeros(size(inDA,1),1)]; inDBf1 = [inDB zeros(size(inDB,1),1)];	Add a column of zeros at the end of each matrix to place tag

for i = 1:size(inDAf1,1)
  if s(inDAf1(i,2))==0
  inDAf1(i,N+3)=1;
  end
end
	If process is not part of product system, scaling vector in that row==0. Tag that row with a 1.

for i = 1: size(inDBf1,1)
  if s(inDBf1(i,2))==0
  inDBf1(i,N+3)=1;
  end
end
	Repeat as above, this time for B matrix.

inDAf1(inDAf1(:,size(inDAf1,2))==1,:)=[]; inDBf1(inDBf1(:,size(inDBf1,2))==1,:)=[];	Delete rows with unused processes that are tagged with 1.

Apply filter (ii) to matrix B:

Iref = 482	Row position for impact type in Q matrix.
envflowsCC = find(Q_mat(Iref,:));	Find the flows in the Q matrix that have a characterization factor for impact *Iref*. The function *find()* returns the index (column) for non-zero values in row *Iref* of the Q matrix.
inDBf2 = inDBf1(ismember(inDBf1(:,1), envflowsCC), :);	Copy to inDBf2 only those flows that have been listed in envflowsCC.

Prepare input matrix for GSA and run GSA:

We can now concatenate the inputs from A and B matrices along with the uncertain foreground parameters and triggers. We have previously stored the randomly sampled foreground input parameters in matrix i*nPar* with each row representing each parameter (including the triggers) and each column the corresponding value for reach MC run. We have also stored the impact assessment results for the impact category in a vector *Ygsa*, with one result for each run.

Xgsa = cat(1,inDAf1, inDBf2);	Concatenate the A and B inputs into a single matrix
Xgsa(:,[1 2]) = [];	Delete first two columns with position information
Xgsa(:,end) = [];	Delete last column with the tag from filter (i)

Xgsa = cat(1, Xgsa, inPar);	Concatenate the A and B inputs with the foreground uncertain input parameters and triggers
Xgsa = transpose(Xgsa);	Transpose the matrix
d = deltamim(Xgsa, Ygsa);	Run *deltafast* function. *d* will contain a vector with the sensitivity indices.

Note: All uncertain inputs in the background and foreground are pre-sampled and stored in arrays, prior to running the Monte Carlo simulation, in order to ensure that the sampling of compared systems is dependent as recommended by Henriksson et al.[104] In each run, the Monte Carlo simulation picks the same pre-stored value for both systems.

A.3.3. Case study: process descriptions and input/output data

A.3.3.1. Fingers: seed layer (nano) inkjet printing

Materials: The pattern to be printed on the cell for the seed layer consists of 6 fingers 2 mm wide, 75 mm long and 0.1 μm thick on average. The total quantity of nanoink required is calculated by the total volume of this pattern multiplied by the density of each nanoink (reported by the manufacturers). To this quantity, we add 10% to account for ink that remains in the filter and is discarded as hazardous waste. Therefore, for each type of ink we have the following inputs, per cell:

 # fingers *Finger width* *Finger length* *Finger thickness* *Ink density* *Loss factor* (Eq. A.3-3)

$$6 \cdot \left(2\ mm \cdot \frac{1\ m}{1E3\ mm}\right) \cdot \left(75\ mm \cdot \frac{1\ m}{1E3\ mm}\right) \cdot \left(0.1\mu m \cdot \frac{1\ m}{1E6\ \mu m}\right) \cdot \frac{1.27E3\ kg}{m^3} \cdot 110\% = 1.25E-7\ kg\ Cu\ ink$$

$$6 \cdot \left(2\ mm \cdot \frac{1\ m}{1E3\ mm}\right) \cdot \left(75\ mm \cdot \frac{1\ m}{1E3\ mm}\right) \cdot \left(0.1\mu m \cdot \frac{1\ m}{1E6\ \mu m}\right) \cdot \frac{1.45E3\ kg}{m^3} \cdot 110\% = 1.44E-7\ kg\ Ag\ ink$$

Printer electricity. The current sample being tested is approx. 10 cm. long and takes 5 minutes to print, with only 2 nozzles in use out of a total possible of 210. We estimate the printing speed as:

$$\frac{10\ cm}{5\ min} \cdot \frac{210\ nozzles}{2\ nozzles} \cdot \frac{60\ min}{1\ h} \cdot \frac{1\ m}{100\ cm} = \frac{126\ m}{h} \quad \text{(Eq. A.3-4)}$$

From the data above, the total length of the 6 printed fingers is 0.45 m, and the printer has a maximum power rating of 1kW. We assume it operates at 75% power on average. To calculate electricity consumption of the printing process (per cell) we have:

$$\frac{0.45\ m}{cell} \cdot \frac{1\ h}{126\ m} \cdot 1\ kW \cdot 75\% = \frac{0.027\ kWh}{cell} \quad \text{(Eq. A.3-5)}$$

A.3.3.2. Fingers: seed layer sintering

Laser electricity: The length of the pattern that must be sintered is calculated from the data in the previous section (0.45 m). We use a laser scan speed of 0.01 m/s, and the optical power delivered by the laser is 1.4 W. The wall-plug to optical efficiency of YAG type lasers is typically around 25% [84], so we estimate the electricity consumption for laser sintering as:

$$\frac{0.45\ m}{cell}\cdot\frac{s}{0.01\ m}\cdot\frac{1\ h}{3600\ s}\cdot 1.4E-3\ kW\cdot\frac{1}{25\%}=\frac{5.6E-5\ kWh}{cell} \quad \text{(Eq. A.3-6)}$$

Materials: Laser-sintering of both Cu and Ag ink is done in open air.

A.3.3.3. Fingers: electroplating

Electroplating consists of submerging the cell with the seed pattern in an electrolyte bath, where the patterned cell will serve as an ion-receiving cathode and a copper anode in the solution will serve as a cathode. The electrolyte solution consists of a mix of cupric sulfate and sulfuric acid. Driving an electric current through the solution will force the metallic ions from the cathode to deposit on the seed pattern until the desired geometry is obtained.

Electricity: A conventional electroplating setup is used, where 10 mA of applied current with an average voltage of 0.5 V provides 250 nm of plating per minute. The electrical power can be calculated from the current and voltage:

$$P=I\cdot V=\left(10\ mA\cdot\frac{1\ A}{1000\ mA}\right)\cdot(0.5\ V)=5E-3\ W=5E-6\ kW \quad \text{(Eq. A.3-7)}$$

The amount of electricity consumed is calculated by multiplying the power by the time required to plate the desired finger thickness of 12.5μm.

$$\frac{5E-6\ kW}{cells}\cdot\frac{1\ min}{0.25\ \mu m}\cdot 12.5\ \mu m\cdot\frac{1\ h}{60\ min}=\frac{4.16E-6\ kWh}{cell} \quad \text{(Eq. A.3-8)}$$

Materials: Pure metal anodes donate the ions that ultimately deposit on the pattern (cathode). The ions are first passed from the electrolyte solution to the cathode and are then replenished from the anode to the solution. Therefore, the anode is sacrificed according to the amount of metal deposited in the cell, and we assume 10% losses.

(Eq. A.3-9)

$$Cu:\ \ 6\cdot\left(2\ mm\cdot\frac{1\ m}{1E3\ mm}\right)\cdot\left(75\ mm\cdot\frac{1\ m}{1E3\ mm}\right)\cdot\left(12.4\ \mu m\cdot\frac{1\ m}{1E6\ \mu m}\right)\cdot\frac{8.96E3\ kg}{m^3}\cdot 110\%=1.09E-4\ kg\ C$$

We consider a standard cupric sulfate electrolyte solution that consists of 200 g cupric sulfate and 25 mL sulfuric acid in sufficient deionized water to prepare 1 L of electrolyte solution. This amount of solution is used for electroplating on one cell; however, we consider that it can be used for the production of 10-100 wafers based on lab experience, and test the sensitivity of this parameter.

A.3.3.4. Busbars: screen printing

Screen printing electricity: We use data from a screen printer running a squeegee motor with a power of 1.16 kW. The printer can process a sheet of 400x400mm in 30 seconds.

$$\frac{1\ sheet}{4\ cells} \cdot 1.16\ kW \cdot 30\ s \cdot \frac{1\ h}{3600\ s} = \frac{2.41E-3\ kWh}{cell} \quad \text{(Eq. A.3-10)}$$

Curating electricity: Cu busbars are grown over the Ag or Cu fingers by screen-printing. However, instead of co-firing, the Cu busbars are curated at lower temperature (250°C) in an atmosphere of pure nitrogen[85]. This is done in a furnace that has a power rating of 3.4 kW and can process 1000 cells per batch, for a curating time of 10 minutes.

$$\frac{3.4\ kW}{1000\ cells} \cdot 10\ min \cdot \frac{1\ h}{60\ min} = \frac{5.67E-4\ kWh}{cell} \quad \text{(Eq. A.3-11)}$$

Materials: We consider 3 busbars, 1 mm wide, 156 mm long and 13.5 µm thick on average. We assume 10% losses from the paste during screen-printing. Per cell, we have:

(Eq. A.3-12)

$$3 \cdot \left(1\ mm \cdot \frac{1\ m}{1E3\ mm}\right) \cdot \left(156\ mm \cdot \frac{1\ m}{1E3\ mm}\right) \cdot \left(13.5\ \mu m \cdot \frac{1\ m}{1E6\ \mu m}\right) \cdot \frac{8.96E3\ kg}{m^3} \cdot 110\% = 6.23E-5\ kg\ Cu$$

A.4. Supplementary information to Chapter 5

A.4.1. Model overview

This risk assessment was conducted in six integrated steps:

- III-V/Si PV electricity demand scenarios: Projected the expected PV demand (in MW_p or GW_p) in each geographical scale over a period of 100 years using logistic growth curves.
- Dynamic stock flows: Determined the quantity of III-V/Si PV panels (in m^2 of PV installation) manufactured, installed, and recycled/incinerated/landfilled in each year to meet the electricity demands of the previous step.
- Emissions: Determined the quantities of III-V materials emitted to the environment from III-V/Si PV panels at each life cycle stage.
    - *Manufacturing:* Emissions from this phase were deemed negligible as all waste goes to underground hazardous waste storage and/or is reused.
    - *Use phase*: Calculated the emissions that may occur from panel breakage which exposes the III-V materials in the PV cells to leaching during rain events.
    - *End-of-life phase*:
        - Recycling: no direct emissions to the environment were considered during PV materials separation and repurposing, only the generation of waste.
        - Incineration: Calculates emissions of III-V materials that vaporize and are not captured by the abatement system, escaping to air.
        - Landfilling: Calculates emissions from III-V materials that leach from the waste to the landfill leachate, and later escape the landfill through uncontrolled leakage to the surrounding soil. Also calculates emissions that can volatize to air in the landfill.
- Environmental fate: Models the distribution of emitted III-V materials (in kg) in each environmental compartment in each scale and calculates the predicted environmental concentrations (PEC).
- Risk Quotient: Evaluates the risk as a ratio of predicted environmental concentrations (PEC) to concentrations at which no observable effects are reported (PNEC).

These steps are described in detail in the following sections, along with the assumptions and calculation notes. The values and probability distributions taken for all model input parameters are listed in Table A.4-2.

A.4.2. Demand scenarios

Demand scenarios for three geographical scales were modelled; one for Europe (continental, "SKY_EUR"), one for the city of Amsterdam (regional, "RES_AMS"), and an intentionally loaded smaller area (~16 km^2) containing a floating utility-scale PV plant with surrounding rooftop PV and EOL treatment facilities within it (local, "UTI_LOC"). The scales are embedded in the model, so that the PV demand (and corresponding emissions) in the local scale is added to the regional scale, and the regional scale is added to the continental scale. In the SimpleBox fate models, materials are allowed to be transported across scales.

With an expected 28% panel conversion efficiency, III-V/Si panels will have a rating of 280 W_p/m^2. This is equivalent to the power output of the panel under standard irradiance conditions of 1000 W/m^2. The rating can also be expressed in terms of efficiency, as the ratio of power output to power input. To translate PV installed capacity to PV installation size (as total Area of panels, in m^2) we used Equation A.4-1.

$$Area = \frac{PV\ Capacity}{Rating} = \frac{PV\ Capacity}{efficiency \cdot 1000\ W/m^2} \quad \text{(Eq. A.4-1)}$$

A.4.2.1. Continental scale: Europe

We modelled a first scenario based on possible future electricity demand in Europe according to the Shell Sky Scenario[105], which sets the most ambitious targets for electrification and solar generation in Europe from the different scenarios presented by Shell. In this scenario, total PV electricity demand will rise to 18.43 EJ (=5,138 TWh) by the year 2100, split equally between distributed and utility. If the IEA's "High GaAs" market shares are taken 15% of the utility share and 5% of the rooftop share would be taken by III-V/Si panels, the installed capacity of III-V/Si panels is 10%, or 513.8 TWh. We translate this electricity demand to installed capacity by assuming a 1200 kWh/kW_p average yield in Europe[106], although this can vary if the location of new PV installations shifts significantly to the north or south. Based on these data, we used a logistic growth curve (equations A.4-2 and A.4-3) to project installed capacity at any given time *C(t)*, starting with an initial capacity addition of $C_0 = 100\ MW_p$ in the year 2031 and stabilizing at $C_f = 430\ GW_p$. We took the growth rate k = 14.1% from the 75th percentile of 1100 different PV deployment scenarios in Europe that were reviewed and harmonized by Jaxa-Rozen et. al.[107]

$$C(t) = \frac{C_f}{1 + A \cdot e^{-kt}} \quad \text{(Eq. A.4-2)}$$

$$A = \frac{C_f - C_0}{C_0} \quad \text{(Eq. A.4-3)}$$

Of the total amount of III-V/Si PV panels produced each year, we assumed 25% would be installed on rooftop installations, while 75% would be installed in utility-scale plants, following the IEA's "High GaAs" scenario.[108] We further assumed that a fraction of utility-scale corresponding to 13.3% of utility (~10% of total generation) is supplied by floating

structures on surface water bodies (lakes) based on projections made by Cazzaniga et al. for floating PV installations.[109] In lieu of data, we assumed an equal split between rooftop installations that drain to freshwater and those that drain to soil (Figure A.4-1).

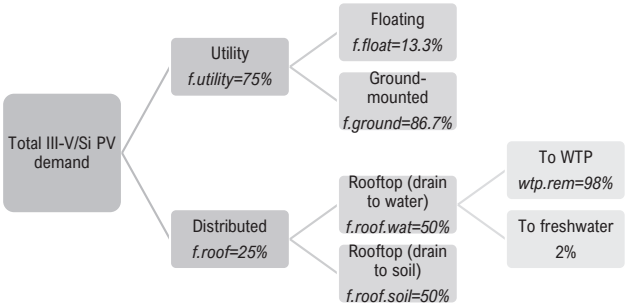

Fig A.4-1. Projected distribution of III-V/Si modules in Europe based on installation type and location.

A.4.2.2. Regional scale: Amsterdam area

The second scenario we modelled was based on the stated policies of the Amsterdam municipality[110]. The number of installed solar panels has grown by approximately 50% annually from 2012 to mid-2019. The city's aspiration is to reach 550 MW by 2030, which is half of the total potential of roofs (large and small). Afterwards, the city is committed to "leave no roof unused", with a roof potential of 1100 MW. Floating PV and ground-based installations will be kept as an option only if the targets are not achievable otherwise. Following these stated aspirations, for this scenario we assume III-V/Si enters the market after 2030 with an initial installed capacity of 100 kWp and grows at the pace of 20% annually to take up 10% of the total rooftop potential. As per Equations A.4-2 and A.4-3, this can be represented by setting C0 = 0.1 MW, Cf = 110 MW, and k = 0.2. The distributions according to type of installation are shown in Figure A.4-2.

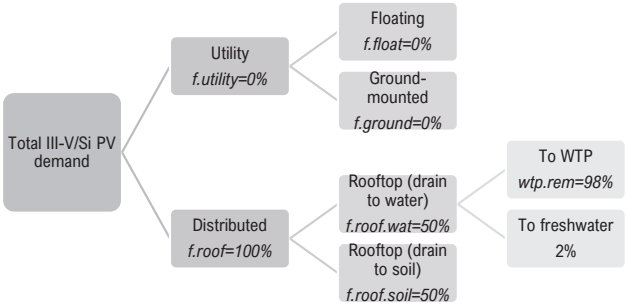

Fig A.4-2. Projected distribution of III-V/Si modules in Amsterdam based on installation type and location.

A.4.2.3. Local scale: Floating utility plant and surrounding rooftop installations

The third scenario represents a very localized situation, largely based on the current status (2020) of the Sloterplas lake area in Amsterdam. The number of rooftop panels currently installed in the encircled area (Figure A.4-3) is approximately 50,000. For this scenario, we

assume all the panels are replaced for III-V/Si panels in 2030. We also assumed all panels in this area will drain directly to soil, or towards the lake. In addition to this, 50 MW of III-V/Si panels are assumed to be installed in 2030 as a floating utility installation on the lake, taking up approximately 20% of the lake area.

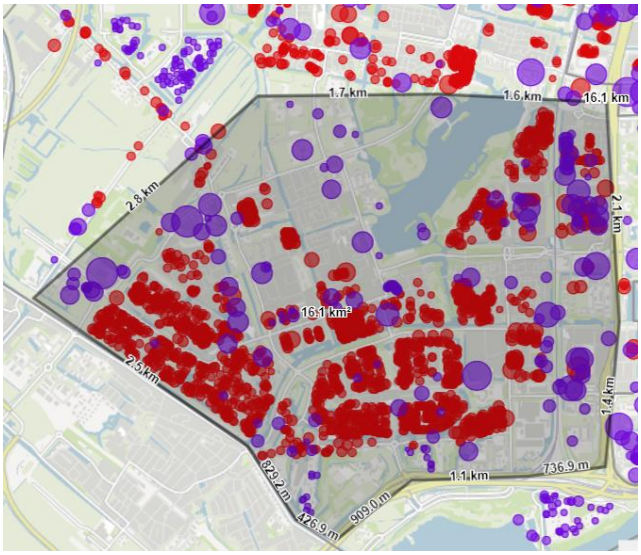

Fig A.4-3. Current PV installations around the Sloterplas lake in Amsterdam (red: on houses, purple: on non-houses or mixed).[*]

A.4.3. Stock flows

According to the current European Union regulations, 85% of solar panels by weight must be collected for recycling.[111] The base (conservative) case considers current PV recycling practices, which largely focus on the aluminum framing, glass, and plastic components of the panel while the cell is discarded (Figure A.4-4). Based on interviews we conducted with industry representatives, it is believed that if an amount of arsenic in the order of 100 ton per year would become available for recycling, then this additional recycling step would become economically feasible. This alternative is tested in a sensitivity analysis where *f.rec.reu=98%* and *f.rec.rej=2%*.

[*]https://maps.amsterdam.nl/zonnepanelen/?LANG=en.

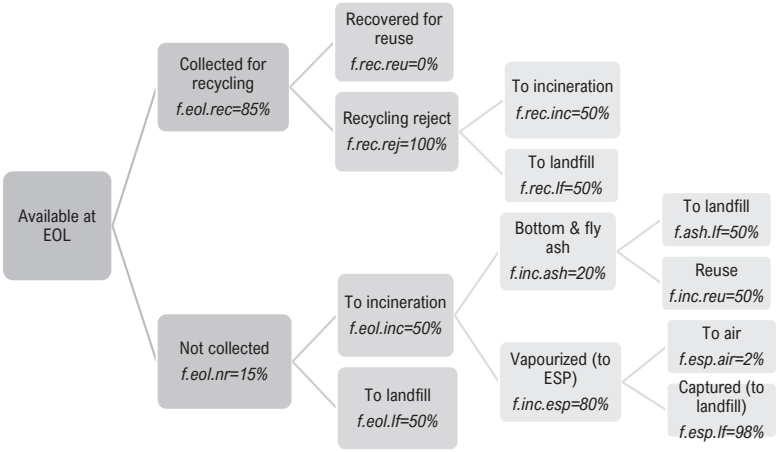

Fig A.4-4. Distribution of III-V/Si panels at EOL. Percentage values represent the base (conservative) case with no arsenic recovery during recycling.

A.4.4. Emissions

A.4.4.1. Use phase[†]

The model supposes III-V materials emissions during the use phase may occur if there is leaching from broken panels during rain events. The potentially released amounts were determined by calculating the release per second per broken panel, and multiplying this by the exposure time to rainwater, number of panels, and fraction of panels with glass breakage. The release of arsenic/gallium/indium per broken panel is dependent on the speciation in the panel which consists of two factors: dissolution at the crack surface of directly exposed material (modelled according to Celik et al.[67]) and transport of arsenic on non-exposed parts that gets dissolved by water ingress and is transported to the crack where it is then released.

The total release can be expressed as:

$$R.system = (R.crack + trans.crack) \cdot t.exp \cdot n.system \cdot f.cracked \quad \text{(Eq. A.4-4)}$$

Where:

R.system = total release of a metal from a specific speciation from the PV system in g/year

R.crack = dissolution rate of metal where the metal is directly exposed to the solvent due to the crack in g/s

trans.crack = transport of dissolved metal from the rest of the panel to the crack in g/s

[†] The "use phase" calculations presented in this section are based on the RIVM/Wageningen University and Research internship report by Matthias Hof, *"Environmental risk assessment of photovoltaic-panels applied on surface waters"* (April 15, 2021). Supervised by Joris Quik, Michiel van Kuppevelt (RIVM), Bart Koelmans (WUR).

t.exp = exposure time to solvent (rainwater) per year in s/year

n.system = number of panels in the PV system

f.cracked = fraction of panels in the system with glass panel breakage

The exposure time to solvent (rainwater) per year is calculated as:

$$t.exp = t.rain \cdot t.removal/365 \quad \text{(Eq. A.4-5)}$$

Where:

t.rain = days of rain per year

t.removal = days until removal after breakage of panel

The dissolution rate of arsenic directly exposed at the cracks of a broken panel can be calculated as:[67]

$$R.crack = A.crack \cdot \left(\frac{D}{d}\right) \cdot (Cs - Cb) \quad \text{(Eq. A.4-5)}$$

Where:

A.crack = cumulative surface area of cracks in m2

D = diffusion coefficient of metal in m2/s

d = thickness boundary layer of diffusion in m

Cs = saturated mass concentration of metal in water in g/m3

Cb = concentration of metal in bulk solvent (rainwater) in g/m3

In Equation A.4-5, the saturated mass concentration *Cs* is given by:

$$Cs = MW \cdot Ss \quad \text{(Eq. A.4-6)}$$

Where:

MW = Molecular weight of metal atom in g/mol

Ss = saturated molar concentration of metal ions in mol/l

The saturated molar concentration *Ss* is:

$$Ss = \left(\frac{x}{y}\right)^{\frac{y}{x+y}} \cdot Ksp^{\frac{1}{x+y}} \quad \text{(Eq. A.4-7)}$$

Where:

x = number of metal ions in soluble speciation

y = number of anions in soluble speciation

Ksp = solubility constant of soluble speciation

Finally, the cumulative crack surface is calculated as:

$$A.crack = n.cr \cdot (W.cr \cdot L.cr) \quad \text{(Eq. A.4-8)}$$

Where:

n.cr = number of cracks

W.cr = width of the crack in m

L.cr = length of the crack in m

In addition to direct dissolution at the crack surface, III-V materials in the rest of the panel may be exposed to the solvent through the ingress of rainwater. We assumed that ingressed water is continuously present in the panel, and the concentration of dissolved III-V materials in the ingressed water was assumed to be saturated due to the long residence time. The release of metal through the crack can thus be described by the transport from its position in the panel to the crack through diffusion.

The transport of dissolved metal to crack is calculated as:

$$trans.crack = J.crack \cdot A.cr.sides \quad \text{(Eq. A.4-9)}$$

Where:

J.crack = the flux of dissolved metal to the crack in $g/m^2/s$

A.cr.sides = the surface of the diffusion interface between the panel and the crack, which is the surface of the sides of the crack in m^2.

The flux of dissolved metal to crack is given by:

$$J.crack = D \cdot \frac{Cs-Cb}{distance.cr} \quad \text{(Eq. A.4-10)}$$

Where:

distance.cr = the average travel distance of the metal from any point in the panel to the crack

The surface of the diffusion interface can be calculated by the width and length of the crack, and the "depth" of the crack, or the thickness of the space between sheets of the panel through which the rainwater can ingress. Due to the possibility of multiple cracks on the panel, the total surface of the diffusion interface is the sum of the sides of multiple cracks. The total surface of the diffusion interface can be calculated as follows:

$$A.cr.sides = (n.cr \cdot 2(W.cr + L.cr) \cdot D.cr \quad \text{(Eq. A.4-11)}$$

Where:

D.cr = depth of crack in m.

If the panel is regarded as a two-dimensional sheet, the average travel distance of dissolved metal from any point in the panel to the crack can be described by the average distance between two random points in a rectangle of a certain size. The average distance between two random points in a rectangle is described by Mathai et al.[112]:

$$avg.dis.panel = 1/15 \cdot ((L.panel\text{^}3)/(W.panel\text{^}2) + (W.panel\text{^}3)/(L.panel\text{^}2) + d(-(L.panel\text{^}2)/(W.panel\text{^}2) - (W.panel\text{^}2)/(L.panel\text{^}2)) + 5/2((W.panel\text{^}2)/(A.panel)\ ln\ ((L.panel + LW)/(W.panel)) + (L.panel\text{^}2)/(W.panel)\ ln\ ((W.panel + LW)/(L.panel))))$$ (Eq. A.4-12)

Where:

avg.dis.panel = the average distance between two random points in a rectangle with sides L.panel and W.panel in m

L.panel = the length of the panel in m

W.panel = the width of the panel in m

$LW = (L.panel^2 + W.panel^2)^{1/2}$

L.panel > W.panel

Because of the possibility of multiple cracks forming on the panel, the actual distance from any point on the panel to the crack would be smaller than the average distance between two points. As far as we are aware, there is no formula for the average distance between multiple random points in a rectangle. To approximate this decrease in distance with multiple cracks, the average distance calculated by Eq. A.4-12 was divided by the number of cracks on the panel:

$$distance.cr = \frac{avg.dis.panel}{n.cr}$$ (Eq. A.4-13)

This underestimates the actual distance when cracks are not uniformly distributed, however this was deemed preferable over overestimating the distance as the latter leads to underestimating the release of metals and resulting ecotoxicological risk.

Finally, the amount of metal that can be released through direct dissolution at the crack with the Celik et al.[67] formula was limited to the amount of metal directly exposed to the outside environment (using an IF statement):

$$IF((R.crack \cdot t.exp) < Mu.crack; (R.crack \cdot t.exp); Mu.crack)$$ (Eq. A.4-14)

The mass of metal directly exposed at crack is equal to:

$$Mu.crack = Mu.spec \cdot f.crack$$ (Eq. A.4-15)

The amount of metal of specific speciation in panel is:

$$Mu.spec = Mu.PVarea \cdot L.panel \cdot W.panel \cdot f.spec$$ (Eq. A.4-16)

The fraction of panel surface exposed by crack is:

$$f.crack = \frac{A.crack}{A.pv.panel}$$ (Eq. A.4-17)

Where:

Mu.crack = amount of metal directly exposed to outside environment in g

Mu.spec = total weight of metal of specific speciation in panel in g

A.crack = total crack surface area in m2

Mu.PVarea = weight of metal per surface aera of PV panel in g/m2

f.spec = ratio of metal from specific speciation to total amount of that metal in the panel

Similarly, the total amount of metal that can be released from the panel trough dissolution in ingressed water and subsequent diffusion can be limited by:

$$IF((trans.crack \cdot t.exp) < Mu.ingress; (trans.crack \cdot t.exp); Mu.ingress) \quad \text{(Eq. A.4-18)}$$

The amount of metal of specific speciation in panel that is not directly exposed by crack is:

$$Mu.ingress = Mu.PVarea \cdot A.pv.panel - Mu.crack \quad \text{(Eq. A.4-19)}$$

Where:

Mu.ingress = weight of metal not directly exposed to outside environment in g.

A.4.4.2. End-of-life

A.4.4.2.1. Landfilling

A simplified landfill model based on EPA's Composite Model for Leachate Migration with Transformation Products (EPACMTP)[113,114] was used to determine how much arsenic will dissolve from the PV discarded in landfills into the landfill leachate, and how much of the leachate containing these elements will escape the landfill into the surrounding environment. For simplicity, we assumed each cohort (yearly installation) will be disposed in a new landfill cell, all of which constitute monofills (only PV waste).

Once a landfill cell has been closed, it is expected that the concentration of an element in the leachate will decrease over time as the available quantity embedded in the waste is depleted. As per the EPACMTP model, this constitutes a "depleting source scenario", where the leachate concentration at a given time (t) is a linear function of the remaining concentration in the waste Cw(t):

$$C_L(t) = K_W \cdot C_W(t) \quad \text{(Eq. A.4-20)}$$

In equation A.4-20, K_W is a waste/leachate partitioning coefficient. K_W values for arsenic were suggested by EPA[115], based largely on previously reported leachate extraction test results and modeling using the MINTEQA2 geochemical speciation model.

A mass balance can then be performed at any given time *t*, where the difference between the initial concentration in the waste and the concentration at time *t* should equal the total amount lost via leaching. Assuming all the waste is composed of the same PV waste (monofil), this mass balance can be expressed as:

$$A_W \cdot D_{LF} \cdot \rho_W \cdot \frac{dC_w}{dt} = A_W \cdot I \cdot C_L(t) \quad \text{(Eq. A.4-21)}$$

C_W can be substituted for C_L using equation A.4-20 and equation A.4-21 can be rearranged to obtain:

$$\frac{dC_L}{dt} = \frac{-I}{D_{LF} \cdot \rho_W \cdot K_W} C_L \quad \text{(Eq. A.4-22)}$$

Equation A.4-22 can be integrated to give:

$$C_L(t) = C_L^0 \cdot exp\left\{\left(\frac{-I}{D_{LF} \cdot \rho_W \cdot K_W}\right) t\right\} \quad \text{(Eq. A.4-23)}$$

In equation A.4-23, C_L^0 represents the initial concentration of the element in the leachate at the time of landfill cell closure.

A small fraction of arsenic present in the landfill waste was assumed to be volatized due to biological processes. We took a range of values of 0.02-0.1% as reported by Webster et al.[116] for microbially mediated volatilization in anaerobic environments. It is likely that or monofils with reduced microbial activity this value is on the lower range if not negligible. This process is assumed to occur within the simulation time step of 1 year, and so is immediately subtracted from the amount available for leakage.

A.4.4.2.2. Incineration

During incineration, arsenic in PV waste can be reduced to bottom ash or volatized. In the latter case, it will join the flue gas which is mostly captured by an electrostatic precipitator (ESP) while a small fraction escapes to air. Arsenic in bottom ash and captured in the ESP (fly ash) are assumed to be sent to the same PV landfill cells used described in section A.4.4.2.1.

We based our assumptions on a study by Uryu et al.[117], who modelled the distribution of arsenic in GaAs FET semiconductors in mobile phones that are burned in hazardous waste incineration plants in Japan. Of the incinerated amount, 90% of arsenic was present in the gas phase at high incineration temperatures. 0.2% of arsenic present in the gas was found to escape to air while the remaining fraction (bottom ash and fly ash) was sent to a landfill.

A.4.5. Environmental fate

The Excel spreadsheets and annotated R scripts to run the fate model as described in Section 5.2.5 of Chapter 5 are available at https://github.com/jormercury/SimpleBox. The emissions were sent to specific compartments in SimpleBox as indicated in Table A.4-1.

Table A.4-1 Receiving compartments for Use and EOL phase emissions

Emission	SKY_EUR	AMS_RES	UTI_LOC
Use phase – leaching, utility (ground)	Continental agricultural soil, s2C	Regional agricultural soil, s2R	Local soil, sL
Use phase – leaching, utility (floating)	Continental freshwater, w1C	Regional freshwater, w1R	Local water, wL
Use phase – leaching, distributed	Continental freshwater, w1C	Regional freshwater, w1R	Local water, wL
EOL phase – incineration	Continental air, aC	Regional air, aR	Local air, aL
EOL phase – landfill leaching	Continental agricultural soil, s2C	Regional natural soil, s1R	Local soil, sL
EOL phase – landfill volatilization	Continental air, aC	Regional air, aR	Local air, aL

Table A.4-2 Model input parameters and uncertainty distributions

			SKY_EUR SCENARIO		RES_AMS SCENARIO		UTI_LOC SCENARIO		
Model input parameter	**Variable name**	**Units**	**Base value**	**Distribution parameters[1]**	**Base value**	**Distribution**	**Base Value**	**Distribution**	**Refs.**
--- Installation parameters									
Panel conversion efficiency	pv.eff	%	28%	P, a=25%, b=28%, c=31%	28%	P, a=25%, b=28%, c=31%	28%	P, a=25%, b=28%, c=31%	82
Panel lifetime	LT	years	30	N, μ=30, σ=5	30	N, μ=30, σ=5	30	N, μ=30, σ=5	82
Mass of element per m^2 cell: arsenic	Mu.PVarea	g/m^2	8.81	U, min=7.93, max=9.69	8.81	U, min=7.93, max=9.69	8.81	U, min=7.93, max=9.69	[2]
Mass of element per m^2 cell: gallium	Mu.PVarea	g/m^2	15.06	U, min=13.55, max=16.57	15.06	U, min=7.93, max=9.69	15.06	U, min=7.93, max=9.69	
Mass of element per m^2 cell: indium	Mu.PVarea	g/m^2	0.02	U, min=0.018, max=0.022	0.02	U, min=7.93, max=9.69	0.02	U, min=7.93, max=9.69	
--- Demand scenarios									
Initial capacity addition	C0	MW	100	N/A	0.1	N/A	64	N/A	[3]
Carrying capacity	Cf	MW	4.3e5	N/A	110	N/A	64	N/A	105,110
Yearly growth rate	k	-	11.4%	N/A	20%	N/A	0	N/A	107
Fraction utility vs. rooftop	f.utility	-	75%	P, a=25%, b=75%, c=90%	0	P, a=0, b=0.1, c=0.2	78.1%	N/A	108
Fraction utility floating vs. ground	f.float	-	13.3%	P, a=5%, b=13.3%, c=20%	0	P, a=5%, b=13.3%, c=20%	100%	N/A	109
Fraction rooftop draining to water vs. soil	f.roof.wat	-	50%	P, a=10%, b=50%, c=90%	50%	P, a=10%, b=50%, c=90%	50%	P, a=10%, b=50%, c=90%	[4]
Collected PV waste for recycling	f.EOL.rec	-	85%	U, min=85%, max=99.9%	85%	U, min=85%, max=99.9%	85%	U, min=85%, max=99.9%	111
Fraction of arsenic recovered for reuse	f.rec.reu	-	95%	U, min=90%, max=99.9%	95%	U, min=90%, max=99.9%	95%	U, min=90%, max=99.9%	118–120

[1] P: PERT, N: Normal, L: Lognormal, U: Uniform, T: Student's T, E: Exponential.
[2] Internal calculations from the SiTaSol project (http://sitasol.com).
[3] Assumed prior, see Chapter 6.
[4] Assumed prior, see Chapter 6.

Fraction of gallium recovered for reuse	f.rec.reu	-	95%	U, min=90%, max=99.9%	95%	U, min=90%, max=99.9%	95%	U, min=90%, max=99.9%	118–120
Fraction of indium recovered for reuse	f.rec.reu	-	95%	U, min=90%, max=99.9%	95%	U, min=90%, max=99.9%	95%	U, min=90%, max=99.9%	118–120
Fraction not recycled to incinerator	f.EOL.inc	-	50%	P, a=25%, b=50%, c=75%	100%	N/A	100%	N/A	[5]
--- Use phase emissions									
Yearly fraction of panels with breakage	f.cracked	-	0.06%	U, min=0% max=0.12%	0.06%	U, min=0.03% max=0.12%	0.06%	U, min=0.03% max=0.12%	121
Number of cracks per panel	n.cr		5	U, min=1 max=10	5	U, min=1 max=10	5	U, min=1 max=10	
Average width of crack	W.cr	mm	1	U, min=0.01 max=1	1	U, min=0.01 max=1	1	U, min=0.01 max=1	67
Average length of crack	L.cr	cm	10	P, a=1, b=10, c=30	10	P, a=1, b=10, c=30	10	P, a=1, b=10, c=30	
Average hours of rain per year	t.rain	h	840	P, a=240, b=840, c=1080	840	P, a=240, b=840, c=1080	840	P, a=240, b=840, c=1080	122
Diffusion coefficient of arsenic	D	m^2/s	1.2e-9	P, a=5e-10, b=1.2e-9, c=1.9e-9	1.2E-9	P, a=5e-10, b=1.2e-9, c=1.9e-9	1.2E-9	P: a=5e-10, b=1.2e-9, c=1.9e-9	123
Diffusion coefficient of gallium	D	m^2/s	7.9e-10	P, a=6e-10, b=7.9e-10, c=1.9e-9	7.9e-10	P, a=6e-10, b=7.9e-10, c=1.9e-9	7.9e-10	P, a=6e-10, b=7.9e-10, c=1.9e-9	124
Diffusion coefficient of indium	D	m^2/s	9.8e-10	P, a=6e-10, b=9.8e-10, c=1.9e-9	9.8e-10	P, a=6e-10, b=9.8e-10, c=1.9e-9	9.8e-10	P, a=6e-10, b=9.8e-10, c=1.9e-9	124
Thickness boundary layer of diffusion	d	mm	0.01	U, min=0.01 max=0.1	0.1	U, min=0.1 max=1	0.1	U, min=0.1 max=1	67
Frac. rooftop drainage removed at WTP	f.roof.wtp	-	99%	U, min=98%, max=99.9%	99%	U, min=98%, max=99.9%	99%	U, min=98%, max=99.9%	125
--- EOL phase emissions: landfill									
Landfill cell depth	lf.d	m	2.9	E, λ=0.35	2.9	E, λ=0.35	2.9	E, λ=0.35	113
PV waste density (compacted)	waste.dens	kg/L	1.38	P, a=1, b=1.38, c=2	1.38	P, a=1, b=1.38, c=2	1.38	P, a=1, b=1.38, c=2	
Fraction of arsenic volatized in landfill	f.lf.air	-	6.5%	U, min=2% max=10%	6.5%	U, min=2% max=10%	6.5%	U, min=2% max=10%	116
Effective infiltration through landfill	lf.inf	m/yr	0.07	P, a=0, b=0.07, c=0.14	0.07	P, a=0, b=0.07, c=0.14	0.07	P, a=0, b=0.07, c=0.14	113

[5] Assumed prior, see Chapter 6.

Waste/leachate partit. coefficient: As	K_W	L/kg	205	L, μ=205, σ=4.5	205	L, μ=205, σ=4.5	205	L, μ=205, σ=4.5	[6]
Waste/leachate partit. coefficient: Ga	K_W	L/kg	1,346	L, μ=1,346, σ=6.4	1,346	L, μ=1346, σ=6.4	1,346	L, μ=1346, σ=6.4	
Waste/leachate partit. coefficient: In	K_W	L/kg	516	L, μ=2,800, σ=2.9	516	L, μ=2,800, σ=2.9	516	L, μ=2,800, σ=2.9	
--- EOL phase emissions: incineration									
Fraction of arsenic volatized incinerator	f.inc.esp	-	50%	U, min=20%, max=80%	50%	U, min=20%, max=80%	50%	U, min=20%, max=80%	126
Fraction of gallium volatized incinerator	f.inc.esp	-	0%	None	0%	None	0%	None	117
Fraction of indium volatized incinerator	f.inc.esp	-	0%	None	0%	None	0%	None	117
ESP removal of volatized arsenic	f.esp.lf	-	99%	U, min=98%, max=99.99%	99%	U, min=98%, max=99.99%	99%	U, min=98%, max=99.99%	126
Fraction of incinerator ash to reuse	f.inc.reu	-	54%	P, a=25%, b=54%, c=75%	54%	P, a=0.25, b=0.54, c=0.75	54%	P, a=0.25, b=0.54, c=0.75	127
--- Substance parameters									
Solid/water partitioning coefficient: As	Kp soil	L/kg	750	L, μ=750, σ=4.5	750	L, μ=750, σ=4.5	750	L, μ=750, σ=4.5	128
Solid/water partitioning coefficient: Ga	Kp soil	L/kg	11,000	L, μ=11,000, σ=6.4	11,000	L, μ=11,000, σ=6.4	11,000	L, μ=11,000, σ=6.4	128
Solid/water partitioning coefficient: In	Kp soil	L/kg	2,800	L, μ=2,800, σ=2.9	2,800	L, μ=2,800, σ=2.9	2,800	L, μ=2,800, σ=2.9	128
--- Environmental fate: SimpleBox landscape & other parameters									
Area of landscape covered by land	AREAland.	m^2	3.7E12	N/A	2.2E8	N/A	1.6E7	N/A	129
Area of landscape covered by sea	AREAsea.	m^2	3.7E12	N/A	0	N/A	N/A	N/A	129

[6] Waste/leachate partitioning coefficients were calculated from the regression equation derived by Allison & Allison[115]: *log Kw = 0.7 log Kpsoil + 0.3*. The relation has a low correlation coefficient (R2 = 0.4) and the obtained values "must be regarded as highly uncertain". To preserve correlations between Kw and Kpsoil, the Kpsoil (solid/water partitioning coefficient) values used in this formula in every model iteration were the same as those used in the SimpleBox fate model (see "Substance parameters" section in this Table).

Fraction of area freshwater	FRACfresh.	-	0.03	N/A	0.24	N/A	0.08	N/A	129
Fraction of area natural soil	FRACnatsoil.	-	0.27	N/A	0	N/A	0	N/A	129
Fraction of area agricultural soil	FRACagsoil.	-	0.60	N/A	0.18	N/A	0	N/A	129
Fraction of area other soil	FRACothersoil.	-	0.70	N/A	0.58	N/A	0	N/A	129
Fraction of soil (local scale)	FRACsoil	-		N/A		N/A	0,92	N/A	129
Temperature	TEMP	°C	12	T, mix=-10, mode=12, max=35	12	T, mix=-10, mode=12, max=35	12	T, mix=-10, mode=12, max=35	130
Average wind speed	WINDspeed.	m/s	4.65	PERT, a=0, b=5.1, c=18	4.65	PERT, a=0, b=5.1, c=18	4.65	PERT, a=0, b=5.1, c=18	130
Mixed height air compartment	HEIGHT.a	m	605	T, min=77, mode=400, max=1338	605	T, min=77, mode=400, max=1338	605	T, min=77, mode=400, max=1338	130
Average rainfall	RAINrate.	mm/yr	925	PERT, a=350, b=700, c=2400	925	PERT, a=350, b=700, c=2400	925	PERT, a=350, b=700, c=2400	130
Average depth freshwater compartments	DEPTHfreshwater	m	4.7	PERT, a=1, b=3, c=15	2.6	PERT, a=1, b=3, c=5	4.7	PERT, a=1, b=3, c=15	130
Mixed depth of freshwater sediment	DEPTH.sd1	cm	4,7	T, min=1, mode=3, max=10	4,7	T, min=1, mode=3, max=10	4,7	T, min=1, mode=3, max=10	130
Mixed depth of marine sediment	DEPTH.sd2	cm	4,7	T, min=1, mode=3, max=10	N/A	N/A	N/A	N/A	130
Volume fraction water in soil	FRACw.s	-	0.29	T, min=0.003, mode=0.2, max=0.67		T, min=0.003, mode=0.2, max=0.67		T, min=0.003, mode=0.2, max=0.67	130
Volume fraction water in sediment	FRACw.sd	-	0.77	T, min=0.5, mode=0.8, max=0.999		T, min=0.5, mode=0.8, max=0.999		T, min=0.5, mode=0.8, max=0.999	130
Mass fraction organic carbon in suspended matter freshwater	CORG.susp1	-	0.1	L, μ=0.1, σ=0.04	0.1	L, μ=0.1, σ=0.04	0.1	L, μ=0.1, σ=0.04	130
Concentration suspended matter in freshwater	SUSP.w1	mg/L	24.4	L, μ=24.4, σ=23.5	24.4	L, μ=24.4, σ=23.5	24.4	L, μ=24.4, σ=23.5	130

Mass fraction organic carbon in suspended matter seawater	CORG.susp2	-	0.1	L, μ=0.1, σ=0.04	N/A	N/A	N/A	N/A	130
Concentration suspended matter in seawater	SUSP.w2	mg/L	24.4	L, μ=24.4, σ=23.5	N/A	N/A	N/A	N/A	130
Mass fraction organic carbon in freshwater sediment	CORG.sd1	-	0.05	L, μ=0.05, σ=0.04	0.05	L, μ=0.05, σ=0.04	0.05	L, μ=0.05, σ=0.04	130
Mass fraction organic carbon in sediment seawater	CORG.sd2	-	0.05	L, μ=0.05, σ=0.04	N/A	N/A	N/A	N/A	130
Mass fraction organic carbon in soil	CORG.s	-	0.05	L, μ=0.05, σ=0.04	0.05	L, μ=0.05, σ=0.04	0.05	L, μ=0.05, σ=0.04	130
Deposition velocity aerosol particles	AEROSOL deprate	m/s	1.0E-3	L, μ=1.0E-3, σ=1.0E-3	1.0E-3	L, μ=1E-3, σ=1.0E-3	1.0E-3	L, μ=1.0E-3, σ=1.0E-3	130
Aerosol collection efficiency	COLLECT eff	-	2.0E4	T, min=5.0E3, mode=2.0E4, max=3.5E4	2.0E4	T, min=5.0E3, mode=2.0E4, max=3.5E4	2.0E4	T, min=5.0E3, mode=2.0E4, max=3.5E4	130
Settling velocity suspended particles	SETTLvelocity	m/s	2.1E-5	T, mix=3.0E-6, mode=2.9E-5, max=3.0E-5	2.1E-5	T, mix=3.0E-6, mode=2.9E-5, max=3.0E-5	2.1E-5	T, mix=3.0E-6, mode=2.9E-5, max=3.0E-5	130
Autochtonous production of suspended matter in freshwater	PRODsusp.w1	$g/m^2/yr$	12	T, min=5, mode=10, max=20	12	T, min=5, mode=10, max=20	12	T, min=5, mode=10, max=20	130
Autochtonous production of suspended matter in seawater	PRODsusp.w2	$g/m^2/yr$	1.2	T, min=0.5, mode=1.0, max=2.0	N/A	N/A	N/A	N/A	130
Partial mass transfer coefficient water side of water/sediment interface	Kwsd.water.w	m/s	4.0E-6	T, min=2.78E-6/3, mode=2.78E-6, max=2.78E-6*3	4.0E-6	T, min=2.78E-6/3, mode=2.78E-6, max=2.78E-6*3	4.0E-6	T, min=2.78E-6/3, mode=2.78E-6, max=2.78E-6*3	130
Partial mass transfer coefficient sediment side of water/sediment interface	Kwsd.sed.sd	m/s	4.0E-8	T, min=2.78E-8/3, mode=2.78E-8, max=2.78E-8*3	4.0E-8	T, min=2.78E-8/3, mode=2.78E-8, max=2.78E-8*3	4.0E-8	T, min=2.78E-8/3, mode=2.78E-8, max=2.78E-8*3	130
Erosion of soil	EROSION.s	mm/yr	0.03	T, min=0, mode=0.03, max=0.06	0.03	T, min=0, mode=0.03, max=0.06	0.03	T, min=0, mode=0.03, max=0.06	130

Volume fraction of precipitation on soil running off to surface water	FRACrun.s	-	0.25	T, min=0, mode=0.25, max=0.50	0.25	T, min=0, mode=0.25, max=0.50	0.25	T, min=0, mode=0.25, max=0.50	130
Volume fraction of precipitation infiltrating into soil	FRACinf.s	-	0.25	T, min=0, mode=0.25, max=0.50	0.25	T, min=0, mode=0.25, max=0.50	0.25	T, min=0, mode=0.25, max=0.50	130
Mineral density sediment and soil	RHOsolid	Kg/m^3	2.5E3	T, min=2.0E3, mode=2.5E3, max=3.0E3	2.5E3	T, min=2.0E3, mode=2.5E3, max=3.0E3	2.5E3	T, min=2.0E3, mode=2.5E3, max=3.0E3	130

References

1. García-Valverde, R., Cherni, J. A. & Urbina, A. Life cycle analysis of organic photovoltaic technologies. *Prog. Photovoltaics Res. Appl.* **18**, 535–558 (2010).
2. Ito, M., Komoto, K. & Kurokawa, K. Life-cycle analyses of very-large scale PV systems using six types of PV modules. *Curr. Appl. Phys.* **10**, S271–S273 (2010).
3. Reijnders, L. Design issues for improved environmental performance of dye-sensitized and organic nanoparticulate solar cells. *J. Clean. Prod.* **18**, 307–312 (2010).
4. Bravi, M., Parisi, M. L., Tiezzi, E. & Basosi, R. Life cycle assessment of a micromorph photovoltaic system. *Energy* **36**, 4297–4306 (2011).
5. Espinosa, N., García-Valverde, R. & Krebs, F. C. Life-cycle analysis of product integrated polymer solar cells. *Energy Environ. Sci.* **4**, 1547 (2011).
6. Fthenakis, V. M. & Kim, H. C. Photovoltaics: Life-cycle analyses. *Sol. Energy* **85**, 1609–1628 (2011).
7. Held, M. & Ilg, R. Update of environmental indicators and energy payback time of CdTe PV systems in Europe. *Prog. Photovoltaics Res. Appl.* **19**, 614–626 (2011).
8. Kim, H. C. & Fthenakis, V. M. Comparative life-cycle energy payback analysis of multi-junction a-SiGe and nanocrystalline/a-Si modules. *Prog. Photovoltaics Res. Appl.* **19**, 228–239 (2011).
9. Espinosa, N., García-Valverde, R. & Urbina, A. A life cycle analysis of polymer solar cell modules prepared using roll-to-roll methods under ambient conditions. *Sol. Energy Mater. Sol. Cells* **95**, 1293–1302 (2011).
10. Şengül, H. & Theis, T. L. An environmental impact assessment of quantum dot photovoltaics (QDPV) from raw material acquisition through use. *J. Clean. Prod.* **19**, 21–31 (2011).
11. van der Meulen, R. & Alsema, E. Life-cycle greenhouse gas effects of introducing nano-crystalline materials in thin-film silicon solar cells. *Prog. Photovoltaics Res. Appl.* **19**, 453–463 (2011).
12. Emmott, C. J. M., Urbina, A. & Nelson, J. Environmental and economic assessment of ITO-free electrodes for organic solar cells. *Sol. Energy Mater. Sol. Cells* **97**, 14–21 (2012).
13. Espinosa, N., Hösel, M., Angmo, D. & Krebs, F. C. Solar cells with one-day energy payback for the factories of the future. *Energy Environ. Sci.* **5**, 5117–5132 (2012).
14. Fthenakis, V. Sustainability metrics for extending thin-film photovoltaics to terawatt levels. *MRS Bull.* **37**, 425–430 (2012).
15. Kim, H. C., Fthenakis, V., Choi, J.-K. & Turney, D. E. Life Cycle Greenhouse Gas Emissions of Thin-film Photovoltaic Electricity Generation. *J. Ind. Ecol.* **16**, S110–S121 (2012).

16. Espinosa, N. *et al.* Life cycle assessment of ITO-free flexible polymer solar cells prepared by roll-to-roll coating and printing. *Sol. Energy Mater. Sol. Cells* **97**, 3–13 (2012).

17. Raugei, M., Isasa, M. & Fullana Palmer, P. Potential Cd emissions from end-of-life CdTe PV. *Int. J. Life Cycle Assess.* **17**, 192–198 (2012).

18. Yue, D., Khatav, P., You, F. & Darling, S. B. Deciphering the uncertainties in life cycle energy and environmental analysis of organic photovoltaics. *Energy Environ. Sci.* **5**, 9163 (2012).

19. Zuser, A. & Rechberger, H. Considerations of resource availability in technology development strategies: The case study of photovoltaics. *Resour. Conserv. Recycl.* **56**, 56–65 (2011).

20. Eisenberg, D. A., Yu, M., Lam, C. W., Ogunseitan, O. A. & Schoenung, J. M. Comparative alternative materials assessment to screen toxicity hazards in the life cycle of CIGS thin film photovoltaics. *J. Hazard. Mater.* **260**, 534–542 (2013).

21. Espinosa, N. *et al.* OPV for mobile applications: an evaluation of roll-to-roll processed indium and silver free polymer solar cells through analysis of life cycle, cost and layer quality using inline optical and functional inspection tools. *J. Mater. Chem. A* **1**, 7037 (2013).

22. Fthenakis, V. & Anctil, A. Direct Te mining: Resource availability and impact on cumulative energy demand of CdTe PV life cycles. in *2012 IEEE 38th Photovoltaic Specialists Conference (PVSC) PART 2* 1–6 (IEEE, 2012). doi:10.1109/PVSC-Vol2.2012.6656725.

23. Kim, H. C. & Fthenakis, V. Life Cycle Energy and Climate Change Implications of Nanotechnologies. *J. Ind. Ecol.* **17**, 528–541 (2013).

24. Mohr, N. J., Meijer, A., Huijbregts, M. A. J. & Reijnders, L. Environmental life cycle assessment of roof-integrated flexible amorphous silicon/nanocrystalline silicon solar cell laminate. *Progress in Photovoltaics: Research and Applications* (2013) doi:10.1002/pip.2157.

25. Parisi, M., Maranghi, S., Sinicropi, A. & Basosi, R. Development Of Dye Sensitized Solar Cells: A Life Cycle Perspective For The Environmental And Market Potential Assessment Of A Renewable Energy Technology. *Int. J. Heat Technol.* **31**, 143–148 (2013).

26. Collier, J., Wu, S. & Apul, D. Life cycle environmental impacts from CZTS (copper zinc tin sulfide) and Zn3P2 (zinc phosphide) thin film PV (photovoltaic) cells. *Energy* **74**, 314–321 (2014).

27. Espinosa, N. & Krebs, F. C. Life cycle analysis of organic tandem solar cells: When are they warranted? *Sol. Energy Mater. Sol. Cells* **120**, 692–700 (2014).

28. Espinosa, N., Hösel, M., Jørgensen, M. & Krebs, F. C. Large scale deployment of polymer solar cells on land, on sea and in the air. *Energy Environ. Sci.* **7**, 855 (2014).

29. Kim, H., Cha, K., Fthenakis, V. M., Sinha, P. & Hur, T. Life cycle assessment of cadmium telluride photovoltaic (CdTe PV) systems. *Sol. Energy* **103**, 78–88 (2014).

30. Mann, S. A., de Wild-Scholten, M. J., Fthenakis, V. M., van Sark, W. G. J. H. M. & Sinke, W. C. The energy payback time of advanced crystalline silicon PV modules in 2020: a prospective study. *Prog. Photovoltaics Res. Appl.* **22**, 1180–1194 (2014).

31. Parisi, M. L., Maranghi, S. & Basosi, R. The evolution of the dye sensitized solar cells from Grätzel prototype to up-scaled solar applications: A life cycle assessment approach. *Renew. Sustain. Energy Rev.* **39**, 124–138 (2014).

32. Wender, B. A. *et al.* Illustrating anticipatory life cycle assessment for emerging photovoltaic technologies. *Environ. Sci. Technol.* **48**, 10531–10538 (2014).

33. Espinosa, N., Laurent, A. & Krebs, F. C. Ecodesign of organic photovoltaic modules from Danish and Chinese perspectives. *Energy Environ. Sci.* **8**, 2537–2550 (2015).

34. Fabini, D. Quantifying the Potential for Lead Pollution from Halide Perovskite Photovoltaics. *J. Phys. Chem. Lett.* **6**, 3546–3548 (2015).

35. Gong, J., Darling, S. B. & You, F. Perovskite photovoltaics: life-cycle assessment of energy and environmental impacts. *Energy Environ. Sci.* **8**, 1953–1968 (2015).

36. Louwen, A., van Sark, W. G. J. H. M., Schropp, R. E. I., Turkenburg, W. C. & Faaij, A. P. C. Life-cycle greenhouse gas emissions and energy payback time of current and prospective silicon heterojunction solar cell designs. *Prog. Photovoltaics Res. Appl.* **23**, 1406–1428 (2015).

37. Espinosa, N., Serrano-Luján, L., Urbina, A. & Krebs, F. C. Solution and vapour deposited lead perovskite solar cells: Ecotoxicity from a life cycle assessment perspective. *Sol. Energy Mater. Sol. Cells* **137**, 303–310 (2015).

38. Prado-Lopez, V. *et al.* Tradeoff Evaluation Improves Comparative Life Cycle Assessment: A Photovoltaic Case Study. *J. Ind. Ecol.* **20**, 710–718 (2016).

39. Scott, R. P. & Cullen, A. C. Reducing the life cycle environmental impacts of kesterite solar photovoltaics: comparing carbon and molybdenum back contact options. *Int. J. Life Cycle Assess.* **21**, 29–43 (2016).

40. Serrano-Lujan, L. *et al.* Tin- and Lead-Based Perovskite Solar Cells under Scrutiny: An Environmental Perspective. *Adv. Energy Mater.* **5**, 1501119 (2015).

41. Wetzel, T. & Borchers, S. Update of energy payback time and greenhouse gas emission data for crystalline silicon photovoltaic modules. *Prog. Photovoltaics Res. Appl.* **23**, 1429–1435 (2015).

42. Zhang, J., Gao, X., Deng, Y., Li, B. & Yuan, C. Life Cycle Assessment of Titania Perovskite Solar Cell Technology for Sustainable Design and Manufacturing. *ChemSusChem* **8**, 3882–3891 (2015).

43. Babayigit, A., Ethirajan, A., Muller, M. & Conings, B. Toxicity of organometal halide perovskite solar cells. *Nat. Mater.* **15**, 247 (2016).

44. Bergesen, J. D. & Suh, S. A framework for technological learning in the supply chain: A case study on CdTe photovoltaics. *Appl. Energy* **169**, 721–728 (2016).

45. Celik, I. *et al.* Life Cycle Assessment (LCA) of perovskite PV cells projected from lab to fab. *Solar Energy Materials and Solar Cells* vol. 156 157–169 (2015).

46. Chatzisideris, M. D. & Laurent, A. Ecodesign perspectives of thin-film photovoltaic technologies: A review of life cycle assessment studies. *Sol. Energy Mater. Sol. Cells* **156**, 2–10 (2016).

47. Hengevoss, D., Baumgartner, C., Nisato, G. & Hugi, C. Life Cycle Assessment and eco-efficiency of prospective, flexible, tandem organic photovoltaic module. *Sol. Energy* **137**, 317–327 (2016).

48. Kim, J., Rivera, J. L., Meng, T. Y., Laratte, B. & Chen, S. Review of life cycle assessment of nanomaterials in photovoltaics. *Sol. Energy* **133**, 249–258 (2016).

49. Leccisi, E., Raugei, M. & Fthenakis, V. The Energy and Environmental Performance of Ground-Mounted Photovoltaic Systems—A Timely Update. *Energies* **9**, 622 (2016).

50. Scott, R. P., Cullen, A. C., Fox-Lent, C. & Linkov, I. Can Carbon Nanomaterials Improve CZTS Photovoltaic Devices? Evaluation of Performance and Impacts Using Integrated Life-Cycle Assessment and Decision Analysis. *Risk Anal.* **36**, 1916–1935 (2016).

51. Tsang, M. P., Sonnemann, G. W. & Bassani, D. M. A comparative human health, ecotoxicity, and product environmental assessment on the production of organic and silicon solar cells. *Prog. Photovoltaics Res. Appl.* **24**, 645–655 (2016).

52. Tsang, M. P., Sonnemann, G. W. & Bassani, D. M. Life-cycle assessment of cradle-to-grave opportunities and environmental impacts of organic photovoltaic solar panels compared to conventional technologies. *Sol. Energy Mater. Sol. Cells* **156**, 37–48 (2016).

53. Celik, I. *et al.* Environmental analysis of perovskites and other relevant solar cell technologies in a tandem configuration. *Energy Environ. Sci.* **10**, 1874–1884 (2017).

54. Celik, I., Mason, B. E., Phillips, A. B., Heben, M. J. & Apul, D. Environmental Impacts from Photovoltaic Solar Cells Made with Single Walled Carbon Nanotubes. *Environ. Sci. Technol.* **51**, 4722–4732 (2017).

55. A. dos Reis Benatto, G., Espinosa, N. & Krebs, F. C. Life-Cycle Assessment of Solar Charger with Integrated Organic Photovoltaics. *Adv. Eng. Mater.* **19**, 1700124 (2017).

56. Hauck, M., Ligthart, T., Schaap, M., Boukris, E. & Brouwer, D. Environmental benefits of reduced electricity use exceed impacts from lead use for perovskite based tandem solar cell. *Renew. Energy* **111**, 906–913 (2017).

57. Itten, R. & Stucki, M. Highly efficient 3rd generation multi-junction solar cells using silicon heterojunction and perovskite tandem: Prospective life cycle environmental impacts. *Energies* **10**, 841 (2017).

58. Khaenson, W., Maneewan, S. & Punlek, C. A comparison of the environmental impact of solar power generation using multicrystalline silicon and thin film of amorphous silicon solar cells: case study in Thailand. *J. Ecol. Eng.* **18**, 1–14 (2017).

59. Monteiro Lunardi, M., Wing Yi Ho-Baillie, A., Alvarez-Gaitan, J. P., Moore, S. & Corkish, R. A life cycle assessment of perovskite/silicon tandem solar cells. *Prog. Photovoltaics Res. Appl.* **25**, 679–695 (2017).

60. Vellini, M., Gambini, M. & Prattella, V. Environmental impacts of PV technology throughout the life cycle: Importance of the end-of-life management for Si-panels and CdTe-panels. *Energy* **138**, 1099–1111 (2017).

61. Zhang, J., Gao, X., Deng, Y., Zha, Y. & Yuan, C. Comparison of life cycle environmental impacts of different perovskite solar cell systems. *Sol. Energy Mater. Sol. Cells* **166**, 9–17 (2017).

62. Alberola-Borràs, J.-A. *et al.* Perovskite Photovoltaic Modules: Life Cycle Assessment of Pre-industrial Production Process. *iScience* **9**, 542–551 (2018).

63. Alberola-Borràs, J.-A. *et al.* Relative impacts of methylammonium lead triiodide perovskite solar cells based on life cycle assessment. *Sol. Energy Mater. Sol. Cells* **179**, 169–177 (2018).

64. Alberola-Borràs, J.-A., Vidal, R. & Mora-Seró, I. Evaluation of multiple cation/anion perovskite solar cells through life cycle assessment. *Sustain. Energy Fuels* **2**, 1600–1609 (2018).

65. Amarakoon, S. *et al.* Life cycle assessment of photovoltaic manufacturing consortium (PVMC) copper indium gallium (di)selenide (CIGS) modules. *Int. J. Life Cycle Assess.* **23**, 851–866 (2018).

66. Celik, I. *et al.* Energy Payback Time (EPBT) and Energy Return on Energy Invested (EROI) of Perovskite Tandem Photovoltaic Solar Cells. *IEEE J. Photovoltaics* **8**, 305–309 (2018).

67. Celik, I., Song, Z., Phillips, A. B., Heben, M. J. & Apul, D. Life cycle analysis of metals in emerging photovoltaic (PV) technologies: A modeling approach to estimate use phase leaching. *J. Clean. Prod.* **186**, 632–639 (2018).

68. Monteiro Lunardi, M. *et al.* A comparative life cycle assessment of chalcogenide/Si tandem solar modules. *Energy* (2018) doi:10.1016/J.ENERGY.2017.12.130.

69. M. Lunardi, M., Alvarez-Gaitan, J. P., Chang, N. L. & Corkish, R. Life cycle assessment on PERC solar modules. *Sol. Energy Mater. Sol. Cells* **187**, 154–159 (2018).

70. Mokhtarimehr, M., Forbes, I. & Pearsall, N. Environmental assessment of vacuum and non-vacuum techniques for the fabrication of Cu_2ZnSnS_4 thin film photovoltaic cells. *Jpn. J. Appl. Phys.* **57**, 08RC14 (2018).

71. Moore, E. A., Babbitt, C. W., Gaustad, G. & Moore, S. T. Portfolio Optimization of Nanomaterial Use in Clean Energy Technologies. *Environ. Sci. Technol.* **52**, 4440–4448 (2018).

72. Munshi, A. H. *et al.* Thin-film CdTe photovoltaics – The technology for utility scale sustainable energy generation. *Sol. Energy* **173**, 511–516 (2018).

73. Pallas, G., Peijnenburg, W., Guinée, J., Heijungs, R. & Vijver, M. Green and Clean: Reviewing the Justification of Claims for Nanomaterials from a Sustainability Point of View. *Sustainability* **10**, 689 (2018).

74. Ravikumar, D., Seager, T. P., Cucurachi, S., Prado, V. & Mutel, C. Novel Method of Sensitivity Analysis Improves the Prioritization of Research in Anticipatory Life Cycle Assessment of Emerging Technologies. *Environ. Sci. Technol.* acs.est.7b04517 (2018) doi:10.1021/acs.est.7b04517.

75. Bani Salim, M., Emre Demirocak, D. & Barakat, N. A Fuzzy Based Model for Standardized Sustainability Assessment of Photovoltaic Cells. *Sustainability* **10**, 4787 (2018).

76. Sinha, P. & Wade, A. Addressing Hotspots in the Product Environmental Footprint of CdTe Photovoltaics. *IEEE J. Photovoltaics* 1–5 (2018) doi:10.1109/JPHOTOV.2018.2802786.

77. Soares, W. M., Athayde, D. D. & Nunes, E. H. M. LCA study of photovoltaic systems based on different technologies. *Int. J. Green Energy* **15**, 577–583 (2018).

78. Stamford, L. & Azapagic, A. Environmental Impacts of Photovoltaics: The Effects of Technological Improvements and Transfer of Manufacturing from Europe to China. *Energy Technol.* **6**, 1148–1160 (2018).

79. Zhou, Z. & Carbajales-Dale, M. Assessing the photovoltaic technology landscape: efficiency and energy return on investment (EROI). *Energy Environ. Sci.* **11**, 603–608 (2018).

80. Billen, P. *et al.* Comparative evaluation of lead emissions and toxicity potential in the life cycle of lead halide perovskite photovoltaics. *Energy* **166**, 1089–1096 (2019).

81. Pallas, G., Vijver, M. G., Peijnenburg, W. J. G. M. & Guinée, J. Life cycle assessment of emerging technologies at the lab scale: The case of nanowire-based solar cells. *J. Ind. Ecol.* jiec.12855 (2019) doi:10.1111/jiec.12855.

82. Blanco, C. F. *et al.* Environmental impacts of III–V/silicon photovoltaics: life cycle assessment and guidance for sustainable manufacturing. *Energy Environ. Sci.* **13**, 4280–4290 (2020).

83. Louwen, A., Van Sark, W. G. J. H. M., Schropp, R. E. I., Turkenburg, W. C. & Faaij, A. P. C. Life-cycle greenhouse gas emissions and energy payback time of current and prospective silicon heterojunction solar cell designs. *Progress in Photovoltaics: Research and Applications* vol. 23 1406–1428 (2015).

84. Paschotta, R. Wall-plug efficiency. *RP Photonics Encyclopedia* (2019).

85. Wood, D. *et al.* Passivated Busbars from Screen-printed Low-temperature Copper Paste. *Energy Procedia* **55**, 724–732 (2014).

86. Wernet, G. *et al.* The ecoinvent database version 3 (part I): overview and methodology. *Int. J. Life Cycle Assess.* **21**, 1218–1230 (2016).

87. Spath, P. L. & Mann, M. K. *Life cycle assessment of hydrogen production via natural gas steam reforming. National Renewable Energy Laboratory* (2001).

88. Mehmeti, A., Angelis-Dimakis, A., Arampatzis, G., McPhail, S. & Ulgiati, S. Life Cycle Assessment and Water Footprint of Hydrogen Production Methods: From Conventional to Emerging Technologies. *Environments* **5**, 24 (2018).

89. Cetinkaya, E., Dincer, I. & Naterer, G. F. Life cycle assessment of various hydrogen production methods. *Int. J. Hydrogen Energy* **37**, 2071–2080 (2012).

90. Balaji, R. *et al.* Development and performance evaluation of Proton Exchange Membrane (PEM) based hydrogen generator for portable applications. *Int. J. Hydrogen Energy* **36**, 1399–1403 (2011).

91. Smith, B. L., Babbitt, C. W., Horowitz, K., Gaustad, G. & Hubbard, S. M. Life Cycle Assessment of III-V Precursors for Photovoltaic and Semiconductor Applications. *MRS Adv.* **3**, 1399–1404 (2018).

92. Guerin, J. An increased portfolio for waste gas abatement. *Compound Semiconductors* 18–22 (2016).

93. Hsu, J.-N., Tsai, C.-J., Chiang, C. & Li, S.-N. Silane Removal at Ambient Temperature by Using Alumina-Supported Metal Oxide Adsorbents. *J. Air Waste Manage. Assoc.* **57**, 204–210 (2007).

94. Pacaud, B., Popa, J.-M. & Cartier, C.-B. Purification of silane gas. (1990).

95. CS Clean Systems. Safety Data Sheet - Cleansorb CS3C. (2014).

96. Wang, X. *et al.* Arsine adsorption in copper-exchanged zeolite under low temperature and micro-oxygen conditions. *RSC Adv.* **7**, 56638–56647 (2017).

97. Li, W.-C. *et al.* Metal Loaded Zeolite Adsorbents for Phosphine Removal. *Ind. Eng. Chem. Res.* **47**, 1501–1505 (2008).

98. Heitmann, U. *et al.* Novel Approach for the Bonding of III-V on Silicon Tandem Solar Cells with a Transparent Conductive Adhesive. in *2018 IEEE 7th World Conference on Photovoltaic Energy Conversion, WCPEC 2018 - A Joint Conference of 45th IEEE PVSC, 28th PVSEC and 34th EU PVSEC* 201–205 (IEEE, 2018). doi:10.1109/PVSC.2018.8548276.

99. Chaudhuri, M. K. *et al.* Process for making metal acetylacetonates. (2002).

100. Matovu, J. B., Ong, P., Leunissen, L. H. A., Krishnan, S. & Babu, S. V. Fundamental Investigation of Chemical Mechanical Polishing of GaAs in Silica Dispersions: Material Removal and Arsenic Trihydride Formation Pathways. *ECS J. Solid State Sci. Technol.* **2**, P432–P439 (2013).

101. Heijungs, R. & Suh, S. *The Computational Structure of Life Cycle Assessment*. vol. 11 (Springer Netherlands, 2002).

102. Borgonovo, E. A new uncertainty importance measure. *Reliab. Eng. Syst. Saf.* **92**, 771–784 (2007).

103. Borgonovo, E. & Iooss, B. Moment-Independent and Reliability-Based Importance Measures. in *Handbook of Uncertainty Quantification* (eds. Ghanem, R., Higdon, D. & Owhadi, H.) 1265–1287 (Springer International Publishing, 2017). doi:10.1007/978-3-319-11259-6_37-1.

104. Henriksson, P. J. G. *et al.* Product carbon footprints and their uncertainties in comparative decision contexts. *PLoS One* **10**, 1–11 (2015).

105. Shell International B.V. Sky Scenario. *Shell Scenarios SKY Meeting the Goals of the Paris Agreement* https://www.shell.com/energy-and-innovation/the-energy-future/scenarios/shell-scenario-sky.html (2018).

106. Global Solar Atlas. https://globalsolaratlas.info/map?c=50.958427,15.512695,4&s=47.338823,5.976563&m=site.

107. Jaxa-Rozen, M. & Trutnevyte, E. Sources of uncertainty in long-term global scenarios of solar photovoltaic technology. *Nat. Clim. Chang.* **11**, 266–273 (2021).

108. IEA. *The Role of Critical Minerals in Clean Energy Transitions*. (2021).

109. Cazzaniga, R. & Rosa-Clot, M. The booming of floating PV. *Sol. Energy* **219**, 3–10 (2021).

110. City of Amsterdam. Policy: Renewable energy. *Policy: Sustainability and energy* https://www.amsterdam.nl/en/policy/sustainability/renewable-energy/.

111. European Parliament; Council of the European Union. *Directive 2012/19/EU of the European Parliament and of the Council of 4 July 2012 on waste electrical and electronic equipment (WEEE)*. (2012). doi:10.3000/19770677.L_2012.197.eng.

112. Mathai, A. M., Moschopoulos, P. & Pederzoli, G. Random points associated with rectangles. *Rend. del Circ. Mat. di Palermo* **48**, 163–190 (1999).

113. U.S. Environmental Protection Agency Office of Solid Waste. *EPA's Composite Model for Leachate Migration with Transformation Products (EPACMTP) Parameters/Data Background Document*. https://www.epa.gov/smm/epas-composite-model-leachate-migration-transformation-products-epacmtp#:~:text=Related Topics%3A-,EPA's Composite Model for Leachate Migration with Transformation Products (EPACMTP,constituents to the subsurface environment. (2003).

114. U.S. Environmental Protection Agency Office of Solid Waste. *EPA's Composite Model for Leachate Migration with Transformation Products (EPACMTP) Technical Background Document*. (2003).

115. Allison, J. D. & Allison, T. L. *Partitioning Coefficients for Metals in Surface Water, Soil and Waste*. https://cfpub.epa.gov/si/si_public_record_report.cfm?Lab=NERL&dirEntryId=135783 (2005).

116. Webster, T. M. *et al.* Anaerobic Disposal of Arsenic-Bearing Wastes Results in Low Microbially Mediated Arsenic Volatilization. *Environ. Sci. Technol.* **50**, 10951–10959 (2016).

117. Uryu, T., Yoshinaga, J. & Yanagisawa, Y. Environmental Fate of Gallium Arsenide Semiconductor Disposal. *J. Ind. Ecol.* **7**, 103–112 (2003).

118. Zhan, L., Wang, Z., Zhang, Y. & Xu, Z. Recycling of metals (Ga, In, As and Ag) from waste light-emitting diodes in sub/supercritical ethanol. *Resour. Conserv. Recycl.* **155**, (2020).

119. Van Den Bossche, A., Vereycken, W., Vander Hoogerstraete, T., Dehaen, W. & Binnemans, K. Recovery of Gallium, Indium, and Arsenic from Semiconductors Using Tribromide Ionic Liquids. *ACS Sustain. Chem. Eng.* **7**, 14451–14459 (2019).

120. Zhan, L., Xia, F., Xia, Y. & Xie, B. Recycle Gallium and Arsenic from GaAs-Based E-Wastes via Pyrolysis-Vacuum Metallurgy Separation: Theory and Feasibility. *ACS Sustain. Chem. Eng.* **6**, 1336–1342 (2018).

121. Köntges, M. *et al. Review of Failures of Photovoltaic Modules*. https://iea-pvps.org/wp-content/uploads/2020/01/IEA-PVPS_T13-01_2014_Review_of_Failures_of_Photovoltaic_Modules_Final.pdf (2014).

122. Hosseinzadehtalaei, P., Tabari, H. & Willems, P. Climate change impact on short-duration extreme precipitation and intensity–duration–frequency curves over Europe. *J. Hydrol.* **590**, 125249 (2020).

123. Tanaka, M. *et al.* The difference of diffusion coefficients in water for arsenic compounds at various pH and its dominant factors implied by molecular simulations. *Geochim. Cosmochim. Acta* **105**, 360–371 (2013).

124. Vanýsek, P. Ionic conductivity and diffusion at infinite dilution. in *Handbook of Chemistry and Physics* (5-111)-(5-113) (CRC Press, 1992).

125. Sun, L., Lu, M., Li, Q., Jiang, H. & Yin, S. Research progress of arsenic removal from wastewater. *IOP Conf. Ser. Earth Environ. Sci.* **218**, 012142 (2019).

126. Jung, C. ., Matsuto, T., Tanaka, N. & Okada, T. Metal distribution in incineration residues of municipal solid waste (MSW) in Japan. *Waste Manag.* **24**, 381–391 (2004).

127. Blasenbauer, D. *et al.* Legal situation and current practice of waste incineration bottom ash utilisation in Europe. *Waste Manag.* **102**, 868–883 (2020).

128. Sheppard, M. I., Sheppard, S. C. & Grant, C. A. Solid/liquid partition coefficients to model trace element critical loads for agricultural soils in Canada. *Can. J. Soil Sci.* **87**, 189–201 (2007).

129. Vermeire, T. G. *et al.* European Union System for the Evaluation of Substances (EUSES). Principles and structure. *Chemosphere* **34**, 1823–1836 (1997).

130. Bakker, J., Brandes, L. J., den Hollander, H. A., van de Meent, D. & Struijs, J. *Validating SimpleBox-Computed Steady-state Concentration Ratios*. (2003).

Summary

This thesis aimed to address the main challenge in the environmental appraisal of emerging technologies to guide safe and sustainable innovation: the uncertainty about future developments which can influence the technology's environmental performance. While uncertainty may be regarded as an 'inconvenience' to conducting meaningful appraisals, this work offers an upside to the inconvenience in that it can be an important source of opportunities for safer and more sustainable designs. This work is motivated by the view that safety and sustainability assessments cannot fall behind to technological or economic drivers of innovations, which already rely on sophisticated methods to deal with uncertainties in these domains. Thus, the overarching aim of this work was to bring forward the practice of ex-ante/prospective life cycle assessment and risk assessment of emerging technologies by relying on novel adaptations of uncertainty analysis and global sensitivity analysis.

In Chapter 1 we introduced the pressing need and challenges in conducting environmental appraisals of technologies while they are still at early research and development stages. We showed how this is especially relevant for emerging photovoltaics (PV) which have seen accelerated growth in deployment and innovation in the past decades. We also introduced the case study of multijunction III-V/silicon tandem solar cells, a promising high-efficiency solar cell design for which no environmental assessments had been conducted prior to this work.

In Chapter 2 we surveyed the PV innovation landscape to investigate whether innovation in the sector as a whole was leading to reduced environmental impacts, as well as to identify environmental hotspots across the proposed technologies. For this we conducted a systematic review and meta-analysis of life cycle assessment (LCA) studies of emerging PV technologies in the period 2010-2020. In most cases, the impacts of emerging PV were lower on average than those of the incumbent technology in 2010, Al-BSF c-Si cells. However, due to large variabilities and heterogeneity we found no discernible trend in time or statistically significant effect of innovation on climate change impact scores. Of the technologies surveyed, most hotspots were found in perovskites vs. other technologies. These hotspots could be mostly attributed to the fluorine-doped tin oxide (FTO) glass component. Life cycle impacts of perovskite cells were magnified because of the perovskite cells' short lifetimes.

In Chapter 3 we conducted a comprehensive LCA of a lab/pilot scale version of the III-V/Si tandem solar cell technology. At this scale, III-V/Si was found to perform better than the Al-BSF c-Si cells which dominated the market until 2015, but slightly worse than PERC c-Si cells which have dominated since. However, our break-even analysis concluded that foreseeable optimizations in energy reduction and/or increased throughput in the MOVPE process could lead to an advantage in environmental performance of III-V/Si over state-of-the-art PERC c-Si cells.

In Chapter 4 we proposed and successfully demonstrated two important modelling enhancements needed to assess technologies beyond lab/pilot scale in an *ex-ante* LCA framework. First, unresolved choices of materials or processing methods (referred to as *technological pathways*) were modelled using binomial distributions which trigger the pathways

stochastically depending on their chances of success. Second, a novel screening algorithm was developed to allow a global sensitivity analysis (GSA) to be conducted on full-scale LCA models with an unprecedented number of uncertain model inputs, including unresolved technological pathways. The joint application of both enhancements to emerging front metal designs for PV cells allowed us to discern which unresolved technological pathways would be the most influential on the cells' future environmental performance. In this case, the choice between laser and chemical sintering methods for the copper ink, and the choice between silver and copper ink were considerably more influential than all other choices.

In Chapter 5 we conducted a prospective ecological risk assessment of the III-V/Si PV technology for high-electrification/high PV demand scenarios in three geographical scales: Europe, Amsterdam region, and a local utility-scale plant. The emissions and risks from III-V/Si PV cells were found to be low in worst-case situations, and negligible in other cases. A GSA identified operational parameters in the landfill end-of-life route as the most influential factors (waste/leachate partitioning and landfill cell depth). These factors were taken as a basis to produce recommendations for safe-by-design of III-V/Si PV panels and ancillary systems, such as increased separation for reuse of the III-V layers, substitution of the ethyl vinyl acetate (EVA) encapsulation for less acid-generating materials, and more vertical landfill cell designs.

Chapter 6 built on the experiences and insights from the previous chapters to propose a generalized framework for *ex-ante*/prospective assessments to guide safe and sustainable innovation. We showed that GSA can be used as a screening tool to identify the most influential factors across different domains (e.g., economic, social, technological, environmental). A hierarchy of risk mitigation strategies was proposed to target these influential factors at the design stage. For the III-V/Si cells we found that, once all foreseeable improvements in cell design and manufacturing are applied, extending the useful life of the panels and/or avoiding early obsolescence can offer the most effective impact reduction strategy. In this chapter we also demonstrated for the first time how the Bayesian approach to probability can be applied and may be better suited than the frequentist approach to deal with uncertainties in *ex-ante*/prospective assessments. We also showed how simple analytical solutions can be used to perform Bayesian inference and further reduce uncertainty on the influential factors identified.

In Chapter 7 we finalized by discussing the strengths of the ex-ante/prospective approach developed in this work, in that it can focus resources much more effectively than approaches relying solely on potentially biased scenario analysis. We also highlight how this approach provides a more transparent way to make design choices in light of numerous underlying assumptions and residual uncertainties.

Samenvatting

Deze dissertatie had tot doel een antwoord te vinden op de belangrijkste uitdaging bij de milieubeoordeling van opkomende technologieën als leidraad voor veilige en duurzame innovatie: namelijk de onzekerheid over toekomstige ontwikkelingen die van invloed kunnen zijn op de milieuprestaties van de technologie. Hoewel onzekerheid kan worden beschouwd als een "ongemak" bij het uitvoeren van zinvolle beoordelingen, biedt dit werk een keerzijde aan het ongemak. Dit proefschrift kan dan ook een belangrijke bron worden van mogelijkheden voor veiliger en duurzamer ontwerpen. Dit werk is ingegeven door de opvatting dat veiligheids- en duurzaamheidsbeoordelingen niet achter mogen blijven bij technologische of economische aanjagers van innovaties, die al gebruik maken van verfijnde methoden om met onzekerheden op deze gebieden om te gaan. Het overkoepelende doel van dit werk was dan ook om de praktijk van ex-ante (een ander woord voor prospectieve) levenscyclusbeoordeling en risicobeoordeling van opkomende technologieën te verbeteren door aanpassingen van onzekerheidsanalyse en globale gevoeligheidsanalyse.

In hoofdstuk 1 introduceerden wij de dringende behoefte aan, en uitdagingen bij, het uitvoeren van milieubeoordelingen van technologieën terwijl deze zich nog in een vroeg stadium van onderzoek en ontwikkeling bevinden. We hebben laten zien hoe dit met name relevant is voor opkomende systemen voor fotovoltaïsche energie (PV) winning, die de afgelopen decennia een versnelde groei in toepassing en innovatie hebben doorgemaakt. We introduceerden ook de case study van multi-junctie III-V/silicium tandem zonnecellen, een veelbelovend zonnecelontwerp met hoog rendement waarvoor voorafgaand aan dit werk nog geen milieubeoordelingen waren uitgevoerd.

In hoofdstuk 2 hebben we het PV-innovatielandschap onderzocht om na te gaan of innovatie in de sector als geheel tot minder milieueffecten leidt, en om milieu-hotspots binnen de voorgestelde technologieën te identificeren. Hiertoe hebben we een systematische review en meta-analyse uitgevoerd van levenscyclusanalyse (LCA) studies van opkomende PV-technologieën in de periode 2010-2020. In de meeste gevallen waren de effecten van opkomende PV-technologieën gemiddeld gezien lager dan die van de gevestigde technologie in 2010, Al-BSF c-Si cellen. Door de grote variabiliteit en heterogeniteit vonden we echter geen waarneembare trend in de tijd of een statistisch significant effect van innovatie op de klimaatveranderings-impact-scores. Van de onderzochte technologieën werden de meeste hotspots gevonden in perovskieten ten opzichte van andere technologieën. Deze hotspots kunnen vooral worden toegeschreven aan de fluor-gedoteerd tinoxide (FTO) glascomponent. De levenscycluseffecten van perovskietcellen waren groter vanwege de korte levensduur van de perovskietcellen.

In hoofdstuk 3 hebben we een uitgebreide LCA uitgevoerd van een laboratorium/proefschaalversie van de III V/Si tandem zonneceltechnologie. Op deze schaal bleek III-V/Si beter te presteren dan de Al-BSF c-Si cellen die tot 2015 de markt domineerden, maar iets slechter dan de PERC c-Si cellen die sindsdien hebben gedomineerd. Onze break-even analyse leidde echter tot de conclusie dat te voorziene optimalisaties in energiebeperking en/of verhoogde doorvoercapaciteit in het MOVPE-proces zouden kunnen leiden tot een voordeel in milieuprestaties van III-V/Si ten opzichte van state-of-the-art PERC c-Si cellen.

In hoofdstuk 4 hebben we twee belangrijke verbeteringen in de modellering voorgesteld en met succes gedemonstreerd. Deze verbeteringen zijn nodig om technologieën die voorbij de laboratorium-/proefschaal zijn, te beoordelen in een ex-ante LCA-kader. Ten eerste werden onopgeloste keuzes van materialen of verwerkingsmethoden (aangeduid als technologische paden) gemodelleerd met behulp van binomiale verdelingen die de paden stochastisch in werking stellen, afhankelijk van hun kans op succes. Ten tweede werd een nieuw screeningalgoritme ontwikkeld om een globale gevoeligheidsanalyse (GSA) te kunnen uitvoeren op grootschalige LCA-modellen met een ongekend aantal onzekere modelinputs, waaronder onopgeloste technologische paden. De gezamenlijke toepassing van beide verbeteringen op opkomende frontmetaalontwerpen voor PV-cellen stelde ons in staat om te bepalen welke onopgeloste technologische paden de meeste invloed zouden hebben op de toekomstige milieuprestaties van de cellen. In dit geval waren de keuze tussen laser- en chemische sintermethoden voor de koperinkt, en de keuze tussen zilver- en koperinkt aanzienlijk invloedrijker dan alle andere keuzes.

In hoofdstuk 5 hebben we een prospectieve ecologische risicobeoordeling uitgevoerd van de III-V/Si PV-technologie voor scenario's met hoge elektrificatie/hoge vraag naar PV op drie geografische schalen: Europa, de regio Amsterdam, en een lokale utiliteitscentrale. De emissies en risico's van III-V/Si PV-cellen bleken laag te zijn in worst-case situaties, en verwaarloosbaar in andere gevallen. Een GSA identificeerde operationele parameters in de eindfase van het storttraject als de meest invloedrijke factoren (verdeling afval/percolaat en diepte van de stortcel). Op basis van deze factoren zijn aanbevelingen gedaan voor een veilig ontwerp van III-V/Si PV-panelen en aanverwante systemen, zoals een grotere scheiding voor hergebruik van de III-V lagen, vervanging van de ethylvinylacetaat (EVA) inkapseling door minder zuurvormende materialen, en meer verticale ontwerpen van stortplaatscellen

Hoofdstuk 6 bouwde voort op de ervaringen en inzichten uit de vorige hoofdstukken om een gegeneraliseerd kader voor ex-ante/prospectieve beoordelingen voor te stellen om veilige en duurzame innovatie te begeleiden. We toonden aan dat GSA kan worden gebruikt als een screeningsinstrument om de meest invloedrijke factoren over verschillende domeinen (bv. economisch, sociaal, technologisch, milieu) te identificeren. Er werd een hiërarchie van risicobeperkingsstrategieën voorgesteld om deze invloedrijke factoren in de ontwerpfase aan te pakken. Voor de III-V/Si-cellen hebben we vastgesteld dat, zodra alle te verwachten verbeteringen in celontwerp en -fabricage zijn toegepast, het verlengen van de nuttige levensduur van de panelen en/of het vermijden van vroegtijdige veroudering de meest doeltreffende strategie voor het beperken van de effecten kan bieden. In dit hoofdstuk hebben we ook voor het eerst laten zien hoe de Bayesiaanse benadering van waarschijnlijkheid kan worden toegepast en wellicht beter geschikt is dan de stochastische benadering om met onzekerheden in ex ante/prospectieve beoordelingen om te gaan. We hebben ook laten zien hoe eenvoudige analytische oplossingen kunnen worden gebruikt om Bayesiaanse inferentie uit te voeren en de onzekerheid over de geïdentificeerde invloedrijke factoren verder te verminderen.

In hoofdstuk 7 bespreken we tot slot de sterke punten van de in dit werk ontwikkelde ex ante/prospectieve benadering, in die zin dat zij de middelen veel doeltreffender kan concentreren dan benaderingen die uitsluitend berusten op een potentieel vertekende

scenario-analyse. We belichten ook hoe deze benadering een transparantere manier biedt om ontwerpkeuzen te maken in het licht van talrijke onderliggende veronderstellingen en resterende onzekerheden.

Acknowledgements

Devoting four years of one's life to the study of one specific topic is a very big commitment. It is a decision to embark on a long journey full of challenges, gratifications, unexpected detours, surprising outcomes, many questions and some answers. In this journey, it would have been very easy to lose my course were it not for the many people willing to share a vision, an insight, an idea, an opinion, or simply lend an ear.

First and foremost, I would like to express my deepest gratitude to my promotors and mentors: Martina Vijver, Stefano Cucurachi and Willie Peijnenburg. I was very lucky to count on their experience and different backgrounds, as well as their keen interest in my development as a PhD student and an academic. I will never forget their support, generosity and openness to share guidance in technical aspects but also towards my personal career development.

Throughout the past 4 years I also had the pleasure and honour to collaborate with highly esteemed colleagues from Leiden University's Institute of Environmental Sciences (CML) and Leiden University College (LUC) on several publications: Paul Behrens, Jeroen Guinée, Reinout Heijungs, Bernhard Steubing, Maarten Koese, Gerard Breeman, Vrishali Subramanian, Joao Rodrigues, Peter van Bodegom and Alexandra Marques. At CML I also encountered a brilliant and inspiring group of colleagues and friends. A special thanks to those who joined me in the Ex-ante LCA Working Group for their wonderful insights and validation of the important work we are doing. And to my students from the Industrial Ecology, Governance of Sustainability and LUC programmes, who trusted me with supervision of their projects from which I also learned a lot. All the above was made possible thanks to the ever-growing and high-visibility platform that our institute director, Arnold Tukker, and the management team at CML have shaped. To them I also owe enormous gratitude for supporting my transition to a new role as Assistant Professor where I will be able to continue this exciting and promising research line.

I owe much of the valuable data and technological insights in this work to the generosity of the SiTaSol project consortium partners, where I would especially like to thank Frank Dimroth, Thomas Bergunde, Jan Bennick, Dietmar Schmitz, Sebastian Nold, Matthew Hull, Roman Trattnig, Nastaran Hayatiroodbari, Mirella El-Gemayel and Leif Jensen. I also benefited greatly from our collaboration with Caterin Salas-Redondo and Lars Oberbeck at L'Institut Photovoltaïque d'Île-de-France (IPVF). The most challenging chapters of this thesis would have been impossible to write without the technical input and insights of Joris Quik and Matthias Hof at the Netherlands Institute for Public Health and the Environment (RIVM).

To my mother, Maria Victoria, thank you for working so hard and against all forces of nature to instil in me the discipline required for this type of work. To my father, Alberto, for imbuing me with admiration for science, philosophy and beauty. To Niall, for the endless supply of extra mental power whenever reserves were running low. To Sammy, for making everything so unbelievably easy.

List of publications

Papers in this thesis

- Blanco, C.F., Cucurachi, S., Dimroth, F., Guinée, J.B., Peijnenburg, W.J.G.M. & Vijver, M.G. (2020), Environmental impacts of III–V/silicon photovoltaics: life cycle assessment and guidance for sustainable manufacturing, *Energy and Environmental Science* 13(11): 4280-4290.
- Blanco, C.F., Cucurachi, S., Guinee, J.B., Vijver, M.G., Peijnenburg, W.J.G.M., Trattnig, R. & Heijungs, R. (2020), Assessing the sustainability of emerging technologies: A probabilistic LCA method applied to advanced photovoltaics, *Journal of Cleaner Production* 259: 120968.
- Blanco ,C.F., Cucurachi, S., Peijnenburg, W.J.G.M., Beames, A. & Vijver, M.G. (2020), Are Technological Developments Improving the Environmental Sustainability of Photovoltaic Electricity? *Energy Technology* 8(11): 1901064.

Related publications

- Koese, M., Blanco, C.F., Breeman, G.E., Vijver, M.G. (2022) Towards a more resource-efficient solar future in the EU: an actor-centered approach, *Environ. Innov. Soc. Transit.* (in review).
- Cucurachi, S., Blanco, C.F., Steubing, B.R.P. & Heijungs, R. (2022), Implementation of uncertainty analysis and moment-independent global sensitivity analysis for full-scale life cycle assessment models, *Journal of Industrial Ecology*: 13194.
- Adrianto, L.R., van der Hulst, M.K., Tokaya, J.P., Arvidsson, R., Blanco, C.F., Caldeira, C., Guillén-Gonsálbez, G., Sala, S., Steubing, B.R.P., Buyle, M., Kaddoura, M., Navarre, N.H., Pedneault, J., Pizzol, M., Salieri, B., van Harmelen, T. & Hauck, M. (2021), How can LCA include prospective elements to assess emerging technologies and system transitions? The 76th LCA discussion forum on life cycle assessment, 19 November 2020, *The International Journal of Life Cycle Assessment* 26(8): 1541-1544.
- Cucurachi, S. & Blanco, C.F. (2019), 31 - Life-cycle assessment of engineered nanomaterials. In: Cucurachi S. & Blanco Rocha C.F. (Eds.) *Nanotechnology in Eco-efficient Construction*. Nanotechnology in Eco-efficient Construction: Woodhead Publishing. 815-846.
- Blanco, C.F., Penedo De Sousa Marques, A. & van Bodegom, P.M. (2018), An integrated framework to assess impacts on ecosystem services in LCA demonstrated by a case study of mining in Chile, *Ecosystem Services* 30(Part B): 211-219.

Curriculum Vitae

Carlos Felipe Blanco was born in Barranquilla Colombia, where he obtained a dual Colombian Bachillerato and U.S. High School degree from Karl C. Parrish School in 1998. Carlos Felipe graduated amongst the top of his class and was awarded with the prestigious *Andres Bello* award from the Colombian Ministry of Education for achieving the highest regional score in the ICFES state examinations.

In 2004, Carlos Felipe obtained his bachelor's degree in Environmental Engineering from Universidad de Los Andes in Bogota, Colombia. Here he was again awarded by the Ministry of Education for ranking amongst the top 10 national scores in the ECAES examinations for the quality of higher education. His thesis project "*Aquamod: An Educational Software Tool to Model Transport of Pollutants in Surface Water*s" was graded with a perfect score.

Carlos Felipe went on to work for 8 years in the mining industry as a Health, Safety, Environment and Community Relations (HSEC) manager in various countries in Latin America including Chile, Argentina, Guyana, Peru, Colombia and Brazil. In this role, Carlos Felipe led social and environmental impact studies for large-scale mining and minerals exploration projects, developed mine closure plans and led several critical incident investigations. He was also tasked with environmental auditing and implementing ISO14001 and OHSAS18001 health and safety standards.

In 2014, Carlos Felipe moved to the Netherlands to pursue a M.Sc. degree in Industrial Ecology at the Institute of Environmental Sciences (CML). In his M.Sc. thesis, Carlos Felipe developed a framework to assess ecosystem services in Life Cycle Assessment (LCA), which was demonstrated by a case study of water supply for the mining industry in the north of Chile. The thesis was awarded the Stans prize by CML in 2016 and later published in the journal *Ecosystem Services*.

Throughout the period 2014-2020, Carlos Felipe also worked part-time as a sustainability consultant for the energy and forestry industries and developed software solutions for stakeholder engagement programs in several large-scale mining projects.

In his free time, Carlos Felipe is an avid reader of geopolitics and philosophy and devotes considerable time to music composition and production. His artistic work can be found in Spotify under the artist name *Galactic Desperates* and the soon-to-be-released collaboration *Chaos, Order and the Lines*.